THE UNIVERSITY
of EDINBURGH

The cellular basis of resistance to Marek's disease

Pankaj Chakraborty

A dissertation submitted for the degree of

Doctor of Philosophy

University of Edinburgh

2015

Declaration

I certify:

(a) that the thesis has been composed by me, and

(b) either that the work is my own, or, where I have been a member of a research group, that I have made a substantial contribution to the work, such contribution being clearly indicated, and

(c) that the work has not been submitted for any other degree or professional qualification except as specified.

Signed:

Date: 21 May 2015

Abstract

Marek's disease (MD) is a highly infectious economically important oncogenic viral disease of chickens. It is found throughout the world and is caused by an alphaherpesvirus, Marek's disease virus (MDV). Though this disease can currently be successfully controlled by vaccination, the virus has continuously evolved to greater virulence over the last several decades. Hence, there is a need for alternative approaches to control MD. Selection and breeding of MD-resistant chickens presents an attractive option for prevention of this disease. MHC-congenic chicken inbred lines, 6_1 and 7_2, which are highly resistant and susceptible to MD, respectively, have been identified, but the cellular and genetic basis for these phenotypes is unknown. The overall aim of this study was to investigate the cellular basis of resistance to MD using an *in vitro* MDV infection model with the hypothesis that resistance is exerted by the innate immune cells. MDV is a highly cell-associated virus which makes *in vitro* studies difficult. *In vivo*, MDV infects APCs (antigen-presenting cells: macrophages and/or dendritic cells [DCs]), B cells and activated T cells. Though both B and T cells can be infected *in vitro*, co-culture infection models have not been described for APCs. Thus, the primary goal was to develop a model for infecting these cells with MDV *in vitro* and to characterise infected and uninfected cells. Developmental studies used APCs derived from outbred chickens. Chicken bone marrow cells were cultured with chCSF-1 (for macrophages) or chIL-4 and chCSF-2 (for DCs) for 4 days and then infected by the addition of chicken embryo fibroblasts (CEFs) infected with recombinant MDV expressing GFP. CEF preparations naturally contain a mixture of CEFs (92-98%) and macrophages (2-8%) and both appear to be

infectable with MDV. Infected CEFs were therefore separated from infected macrophages by FACS before adding to the bone marrow-derived APCs. Infected and uninfected APCs were sorted by FACS using GFP expression and APC-specific mAb staining (KUL01 and anti-CD45). Characteristic virus-infected and uninfected APCs were revealed via examination with live cell confocal microscopy. The presence of herpesvirus specific immediate early (ICP4), early (pp38), late (gB) transcripts and MDV specific transcript, L-Meq, in infected APCs was confirmed by RT-PCR providing evidence for MDV replication. Hence, a new *in vitro* MDV infection model of APCs has been established. Using the infected macrophages to infect CEFs showed that the infection was productive.

This model was then extended to infect APCs of lines 6_1 and 7_2. Flow cytometric analysis revealed that a higher percentage of macrophages were infected in the susceptible line (7_2) than in the resistant line (6_1). To analyse this in detail, RNA-Seq was carried out to identify differentially expressed (DE) genes between the two lines pre- and post-MDV infection. From these DE genes, potential candidate genes involved in MD resistance and susceptibility were identified. Functional analysis of DE genes support the hypothesis that resistance to MD is determined at the macrophage level of the resistant line (6_1) and the JAK-STAT signalling pathway is at least one anti-viral mechanism by which this signature is expressed.

Lay Summary

Marek's disease (MD) is an economically important cancerous disease of chickens caused by Marek's disease virus (MDV). Despite successful control by vaccination, the virus has continuously evolved to greater virulence over the last several decades. Hence, there is a need for alternative approaches to control MD. Selection and breeding of MD-resistant chickens presents an attractive option for prevention of this disease. Two chicken inbred lines, 6_1 and 7_2, which share the same MHC (major histocompatibility complex) genes and are highly resistant and susceptible to MD, respectively, have been identified, but the cellular and genetic basis for MD-resistance is still unknown. MDV infects APCs (antigen-presenting cells: macrophages and/or dendritic cells [DCs]), B cells and activated T cells in its life cycle in chickens. The overall aim of this study was to investigate the cellular basis of resistance to MD using an in vitro (in cell culture) MDV infection model with the hypothesis that resistance is exerted by the APCs. Though both B and T cells can be infected in vitro, co-culture infection models have not been described for APCs. Thus, the primary goal was to develop a model for infecting these cells with MDV in vitro and to characterise infected and uninfected cells. Developmental studies used APCs derived from outbred chickens. Chicken bone marrow-derived macrophages and DCs were cultured with chicken specific cytokines for 4 days and then infected by the addition of chicken embryo fibroblasts (CEFs) infected with a MDV expressing GFP (green fluorescent protein). CEF preparations naturally contain a mixture of CEFs and macrophages and both appear to be infectable with MDV. Infected CEFs were therefore separated from infected macrophages by cell sorter

before adding to the bone marrow-derived APCs. Infected and uninfected APCs were sorted using GFP expression and APC-specific antibody staining. Characteristic virus-infected and uninfected APCs were revealed via examination with live cell confocal microscopy. The presence of herpesvirus and MDV specific transcripts in infected APCs was confirmed by RT-PCR providing evidence for MDV replication. Hence, a new in vitro MDV infection model of APCs has been established.

This model was then extended to infect APCs of lines 6_1 and 7_2. Flow cytometric analysis revealed that a higher percentage of macrophages were infected in the susceptible line (7_2) than in the resistant line (6_1).To analyse this in detail, RNA-Sequencing was carried out to identify differentially expressed (DE) genes between the two lines pre- and post-MDV infection. From these DE genes, potential candidate genes involved in MD resistance and susceptibility were identified. Functional analysis of DE genes support the hypothesis that resistance to MD is determined at the macrophage level of the resistant line (6_1) and the JAK-STAT signalling pathway is at least one anti-viral mechanism by which this signature is expressed.

List of Contents

List of Tables

List of Tables

List of Figures

List of Figures

List of Figures

List of Figures

List of Figures

Acknowledgements

I am extremely grateful to my supervisor Professor Pete Kaiser for his support, advice and inspirations during my PhD studies and therefore would like to give big thanks to him. I would also like to extend big thanks to my co-supervisor Dr. Bernadette M. Dutia for her invaluable advice and support.

I would also like to give very special thanks to Dr. Lonneke Vervelde for her help and ideas related to flow cytometry which completely changed the whole scenario of my PhD. Many thanks to Dr. Robert Dalziel for providing the recombinant virus as a kind gift.

Thanks to all the members of Kaiser group for their support during my PhD. Special thanks will go to Dr. Lisa Rothwell and Dr. Zhiguang Wu for their help and advice regarding TaqMan qRT-PCR and flow cytometry, respectively. I will remain ever grateful to Dr. Suzanne Esper, Dr. Kate Sutton, Anuruddika Fernando and Dominika Borowska for their help and technical training at the initial stages of my PhD.

Many thanks to Dr. Michail Karavolos for providing samples in my experiments. I would like to thank Richard Kuo for RNA-Seq data analysis and Dr. Jacqueline Smith for helping me to do functional analyses of DE genes. Many thanks to Robert Fleming and Graeme Robertson for their support in FACS. I would like to acknowledge the staffs in the Poultry Unit of The Roslin Institute for their support in taking care of chickens used in my experiments.

I would like to give very special thanks to my lovely wife Sumika Bhattacharjee for her sacrifice, love and support in my life. I would like to thank my beloved son Aryan Chakraborty for filling my life with happiness. Special thanks to my parents who have given great love and support over the years.

Thanks to University of Edinburgh for providing scholarships to support my study and stay at Edinburgh.

Finally, I would like to thank all my friends and well-wishers whom I met during my life at Edinburgh for their continuous encouragement and help.

Abbreviations and acronyms

$	Dollar
%	Percentage
^{o}C	Degree Celsius
µg	Microgram
µl	Microlitre
µm	Micrometre
7-AAD	7-aminoactinomycin D
aa	Amino acid
Ab	Antibody
ADCC	Antibody-dependent cell-mediated cytotoxicity
AEC	3-amino-9-ethylcarbazole
APC	Antigen-presenting cell
BAC	Bacterial Artificial Chromosome
BMDC	Bone marrow-derived DC
BMDM	Bone marrow-derived macrophages
bo	Bovine
bp	Base pairs
BSA	Bovine serum albumin
bZIP	Basic leucine zipper
Ca^{2+}	Calcium ions
CD	Cluster of differentiation
cDNA	Complementary DNA
CEF	Chicken embryo fibroblasts
ch	Chicken
ChIP	Chromatin immunoprecipitation
CISH	Cytokine-inducible SH2-containing protein
CME	Clathrin mediated endocytosis
cMGF	Chicken myelomonocytic growth factor
CMV	Cytomegalovirus
ConA	Concanavalin A

CPE	Cytopathic effects
CpG	Cytosine-phosphate-Guanine
CS	Chicken serum
CSF	Colony stimulating factor
Ct	Cycle threshold
CtBP	C-type binding protein
CTLA-4	Cytotoxic T-lymphocyte associated antigen-4
CTLs	Cytotoxic T lymphocytes
DAVID	Database for Annotation, Visualization and Integrated Discovery
DC	Dendritic cell
DEAE	Diethylaminoethyl
DENV	Dengue virus
DEPC	Diethyl pyrocarbonate
DMEM	Dulbecco's modified Eagle's medium
DMSO	Dimethyl sulphoxide
DNA	Deoxyribonucleic acid
DNMT	DNA methyltransferase
dNTP	Deoxyribonucleotide triphosphate
dsRNA	Double-stranded RNA
DTT	Dithiothreitol
E. coli	*Escherichia coli*
EARCs	Ellipsoid-associated reticular cells
EBV	Epstein-Barr virus
edgeR	Empirical analysis of digital gene expression in R
EDTA	Ethylenediaminetetraacetic acid
FACS	Fluorescence-activated cell sorter
FAM	5-carboxyfluorescein
FBS	Foetal bovine serum
FDR	False discovery rate
FFE	Feather-follicle epithelium
FHL3	Four and a half LIM domain protein 3
FITC	Fluorescein isothiocyanate

FSC	Forward scatter
g	Relative centrifugal force
g	Glycoprotein
GaHV-2	*Gallid herpesvirus 2*
GaHV-3	*Gallid herpesvirus 3*
GFP	Green fluorescent protein
GH	Growth hormone
GM-CSF	Granulocyte-macrophage colony-stimulating factor
GO	Gene ontology
h	Hour
HHV-8	Human herpesvirus-8
HIV	Human immunodeficiency virus
HRP	Horseradish peroxidise
HSV	Herpes Simplex Virus
HTLV-I	Human T-cell lymphotropic virus type I
HVT	Herpesvirus of Turkey
ICP	Infected cell protein
IE	Immediate early
IFITM	Interferon induced transmembrane protein
IFN	Interferon
Ig	Immunoglobulin
IL	Interleukin
iNOS	Inducible nitric oxide synthase
IPA	Ingenuity pathway analysis
IRES	Internal ribosomal entry site
IRF	Interferon regulatory factor
IRG1	Immune-responsive gene 1
IR_L	Inverted internal-long
IR_S	Inverted internal-short
ISGs	IFN-stimulated genes
JAK-STAT	Janus Kinase -Signal transducers and activators of transcription
kDa	KiloDalton

KEGG	Kyoto Encyclopedia of Genes and Genomes
LATs	Latency-associated transcripts
LB	Luria Borth
LL	Lymphoid leucosis
LPS	Lipopolysaccharide
LTBP1	Latent TGF-β binding protein 1
M	Molar
m	Murine
mAb	Monoclonal antibody
MAPK	Mitogen activated protein kinase
MD	Marek's disease
MDCC	MDV-transformed chicken cell-line
MDM	Monocyte-derived macrophages
MDV	Marek's disease virus
Meq	MDV EcoRI-Q
MFI	Mean fluorescent intensity
mg	Milligram
$MgCl_2$	Magnesium chloride
MHC	Major Histocompatibility Complex
min	Minute
miRNA	MicroRNA
ml	Millilitre
mM	Millimolar
mMDV	Mild MDV
MOI	Multiplicity of infection
mRNA	Messenger RNA
MSRs	MDV small RNAs
MZF1	Myloid zinc finger 1
$NaHCO_3$	Sodium bicarbonate
NEAA	Non-essential amino acids
NF-κB	Nuclear factor kappa-light-chain-enhancer of activated B cells
ng	Nanogram

NK	Natural killer cells
nm	Nanometre
NO	Nitric oxide
OD	Optical density
ORF	Open reading frames
OriLyt	Origin of lytic replication
ov	Ovine
PAMP	Pathogen-associated molecular pattern
PBS	Phosphate-buffered saline
PCR	Polymerase chain reaction
PE	Pathway express
pfu	Plaque forming unit
pp	Phosphoprotein
PRR	Pattern-recognition receptor
PRV	Pseudorabies virus
qRT-PCR	Quantitative real-time-PCR
QTL	Quantitative trait loci
RNA	Ribonucleic acid
RPMI	Roswell Park Memorial Institute medium
rRNA	Ribosomal RNA
RT	Room temperature
RT-PCR	Reverse transcription-PCR
s	Second
SCA2	Stem cell antigen 2
SHFV	Simian haemorragic fever virus
SOCS	Suppressor of cytokine signalling
SSC	Side scatter
ssRNA	Single-stranded RNA
TAE	Tris-Acetate EDTA
TAMRA	Tetramethylrhodamine
Taq	*Thermus aquaticus*
TCR	T cell receptor

TF	Transcription factor
TGF-β	Transforming growth factor-beta
Th	T helper
TLR	Toll-like receptor
TNF	Tumour necrosis factor
TR_L	Terminal repeat-long
TR_S	Terminal repeat-short
U_L	Unique-long
U_S	Unique-short
v/v	Volume per volume
vCXC	Viral CXC
vIL-8	viral interleukin-8
vMDV	Virulent MDV
vTR	Viral telomerase RNA
vv^+MDV	Very virulent plus MDV
vvMDV	Very virulent MDV
VZV	Varicella Zoster Virus
w/v	Weight per volume
ZNF	Zinc finger protein

Chapter 1:

Introduction

1.1 Marek's disease - the early events

The story began in 1907 when József Marek, a Hungarian scientist, first described Marek's disease (MD), so named in his honour later in 1960 by Peter M. Biggs (Biggs, 1961). József Marek described the disease as fowl paralysis in chickens, causing polyneuritis or inflammation of the major nerves, specifically the sciatic nerve and certain areas of the spinal cord (Marek, 1907). Later, Pappenheimer et al. (1929a; 1929b) suggested the name 'neurolymphomatosis gallinarum' for this disease. Because, along with nerve tissues, tumorous lesions were observed in various visceral organs and there was also similarity in the cytological composition of the visceral lymphomas to those in nervous tissues. Coincidentally, a disease causing lymphatic leukosis, now known as lymphoid leukosis (LL), with very similar symptoms to MD, had also been described around the same time (Ellermann, 1921). Unfortunately, MD was often confused with LL and for several decades of research was carried out trying to classify MD and LL based only on pathological lesions as there was no aetiological basis until late 1960s, when the causal agent of MD was first identified as a herpesvirus by an electron microscopic examination of infected chicken kidney cell cultures (Churchill and Biggs, 1967).

1.2 Herpesviruses - a brief biology

Herpesviruses are important pathogens that cause diseases in mammals and birds. They are DNA viruses belonging to the family *Herpesviridae*. The name 'Herpes' is derived from the Greek word *"herpein"* (to creep), referring to the skin conditions such as eczema and cancer, that were evident in ancient times (Wildy, 1973). All herpesviruses can establish latent infection within specific tissues, which are

characteristic for each virus. In the latent phase of infection, the viral genome remains in the host cell with the expression of only a few viral genes. Herperviruses have a unique four-layered structure: a core containing the large, double-stranded DNA genome is enclosed by an icosahedral capsid which is composed of capsomers. The capsid is surrounded by an amorphous protein coat called the tegument, which is again encased in a glycoprotein-bearing lipid bilayer envelope (Davison, 2010). Transcription, genome replication and capsid assembly occur in the host cell nucleus. Genes are replicated in a specific order: (1) immediate-early genes, which encode regulatory proteins; (2) early genes, which encode enzymes for replicating viral DNA and (3) late genes, which encode structural proteins.

The family *Herpesviridae* is divided into three subfamilies, such as Alphaherpesvirinae, Betaherpesvirinae and Gammaherpesvirinae (Davison, 2010). The alphaherpesviruses usually have a short replicative cycle, induce cytopathology in monolayer cell culture and have a broad host range. The general replicative cycle of betaherpesviruses is long and has a restricted host range; and the gammaherpesviruses have a long replicative cycle with a very restricted host range. Marek's disease virus (MDV), the causal agent of MD, belongs to the Alphaherpesvirinae family.

1.3 MDV and its gene contents

MDV belongs to the genus *Mardivirus* (Marek's disease like viruses) in the Alphaherpesvirinae family. MDV was initially considered as a member of *Gammaherpesvirinae* because it grows slowly in cell culture and induces T cell lymphomas, characteristic biological properties which are also observed with the

infection of the *Gammaherpesvirinae* members, such as Epstein-Barr virus (EBV) (Osterrieder et al., 2006). However, molecular characterisation and genome sequencing revealed that MDV and HVT (Herpes virus of Turkey) have similarity to alphaherpesviruses, such as Herpes Simplex Virus (HSV) or Varicella Zoster Virus (VZV) (Fukuchi et al., 1984; Buckmaster et al., 1988; Tulman et al., 2000). There are three serotypes of the *Mardivirus* genus which were initially classified using indirect immunofluorescence tests (Bulow and Biggs, 1975). The serotypes are MDV-1, which includes all the oncogenic strains and their attenuated forms; MDV-2 includes all the non-oncogenic strains isolated from chickens and serotype 3 includes all the non-oncogenic strains isolated in turkeys, herpesvirus of turkeys (HVT) (Davison, 2002; Nair, 2005; Gimeno, 2008).

A detailed classification of the genus *Mardivirus* in the context of MDV is given in Table 1.1. MDV-1 is now classified as *Gallid herpesvirus 2* (GaHV-2), MDV-2 as *Gallid herpesvirus 3* (GaHV-3) and HVT as a *Meleagrid herpesvirus* (Schumacher et al., 2000), though Osterrieder and Vautherot (2004) proposed changing the nomenclature of MDV serotype 1 to be referred to as MDV, because only MDV-1 is virulent and thus capable of causing tumours; a feature which is absent in MDV-2 and HVT as they are avirulent.

The general genome organizations of *Herpesviridae* are categorised into six classes, from A to F, of which, only class D and E are found in the *Alphaherpesvirinae* and all the members of the *Mardivirus* demonstrate class E genomes which represent two unique sequences (Figure 1.1), a long (unique-long, U_L) and a short (unique-short, U_S), each of which is again linked by inverted internal (IR_L and IR_S) and terminal repeats (TR_L and TR_S) (Fukuchi et al., 1984). Genome sequencing of *Mardivirus*

genus revealed that all the members have approximately similar gene contents but they differ in terms of GC (guanine and cytosine) content, with 44.1% in MDV-1 and 53.6% in MDV-2, while in HVT it is 47.2% (Lee et al., 2000a; Tulman et al., 2000; Afonso et al., 2001; Kingham et al., 2001). There are several MDV-1 specific genes which are not expressed by MDV-2 or HVT, such as Meq (MDV EcoR1-Q) (Jones et al., 1992), pp38 (phosphoprotein 38) (Cui et al., 1990) and vIL-8 (viral interleukin-8) (Parcells et al., 2001) and two small open reading frames (ORF), BamHI-H family of transcripts (pp14 and RLORF9) (Hong and Coussens, 1994; Tahiri-Alaoui et al., 2009).

Genus - *Mardivirus*			
Taxon name	**Common name**	**Acronym**	**Strain(s) with available sequences**
Gallid herpesvirus 2	Marek's disease virus type 1 (MDV-1)	GaHV2	Md5 GA CU-2 Md11 CVI988 RB1B 584A
Gallid herpesvirus 3	Marek's disease virus type 2 (MDV-2)	GaHV3	HPRS24
Meleagrid herpesvirus 1	Turkey herpesvirus (HVT)	MeHV1	FC126

Table 1.1. *Classification of the genus Mardivirus. Adapted and modified from Davison (2010).*

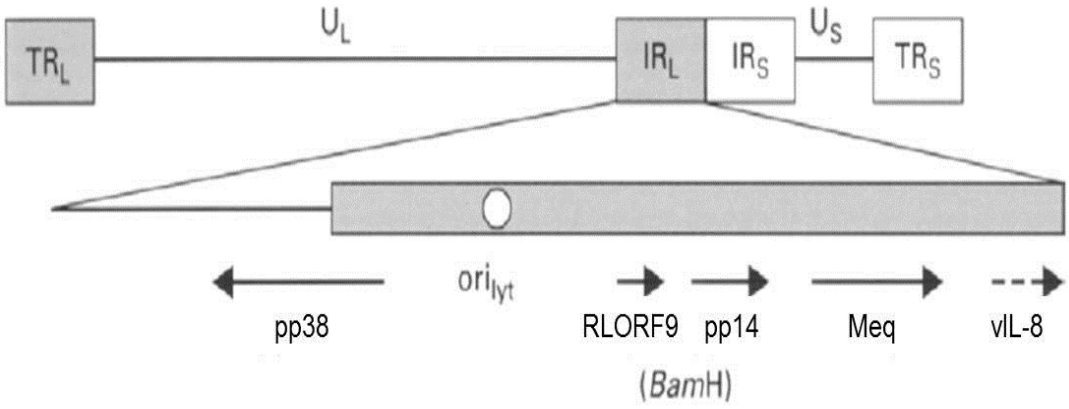

Figure 1.1. *Structure of the MDV genome. Two unique regions (U_L and U_S) are flanked by the repeats TR_L and IR_L and TR_S and IR_S, respectively. The enlarged IR_L region with the major open reading frames is shown. Adapted and modified from Nair and Kung (2004) with permission from Elsevier.*

1.3.1 pp38 complex

pp38 is a complex of two related phosphoproteins, pp24 and pp38 (Cho et al., 1998) and was initially described as a gene having a potential role in oncogenesis, as it was expressed on tumour cells and lymphoid cell lines (Cui et al., 1990). Xie et al. (1996) also mentioned that pp38 plays a role in the proliferation of lymphoblastoid cells. However, deletion of pp38 in a vv (very virulent) MDV strain resulted in severe impairment of *in vivo* early lytic replication with the retention of low levels of oncogenicity, indicating that pp38 is involved in early cytolytic infection and dispensable for induction of tumours (Reddy et al., 2002).

1.3.2 Meq

Meq is a 339-amino acid (aa)-long protein encoded within the genome of MDV-1 strains. A variant of Meq is L-Meq which has an insertion of 59 aa of the proline-rich repeat and it is found in the MDV-1 vaccine strain (CVI988) (Lee et al., 2000b) and in the low virulent strains. Meq is a major determinant of MDV virulence as

indicated by its expression in both latent and transformation stages (Jones et al., 1992; Lupiani et al., 2004; Spatz et al., 2007; Lee et al., 2008). Meq is characterised by an N-terminal bZIP (basic leucine zipper) domain and a proline-rich C-terminal transactivation domain (Jones et al., 1992). The bZIP domain of Meq protein structurally and functionally resembles oncoproteins of the bZIP family, such as c-Jun and c-Fos (Qian et al., 1995).

1.3.3 vIL-8 or vCXC

MDV genome encodes a highly spliced CXC chemokine gene which was originally identified as an IL-8 homologue (Liu et al., 1999; Parcells et al., 2001). Davison and Kaiser (2004) proposed the name vCXC for vIL-8 because, like the B-lymphocyte chemoattractant CXC chemokines, vIL-8 gene consists of three exons and two introns and lacks the ELR (glutamic acid-leucine-arginine) motif. The vIL-8 has a significant role in MDV pathogenesis as deletion of vIL-8 in a vvMDV strain resulted in highly reduced disease and tumour incidence, when compared to the parental virus (Cui et al., 2005).

1.3.4 BamHI-H family of transcripts

The MDV BamHI-H region first came into focus as a pathogenic determinant when it was revealed that an expansion of the 132 bp tandem repeats takes place within the BamHI-D/BamHI-H region during attenuation, though it was reported later that this expansion was not the sole determinant for attenuation (Niikura et al., 2006a; Silva and Gimeno, 2007). The BamHI-H transcripts include the 1.8 kb transcript which is a member of a family of mRNAs expressed as immediate-early genes (Hong and Coussens, 1994; Hong et al., 1995). It has two open reading frames (ORF). The first ORF encodes a 14 kDa polypeptide and the second ORF, also known as RLORF9,

encodes a 12 kDa protein, which is expressed through an internal ribosomal entry site (IRES) (Tahiri-Alaoui et al., 2009). Though the precise roles have not been explored yet, the 1.8 kb family of transcripts were shown to be involved in the induction and maintenance of MDV latency (Peng et al., 1994; Hong and Coussens, 1994; Hong et al., 1995; Hayashi et al., 1999).

1.4 MD - an evolving viral infection

Based on the pathogenicity of the virus, MDV-1 can be grouped into four pathotypes: (i) mild (mMDV), (ii) virulent (vMDV), (iii) very virulent (vvMDV) and (iv) very virulent plus (vv^+MDV) (Witter, 1997; Witter and Schat, 2003). These pathotypes have been identified on a regular basis over the years, hence indicating a continuous evolution of MDV towards greater virulence (Witter, 1997). The pathotype was thought to be a mild form of the virus (mMDV) until 1950s based on lesions caused by the disease, although there was no isolated virus from this time period. The lesions caused by mMDV strains are mainly restricted to nerve tissues and sometimes a low incidence of ovarian lymphomas (Witter, 1997). Then, from the late 1950s through the 1960s an acute form of MD emerged that caused major outbreaks and led to very high mortality (40%) in layers. These virulent strains of MDV (vMDV) caused high incidence of visceral and neural lymphomas (Witter, 1997). The very virulent form of the virus (vvMDV) was discovered in the late 1970s. This form was able to cause severe acute cytolytic diease and bursal and thymic atrophy resulting in early death of the bird (Witter et al., 1980). The increase in virulence continued into the late 1990s when very virulent plus strains (vv^+MDV) were first discovered that can cause high incidence of lymphomas and can even be oncogenic in bivalent-vaccinated chickens (Witter, 1997).

1.5 Pathology and clinical stages of MD

Pathologically MD is characterized by viraemia (Lee et al., 1981), infection of feather-follicle epithelium (Moriguchi et al., 1982), central and peripheral neuropathy (Burgess et al., 2001; Gimeno et al., 2001), visceral lymphomatosis (Payne and Rennie, 1976), atherosclerosis (Fabricant et al., 1978) and ocular lesions (Ficken et al., 1991). MDV clinical signs vary greatly according to the stage of infection and the virulence of the virus. The disease has many clinical forms including classical MD, lymphomatosis, early mortality syndrome, skin form, ocular form and atherosclerosis.

1.5.1 Classical form of MD

The classical form of MD is also known as Fowl paralysis which is characterised by both peripheral neuropathy, usually associated with the gross enlargement of the peripheral nerves and lymphomatosis in visceral organs, predominantly in the ovaries. The disease appears as asymmetrical spastic leg paralysis and gradual death of birds (Biggs and Payne, 1967).

1.5.2 Lymphomatosis

In this form of MD, visceral lymphomas might occur in the gonads, lung, heart, mesentery, kidney, liver, spleen, bursa, thymus, adrenal gland, pancreas, proventriculus, iris, skeletal muscle and skin due to multifocal lymphoid proliferation along with the presence or absence of gross nerve lesions (Payne and Rennie, 1976; Witter and Schat, 2003; Payne, 2004). The affected birds usually have no particular clinical signs, but sometimes show varying signs from general depression to total comatose. As described in Witter and Schat (2003), MDV lymphoma generally

appears as an enlargement of the affected organ with diffuse or nodular white or grey discoloration, whereas in the ovary it has a distinct cauliflower-shaped appearance.

1.5.3 Early mortality syndrome

This form was reported in the infection with vv and vv^+MDV strains. Though the clinical signs of the early mortality syndrome vary according to the susceptibility of birds to MD, it is generally characterised by acute cytolytic infection that leads to high rates of early morality. The acute cytolytic infection of vvMDV strains is characterised by marked atrophy in the bursa and thymus and increased splenic necrosis compared to other low virulent MDV strains (Witter et al., 1980; Witter, 1983). These strains can induce lymphoma in HVT vaccinated birds and in birds genetically resistant to less virulent strains (Witter et al., 1980). The vv^+MDV strains can cause severe brain oedema and acute death and are oncogenic in birds vaccinated with bivalent vaccines (Witter, 1997; Gimeno et al., 1999).

1.5.4 Skin form

Feather-follicle epithelium (FFE) of skin is the only site in the chicken where MDV infection is fully productive. The FFE infection starts usually after 1-2 weeks of primary infection, and continues for many weeks. The cells in the corneous and transitional layer of the FFE are commonly affected and cloudy swelling and hydropic degeneration can be noticed in these cells, followed by local perivascular and perifollicular aggregation and proliferation of lymphoid cells (Moriguchi et al., 1982). Skin biopsies of the perifollicular skin lesions revealed that two distinct patterns could be developed in this area: a tumour-associated pattern and a non-tumour-associated pattern (Cho et al., 1996).

1.5.5 Ocular form

The ocular form of MD is observed in sporadic cases. The main clinical manifestation of this outbreak is blindness in the infected birds (Ficken et al., 1991), due to the infiltration of mononuclear cells mainly in the iris, ciliary body and conjunctiva. The gross pathology of the eye is characterised by acute uveitis and corneal oedema.

1.5.6 Atherosclerosis

Atherosclerosis is thickening in the artery walls as a result of deposition of cholesterol and other lipid droplets. Infection with MDV is sometimes associated with atherosclerosis in the aorta, coronary arteries and other large arteries, which appears as a marked narrowing in the lumen of the affected artery with small focal plaques 1-2 mm in diameter usually occurring one month after the infection (Minick et al., 1979). The association between atherosclerosis and MDV infection was investigated by Fabricant et al. (1978) and it was suggested that virus-induced necrosis of the medial layer is a crucial factor in the development of atherosclerosis. MDV antigens were readily detectable in the medial layer of affected arteries by immunofluorescence (Fabricant et al., 1978; Minick et al., 1979; Hajjar et al., 1986).

1.6 Economic impact of MD in poultry industry

MD has a tremendous economic impact on the global poultry industry, firstly, because of the continuing losses due to the disease and secondly, because of the costs of vaccination. The vaccination can prevent formation of tumours but not the generation of infectious viruses. Despite the widespread and successful use of vaccines since the 1970s, MDV strains have shown continuous evolution in virulence conveying the ability to overcome the immune responses induced by the vaccine

(Witter, 1997). The crude estimation of worldwide MD-induced loss is thought to be US$1-2 billion per annum (Morrow and Fehler, 2004) which validates the importance of developing further control strategies for MD.

1.7 Major approaches to control MD

MD is largely a lymphoproliferative disease which can be effectively controlled by vaccination.

1.7.1 Control by vaccination

MD is the first virus-induced tumour disease to be prevented by vaccination (reviewed in Baigent et al., 2006). Though, as mentioned above, despite successful vaccination, the virulence of MDV has increased in the course of time. Nair (2005) described a periodic step-wise evolution of MDV with the vaccines implemented over the last several decades (Figure 1.2).Various vaccines developed from different strains of MDV have been introduced since the 1970s. The first vaccine for MD was prepared from the oncogenic HPRS-16 strain of MDV-1, which was attenuated by serial passages through chicken kidney cell cultures (Churchill et al., 1969). This was very soon replaced by the widely used HVT vaccine, developed from the FC126 strain (Okazaki et al., 1970) to control vMDV strains (Figure 1.2). Both 'cell-free' and 'cell-associated' types of HVT vaccines are available and they are still in use either alone, or in combination with other vaccines (Bublot and Sharma, 2004). Later, Schat and Calnek (1978) introduced another widely used vaccine, SB-1, which was developed from MDV-2, and had synergistic activity when administered with HVT (Calnek et al., 1983; Witter and Lee, 1984). Bivalent vaccines were used for controlling vvMDV strains (Figure 1.2). Meanwhile in the early 1970s, a vaccine was developed from an attenuated strain (CVI988) of MDV-1, also called 'Rispens'

vaccine (Rispens et al., 1972a; 1972b), which has been in widespread use and is now considered as the 'gold standard' for MD vaccines (Bublot and Sharma, 2004).

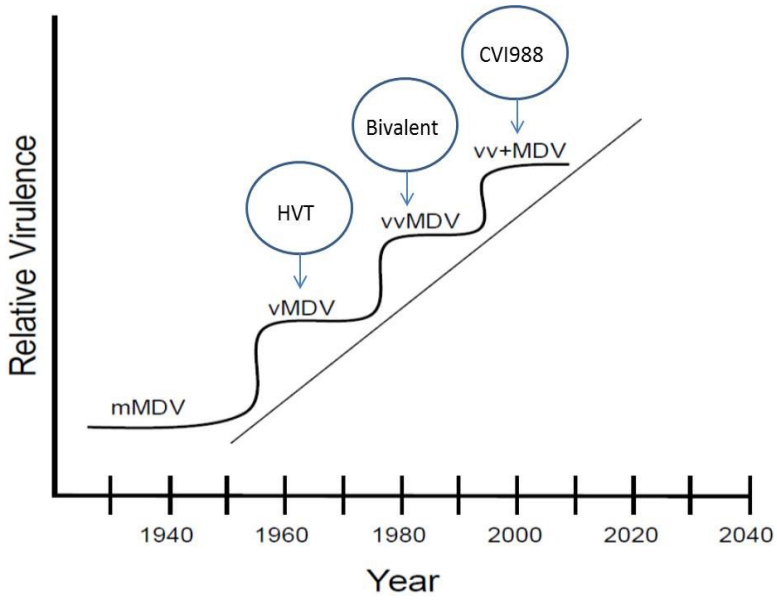

Figure 1.2. *Periodic step-wise evolution of MDV in response to the introduction of different types of vaccines. Adapted and modified from Nair (2005) with permission.*

This vaccine has protective efficacy against vv^+ field strains of MDV (Figure 1.2) because, being serotype 1, it has a close antigenic relationship with those field strains (Baigent et al., 2006). Although vaccination against MD is highly effective, it has apparently contributed to the evolution of field strains towards increased virulence.

1.7.1.1 Future of MD vaccination

Though MD vaccines are capable of reducing disease incidence, virus replication and tumour formation, they do not confer sterile immunity. Vaccination cannot halt superinfection with virulent strains and hence, cannot stop virus shedding, resulting in the spread of MDV from vaccinated birds to other uninfected birds. Besides this, the diffident nature of vaccinal immunity might lead to the evolution of viral pathogenicity and emergence of more virulent strains (Gimeno, 2008). The

increasing virulence of MDV could also be the cumulative effect of some other events which have happened globally over the last few decades, such as the intensification of poultry production, changes in host genetics, and vaccination pressure (Witter, 1997).

Though the vaccines from the CVI988 strain are still successfully capable of controlling MD, it is a matter of great concern that this is one of the last effective vaccines currently used and if its efficacy declines in the foreseeable future, the result would be disastrous for the global poultry industry (Nair, 2005; Spatz et al., 2007). To overcome this, one of the areas of research is now focused on modifying the MDV genome and hence, building a way for a new generation of molecularly defined vaccines, such as vaccines produced by BAC (Bacterial Artificial Chromosome) technology (Nair, 2005).

1.7.1.1.1 BAC and BAC-derived MDV vaccines

BACs are derivatives of the naturally occurring F (Fertility)-plasmid DNA found in *E. coli* (Kim et al., 1992; Shizuya et al., 1992). Large DNA fragments from various genomic sources can be cloned into *E. coli* using the BAC system, where the DNA is easy to manipulate and highly stable due to its low copy number (Shizuya et al., 1992). Messerle et al. (1997) constructed the first herpesvirus BAC mutant for murine cytomegalovirus (MCV) and since then this technology has proved to be a vital tool for studying herpesvirus pathogenesis (Warden et al., 2011).

Several BAC clones have so far been developed for different strains of MDV. Schumacher et al. (2000) first reported a MDV BAC clone of the attenuated MDV-1 strain, 584Ap80C, which was constructed by inserting the F-plasmid into the US2

region of the virus by homologous recombination, emphasising the fact that the US2 ORF was non-essential for MDV growth (Petherbridge et al., 2003).

The BAC mutants grew and replicated as well as their parental strain (Schumacher et al., 2000). Subsequently, the vaccine strain CVI988 (Rispens), the virulent Md11 strain and the very virulent RB1B strain were cloned as infectious BACs (Petherbridge et al., 2003; Niikura et al., 2006b).

MDV BAC clones can be used to study the role of various genes in virus growth and replication. For example, UL46-UL49 genes have been studied which encode the major tegument proteins (Dorange et al., 2002), and also the viral membrane glycoprotein encoding genes, UL10 (gM) and UL49.5 (Tisher et al., 2002).

Apart from the study of virus genes and their role in virus growth and pathogenesis, BACs can also be used to develop new vaccines. Using BAC technology, the large sized herpesvirus genome can be easily manipulated. For example, genes which are not essential for effective *in vitro* or *in vivo* viral replication can be deleted or replaced with any marker gene, a feature which made herpesvirus BACs suitable candidates for prospective vaccine vectors (Brun et al., 2008).

Wasson (2011) constructed several mutants of CVI988 BAC strain by replacing UL41, US10 and UL50 genes with GFP (Green Fluorescent Protein) as a first step to create MDV vaccine vectors that could deliver influenza genes. A Meq-deleted MDV BAC vaccine has been developed which was non-oncogenic *in vivo* and provided greater protection than that of the CVI988 or Rispens strain (Silva et al., 2010). A cosmid-derived Meq-deleted vaccine of a vvMDV strain (Md5) was also shown to confer a better or equal efficacy compared to the CVI988 vaccines but caused significant lymphoid organ (bursa and thymus) atrophy and body weight loss

in chickens with no maternal antibodies (Lee et al., 2008), though it was later revealed that the lesions could be attenuated by serial passage of the vaccine strain *in vitro* (Lee et al., 2013).

1.7.2 Alternative control method - selection and breeding of MD-resistant chickens

Another key control measure of MD could be the selection and breeding of MD-resistant chickens for meat and high egg production (von Krosigk et al., 1972). The estimates of heritability of MD resistance were 61% (reviewed in Gavora and Spencer, 1979) suggesting good potential for genetic improvement by selection and breeding. Genetic resistance to MD and the accompanying immune responses to MDV infection are complex, as they are controlled by many genes within and outside of the MHC. Moreover, each gene has only a small effect that can also be influenced by environmental conditions and other genes (Liu et al., 2001).

1.7.2.1 The chicken major histocompatibility complex (MHC)

The chicken MHC is much more compact and simple than the mammalian MHC. It contains only 19 genes in a 92 kb region of the B locus of the chicken microchromosome 16, making the chicken MHC approximately 20-fold smaller than the human MHC (Kaufman et al., 1999). The B-F/B-L region of B locus has all of the features of the MHC (Figure 1.3) identified in mammals, as it contains classical class I and class II genes and determines serological alloantigens, rapid allograft rejection, strong mixed lymphocyte reactions and cellular cooperation in the immune response. Briles et al. (1983) suggested that a gene or genes from this region are responsible for determining resistance to MD.

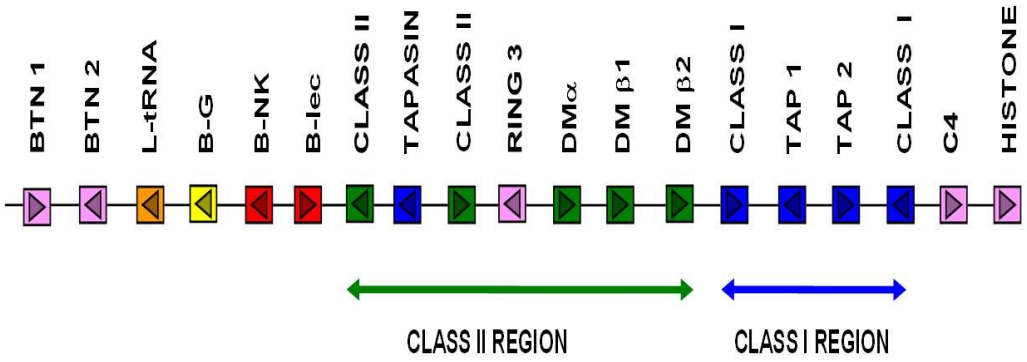

Figure 1.3. *The chicken MHC. Adapted and modified from Bumstead and Kaufman (2004) with permission from Elsevier.*

1.7.2.1.1 Role of the MHC in resistance to MD

Within the chicken MHC (B-F/B-L region), there are two classical class I genes (Figure 1.3), of which only one is highly expressed. Shaw et al. (2007) proposed that drifting and selection within stable MHC haplotypes led to predominant expression of a single class I molecule, which in turn led to strong associations of the chicken MHC with resistance to infectious pathogens and response to vaccines. Among MHC haplotypes, the B21 haplotype confers the highest order of resistance to MD compared to the B4, B12, B15 and B19 haplotypes (reviewed in Kaufman et al., 1995). Overall, B21 haplotypes have the lowest and B19 have the highest levels of MHC class I expression on the cell surface (Kaufman and Venugopal, 1998).

This MHC-dependent resistance or susceptibility of various haplotypes to MD has been studied extensively. The C-type lectin-like receptor genes, B-NK (also called BNK or Blec2 (Rogers and Kaufman, 2008)) and B-lec (also called Blec or Blec1 (Rogers and Kaufman, 2008)) are located next to each other in opposite orientations in the chicken MHC (Figure 1.3). They have been considered as potential candidate genes for the MHC-mediated resistance to MD as previous reports (Lee et al., 2001b; Iizuka et al., 2003) showed that the C-type lectin-like receptors in mouse and rat

(Ly49H, NKR-P1 and Clr) are associated with resistance to another herpesvirus, cytomegalovirus (CMV). Sequence examination revealed that B-lec is well conserved between different haplotypes. In contrast, B-NK has high allelic polymorphism and moderate sequence diversity. B-NK is also polymorphic at the protein level, and modelling demonstrates significant variation between haplotypes in the predicted ligand binding face of B-NK (Rogers and Kaufman, 2008), which could be a factor in differing MHC-based resistance to MD in various haplotypes. An up-regulation of both MHC class II (Niikura et al., 2007) and vitamin D receptor (VDR), which modulates MHC class II cell surface expression and is thus associated with MD resistance (Praslickova et al., 2008), was observed following MDV infection, suggesting MHC class II as a candidate gene for MD resistance.

1.7.2.2 Genes outside the MHC

Resistance to MD is not just influenced by genes in the MHC. Non-MHC genes also play a pivotal role in MD resistance. At least 21 separate QTL (quantitative trait loci) are involved (Yonash et al., 1999; McElroy et al., 2005). This can be most clearly explained by the examples of two inbred chicken lines (6_1 and 7_2), which are homozygous for the B2 haplotype (Cole, 1968). Lines 6_1 and 7_2 are highly resistant and highly susceptible to clinical MD, respectively, which is reflected by great differences in viraemia levels when challenged with MDV (Lee et al., 1981; Bumstead et al., 1997). Bumstead (1998) suggested that a cluster of genes (the MDV1 locus) on chicken chromosome 1 are involved in MD resistance in these lines. This region has conserved synteny with the lectin-like natural killer (NK) cell antigen complex in mice and human (Yabe et al., 1993; Lanier and Phillips, 1996). It is notable that the gene Cmv1 in mice, which accounts for resistance to murine

cytomegalovirus, also maps to this region (Scalzo et al., 1995; Brown et al., 2001; Lee et al., 2001a). The chicken protein-protein interactions during MDV infection also provided evidence that various non-MHC genes, such as GH (growth hormone), SCA2 (Stem cell antigen 2), are associated with MD resistance because the transcripts for these genes were differentially expressed between MD-resistant and -susceptible birds following MDV infection (Liu et al., 2001; Liu et al., 2003). The allele frequencies of GH have also altered in response to selection for MD resistance (Kuhnlein et al., 1997), suggesting GH as an MD resistance gene. An allele-specific expression analysis (Meydan et al., 2011) revealed that the allelic ratios of CD79B alter in bursa and thymus in response to MDV infection at 4 and 15 dpi. CD79B plays a crucial role in the immune response and, is transcriptionally combined with GH, one of the previously identified MD resistance genes.

Using microarray techniques, Smith et al. (2011) analysed genes differentially expressed in the spleen between lines 6_1 and 7_2 and identified sixteen genes as potential candidates for involvement in MD resistance. Furthermore, by conducting ingenuity pathway analysis (IPA) it was shown that one of these genes, immune-responsive gene 1 (IRG1), was highly expressed in the susceptible line following MDV infection. The precise function of IRG1 remains to be determined but it is likely to be involved in apoptosis as it clusters with other genes in its expression patterns, which are known to be involved in apoptosis or its regulation. This study also revealed a unique pathogenicity mechanism of MDV infection in which genes, involved in anti-tumour regulation, were down-regulated as early as 4 days after infection. In a separate microarray-based study, Yu et al. (2011) identified a total of 108 candidate genes for MD resistance and 121 candidate genes for MD

susceptibility which were up-regulated in spleen at 5, 10 and 21 dpi. Of these, genes involved in more than 5 bio-functions, such as CD8α, IL-8, USP18, and CTLA-4 (cytotoxic T-lymphocyte associated antigen-4) were considered to be potentially important genes regarding MD resistance or susceptibility. Recently, Haunshi and Cheng (2014) reported a differential expression of several non-MHC genes, such as TLR3 along with cytokines, IL-6 and IL-8 between CEFs (chicken embryo fibroblasts) from resistant and susceptible lines, suggesting an important role for these genes in resistance to MD.

1.7.2.3 Role of host microRNAs in genetic resistance to MD

MicroRNAs (miRNA) are small (19-24 nucleotides) non-coding RNAs generated from longer precursor RNAs and involved in RNA silencing and post-transcriptional regulation of gene expression (Treiber et al., 2012). Host miRNAs may also play important roles to determine resistance or susceptibility to MD as Zhang et al. (2014) reported a significantly differed expression of 34 and 21 miRNA genes between resistant and susceptible lines in the control and MDV challenged groups, respectively.

1.8 MDV life cycle

The well-established 'Cornell Model' (reviewed in Calnek, 2001) describes natural infection with MDV in susceptible chickens in four phases: (1) early cytolytic (2) latent (3) late cytolytic, and (4) transformation. Later, Baigent and Davison (2004) re-described it with some elaborations which are outlined below.

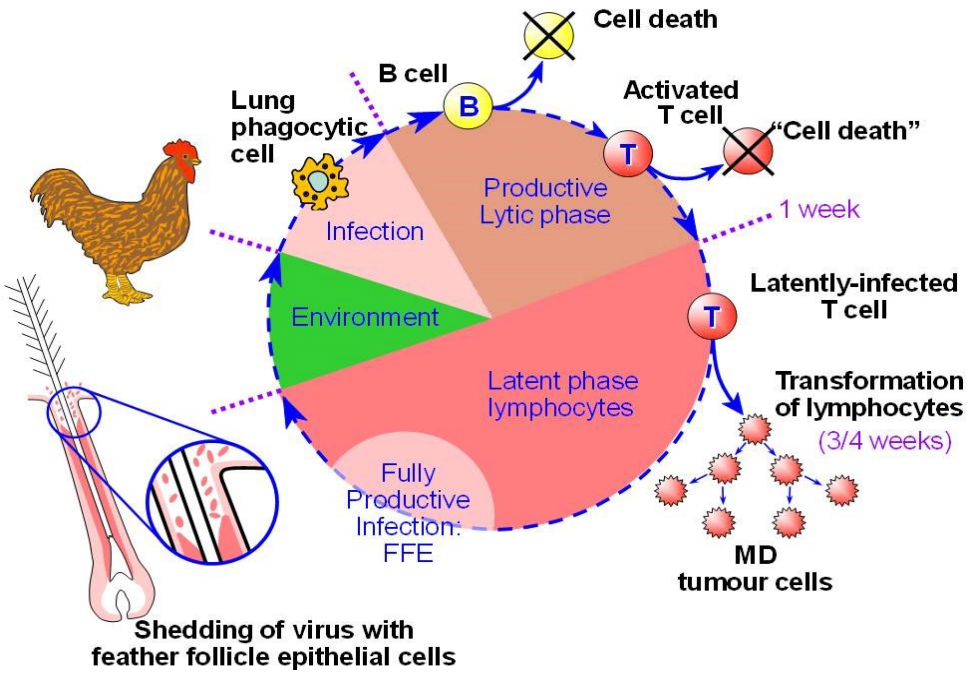

Figure 1.4. *The life cycle of MDV. Picture kindly provided by Prof. Venugopal Nair, The Pirbright Institute.*

1.8.1 Mode of MDV infection

MDV is a highly contagious virus and the natural infection occurs with cell-free virus through the respiratory tract. The FFE is the only site in infected birds where fully productive infection of MDV takes place and infectious, cell-free viruses are shed in the environment. Cell-free MDV can be found in two forms in the poultry dust. In one form, cell-free viruses are mixed with keratin, which are highly infectious but labile, whereas in another form, virus particles remained keratin-wrapped which are less infectious but more stable in the environment and can remain infectious for several months (Carrozza et al., 1973). The MDV-infected poultry dust and dander are inhaled by birds and hence, natural infection occurs.

Following initial infection, MDV is thought to be taken up by macrophages in the respiratory tract (Calnek, 2001). However, the actual site(s) and cellular

mechanism(s) involved with uptake have not yet been clearly identified. Little is also known about host immune responses induced by MDV in lungs.

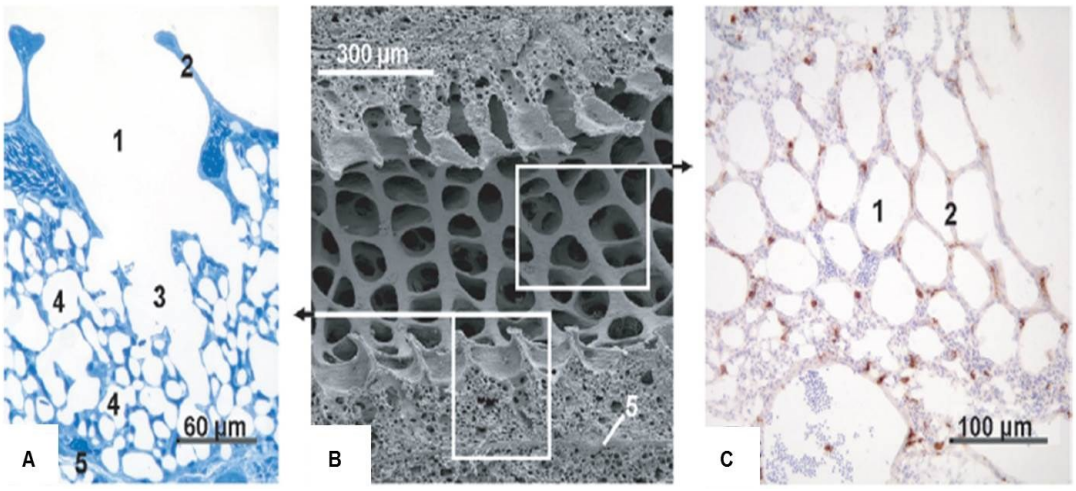

Figure 1.5. *Microscopic section of parabronchus of a chicken lung. (A) Longitudinal section (methylene blue staining) of the parabronchus wall. 1 – atrium; 2 – interatrial septum; 3 – infundibulum; 4 – air capillaries; 5 – interparabronchial septum. (B) Scanning electron micrograph of a parabronchus cut in longitudinal section. (C) Horizontal section of the atria demonstrating macrophages in the interatrial septa by immunohistochemistry (stained with mAb KUL01). Adapted from Reese et al. (2006) with permission from EDP Sciences.*

The avian lung differs significantly from its mammalian counterpart in several ways (reviewed in Reese et al., 2006). Firstly, it differs morphologically as birds use air sacs to ventilate their lungs in the absence of a diaphragm and unlike mammals, the avian lung has unidirectional airflow. The avian lung also lacks alveoli but owns tertiary bronchi or parabronchi which are surrounded by a network of blood capillaries and are considered as the functional units of gas exchange. A microscopic section of the parabronchus is shown in Figure 1.5. A parabronchus is surrounded by the interparabronchial septa (5). Air from the lumen of the parabronchus enters into the atria (1) and by crossing the interatrial septum (2) into the infundibula (3). The

gaseous exchange then takes place in the blood capillaries (4) that surround the infundibulum. The second and most striking difference between the mammalian and avian lungs is immunological as avian lungs do not have draining lymph nodes and also lack alveolar macrophages due to the absence of alveoli. Hence, the avian lungs differ from mammals in terms of immune strategies. Though they have fewer surface (free) macrophages, a large population of sub-epithelial macrophages is present. The lining epithelial cells of atria and infundibula are phagocytic and also a significant number of intravascular macrophages are present in lungs (Maina, 2002).

It is not exactly known whether lung macrophages directly pick up MDV or become infected after an initial round of replication in epithelial cells as seen in the respiratory tract infection with VZV (Varicella Zoster virus) (Zerboni et al., 2014). Abdul-Careem et al. (2009b) reported a significantly increased number of macrophages in lungs of infected chickens compared to uninfected control birds based on an aerosol-based infection model with cell-free MDV via the respiratory route, suggesting a potential role of macrophages at the primary stages of MDV infection.

1.8.2 Early cytolytic phase

Macrophages are not only excellent candidates for transporting MDV to primary lymphoid organs but they can also be cytolytically infected. Barrow et al. (2003) first presented evidence in support of this as viral antigens were identified in the splenic macrophages following MDV infection. However, to date no research has been carried out regarding MDV-DC (dendritic cell) interaction and it is certainly possible that DCs are also infected and transport the virus. From the lungs, MDV is transported to most lymphoid organs, such as the spleen, the bursa of Fabricius,

caecal tonsil, the thymus and the early cytolytic phase of infection is then evident in these tissues with the expression of large amounts of pp38 (MDV early protein) and with the presence of MDV genome, between 1 and 7 days post-infection (dpi) (Schat et al., 1981). During MDV infection, B lymphocytes are cytolytically infected first (Schat, 1981), resting T cells are not, but in turn are cytolytically infected when activated, presumably through the cytolytic infection of the B cells (Calnek et al., 1984b). The cytolytic infection is therefore characterised by lymphocytolysis, resulting in necrosis as well as infiltration of inflammatory cells (Baigent and Davison, 2004).

B cells are the primary targets of acute cytolytic infection and in various lymphoid tissues, almost 90% of cytolytically infected cells are B lymphocytes, with only 3-6% cells being $CD4^+$, $CD8^+$ and $TCR\alpha\beta^+$ T lymphocytes (Baigent et al., 1998). In the spleen, the reason for B lymphocytes to be the main target of cytolytic infection is perhaps the anatomical structure, where B cells are directly surrounded by ellipsoid-associated reticular cells (EARCs). The EARCs are phagocytic and MDV antigens can be detected in these cells (Jeurissen et al., 1989). Though infection of B cells leads to the activation of T cells, B cells are not absolutely required to activate T cells as it was observed in bursectomised chicks that T cells could possibly be directly infected by macrophages (Calnek et al., 1984b).

A microarray analysis revealed an increased expression level (2 to11 fold) of more than 78 MDV genes during the cytolytic infection compared to the latent infection. Of these, pp38, UL49.5, vLIP, US3 and vIL-8 (vCXC) play critical roles in virus pathogenesis (Heidari et al., 2008b). As mentioned above, pp38 is an early protein involved in lytic replication and also plays a role in reactivation from latency (Reddy

et al., 2002; Lee et al., 2005). UL49.5 is a non-glycosylated transmembrane protein involved in down-regulation of MHC class I (Tischer et al., 2002), which is the hallmark of lytic infection (Osterrieder et al., 2006). The MDV genome encodes a secreted glycoprotein, vLIP, with homology to the pancreatic lipases, which forms a covalent bond with lipids and is essential for efficient lytic replication (Kamil et al., 2005). The US3 orthologue of MDV is involved in virus spread and rearrangement of the actin cytoskeleton; and is also essential for growth of some virulent MDV strains (Schumacher et al., 2005).

vIL-8 or vCXC has a significant role during lytic infection as a vIL-8-deleted MDV strain showed decreased level of lytic infection (Parcells et al., 2001), though deletion of vIL-8 could not prevent the virus either from entering latency or to maintain oncogenicity (Cui et al., 2004). However, infection of birds with a mutant MDV strain that lacked secreted vIL-8 but not Meq-vIL-8 splice variants resulted in significantly reduced disease and tumour incidence (Engel et al., 2012). vIL-8 also has a role in recruiting target cells for both lytic and latent infection as it acts as a chemoattractant for B and $CD4^+$ $CD25^+$ T cells *in vitro* (Engel et al., 2012).

The influence of the host immune system may also direct the course of early MDV pathogenesis. Kaiser et al. (2003) reported the role of cytokines during the early stage of MDV infection (between 3 and 10 dpi) in resistant and susceptible lines. Differences between inbred lines were observed for IL-6 and IL-18, with splenocytes from susceptible chickens expressing high levels of both cytokines which might play a role in formation of lymphoma in these birds, while splenocytes from resistant birds did not express any of these cytokines suggesting their role in promoting latency in these chickens. Heidari et al. (2008a) reported a significant up-regulation

of the mRNA expression levels of IL-1β, IL-4, IL-6, IL-10, IL-12p35, and IL-13, IFN-α, IFN-β, and IFN-γ, chicken myelomonocytic growth factor (cMGF), granulocyte-macrophage colony-stimulating factor (GM-CSF), and inducible nitric oxide synthase (iNOS) in the splenic tissues of chickens infected with a vv^+ strain of MDV at 5 days post-inoculation (lytic infection).

1.8.3 Latent phase

Establishing latent infection inside host cells is an innate feature of Herpesviruses. MDV infection shifts from lytic to latent at around 6-7 dpi and a cell-associated viraemia (i.e. latent infection of peripheral blood lymphocytes) can be detected. In contrast to the cytolytically infected cells, the majority of latently infected lymphocytes are T cells with only a smaller proportion of B cells (Calnek et al., 1984b; Morimura et al., 1998). The cell-mediated rather than the humoral immune responses are crucial in the latent phase because the establishment of latency can be delayed by thymectomy but not by bursectomy (Schat et al., 1981).

In the latent phase of infection, the viral genome remains in the host cell with the expression of only a few viral genes. Also there is no production of infectious virus apart from reactivation of virus. Both host determined and viral factors are evident in the switch from cytolysis to latency. However, it is yet to be determined specifically whether host-innate immunity or sequential events during MDV pathogenesis switch the infection from cytolytic to latent phase (reviewed in Nair, 2013).

A lack of expression of pro-inflammatory cytokines, such as IL-6 and IL-18 may contribute to the establishment and maintenance of latency in MD-resistant lines (Kaiser et al., 2003). Soluble mediators like nitric oxide (NO), produced by host macrophages, probably play an important role in the control of MDV replication

(Xing and Schat, 2000), thus creating an environment hostile to the virus which in turn might lead to latency. MDV expresses a number of genes during latency, such as pp14, Meq and latency-associated transcripts (LATs) and also represses the genes from the pp38 family, which in turn play a role in the balance between latent and lytic infections (Parcells et al., 2003). MDV LATs include two small spliced, non-polyadenylated RNAs which are called MDV small RNAs (MSRs) and a 10 kb polyadenylated RNA. The LATs are antisense to the MDV major immediate early regulatory protein, ICP4 (infected cell protein 4), and are thought to interfere with translation of ICP4, suggesting their role in suppression of lytic infection (Cantello et al., 1994; 1997). Among the genes expressed, Meq plays an important role in maintaining MDV latency by blocking the apoptosis of latently infected $CD4^+$ T cells and also by transactivating gene expression (Parcells et al., 2003). Microarray analysis revealed that a 23 kDa nuclear protein, Meq, and RLORF5 were among the few viral genes that were expressed in both lytic and latent phases of infection (Heidari et al., 2008b).

1.8.3.1 Role of MDV microRNAs in latency

MDV miRNAs have a potential role in the induction and maintenance of latency. Burnside et al. (2006) first reported MDV-encoded miRNAs in CEFs infected with a very virulent strain (RB1B). A total of 14 pre-miRNA sequences, producing 26 mature miRNAs, have so far been identified in the MDV-1 genome (www.mirbase.org, v.21). As in other herpesviruses, MDV miRNAs are located in genomic repeat regions. They are located in two major clusters; the first cluster maps to the oncogene Meq, and the second cluster maps ICP4-LAT region (reviewed in Hicks and Liu, 2013).

The functions of most MDV-1 miRNAs are yet to be explored. To date, the well characterized MDV-1 miRNA is miR-M4, an orthologue of host miR-155, located in the Meq cluster (reviewed in Hicks and Liu, 2013). MDV-1-miR-M4-3p acts to maintain latency by down-regulating the production of UL28 and UL32 which are involved in the cleavage or packaging of herpesvirus DNA (Muylkens et al., 2010). MDV microRNAs produced from LAT transcripts may also contribute to establish and/or maintain latency. For example, MDV-1-miR-M7-5p targets MDV immediate-early (IE) genes ICP4 and ICP27 to down-regulate their expression and thus establish latency (Strassheim et al., 2012).

1.8.3.2 Epigenetic regulations of latency

Recent studies suggest that the epigenetic machineries, such as histone modifications and DNA methylation also play a role in maintaining MDV latency. MDV gene expression during latency is mostly restricted to the repeat regions of the viral genome (Sugaya et al., 1990). Meq and several noncoding RNAs, including two miRNA clusters, are expressed from the repeats of the MDV genome during latent infection of T cells. Brown et al. (2012) carried out chromatin immunoprecipitation (ChIP) analysis to identify distinct regions of histone modifications in the viral genome in MDV-transformed T cell lines and revealed the presence of active histone marks, such as H3K9 acetylation and H3K4 trimethylation around the promoters for Meq and the miRNAs, but there were no active histone marks in the lytic origin of replication (OriLyt), suggesting a role for Meq in the epigenetic regulation of the MDV genome repeats. Abundant DNA methylation was also observed across the repeats but that was significantly reduced or absent around the active promoters (Brown et al., 2012). A recent study suggests that DNA methylation in the host might

be associated with disease resistance or susceptibility as DNMT3a and 3b (DNA methyltransferase) were differentially expressed in chicken MD-resistant line (6_3) and MD-susceptible line (7_2) at 21 day post-MDV infection (Tian et al., 2013).

1.8.4 Late cytolytic phase

In the resistant chicken genotypes, latent infection persists at a low level in the spleen and blood lymphocytes without additional effects. However, in susceptible birds, or those infected with a vvMDV pathotype, a second wave of cytolytic infection begins 2-3 weeks after primary infection. It is assumed that the virus is carried to the thymus, bursa and some epithelial tissues, including the FFE, kidney, adrenal gland and proventriculus by latently infected cells, where it becomes reactivated due to a secondary phase of immunosuppression. Reactivation from latency is most likely associated with a significant increase in expression of the lytic protein pp38. Parcells et al. (2003) reported that during reactivation to lytic infection, a number of splice variants of Meq predominate which lack several of the domains important to Meq trans-activation and trans-repression. At this point, a family of genes, including pp38 are expressed from the OriLyt region during early stages of reactivation. Recently, Jarosinski and Du (2014) reported the expression of RLORF4 gene during reactivation, though its precise role is yet to be elucidated. Lymphocytic and epithelial necrosis, associated with marked inflammation, infiltration of mononuclear cells with severe atrophy, is observed in the above mentioned organs in the late cytolytic phase of infection (Baigent and Davison, 2004).

1.8.5 Fully productive infection in the FFE

MDV infects various cell and tissue types but only the skin and associated FFE cells support the production of cell-free, enveloped, fully infectious virus (Calnek et al.,

1970). The virus can be detected in the skin from 10-12 dpi, where it is thought to be carried by latently infected peripheral blood lymphocytes, however Abdul-Careem et al. (2008) reported detecting MDV in the FFE as early as 4 dpi. Lymphoproliferative skin lesions are also associated with the FFE due to virus infection. Induction of host responses against MDV is manifested by the infiltration of inflammatory cells, consisting of lymphocytes and heterophils into the feather pulp region (Moriguchi et al., 1987; Abdul-Careem et al., 2008). Though it is a suitable site for production and release of infectious cell-free virus, no cellular component has been identified so far to be associated with the productive viral replication in the FFE. It is most likely the gradually keratinising cells in the FFE that show less lysosomal activity which perhaps protects the virus from degradation (Baigent and Davison, 2004). The MDV glycoprotein D (gD) (encoded by US6 gene) might also play a crucial role in the production of cell-free virus *in vivo*, as it is expressed only in the FFE (Niikura et al., 1999). The role of gD expression in the FFE is still unclear because the US6 gene is not required for horizontal transmission of MDV (Anderson et al., 1998). The tegument protein VP13/14 (encoded by the UL47 gene) is also highly expressed in the FFE of infected chickens (Jarosinski et al., 2012), though its association with high viral productivity in the FFE has not been investigated. Infected chickens, regardless of their genotypes, shed cell-free virus all through their life spans.

1.8.6 Transformation

The eventual outcome of interaction of MDV with the host cell is the neoplastic transformation of latently infected lymphocytes to lymphoblastoid tumour cells which starts three weeks post-infection. Neoplastic lesions can be found in various visceral organs including spleen, kidneys, gonads, proventriculus and also in nerve

tissues, resulting in blindness, paralysis and mortality (Calnek, 2001). The spleen is likely to be the main, but not only, site for initial proliferation of transformed cells, as neoplastic MD lesions can also be seen in splenectomised birds (Schat, 1981). MDV-infected neoplastic cells show higher expression of a host-encoded extracellular antigen, CD30, which can be identified in the spleen and blood of both resistant and susceptible chickens at the later phase of cytolytic infection (Baigent et al., 1998; Burgess and Davison, 2002). The vast majority (about 75%) of the cells involved in visceral lymphomas are T ($CD4^+$) lymphocytes, whereas only around 15% are B lymphocytes (Payne and Rennie, 1976). This could be because integration of viral DNA into the host cell genome requires cell proliferation; a condition easily fulfilled by the population of activated, latently infected T cells, but perhaps not by the depleting B cells (Baigent and Davison, 2004). Massive proliferation of $CD4^+TCR\alpha\beta^+$ T cells totally replaces normal tissues in susceptible birds and these cells form mature lymphomas by 50 dpi, but in resistant birds $CD8\alpha^+$ T cells prevail and the lesions usually disappear from 30 dpi, accompanied by apoptosis (Burgess et al., 2001).

Immunological mediators, produced by MD tumour cells, may be able to down-regulate immune responses resulting in development of tumour lesions. For example, MD tumour cells can express IL-10 and IL-10R, suggesting a strategy of MDV to evade host response, which suppresses anti-tumour immunity by increasing Treg responses, thereby inhibiting cytotoxic T lymphocyte differentiation and cytokine production (Buza and Burgess, 2007). Based on a proteomic approach, Kumar et al. (2009) demonstrated that MDV-induced tumours are enriched for expression of certain molecules, such as CTLA-4, which could indicate an immune regulatory or

suppressive environment. Among the MDV genes, Meq plays potential roles in transformation of cells *in vitro* (Levy et al., 2005). Various biochemical and genetic studies have revealed that Meq is the principal oncogene of MDV (Parcells et al., 2001). Along with Meq, telomerase RNAs (vTR) and miRNAs also have important roles in MDV oncogenesis.

1.8.6.1 Role of Meq

As mentioned before, the oncogene Meq is unique to MDV-1 and is one of the most widely studied MDV proteins (reviewed in Nair, 2013). The expression of Meq is observed in latency and transformation stages (Qian et al., 1995). Meq is a bZIP protein and to show oncogenic property, Meq needs to dimerize with itself and a number of other bZIP- and non-bZIP proteins (Brown et al., 2006, Reinke et al., 2010). Meq plays an important role in oncogenesis as deletion or mutation of Meq can prevent tumourigenesis. A Meq-deleted mutant of a vvMDV strain of MDV (Md5) did not able to form lymphomas *in vivo* (Lupiani et al., 2004). The non-bZIP interaction of Meq with the CtBP (Carboxyl-terminal binding protein) through the PLDLS (proline-leucine-aspartic acid-leucine-serine) motif was shown to be crucial for the oncogenicity of the virus, as mutations in the CtBP-interaction domain completely eliminated lymphomatosis by MDV (Brown et al., 2006). However, Meq is not exclusively required for the induction of tumours by the virus, as Meq encoding MDV-1 vaccine strains (such as CVI988) cannot induce tumours, though CVI988-encoded Meq proteins are weak transactivators compared to their virulent counterparts (Ajithdoss et al., 2009).

1.8.6.2 Role of MDV telomerase RNA (vTR)

The IR_L-TR_L region of the oncogenic MDV genome encodes a telomerase RNA (vTR) which has a potential role in tumourigenesis (Fragnet et al., 2003). The vTR is a noncoding RNA having structural and functional similarity to the telomerase RNA. The enzyme telomerase is involved in preserving the integrity of chromosomes during the cell cycle by maintaining the length of telomeres (Greider and Blackburn, 1985; Yu et al., 1990). It is presumed that vTR might play a role in the generation of telomeric elongations at the ends of the viral genome which is crucial for integration of MDV genome to the host genome (Morissette and Flamand, 2010). Telomerase is a ribonucleoprotein complex consisting of two essential components: a protein component (TERT), which is essentially reverse transcriptase (Lingner et al., 1997), and an RNA component (TR) which acts as a template for TERT (Greider and Blackburn, 1989; Yu et al., 1990). However, MDV-induced lymphomagenesis does not require the interaction of vTR with the telomerase protein component (TERT) (Kaufer et al., 2010). Shkreli et al. (2007) demonstrated the involvement of c-Myc oncoprotein in the transcriptional regulation of vTR during MDV-induced lymphomagenesis. While an elevated expression of vTR was essential for the induction of tumours (Kaufer et al., 2010), a deletion of vTR substantially reduced the ability to induce T cell lymphomas by MDV (Trapp et al., 2006; Kaufer et al., 2011).

1.8.6.3 Role of microRNAs in MDV oncogenesis

MiRNAs are a key component of MDV pathogenesis especially in the transformation stage. It was reported that MDV1-miR-M4 is the highest expressed miRNA in MD tumours, representing 72% of all MDV miRNAs (Morgan et al., 2008). MiR-M4 is

involved in regulating host genes that are involved in several cellular processes, such as modulation of lymphocyte proliferation and differentiation and regulation of lymphoid-specific transcription (spleen focus forming virus pro-viral integration oncogene spi1 [SPI1]), signifying its role in MDV oncogenesis (Hicks and Liu, 2013). The *in vivo* role of miR-M4 in the induction of lymphoma has also been demonstrated, as viruses deleted in or having a 2-nucleotide mutation in the seed region of miR-M4 failed to induce lymphomas (Zhao et al., 2011). An elevated expression of the MDV-1 miRNAs, miR-M4, miR-M8, and miRM12 was observed in tumour tissues compared to non-tumour tissues in chickens infected with RB1B, suggesting a role for these miRNAs in MDV-induced transformation (Xu et al., 2008). MDV encoded miRNAs are also directly involved in modulating antiviral cellular factors including apoptosis. For example, MDV-1-miR-M3 blocked cisplatin (a chemotherapy drug)-induced apoptosis by down-regulating the protein level expression of Smad2, a crucial element of the TGF-β (transforming growth factor beta) signalling pathway, suggesting a pre-emptive role of this miRNA to create a cellular environment suitable for viral latency and oncogenesis (Xu et al., 2011). Recently, the role of MDV-1-miR-M4-5p in MDV tumourigenesis has been investigated. Luo et al. (2014) identified the latent TGF-β binding protein 1 (LTBP1) as a critical target of miR-M4-5p. Down-regulation of LTBP1 leads to the suppression of TGF-β which in turn activates the expression of c-myc, a well-known oncogene which is crucial for the virus-induced oncogenesis.

1.9 Mode of spread of MDV

MDV entry and exit during *in vivo* infection are mediated by cell-free viruses, but unlike other alphaherpesviruses, MDV remains strictly cell-associated *in vitro* as its

infectivity cannot be recovered from supernatant or even from cell lysates. Moreover, free enveloped infectious virus particles cannot be detected in the culture medium of infected cells, either directly by microscopy techniques or indirectly by infectivity assays, which again strongly supports the theory of high cell-associated nature of MDV in culture (reviewed in Denesvre, 2013). Nevertheless, MDV spreads from cell-to-cell though the exact mechanism(s) is not yet known.

On the basis of morphology and location, all types of intracellular MDV particles, i.e., naked nuclear and cytoplasmic capsids, as well as the primarily and secondarily enveloped virions can be identified, but the number of enveloped virions is very low and cannot be found in all cells (Denesvre, 2013). Moreover, no extracellular virions can be detected, suggesting that MDV is deficient in three crucial steps of herpesvirus morphogenesis: the release from the nucleus, the secondary envelopment, and the exocytosis of cell-free viruses (Denesvre, 2013). Hence, a requirement for cell-to-cell transmission of MDV particles could be predicted.

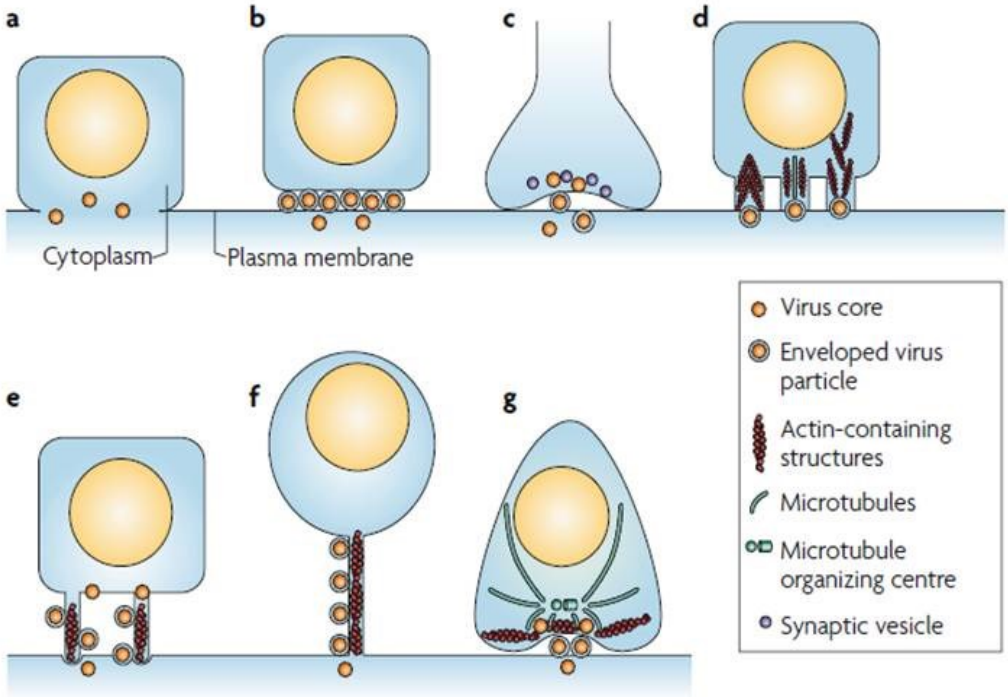

Figure 1.6. *Mechanisms of virus cell-to-cell spread. (a) Cell-to-cell plasma membrane fusion followed by movement of infectious viral material (viral core) into the uninfected target cell. Herpesviruses, paramyxoviruses and retroviruses can spread by cell-cell plasma membrane fusion. (b) Passage of virions across a tight junction. The virus exits basolaterally from an infected cell and is trapped between the infected and uninfected cell membranes at the tight junctions. Virions fuse with and penetrate the uninfected target cell within the tight junctions. Herpesviruses can move across tight junctions. (c) Movement of virions across a neural synapse. Virions either bud through the membrane into the synaptic space or are released from synaptic vesicles into the cleft. Virions then either fuse directly with the opposing synaptic cell or are endocytosed. Rhabdoviruses, herpesviruses and paramyxoviruses move across neural synapses. (d) Viral induction of actin- or tubulin-containing structures. Poxviruses project from infected to uninfected cells using actin tails (left). Herpesviruses can induce actin- and tubulin-containing structures that project virions toward adjacent cells (middle). Afsavirus-induced actin-containing filopodia project virions towards adjacent cells (right). (e) Viral subversion of actin-containing structures. Virus-infected cells stably anchor filopodia that project from uninfected cells, which allows virions to travel from an infected to an uninfected cell in an actin-myosin-dependent manner. Only retroviruses have so far been shown to use this method of spread. (f) Membrane nanotube subversion. Nanotubes can form between immune cells, including myeloid and lymphocytic cells. Nanotubes appear to be continuous with the plasma membrane, contain actin but not tubulin. HIV-1 virions that bud from an infected cell can move along nanotubes and infect distant target cells. (g) Virological synapses. Immune cells are not constitutively polarised, but contain machinery that allows them to polarise their secretory apparatus towards a second cell that is involved in an immunological synapse. This machinery can be subverted by retroviruses so that an infected cell can polarise viral budding towards the receptor-expressing target cell in a structure called a virological synapse. Virions bud from the infected cell into a synaptic cleft, from which they fuse with the target-cell plasma membrane. Adapted from Sattentau (2008) with permission of the Nature Publishing Group.*

Several possible routes were described for the movement of infectious virus particles from cell-to-cell in case of human viruses (Figure 1.6) (Sattentau, 2008), a number of which could potentially be used by herpesviruses. Cell-to-cell communication is essential for the immune system because by establishing intercellular connectivity networks, the cell protrusions may enable immune cells to amplify protective responses without relying on the slower process of diffusion (Watkins and Salter, 2005). However, pathogens may hijack these communication processes to undergo cell-to-cell spread. For example, HIV-1 (human immunodeficiency virus type-1) utilises a specialised area of immune contact known as virological synapse to spread from DCs or macrophages to $CD4^+$ T cells (Fackler et al., 2007). Moreover, like other retroviruses, HIV-1 can use intercellular channels for efficient cell-to-cell transmission (Sherer et al., 2007). Murid herpesvirus-4 (MuHV-4) also induces large-scale cytoskeletal reorganisation in infected myeloid cells (Smith et al., 2007). *In vitro* transmission of MDV in chicken embryo cells requires polymerisation of actin cytoskeleton, but not microtubulin (Schumacher et al., 2005). Denesvre (2013) proposed two hypotheses to explain the cell-to-cell spread of MDV. The first hypothesis suggested the extracellular appearance of a few fully mature virions from infected cells which rapidly enter into adjacent cells most likely at specific cell-cell contacts, a feature which is also followed by the Human T-cell lymphotropic virus type I (HTLV-I) (Majorovits et al., 2008). The second hypothesis proposed that intercellular transmission of virions occurred through direct connections between two cells. However, the author preferred the first hypothesis because intercellular junctions for travelling MDV nucleocapsids of 100 nm or larger in diameter have never been demonstrated before and furthermore, like other herpesviruses MDV

requires gB, gH, and gL (fusion glycoproteins) for replication and cell-to-cell spread (Schumacher et al., 2000; Wu et al., 2001), which also suggests an extracellular state of the virus.

1.10 Host immunity against MD

The outcome of MD is determined not only by the virulence of the virus but also by the result of the complex interaction between the components of host immune systems. Effective immunity to MD requires involvement and a coordinated activity of both the innate and adaptive immunity. These include immune mediators, such as cytokines, soluble factors, antibodies, as well as cells, such as macrophages, natural killer (NK) cells, T helper (Th) cells, cytotoxic T lymphocytes (CTLs) (Baaten et al., 2004). Host immunity to MDV is a complex phenomenon and, though various components of the innate and adaptive immune systems may differ, there is accumulating evidence that both these host responses are in a close and constant interaction in infected birds. Following entry through the respiratory tract, cell-free MDV is most likely picked up by the phagocytic cells, although the actual site(s) and cellular mechanism(s) involved is not yet fully understood. Various receptors, cytokines and cells from the innate and adaptive immune systems play crucial roles during MDV infection.

1.10.1 Receptors

Pathogens of distinct entity have conserved molecular patterns known as pathogen-associated molecular patterns (PAMPs). PAMPs can be of either exogenous or endogenous origin, which includes lipoprotein, peptidoglycan, LPS and pathogen nucleic acids, such as dsRNA, ssRNA and CpG DNA. These PAMPs are recognised by pattern-recognition receptors (PRRs) expressed on a number of cells of the innate

immune system, such as NK cells, macrophages and DCs. Of the various PRRs, TLRs (toll-like receptors) are the best characterised family, though the interactions of TLRs with MDV have not yet been fully investigated. An up-regulation of TLR3 and TLR7 was measured in the lungs of chickens infected with cell-free MDV, presumably expressed by the epithelial cells or macrophages in the lungs (Abdul-Careem et al., 2009b). The mRNA expression level of TLR15 was increased in the spleen of MDV-infected chickens at 4, 14 and 21 dpi and the expression of TLR3 and TLR15 was also up-regulated in MDV-infected bursa at 7 and 14 dpi, respectively (Jie et al., 2013). Recently, a higher expression of TLR3 was observed in CEFs from a resistant line compared to a susceptible line, indicating a role for this gene in exerting resistance to MD (Haunshi and Cheng, 2014). The chicken TLR3 and TLR7 are intracellular receptors that interact with viral dsRNA and ssRNA, respectively (Philbin et al., 2005; Schwarz et al., 2007). TLR15 binds with a variety of ligands including viral CpG (Ciraci and Lamont, 2011). MDV is a dsDNA virus, therefore the correlation between elevated TLRs (3 and 7) and MDV infection needs to be elucidated. However, DNA viruses such as adenovirus, HSV (herpes simplex virus) and vaccinia virus can produce dsRNA during their replication cycles within a few hours of infection (Weber et al., 2006). An up-regulation of MDA-5 (melanoma differentiation-associated gene-5) was also measured in the splenocytes of MDV-infected chickens at 4, 7 and 21 dpi, indicating that MDA-5 might be involved in detecting MDV in chicken (Feng et al., 2013). MDA-5 is another PRR from the RLR (retinoic-acid-inducible-gene-I- (RIG-I-) like receptors)-family which recognises viral dsRNA (Kato et al., 2008).

1.10.2 Role of cytokines

1.10.2.1 Interferons

Like mammals, all the members of type I interferons (IFN) are present in chickens with the exception of IFN-τ (Kaiser, 2010). IFN-α is down-regulated in various Herpesvirus infections (Ambagala and Cohen, 2007; Wu et al., 2009). For example, the mRNA expression level of IFN-α was down-regulated in blood of MD-resistant chickens compared to the susceptible birds from 1 to 7 dpi with either MDV (RB1B strain) or HVT (Quere et al., 2005). The absence of IFN-α transcripts was also reported in the latently infected splenocytes of MDV infected birds (Xing and Schat, 2000). However, Jarosinski et al. (2005) detected an increased expression of IFN-α along with other pro-inflammatory cytokines in the chicken brain, suggesting a crucial role of pro-inflammatory responses in the development of neurological lesions in birds infected with vv^{+}MDV strains. Type I IFNs are also involved in the induction of interferon regulatory factors (IRFs), a family of transcription factors that take part in antiviral defence, cell growth, and immune regulation. Microarray analyses revealed an up-regulation of IRF-1 (Morgan et al., 2001) and IRF-3 (Karaca et al., 2004) in the CEFs infected with MDV and HVT, respectively.

Buscaglia and Calnek (1988) suggested that IFN-γ (type II interferon) might play a role in maintaining MDV latency. However, IFN-γ expression was elevated in the splenocytes of chickens at the cytolytic phase of MDV infection (Xing and Schat, 2000; Djeraba et al., 2002a). Quere et al. (2005) reported a down-regulation of IFN-γ mRNA level in the blood of susceptible but not in resistant lines of chickens at 1 and 7 dpi. A significantly higher expression of IFN-γ transcripts was observed in the feathers of susceptible chickens than those of resistant lines at the early stage of

infection with a virulent MDV strain (JM-16) (Abdul-Careem et al., 2009a). Heidari et al. (2014) also reported an increased mRNA expression level of IFN-γ in the caecal tonsils of MD-susceptible chickens compared to that of resistant line during cytolytic phase of infection. However, Kaiser et al. (2003) did not observe any differential expression of IFN-γ in the splenocytes between resistant and susceptible lines at 3 and 10 dpi. An earlier onset of IFN-γ production along with delayed virus replication was evident in leukocytes of resistant chicken lungs compared to susceptible birds following intratracheal infection with MDV (Baaten et al., 2009). Recently, an up-regulation of the mRNA expression level of IFN-γ was observed in the lung mononuclear cells of chickens infected with RB1B strain of MDV at cytolytic and latent phases of infection (Parvizi et al., 2014).

1.10.2.2 Interleukins

A group of interleukins, including IL-6, IL-10 and IL-18, was up-regulated in MDV infection which was more likely associated with disease development rather than protection from the disease (Abdul-Careem et al., 2007). Kaiser et al. (2003) reported a significant up-regulation of IL-6 and IL-18 in the splenocytes of MD-susceptible chickens, whereas neither of the two transcripts was expressed in resistant lines. Jarosinski et al. (2005) observed an elevated expression of IL-1β, IL-6, and IL-8 in the chicken brain infected with a vv^{+}MDV strain (RK-1). Chickens infected with a vvMDV strain (RB1B) also showed higher expression of IL-6 and IL-18 in their brain tissues (Abdul-Careem et al., 2006). The mRNA expression level of IL-10 was increased in the lung mononuclear cells of chickens infected with RB1B strain of MDV (Parvizi et al., 2014). An up-regulation of IL-6, IL-10, IL-13 and IL-18 mRNAs were observed in the caecal tonsils of MD-susceptible chickens compared to

that of resistant line during cytolytic phase of infection (Heidari et al., 2014). The mRNA expression of IL-6 and IL-8 was increased in CEFs from resistant line than those of susceptible line following MDV infection, suggesting an important role for these cytokines in resistance to MD (Haunshi and Cheng, 2014).

1.10.3 Role of NK cells

NK cells have potent anti-viral activity in the context of herpesvirus infections (Paludan et al., 2011). Sarson et al. (2008a) reported elevated expression levels of cytolytic proteins, granzyme A and NK lysin in MDV-infected birds, suggesting a role of NK cells in the host response in the early stage of MDV infection. An increased cytotoxic activity of NK cells was also observed in MD-resistant and vaccinated chickens compared to MD-susceptible and unvaccinated chickens (Sharma and Okazaki, 1981; Heller and Schat, 1987; Garcia-Camacho et al., 2003). NK cells might also play a role during the transformation phase and can target MD-tumour cells *in vitro* (Quere and Dambrine, 1988). Bumstead (1998) reported that NK cells are also strongly associated with MD-resistance as the MDV-1 locus on chicken chromosome 1 has synteny with the NK-cell receptor locus on mouse chromosome 6 and human chromosome 12.

1.10.4 Role of macrophages

Macrophages play a number of crucial roles in MDV infection (Baaten et al., 2004). They were primarily thought to be the carrier cells that phagocytose MDV and transport it to the lymphoid tissues. Barrow et al. (2003) first showed MDV replication in splenic macrophages *in vivo*, though *in vitro* studies could not mimic this (Haffer et al., 1979; Barrow et al., 2003). Macrophages can produce large quantities of NO (nitric oxide) by the increased activity of iNOS and they have

inhibitory effects on *in vitro* and *in vivo* replication of MD virus in the cytolytic and latent phase of MDV infection (Xing and Schat, 2000; Djeraba et al., 2002a). Furthermore, genetically resistant chickens produce higher levels of NO than susceptible chickens after infection with vMDV (Jarosinski et al., 2002). This is perhaps due to an increased arginase production, which inhibits the iNOS pathway in susceptible chickens (Djeraba et al., 2002b). Higher levels of NO are produced in the infection with vv^{+}MDV strains *in vivo* than infection with vMDV strains, which could initiate NO-induced immunosuppression by prompting apoptosis (Schat, 2004). NO induced apoptosis is thought to be caused by mitochondrial dysfunction (Bustamante et al., 2000). Macrophages, either isolated from MD tumours or stimulated with LPS, are also able to kill MDV-transformed chicken cell-line (MDCC) cells (Sharma, 1983; Qureshi and Miller, 1991).

1.10.5 Role of B lymphocytes and antibodies

B lymphocytes play an important role in MDV infection as indicated by a delay in latency and tumourigenesis in bursectomised birds (Schat et al., 1981). In the acute cytolytic phase of MDV infection, splenic B cells are the primary targets and cytolytic infection of B cells induces activation of T cells (Schat, 1981), which in turn play an important role in the context of cell-mediated immunity against MDV. Shek et al. (1983) also observed that the primary targets of the cytolytic MDV infection were B cells, whereas the subsequent latent infection was found mostly in non-B lymphocytes. A rapid depletion of pulmonary B cells was observed in MD-susceptible chickens which reduced viraemia and substantially affected pathogenesis compared to resistant birds following an intratracheal infection with MDV, suggesting a role of pulmonary B cells as the primary and predominant target cells

during cytolytic phase of MDV pathogenesis (Baaten et al., 2009). A vIL-8 (vCXC) mediated recruitment of B and $CD4^+$ $CD25^+$ T cells was reported as potential targets for both lytic and latent infection, which further demonstrates an important role of B cells in MDV infection (Engel et al., 2012). The exact role of the antibody mediated immune response has not been clearly established in MDV infection as the virus is highly cell-associated. Antibodies are produced against MDV glycoproteins, such as gB, gE, and gI and there is evidence that antibodies play a role in immunity against the virus by neutralizing cell-free viruses, blocking entry of virus into cells, and antibody-dependent cell-mediated cytotoxicity (ADCC) (Kodama et al., 1979). However, maternally derived antibodies (MDA) can play a dual role during infection and vaccination stages. For example, naturally acquired MDA via the egg can delay the progression of clinical MD, provide protection against MD-morbidity and mortality as well as tumour formation (Burgoyne and Witter, 1973; Lee and Witter, 1991). On the other hand, MDA can neutralise cell-free HVT vaccines and thus reduce host immune response to MDV (Calnek, 1972; Sharma and Graham, 1982).

1.10.6 T cells and MDV infection

Although resting T cells are refractory to MDV infection in the cytolytic phase, activated T lymphocytes are the predominant target for latent infection and transformation (Calnek, 2001). The close immunological and anatomical proximity between B and T cells facilitates the spread of MDV to T cells (Baigent and Davison, 2004). Antiviral immunity against MDV is principally mediated by $CD8\alpha\beta^+$ CTLs and $CD4^+$ T helper cells, though it is difficult to demonstrate which subset of T lymphocytes plays the more crucial role, due to the highly cell-associated nature of the virus. However, Morimura et al. (1998) suggested that $CD8^+$ T cells have an

important antiviral effect that controls the course and outcome of MD, as depletion of $CD8^+$ T cells led to higher MDV titres in $CD4^+$ T cells. Omar and Schat (1996) reported the cytotoxic activity of $CD8^+$ T cells against cells expressing immediate-early (ICP4), early (pp38) and late (gB) MDV antigens, whereas no activity of $CD4^+$ and γδ T cells was observed for the elimination of these cells. Other studies have also confirmed the effect of $CD8^+$ CTLs against various MDV glycoproteins (Omar et al., 1998; Markowski-Grimsrud and Schat, 2002). CTL responses may also play a role in genetic resistance to MD. MDV-stimulated splenocytes demonstrated syngeneic cell-mediated immune responses against MDV protein ICP4, only in the MD-resistant MHC haplotype (B21) but not in the susceptible one (B19), suggesting a protective role by inhibiting the secondary cytolytic infection and subsequent lymphoma formation in resistant genotype (Omar and Schat, 1996). Using a microarray approach, Sarson et al. (2006) showed an increased expression of granzyme A and CD8α genes at 7, 14 and 21 dpi, which is suggestive of an up-regulation of CTL activity in infected birds following infection with MDV. Another microarray study (Yu et al., 2011) also showed that the CD8α gene was significantly up-regulated at 10 dpi in the splenocytes of MD-resistant chicken line (6_3), but down-regulated in the MD-susceptible chicken line (7_2). On the other hand, the fold change of CTLA-4 gene was much lower in line 6_3 than in line 7_2 at 10 dpi, indicating a lower level of CTLA-4 could possibly be involved in anti-tumor immune response in resistant chickens (Yu et al., 2011).

1.11 Aims and hypothesis

Resistance to MD in the inbred lines 6_1 and 7_2, in terms of viral load, is established as early as 3 dpi (Burgess and Davison, 2002; Smith et al., 2011). By this time, the

virus has infected APCs (macrophages and/or DCs), B cells and activated T cells. Hence, the resistance mechanisms could be exerted in any or all of these cell types. However, it is still unclear at what stage of infection and in/or by which immune cells those resistance mechanisms or genes are expressed. Therefore, the overall aim of this study is to explore the cellular basis of resistance to MD by developing a new *in vitro* MDV infection model.

Though the *in vivo* infection of MDV in macrophages has been reported previously (Barrow et al., 2003), *in vitro* MDV infection of macrophages or DCs has not been established yet. In fact, several previous *in vitro* attempts with macrophages derived from blood and bone marrow were not successful (Haffer et al., 1979; von Bulow and Klasen, 1983; Barrow et al., 2003) and this led to the belief that MDV-macrophage infection absolutely requires *in vivo* conditions (Barrow et al., 2003). Therefore, the foremost aim is to set up an *in vitro* MDV infection model of APCs which will eventually bring the opportunity to study the cellular basis of resistance in MD resistant (6_1) and susceptible (7_2) chickens. Macrophages and DCs will be cultured from the chicken bone marrow to establish the model. Macrophages will be cultured with CSF-1 (Garceau et al., 2010), whereas DCs will be cultured with recombinant chicken cytokines, IL-4 and GM-CSF (CSF-2) (Wu et al., 2010).

In vitro infection of B and T lymphocytes with MDV-infected CEFs has been established (Calnek et al., 1984a; Kaspers, 2014). It remains to be established if the virus infection can be transmitted from APCs to these cells *in vitro*. B and T lymphocytes will be isolated from spleen rather than bursa or thymus as MDV is first carried to the spleen *in vivo*, presumably by lung phagocytes (macrophages and/or DCs). T lymphocytes will be activated by a suitable mitogen, e.g. ConA.

The *in vitro* model system will be established first in outbred chickens, using cell (CEF)-associated recombinant GFP-MDV. The model will be developed in several steps. In the first step, cell-associated MDV will be co-cultured with macrophages and DCs. Infected cells will be separated from uninfected ones using flow cytometry based on the presence of GFP-MDV. The aim of this step is to measure and characterise the potential *in vitro* MDV-APC infections.

In the second step, infected APCs will be co-cultured with B and activated T cells with the aim to establish the transmission of MDV infection from APCs to lymphocytes. Infected and uninfected lymphocytes will then be characterised.

In the third step, once the *in vitro* model is established with cells from outbred birds, the model will be repeated with the cells from the inbred resistant (6_1) and susceptible (7_2) chickens. Following infection, infected and uninfected cells will be sorted by fluorescence-activated cell sorter (FACS). The complete transcriptome of infected vs. uninfected sorted cells from each line will then be sequenced by RNA-Seq, and compared to identify signatures of expression associated with infection and with resistance. The events of differential viraemia (Burgess and Davison, 2002) and gene expression profiles (Smith et al., 2011) occur at the very early stages of infection in these two lines, suggesting that the differences between lines 6_1 and 7_2 are due to innate rather than an adaptive host immune responses (Bumstead and Kaufman, 2004). Therefore, in this study the hypothesis is that transcriptional signatures pre- and post-infection *in vitro* of APCs from the two inbred lines will indicate the gene(s) and possible mechanism(s) involved in resistance or susceptibility to MD.

Chapter 2:

Materials and Methods

2.1 Bacterial techniques

2.1.1 Bacterial strains

E. coli strains JM109 (Promega) and DH5α (Invitrogen), were routinely used for propagation of plasmids and BACs (Bacterial Artificial Chromosome).

Chromosomal genotype of JM109: *end*A1 *rec*A1 *gyr*A96 *thi hsd*R17 (rk^-, mk^+) *rel*A1 *sup*E44 D(*lac-pro*AB) [F´*tra*D36 *pro*AB *laq*I^qZΔM15].

Chromosomal genotype of DH5α: F^- Φ80*lac*ZΔM15 Δ(*lac*ZYA-*arg*F) U169 *rec*A1 *end*A1 *hsd*R17 (rk^-, mk^+) *pho*A *sup*E44 λ^- *thi*$^-$1 *gyr*A96 *rel*A1.

2.1.2 Preparation of bacterial glycerol stocks

Bacterial strains containing plasmids of interest or BAC DNA were stored in glycerol at -80ºC. A bacterial glycerol containing MDV BAC DNA was kindly provided by Dr. Bob Dalziel (The Roslin Institute). A single bacterial colony was used to inoculate 3 ml of LB medium containing the appropriate antibiotics (see section 2.1.3). Cultures were incubated overnight at 225 rpm in an orbital shaker at 37ºC until the culture had an absorbance reading of OD_{600} 0.6. 850 µl of culture were mixed with 150 µl sterile glycerol in a 1.8 ml screw-cap cryovial (Thermo FisherScientific, UK) and incubated on ice for 2 h before storage at -80ºC.

2.1.3 Bacterial culture

E. coli strains were grown in Luria Broth (LB) medium or on LB plates with 1.5 % (w/v) agar (see Appendix 1). Autoclaved solid agar was broken up using a sterile pipette and melted, followed by cooling to 56ºC in a pre-heated water-bath for at least 1 h to ensure the agar was not too hot to deactivate the antibiotics added subsequently. LB agar was supplemented with the appropriate antibiotic and poured into 10 cm diameter petri dishes. Ampicillin (100 µg/ml) and chloramphenicol (20

μg/ml) (Sigma, UK) were used to propagate *E. coli* containing plasmids and BACs, respectively. Bacteria were plated onto LB agar by streaking with a sterile plastic loop and incubated inverted, overnight at 37ºC. A single colony was isolated from glycerol stocks and inoculated into 5 ml of LB medium supplemented with the selective antibiotic. This starter culture was incubated at 37ºC for 5-6 h in an orbital shaker at 225 rpm. 2.5 ml of the starter culture were used to inoculate 200 ml of LB medium, supplemented with the appropriate antibiotic, in a sterile 500 ml Erlenmeyer flask. The culture was incubated overnight at 225 rpm in an orbital shaker at 37ºC.

2.1.4 Plasmid DNA extraction

An Endofree Plasmid Maxi Kit (Qiagen, UK) was used for large-scale isolation of plasmid DNA. Details of the buffer compositions are given in Appendix 1. The procedures were carried out according to the manufacturer's instructions. Liquid bacterial cultures were incubated overnight at 37ºC in an orbital shaker (section 2.1.3). On the following day, bacteria were harvested by centrifugation at 6000 *g* for 20 min at 4ºC. The bacterial pellet was resuspended in 10 ml buffer P1, before being lysed by the addition of 10 ml lysis buffer P2 with vigorous inversion. The mixture was then incubated at room temperature (RT) for efficient lysis to take place. The lysis reaction was stopped by the addition of 10 ml chilled buffer P3, mixed thoroughly by vigorously inverting the sealed tube 4-6 times and centrifuged at 1500 *g* for 10 min. Addition of buffer P3 enhanced the precipitation of genomic DNA, proteins and cell debris which were removed by passing the lysate through a QIAfilter Cartridge. 2.5 ml buffer ER were then added to the filtered lysate, mixed

by inverting the tube approximately 10 times, and incubated on ice for 30 min to remove the endotoxin.

Meanwhile, a QIAGEN-tip 500 was equilibrated by applying 10 ml of buffer QBT. The filtered lysate was then applied to the column and allowed to drain through the QIAGEN-tip. The ER-treated plasmid solution passes through the column by gravity flow and plasmids bind to the column. The flow through was discarded and the column was washed twice with 30 ml wash buffer QC. Plasmid DNA was eluted using 15 ml of Buffer QN. To precipitate the plasmid DNA, 10.5 ml RT isopropanol were added to the elution solution, mixed by inversion and centrifuged immediately at 3220 *g* for 60 min at 4ºC. The pelleted DNA was washed with 5 ml of endotoxin-free RT 70% ethanol. The sample was centrifuged again at 3220 *g* for 10 min, the supernatant was removed and the pellet was redissolved in 200 µl TE buffer after air drying and stored at -20ºC.

2.1.5 BAC DNA extraction

BAC DNA extraction was performed using a NucleoBond® BAC 100 Kit (Macherey-Nagel GmbH, Germany). Buffer compositions are documented in Appendix 1. Bacteria were harvested from LB culture by centrifugation at 6000 *g* for 15 min at 4ºC. Supernatants were discarded and the bacterial cell pellet was resuspended in buffer S1 containing RNase A. Resuspended cells were lysed by adding lysis buffer S2 and incubated at RT for 2-3 min. Pre-cooled neutralisation buffer S3 was added to the suspension, mixed immediately by inverting the tube 6-8 times until a homogenous suspension containing an off-white flocculate was formed and incubated on ice for 5 min. In the meantime, a NucleoBond BAC 100 column was equilibrated using buffer N2 and the bacterial lysate was cleared by loading it

through a NucleoBond Folded Filter placed in a funnel of appropriate size. BAC DNA binding to the column was carried out by allowing the column to empty by gravity flow. The column was then washed twice with buffer N3 and the flow-through was discarded. DNA was eluted with pre-heated buffer N5 and subsequently precipitated by centrifuging at 3220 *g* for 60 min at 4ºC after adding RT isopropanol. Pelleted DNA was washed with RT 70% ethanol and centrifuged at 3220 *g* for 30 min at 20ºC. The ethanol was removed carefully and the pellet was allowed to dry at RT for 15-20 min. DNA was reconstituted by dissolving the pellet in 150 µl sterile nuclease-free H_2O.

2.2 Cell culture work

2.2.1 Common reagents for cell culture

Cell culture media were purchased from Gibco Life Technologies (Paisley, UK) or Sigma-Aldrich (Poole, UK). Supplementary components for optimal cell growth, such as 100× penicillin-streptomycin (pen-strep) containing 5000 U of penicillin and 5 mg of streptomycin per ml, 100× L-glutamine (200 mM), 100× non-essential amino acids (NEAA), 100 mM sodium pyruvate, foetal bovine serum (FBS, EU approved, South American origin), chicken serum (CS, New Zealand origin), 2.5% trypsin and 1× versene were all purchased from Gibco Life Technologies. Heat-inactivated FBS, specifically for macrophage cultures, was purchased from PAA Laboratories. 0.4% Trypan-blue solution was obtained from Sigma-Aldrich. FBS (Gibco) and CS were thawed and incubated at 56ºC for at least 1 h in a water-bath for heat-inactivation.

2.2.2 Growth and maintenance of COS-7 cell line

COS-7 cells (an African green monkey kidney cell line) were cultured in Dulbecco's Modified Essential Medium (DMEM) (Gibco, UK), supplemented with 10% (v/v) FBS (Gibco), 1% (v/v) L-glutamine and 1% (v/v) NEAA. Cells were maintained in T_{75} tissue culture flasks (ThermoFisher Scientific, UK) and grown in a 37ºC incubator with 5% CO_2. Cell monolayers were split every three to four days. Confluent cells were rinsed once with 10 ml PBS followed by addition of 5 ml trypsin (2.5%)/versene solution (1:9) per flask and then incubated at 37ºC for 4-5 min. The effect of trypsin was neutralised by adding 10 ml complete DMEM per flask and centrifuged for 5 min at 500 *g* to pellet cells in a bench-top centrifuge. Supernatant was discarded, the cell pellet resuspended in 10 ml DMEM and live cells counted using a haemocytometer (20 µl cell suspension and 20 µl trypan blue solution). Viable cell numbers were calculated using the following equation:

$$\text{Cells/ml} = \frac{\text{Number of viable cells in middle 25 squares (haemocytometer)}}{} \times 10^4 \times \text{dilution factor}$$

A density of 7.5×10^5 cells was used to seed each T_{75} flask for routine growth while, for transfection purposes, the concentration was 6×10^6 cells per flask in 12-15 ml media.

2.2.3 Transfecting COS-7 cells for the expression of recombinant cytokines

COS-7 cells were transfected with the mammalian expression vector pCI-neo (Promega, UK) containing the gene of interest (IL-4 or CSF-2) and pTARGET (Promega, UK) containing CSF-1, for high level, transient expression. Plasmid DNAs were extracted previously (section 2.1.4). Transfection was performed using a

diethylaminoethyl (DEAE)-dextran/DNA method. On the day before transfection, 6×10^6 cells were seeded per T_{75} flask and incubated at 37°C with 5% CO_2. Once cells were ready for transfection, a DNA/DEAE complex was prepared as follows: 15 ml of serum-free DMEM was added to a Universal and 150 µl chloroquine (10 M), 112.5 µg plasmid DNA and 90 µl DEAE/dextran were added into the medium sequentially. The DNA/DEAE complex was added to the flask after washing the cell monolayer twice with PBS and incubated for 3-3.5 h at 37°C with 5% CO_2. Following incubation, the complex was removed and the cells were washed once with PBS. 10% dimethyl sulfoxide (DMSO) in PBS was added to the flask and kept at RT for 2 min. This was then removed and replaced with 15 ml DMEM containing 10% FBS and incubated for 16-24 h at 37°C with 5% CO_2. Medium was changed to serum-free medium after incubation. Supernatants were harvested on day 3 post-media change by removing supernatant to a Universal and centrifuging at 200 *g* for 5 min to pellet cell debris. Supernatants, containing recombinant cytokine, were stored at 4°C.

2.2.4 Chickens

The outbred vaccinated chickens used in this study were Brown Leghorn J line birds, bred and reared in the poultry unit of The Roslin Institute. The unvaccinated inbred line 6_1 birds were bred in the Poultry Production Unit at the Institute for Animal Health, Compton, UK and reared in the poultry unit of The Moredun Research Institute, while unvaccinated inbred line 7_2 chickens were hatched and reared at The Roslin Institute's poultry unit.

2.2.5 Generation of chicken bone marrow-derived dendritic cells (BMDC)

Dendritic cells (DCs) were cultured following procedures described in Wu et al. (2010). Femurs and tibia from 3 to 6 week-old birds were removed using sterile instruments, after the birds were killed by cervical dislocation, and submerged in phosphate-buffered saline solution (PBS) on ice until use. Both ends of the bones were cut with scissors and each end was flushed with pre-warmed PBS with a 0.45 mm diameter needle (21 G). Cells were washed once in PBS, pelleted by centrifugation and then resuspended in PBS. The cell suspension was then loaded onto Histopaque 1077 (Sigma-Aldrich) and centrifuged for 25-30 min at 1200 *g* with the brakes off. Cells from the interface were removed using Pasteur pastettes and washed twice in PBS. Cell numbers and viability were assessed with a haemocytometer and trypan blue staining (section 2.2.2). The cell concentration was then adjusted to 1×10^6 cells/ml with pre-warmed complete RPMI-1640 medium (Sigma-Aldrich) containing 10% heat-inactivated CS, 1% L-glutamine and 0.1% pen-strep. Recombinant chicken interleukin-4 (chIL-4) and granulocyte-macrophage colony stimulating factor (chCSF-2) were added to the culture medium. A 1:285 dilution of each cytokine was found to be sufficient for optimal DC growth after testing a series of different dilutions. Cells were seeded in 6-well plates (3 ml/well) and incubated at 41°C with 5% CO_2. On day 2 and 4 of culture, three-quarters of the media were replaced with fresh pre-warmed complete RPMI-1640 media containing cytokines.

2.2.6 Generation of chicken bone marrow-derived macrophages (BMDM)

Leg bones (femurs and tibia) from 3 to 6 week-old birds were removed and processed to isolate cells as in the previously described method (Wu et al., 2010). For flow cytometric analysis, cells were cultured at a final concentration of 1×10^7 cells/15 ml in Sterilin non-compartmentalised (single-square) tissue culture plates (Thermal Scientific, UK) with pre-warmed RPMI-1640 complete medium containing 10% FBS (PAA), 1% L-glutamine and 0.1% pen-strep. Cells were also seeded at 1×10^6 cells/well of Sterilin compartmentalised (25-square) plates (Thermal Scientific, UK) specifically for TaqMan qRT-PCR experiments. ExCOS-7 cell culture supernatant containing recombinant chCSF-1 (2.5%) was added to the culture medium. Cells were incubated at 41^{o}C with 5% CO_2. The medium was replaced with fresh, pre-warmed complete RPMI-1640 medium containing CSF-1 on day 2 and 5 of culture. On day 7 of culture, cells were used for further studies.

2.2.7 Stimulation of DCs and macrophages with lipopolysaccharide

To induce maturation, cultured DCs were stimulated with lipopolysaccharide (LPS: 200 ng/ml, Sigma-Aldrich) on day 6 of culture for 24 h, while macrophages were stimulated on day 7 of culture with LPS (100 ng/ml) for the time-point mentioned above by replacing old culture media with fresh medium containing no cytokines.

2.2.8 Phagocytosis assay

This assay was used to determine whether cultured macrophage-like cells are phagocytic, by their ability to engulf fluorescently labelled, heat- or chemically-killed yeast particles (*Saccharomyces cerevisiae*), called zymosan particles (Invitrogen, UK). The procedure was as follows. On day 7 of culture, the culture

media were replaced with fresh media containing zymosan bioparticles (at a ratio of 50 particles per cell) after washing with pre-warmed PBS. The cells were then incubated at 41ºC, 5% CO_2 for 1 h to allow particle uptake by the cells. Ice-cold PBS was used to stop phagocytosis and then the cells were washed four times with cold PBS. Fresh media were added into wells before the cells were examined under a fluorescence microscope.

2.2.9 Culturing BMDM and BMDC in T_{75} flasks

Sterilin single-square plates were found to be unsuitable for culturing CEFs and co-culturing of CEFs and DCs could not be achieved in 6-well plates as these plates could not accommodate required numbers of CEFs. Thus, both macrophages and DCs were cultured in T_{75} flasks for subsequent co-culturing with CEFs. Bone marrow cells were collected and processed as described previously (Wu et al., 2010) and cells were resuspended in appropriate cell culture medium and cytokines for macrophages (section 2.2.6) and DCs (section 2.2.5). Cells were seeded at a concentration of 1.3×10^7 cells/12 ml for macrophages and 1.6×10^7 cells/13 ml for DCs per flask as repeated trials, in both cases, revealed that it had been possible to harvest around 1×10^7 cells from this amount of seeded cells. Cultured cells were incubated at 41ºC with 5% CO_2 for 4 days and then harvested using 100 mM EDTA (section 2.4.3.2). Phenotypic expression of various molecules in these cells was examined by flow cytometry before infecting with MDV.

2.2.10 Collection and culture of chicken embryo fibroblasts (CEFs)

Fertile eggs from Brown Leghorn chickens were incubated at 37.5ºC with 40-50% humidity for up to 9-11 days. Chicken embryos were collected aseptically by breaking egg shells and decapitation was carried out as soon as possible. Portions of

the limbs, wings and visceral organs were also removed. The embryo bodies were then chopped into pieces, 4 to 5 were pooled and placed into a 15 ml Falcon tube containing 1× trypsin-EDTA (Sigma-Aldrich). The tissues were then incubated for 15 min at 37°C for proper digestion with vigorous shaking after every 5 min. The digestion process was stopped by adding M-199 medium (Gibco) containing 10% FBS (Gibco). Cells were pelleted by centrifugation at 500 *g* for 8 min and resuspended with pre-warmed complete M-199 medium containing 10% (v/v) tryptose phosphate broth (Invitrogen), 2.7% (v/v) $NaHCO_3$ (Sigma-Aldrich), 5% (v/v) FBS (Gibco), 1% (v/v) pen-strep, 0.5% (v/v) gentamycin and 0.001% (v/v) fungizone (amphotericin B, 250 µg/ml) (Thermo Scientific). Complete CEF media were prepared using a range of FBS concentrations (0.5% to 10%), which were used for maintenance and vigorous proliferation of cells, respectively. CEFs were seeded in T_{175} flasks at a concentration of 1.7×10^7 cells per flask and then incubated at 38.5°C with 5% CO_2. Once confluent, cells were harvested by trypsinisation. Cell monolayers were rinsed with 10 ml PBS followed by addition of 6.5 ml trypsin/PBS (1:7.5) per flask and then incubated at 37°C for 6-8 min. Trypsin digestion was stopped by adding 10 ml M-199 medium containing 10% FBS. Harvested cells were pelleted by centrifuging at 500 *g* for 5 min. Pelleted cells were counted using a haemocytometer (section 2.2.2), resuspended in freezing medium and stored at -80°C (section 2.2.11).

2.2.11 Preparation of cells for long-term storage

For CEFs and COS-7 cells, confluent cell monolayers were harvested with trypsin/PBS (section 2.2.10) and counted as described previously (section 2.2.2). The cells were pelleted by centrifugation at 500 *g* for 5 min and resuspended in 1 ml of

freezing medium (95% v/v FBS, 5% v/v DMSO). COS-7 cells were resuspended at a concentration of 5×10^6 cells per ml. CEFs were resuspended at a concentration of 2×10^7 cells per ml. For macrophages and DCs, following Histopaque 1077 centrifugation, cells from the intermediate layer were collected, washed twice with PBS and centrifuged at 500 *g* for 5 min. Pelleted cells were resuspended in freezing media containing 1 volume FBS (Gibco) and 1 volume of 80% RPMI-1640, 20% DMSO. Cells were aliquoted into cryovials, a total of 5×10^7 cells were resuspended per vial. Cryovials were then wrapped with cotton wool, kept in a polystyrene box containing RT isopropanol and frozen at -80ºC for 24-48 h. Samples were transferred into boxes previously kept at -80ºC or in liquid nitrogen for long-term storage.

2.2.12 Resurrection of cells from frozen stocks

Recommended media were pre-warmed to 37ºC. Cryovials were removed from liquid nitrogen and kept on ice until ready to thaw. Cells were thawed rapidly in a 37ºC water bath and transferred immediately to a Universal containing 10 ml of the appropriate culture medium. Cells were pelleted by centrifuging at 500 *g* for 5 min, resuspended in 10 ml of fresh medium and transferred to culture flasks or plates, depending on the experiment. Resurrected cells were always counted prior to culture and usually $6\text{-}8\times10^6$ CEFs were seeded in an T_{75} flask (12-15 ml media), while the numbers were $10\text{-}12\times10^6$ CEFs per T_{175} flask in complete M-199 media (32-35 ml) (section 2.2.10).

2.2.13 Transfection of BAC DNA into CEFs using lipofectamine

Lipofectamine™ 2000 (Invitrogen) mediated transfection of CEFs with MDV BAC DNA was carried out using the 'reverse transfection' method described by Morgan et al. (1990). According to this method, DNA was introduced to CEFs at the seeding

stage, rather than once the CEF monolayer was formed. CEFs, previously stored at -80°C, were cultured in T_{75} flasks at 6-8×10^6 cells/flask 3-4 days prior to transfection. On the day of transfection, 1 µg of BAC DNA (section 2.1.5) was made up to 100 µl in volume with Opti-MEM® reduced serum medium (Gibco, UK) for each well of a 6-well plate and 5 µl of lipofectamine were mixed with 95 µl of Opti-MEM medium in a separate tube. The DNA and lipofectamine samples were then mixed and incubated for 45-60 min at RT. During this incubation, CEFs were removed from the T_{75} flask using trypsin/EDTA and resuspended in 10 ml of Opti-MEM after pelleting cells by centrifugation. A cell count was carried out as described previously (section 2.2.2). For each well, the DNA:lipofectamine solution was diluted in 600 µl Opti-MEM and the total 800 µl of BAC DNA:lipofectamine was mixed with 1×10^6 CEF cells. The DNA:lipofectamine:CEF complex was then made up to 3 ml with Opti-MEM and added to one well of a 6-well plate. Seeded plates were incubated at 38.5°C with 5% CO_2. Culture media were changed from reduced-serum Opti-MEM to pre-warmed 8% CEF media after 7 h. Depending on the confluency of cells, media were changed to pre-warmed CEF media containing 0.5-5% FBS the following day.

2.2.14 Co-culturing macrophages with MDV-infected CEFs in Sterilin single-square plates

On day 4 of macrophage culture in Sterilin single-square plates, cells were infected with virus infected CEFs (section 2.2.15) at the MOI of 0.1.

The optimum level of infection was determined by this formula:

Number of cells to be infected × MOI/ titre of virus.

Here, MOI represents multiplicity of infection which is determined by the number of viruses or plaques (pfu) used to infect a single cell. For example, if 1 plaque per cell is added, the MOI is 1.

For 1×10^7 macrophages, 5 ml of cell-associated MDV were added to the culture plate with a total 15 ml of co-culture media (section 2.2.15) and incubated at 41°C with 5% CO_2.

2.2.15 Co-culturing antigen-presenting cells (APCs) with infected CEFs in T_{75} flasks

Due to the cell-associated nature of MDV, to infect APCs infected CEFs were used in co-culture with the previously cultured chicken bone marrow-derived APCs (macrophages and DCs) in T_{75} flasks. Co-culture infection procedures were carried out using either virus-infected whole CEFs or with pre-sorted infected CEFs. On day 4 of culture, APCs were infected with a range of infected CEFs ($2\text{-}5\times10^6$ for sorted cells or 1×10^7 for whole CEFs). One flask of uninfected CEFs were also grown and added to one flask of macrophage or DC culture on the day of infection as control during cell sorting experiments. Co-culture medium was RPMI-1640 containing 2-10% FBS (Gibco), 1% pen-strep and 1% L-glutamine. Medium for DCs was also supplemented with 5% CS. Depending on the experiments, co-cultured cells were incubated at 41°C with 5% CO_2 for 1, 3 or 5 days post infection (dpi) and then harvested (section 2.4.3.2) for downstream experiments, such as flow cytometry or cell-sorting analyses.

2.2.16 Isolation and culture of chicken splenocytes

The spleen was removed aseptically in PBS, after killing the bird by cervical dislocation, and mashed through a 70 μm cell strainer using the end of a syringe

plunger. The single cell suspension was then transferred into a 20 ml Universal, avoiding any large clumps of tissue, and allowed to settle. In a 50 ml Falcon tube, 10 ml Histopaque 1077 were added and the cell suspension was slowly pipetted into the tube to form a discrete layer above the Histopaque. The cells were then centrifuged at 400 *g*, with brakes off, for 20 min at RT. After centrifugation, cells were taken off from the density gradient interface and washed by pelleting the cells twice with PBS. Cells were seeded in T_{75} flasks at 2.5×10^7 cells/flask after resuspending in complete RPMI-1640 medium containing 10% FBS, 5% CS, 1% pen-strep and 1% L-glutamine, and incubated at 41ºC with 5% CO_2. Cells were then harvested by pipetting and resuspended in FACS buffer (PBS containing 1% BSA (bovine serum albumin) and 0.1% sodium azide).

2.2.17 Co-culturing splenocytes with MDV-infected CEFs

To determine if MDV infection could be transmitted from CEFs to B and T lymphocytes, splenocytes were co-cultured with MDV-infected CEFs. Lymphocytes were isolated from the spleen using methods described previously (section 2.2.15). Infected CEFs were also harvested and sorted on the same day (section 2.4.3.1). RPMI-1640 containing 10% FBS, 5% CS, 1% pen-strep and 1% L-glutamine was used for co-culturing and infection occurred in T_{75} flasks at a 1:5 ratio (2.5×10^7 lymphocytes were infected with 5×10^6 MDV-infected CEFs). On 2 dpi, cells were harvested by pipetting and analysed by flow cytometry (section 2.4.2).

2.2.18 Co-culturing B lymphocytes or splenocytes with MDV-infected macrophages

MDV-infected macrophages were co-cultured either with splenocytes or pre-sorted B lymphocytes to explore transmission of virus infection from macrophages to B or T

cells. B lymphocytes were sorted from the spleen using an AutoMACS Pro Separator (section 2.4.4) and mixed with MDV-infected macrophages. Macrophages, infected with GFP-MDV-CEFs, were sorted on 3 dpi as described in section 2.4.3.2 and mixed with B cells or with splenocytes at infection ratios of 1:5 to 1:20 (infected macrophages:B cells or splenocytes). Cells were placed in 6-well plates (for macrophages and B cells/splenocytes) or in T_{75} flasks (for macrophages and splenocytes) in RPMI-1640 containing 20% FBS, 5% CS, 1% pen-strep and 1% L-glutamine, and incubated at 41ºC with 5% CO_2. The culture medium was supplemented with CSF-1 (1:25).

To infect positively sorted B cells, 2×10^6 B lymphocytes were co-cultured with 1×10^5 pre-sorted MDV-infected macrophages at an infection ratio of 1:20 (infected macrophages: positively sorted B cells). Cells were placed in 6-well plates, incubated at 41ºC with 5% CO_2 for 2.5 days. On the other hand, 2.5×10^6 negatively sorted B cells were co-cultured with 0.5×10^6 pre-sorted MDV-infected macrophages at an infection ratio of 1:5 (infected macrophages:negatively sorted B cells) in 6-well plates and incubated at 41ºC with 5% CO_2 for 1 day.

While infecting splenocytes in 6-well plates, 2.5×10^6 splenocytes/well were infected with 0.5×10^6 pre-sorted infected macrophages, and in T_{75} flasks, 2.5×10^7 splenocytes were infected with 5×10^6 pre-sorted MDV-infected macrophages. In both cases, the infection ratio was 1:5 (infected macrophage:splenocyte).

2.2.19 Re-infection of CEFs with infected macrophages

In vivo MDV-macrophage infection was previously reported as a possible abortive infection (Barrow et al., 2003). Freshly cultured CEFs were co-cultured with MDV-infected macrophages to determine if this was the case. CEFs were cultured in 6-well

plates at 5-7×10^5 cells per well with 7-8% CEF media 2-3 days prior to addition of MDV-infected macrophages. In parallel, newly-isolated macrophages were infected with GFP-MDV-CEFs. On day 3 post-infection, infected macrophages were sorted and added to the freshly cultured CEFs with co-culture medium (3 ml/well) (section 2.2.14) containing 0.5-1% FBS and CSF-1 (40 µl/ml). Cells were incubated at 41ºC with 5% CO_2. Transmission of virus infection was explored by observing fluorescence plaques formed in the CEF monolayers.

2.3 Virus growth and propagation

2.3.1 Virus

The virus, CVI988 UL41 (Rep) GFP (R), used in this study was generated from a BAC construct of vaccine strain CVI988 (Rispens) of MDV serotype 1, in which the UL41 gene was replaced with GFP (green fluorescent protein). This was a kind gift from Dr. Bob Dalziel (The Roslin Institute). This mutant strain was constructed as part of a PhD project, the aim of which was to identify an MDV vector that could deliver influenza antigens to poultry, thus stimulating both humoral and cellular immune responses (Wasson, 2011). Previously, a MDV CVI988 BAC had been constructed to allow genes of interest to be inserted or deleted using mutagenesis (Petherbridge et al., 2003). The viral host shut-off (VHS) gene, UL41, was then identified as a non-essential gene to be replaced by the gene of interest. A UL41 deletion mutant replicates as well as the parental strain *in vitro* (Gimeno and Silva, 2008). Thus, the non-essential gene UL41 was replaced with the GFP gene, inserted into the MDV genome by BAC mutagenesis in the 'reverse' orientation (R) (Wasson, 2011).

2.3.2 Preparation of cell-associated MDV master stocks

CEF cells, transfected with MDV BAC DNA (see section 2.2.13), formed plaques after 5-7 days, displaying the cytopathic effect of MDV infection. The entire cell monolayers of three wells of a 6-well plate were removed using 750 µl of trypsin/versene solution (1:9) per well. The infected cells were resuspended in 10 ml of 5% CEF medium after centrifugation at 500 *g* for 5 min. The supernatant was discarded and the pellet was resuspended in 10 ml pre-warmed 5% CEF media. Cryovials containing CEF cells, stored at -80ºC, were removed and kept on ice until ready to thaw. The cells were thawed rapidly in a 37ºC water bath, transferred to a Universal containing 10 ml of pre-warmed 5% CEF media and pelleted by centrifugation at 500 *g* for 5 min. Pelleted cells were resuspended in 10 ml of fresh 5% CEF media, counted and 6-8×10^6 cells were transferred to each T_{75} flask. Ten ml of infected CEFs were transferred to the flask, which was then incubated at 38.5ºC with 5% CO_2.

Flasks were observed daily until extensive cytopathic effect was seen, after approximately 4-5 days. The infected cell monolayers were removed using trypsin/PBS as described previously. The cells from each T_{75} flask were resuspended in 10 ml 5% CEF media and pelleted by centrifugation at 500 *g* for 5 min. Cryovials containing CEF cells were removed from the -80ºC freezer (section 2.2.11) and kept on ice until ready to thaw. The cells were thawed rapidly in a 37ºC water bath and transferred to a Universal containing 10 ml of pre-warmed 5% CEF media. Cells in Universals were pelleted by centrifugation at 500 *g* for 5 min. Pelleted cells were resuspended in 10 ml of fresh 5% CEF media, counted in a haemocytometer and 8-10×10^6 cells were transferred to a labelled T_{175} flask (ThermoFisher Scientific, UK).

Infected cells from each T_{75} flask, as well as 25 ml pre-warmed 5% CEF media, were transferred to each T_{175} flask. Flasks were incubated in a 38.5°C incubator with 5% CO_2. Once extensive cytopathic effects (CPE) were visible, the infected cell monolayers were removed using trypsin/PBS and pelleted by centrifugation at 500 *g* for 5 min. Pelleted cells in each T_{175} flask were resuspended in 2 ml freezing media and aliquoted into cryovials (200-400 µl/cryovial). All cryovials were stored at -80°C.

2.3.3 Infection of CEFs with MDV for plaque assays

Previously stored CEFs (section 2.2.11) were cultured in 6-well plates at $5\text{-}7\times10^5$ cells/well with 5-7% complete M-199 medium (section 2.2.10) and grown to confluence in 2-3 days. The cells were then infected with stock GFP-MDV (100 µl) in a serial dilution from 10^{-1} to 10^{-6}.

CEF cells, infected with MDV UL41 GFP R, developed focal CPE, also referred to as plaques, which consist of rounded, highly refractile cells, after 3-4 days. Cells were washed twice with PBS and fixed in ice-cold acetone: methanol for 2 min at RT. Fixatives were removed and 1 ml blocking buffer (CAS-Block, Invitrogen, UK) was added per well to block any non-specific binding. Plaques were then stained using diluted primary antibody HB3 (500 µl/well), specific for the MDV glycoprotein B (gB), and incubated at RT for 1 h. Cell monolayers were washed three times with 0.05% PBST (PBS and Tween-20) following incubation and the secondary antibody (rabbit anti-mouse IgG conjugated with horseradish peroxidase) was added (500 µl/well) and incubated again at RT for 1 h. Cell sheets were briefly washed three times with PBST and then combined with the specific developing solution, 3-amino-9-ethylcarbazole (AEC) (Sigma-Aldrich), and incubated at RT

until the colour developed. Red-colour plaques were visualised under an inverted microscope and counted on the day of staining.

2.3.4 Growth and storage of MDV working stocks

To prepare working stocks of MDV, CEFs were seeded in T_{175} flasks at a concentration of $1.1\text{-}1.2\times10^7$ cells/flask with 35 ml 8-10% complete CEF media in the 38.5^{o}C incubator with 5% CO_2. On day 2 of culture, when cells were 80-90% confluent, the cells in each flask were infected with 400 µl of stock virus (section 2.3.2) with 0.5% 35 ml CEF media. Cells were incubated for 48 h and then harvested using trypsin/PBS as described previously (section 2.2.10). Harvested cells from each flask were pooled together, resuspended in 5% complete CEF media and reseeded in an equal number of T_{175} flasks containing 35 ml 5% CEF media. Reseeded cells were incubated for a further 48 h and then harvested with trypsin/PBS, resuspended in freezing media, aliquoted (250-500 µl/cryovial) and stored at -80^{o}C as described previously (section 2.2.11).

2.3.5 Improvement of virus titre

MDV-infected CEFs were grown in large numbers and then pooled together to obtain a high virus titre. In two separate experiments, six and twelveT_{175} flasks of CEFs were grown and infected with MDV as described previously (section 2.3.4). Once plaques formed, cells were harvested using trypsin/PBS (section 2.2.10). Cells from six T_{175} flasks were pooled into one tube and resuspended in 2 ml freezing medium and stored at -80^{o}C (section 2.2.11). Cells in the second experiment, with twelve T_{175} flasks of infected CEFs, were also treated as described above. Plaque assays for the virus stock from both the experiments were carried out according to procedures in section 2.3.3.

2.3.6 Culture and growth of viruses from working stock for the infection of APCs

Infected CEFs were grown and then sorted by FACS on the day they were to be used to infect macrophages and DCs. CEFs were cultured in T_{175} flasks for 6 days prior to the day of sorting at a concentration of $1.1\text{-}1.2\times10^7$ cells/flask with 35 ml 8-10% CEF media and then infected with 250 µl of working virus on day 2 of culture. Virus-infected CEFs were passaged to an equal number of flasks on day 4, after harvesting with trypsin/PBS as described in section 2.2.10. On day 6, cells were harvested and prepared for sorting (section 2.4.3.1). CEFs were also seeded at $6\text{-}7\times10^6$ cells/flask and then infected with stock MDV (100 µl/flask) while culturing them in T_{75} flasks for specific experiments.

2.3.7 Preparation of cell-free MDV stock

Due to problems in the co-culture experiments with cell-associated MDV, an attempt was made to isolate a stock of cell-free MDV preparation as per methods used to prepare cell-free murid herpervirus 4. To do this, twenty T_{175} flasks of GFP-MDV-infected CEFs were grown in complete M-199 medium as described in section 2.3.5. Once CPE were observed, medium from each flask was removed and the cells washed with 10 ml PBS. The cell monolayer was disrupted in PBS by pipetting up and down and collected in a 50 ml Falcon tube. The samples were centrifuged at 350 *g* for 10 min at 4ºC and the supernatants were discarded. Cell pellets from all tubes were pooled together and resuspended in 6 ml of suspension buffer (SPGA-EDTA buffer + 10% sorbitol) (Appendix 1). The cell pellet was then homogenised with a sterile dounce 25-30 times. The cell suspension was transferred to a sterile glass Universal and sonicated in an ice bath for 4 min. After sonication, the cell suspension

was poured into 1.5 ml Eppendorf tubes and centrifuged at 8000 *g* for 1 h at 4ºC. Supernatants were collected in a Universal and kept on ice. The pellets were resuspended with suspension buffer, and homogenised again in the dounce with further centrifugation as described above. Supernatants were collected, pooled with the previous ones, aliquoted at100 µl into cryovials and stored at -80ºC.

2.3.8 Infection of macrophages with cell-free MDV

Macrophages were grown in Sterilin compartmentalised (25-square) plates at 1×10^6 cells/well as described in section 2.2.6. On day 4, culture medium was removed from each well. Cell-free virus was thawed and 200 µl virus was mixed with 1 ml co-culture medium (section 2.2.14) added per well and incubated at 41ºC with 5% CO_2.

2.4 Immunofluorescence techniques

2.4.1 Antibodies

Antibodies used in this study are shown in Table 2.1.

2.4.2 Flow cytometry

Depending on the experiment, cultured cells were harvested at different days of culture, stained with various antibodies to bind cell surface antigens and then analysed by flow cytometry to confirm their identity as immune cells.

Cells were harvested with vigorous pipetting when cultured in 6-well plates or square plates and with 100 mM EDTA while cultured in T_{75} flasks (section 2.4.3.2). Harvested cells were pelleted by centrifugation at 500 *g* for 5 min and then resuspended in FACS buffer. Cells were counted and adjusted to $1\text{-}2\times10^6$ per 100 µl, plated at 100 µl/well in a U-bottomed 96-well plate and pelleted by centrifugation at 250 *g* for 2 min. Supernatants were discarded. The antibodies were diluted in FACS

Antigen	Species	Clone/ Subclass	Conjugate	Dilution	Company/ Provider
chMHC II	Mouse	2G11/ IgG1	FITC	1:500	SouthernBiotech
chMHC II	Mouse	2G11/ IgG1	-----	1:500	The Pirbright Institute
chCD40	Mouse	AV79/ IgG2a	-----	1:500	Serotec
chCD11	Mouse	8F2/IgG1	-----	1:500	University of Munich
chBu-1	Mouse	AV20/ IgG1	-----	1:250 and 1:1000	SouthernBiotech
chCD3	Mouse	CT-3/ IgG1		1:250 and 1:1000	SouthernBiotech
Chicken monocyte/macrophages	Mouse	KUL01/ IgG1	-----	1:250	SouthernBiotech
Chicken monocyte/macrophages	Mouse	KUL01/ IgG1	FITC	1:500	SouthernBiotech
chCD45	Mouse	AV53/ IgG1	-----	1:250	The Roslin Institute
ovNKp46	Mouse	Gr 13.1/ IgG1	-----	1:4	The Roslin Institute
boCD8	Mouse	ILA 105/ IgG2a	-----	1:5	The Roslin Institute
mIgG	Goat	Polyclonal	FITC	1:500	SouthernBiotech
mIgG1	Goat	Polyclonal	Alexa Fluor 647	1:500	Invitrogen
MDV gB	Mouse	Monoclonal	-----	1:100	The Roslin Institute
mIgG	Rabbit	Polyclonal	HRP	1:100	Dako
mIgG	Goat	Polyclonal	Microbeads	Neat	Miltenyi Biotec

Table 2.1. *Antibodies used in this study. Ch: chicken; ov: ovine; bo: bovine; m: mouse.*

buffer and 50 µl per well of primary mAb added to the wells, mixed thoroughly on a plate shaker and incubated on ice for 20 min.The cells were pelleted as before and washed twice with 100 µl FACS buffer. Secondary Abs (conjugated with different fluorescent dyes) were added to wells (50 µl/well) and incubated on ice for 20 min. The cells were pelleted again and the cell pellet washed once as before. The cells in

each well were then resupended in 100 µl FACS buffer, transferred to a FACS tube (12×75 mm polypropylene tube (BD Falcon, UK)) and topped up to 500 µl with FACS buffer. The cell viability dye, 7-AAD (7-aminoactinomycin D) (Life Technologies), was added occasionally at 5 µl per tube to allow exclusion of dead cells from the analysis. The cells were analysed by flow cytometry using a FACSCalibur instrument (BD Biosciences). Viable cells were gated based on 7-AAD staining and the resulting data were analysed with FlowJo software.

2.4.3 Cell sorting by FACSAria™ III cell sorter

2.4.3.1 Harvesting CEFs and preparation for sorting

CEFs were grown in T_{175} flasks and infected with GFP-MDV. On the day of APC infection, CEFs were harvested by trypsinisation. After removing medium from each flask, cell monolayers were washed once with 10-12 ml PBS. Then 6.5 ml of trypsin/PBS (1:7.5) was added to each flask and incubated at 37^{o}C for 6-8 min. Following incubation, 10 ml M-199 medium containing 10% FBS were added to each flask to stop the digestion process. Harvested cells were pelleted by centrifugation at 500 *g* for 5 min. The cell pellets were resuspended in cell sorting buffer (PBS and 1% BSA) and staining procedures were carried out with primary (mouse anti-chicken CD45) and secondary antibodies (goat anti-mouse IgG1 conjugated with Alexa Fluor 647), respectively, as described in section 2.4.2. Prior to the sort, antibody-stained cells were passed through a 70 µm cell strainer to prevent clogging of cells in the nozzle of the cell sorter and flow-through fluids were then collected in sterile FACS tubes. 500 µl of co-culture media (section 2.2.14) were taken into each 15 ml Falcon tube to collect the sorted cells. A total of 2.5×10^{6} sorted

cells was collected in each 15 ml Falcon tube and cell sorting analyses were done using FACSDiva v 6.1.3 software.

2.4.3.2 Harvesting macrophages and DCs and preparation for sorting

Both macrophages and DCs were harvested following the same procedures. After washing the cell monolayers once with 10 ml PBS, 5 ml of 100 mM EDTA (1 ml 0.5 M EDTA and 4 ml PBS) were added to each T_{75} flask and incubated at 41ºC for 10-12 min. Cells were collected in a 50 ml Falcon tube after incubation and remaining adherent cells were harvested using a cell scraper. Cells were then pelleted by centrifugation and stained with primary and secondary antibodies as previously (section 2.4.2) and prepared for sorting (section 2.4.3.1).

2.4.4 B-cell sorting by AutoMACS

Magnetically-labelled splenic B lymphocytes were sorted either positively or negatively with an AutoMACSPro Separator (Miltenyi Biotec). An aseptically collected spleen was mashed in PBS and passed through a 70 μm cell strainer. Red blood cells were separated using Histopaque 1077 by centrifugation at 400 *g* for 25-30 min. Cells from the interface were collected carefully with Pasteur pastettes and washed twice with PBS. For positive B cell sorting, cells were stained with primary antibody, mouse anti-chicken Bu-1 (1:1000), while for negative sorting, cells were stained with anti-CD3 (1:1000) and incubated on ice for 20 min. Following incubation, the cells were washed once with AutoMACS Pro running buffer, stained with goat anti-mouse IgG microbeads, mixed well and incubated for 45 min on ice. Cell separation was then performed with an AutoMACS Pro Separator into collection tubes (15 ml Falcon tubes).

2.5 Molecular techniques

2.5.1 Extraction of RNA

RNA extraction was carried out using RNeasy Mini Kits (Qiagen, UK). Buffer compositions are listed in Appendix 1. Target cell pellets were lysed with 350 µl buffer RLT, mixed with 1 volume of 70% ethanol and transferred to RNeasy mini columns. Columns were centrifuged for 30 s at 8000 *g* and the flow-through was discarded. 700 µl of wash buffer RW1 were added to the column, centrifuged at 8000 *g* for 30 s, and the flow-through discarded. The column was then washed twice with 500 µl buffer RPE, which includes centrifugation and discarding the flow-through as above. RNeasy spin columns were then placed in new 2 ml collection tubes and centrifuged at 10000 *g* for 1 min. RNA was eluted in fresh 1.5 ml low retention collection tubes (Sigma-Aldrich) by adding 30-70 µl RNase-free H_2O to the column and centrifugation at 8000 *g* for 1 min.

2.5.1.1 DNase treatment of RNA

Ambion Turbo DNA-free Kits (Life Technologies) were used to remove contaminating genomic DNA from RNA derived from virus infection experiments. Details of the buffer compositions are given in Appendix 1. A 0.1 volume of 10× Turbo DNase buffer and 1 µl Turbo DNase were added to the previously extracted RNA (section 2.5.1) and mixed gently. The mixture was incubated at 37ºC for 20-30 min. DNase inactivation reagent (0.1 volume) was added after incubation, mixed well and incubated at RT for 5 min with occasional mixing. DNase-treated RNA was then collected in a fresh tube by centrifuging at 10000 *g* for 1.5 min.

2.5.2 Quantification of nucleic acids

DNA and RNA concentrations were determined with a NanoDrop Nd-1000 spectrophotometer (ThermoFisher Scientific) at absorbances of OD_{260} and OD_{280}. TE buffer for plasmids, nuclease-free H_2O for BAC DNA and RNase-free H_2O for RNA were used as negative controls.

For RNA-Seq, RNA samples were also quantified precisely using the Qubit RNA Assay Kit with the Qubit 2.0 Fluorometer (Invitrogen). The kit contents are listed in Appendix 1. Qubit working solutions were made by diluting the Qubit RNA reagent 1:200 in Qubit RNA buffer. Each standard tube (1 and 2) contained 190 µl of Qubit working solution and 10 µl of Qubit RNA standard. Each sample tube consisted of 199 µl of Qubit working solution and 1 µl of RNA sample. The solutions in assay tubes were mixed by vortexing for 2-3 s, incubated at RT for 2 min and then read on the Fluorometer. The RNA concentrations were calculated using the following equation: concentration of sample = QF value × (200/x); where 'QF value' is the value given by the Qubit 2.0 Fluorometer and 'x' is the number of microliters of sample added to the assay tube.

2.5.3 Reverse transcription of RNA

Superscript III reverse transcriptase (Invitrogen, UK) was used for reverse transcription of RNA. As per the manufacturer's instructions, extracted RNA (5-12 ng) was mixed with 1 µl of oligoDT (50 µm), 1 µl of dNTP mix (10 mM) and made up to 13 µl with sterile, nuclease-free H_2O. The mixture was heated to 65^{o}C for 5 min and then chilled rapidly on ice for 1 min. The contents were then collected by brief centrifugation and 4 µl 5× First strand buffer, 1 µl 0.1 M Dithiothreitol (DTT), 1 µl RNasin and 1 µl Superscript III reverse transcriptase were added to the mixture.

After a brief vortex and centrifugation, the samples were incubated at 50°C for 1 h, followed by 70°C for 15 min. The cDNA samples were stored at -20°C.

2.5.4 Real-time quantitative RT-PCR analysis

Total RNA from cells was extracted using RNeasy Mini kits (Qiagen). Cytokine mRNA expression levels were assessed using TaqMan real-time quantitative RT-PCR (qRT-PCR) by a well-described method (Kaiser et al., 2000; Kaiser et al., 2003; Wu et al., 2010). Primers and probes used in this study for cytokines and 28S RNA-specific amplification are given in Table 2.2. All probes were labelled with the fluorescent reporter dye 5-carboxyfluorescein (FAM) at the 5′ end and the quencher N,N,N,N′-tetramethyl-6-carboxyrhodamine (TAMRA) at the 3′ end. QRT-PCR was performed using the TaqMan Fast Universal PCR master mix and one-step RT-PCR master mix reagents (Applied Biosystems, Cheshire, UK).

RNA target	Probe/primer sequence (5'-3')
28S	Probe (FAM)-AGGACCGCTACGGACCTCCACCA-(TAMRA)
	F GGCGAAGCCAGAGGAAACT
	R GACGACCGATTTGCACGTC
IL-6	Probe (FAM)-AGGAGAAATGCCTGACGAAGCTCTCCA-(TAMRA)
	F GCTCGCCGGCTTCGA
	R GGTAGGTCTGAAAGGCGAACAG
IL-18	Probe (FAM)-CCGCGCCTTCAGCACGGATG-(TAMRA)
	F AGGTGAAATCTGGCAGTGGAAT
	R ACCTGGACGCTGAATGCAA

Table 2.2. *Primers and probes for TaqMan qRT-PCR. F: forward primer; R: reverse primer.*

Amplification and detection of specific products in a 10 µl reaction were performed using the 7500 Fast Real-Time PCR System with the following cycle conditions: one cycle of 48°C for 30 min, one cycle of 95°C for 20 s, 40 cycles of 95°C for 3 s, and

40 cycles of 60ºC for 30 s. Quantification of mRNA was based on the increase in fluorescence detected by the 7500 Fast Sequence Detection System as a result of hydrolysis of the target-specific probes by the 5′ exonuclease activity of the DNA polymerase during PCR amplification. The passive reference dye, 6-carboxy-c-rhodamine, was used for normalisation of the reporter signal. Variations in sampling and RNA preparation for the C_t values for each cytokine or chemokine were normalized using the C_t value of the 28S rRNA product for the same sample (C_t indicates threshold cycle value - the cycle at which the change in the reporter dye passes a significance threshold). Standard plots of C_t against $\log_{10}$ [RNA] were obtained for all genes including 28S RNA. Normalized C_t values were calculated by the formula: $C_t + (N'_t - C'_t) * S/S'$, where N'_t is the mean C_t for 28S RNA among all samples, C'_t is the mean C_t for 28S RNA in the sample, S and S' are the slopes of the regressions of the standard plots for the cytokine mRNA and the 28S RNA, respectively. Results are expressed as 40-C_t to get the actual C_t value by deducting each threshold cycle value from the total number of cycles (40).

2.5.5 Polymerase Chain Reaction

Polymerase Chain Reactions (PCRs) were performed on a Mastercycler Thermo cycler (Eppendorf, UK). Recombinant *Taq* DNA polymerase (Invitrogen) was used in all the PCR reactions. Primers used in this study are listed in Table 2.3. Primers were designed using Primer 3 software and supplied by Sigma.

According to the manufacturer's instructions, the reaction mixtures for pp38, gB and L-Meq contained 5 µl 10× PCR buffer minus Mg^{2+}, 2 µl 50 mM $MgCl_2$, 1 µl 10 mM dNTP mixture, 1.5 µl 10 µM forward primer, 1.5 µl 10 µM reverse primer, 0.8 µl *Taq* polymerase (5 Units/µl), 2 µl cDNA template and H_2O to 50 µl. For ICP4, the

mixtures contained 5 µl 10× PCR buffer minus Mg^{2+}, 1.5 µl 50 mM $MgCl_2$, 1 µl 10 mM dNTP mixture, 1 µl 10 µM forward primer, 1 µl 10 µM reverse primer, 0.6 µl *Taq* polymerase (5 Units/µl), 2 µl cDNA template and H_2O to 50 µl. Cycling conditions were: denaturation at 95ºC for 3 min, then amplification with 30 cycles of 94ºC for 1 min, 59ºC for 1 min, and 72ºC for 30 s. The PCR was extended for 6 min at 72ºC, and PCR products were stored at 25ºC if used on the same day or at -20ºC for later use.

Primers	Sequence (5'-3')	Ensembl Accession No.
ICP4 F	GGTGATCCTGGCCTTGTAAA	M75729
ICP4 R	TGGGTGGATTTAATGGGAGA	
pp38 F	GCTAACCGGAGAGGGAGAGT	M73484
pp38 R	TCCGCATATGTTCCTCCTTC	
gB F	CCGCTCTGTGTTTCCGTATT	AY129968
gB R	CTTGACTGGAAGGCTTGCTT	
L-Meq F	GTCGACTTCGAGACGGAAAA	AB033119
L-Meq R	GCAGCTCTTCACATGCTTCA	

Table 2.3. *Primers used for PCR.*

2.5.6 Agarose gel electrophoresis

DNA analyses were carried out using agarose gel electrophoresis. PCR products up to 50 µl were mixed with 5-8 µl 6× DNA loading dye (Thermo Scientific) (see Appendix 1) and loaded into 2% (w/v) agarose gels with 5 µl SYBR® Safe DNA gel stain (Invitrogen) placed in a horizontal tank containing Tris-Acetate EDTA (TAE) buffer (see Appendix 1). Electrophoresis was performed at 400 mA and 140 V/cm^2. The size of the DNA products was estimated by comparing with a GeneRuler DNA ladder mix (Thermo Scientific). Following the run, gels were visualised on a UV transilluminator and photographed.

2.6 Imaging and Image processing

2.6.1 Live cell confocal microscopy

Infected and uninfected cells were sorted and then examined under a confocal microscope to reveal the detailed morphology of macrophages and DCs on day 3 post-MDV infection. Prior to the sort, cells were stained with CD45 as per methods described in section 2.4.3.2. After sorting, cells were centrifuged at 1200 *g* for 5 min at 4ºC and then resuspended in 1 ml co-culture media (section 2.2.14). Resuspended cells were placed in sterile chamber slides mounted on borosilicate cover glass (Nunc, ThermoFisher Scientific, USA) and incubated at 41ºC for at least 2 h. Once settled, cells were examined under a Zeiss LSM710 confocal microscope and images were taken. Captured images were then analysed with Zen2011 image processing software.

2.6.2 Time-lapse confocal video microscopy

Video microscopy was carried out to explore the possible mode(s) of virus infection of macrophages on the day of MDV infection. Cells, after processing as described in section 2.2.6, were cultured in sterile chamber slides, at a concentration of 1×10^6 cells/chamber, and infected on day 4 by addition of 1×10^5 sorted infected CEFs/chamber. Following infection, cells were placed under a Zeiss LSM710 confocal microscope maintaining proper culture conditions with photos captured every 10 s. Pictures from an approximately 10 min long experiment were combined to create a movie.

2.7 Statistical analysis

All data were checked for normality and pairwise statistical comparisons between means in three groups (control, infected and uninfected) of the two inbred chicken

lines (6_1 and 7_2) were carried out with a General linear model with Tukey (95% confidence interval) and the mean difference of infected macrophages between the two inbred lines during cell sorting experiments was measured with 2-sample T-test (95% confidence interval) using Minitab 16 software (State College, USA). Statistical significance was determined as $p<0.05$.

2.8 RNA-Sequencing (RNA-Seq)

2.8.1 Cells and sample preparation

BMDM and BMDC from inbred chicken lines 6_1 and 7_2 were infected with pre-sorted MDV-infected CEFs as described previously (section 2.2.15). The infection ratio for macrophages was 1:5 (CEF:macrophage) for cell-sorting experiments on 1 dpi and for DCs it was 1:2.5 (CEF:DC). Following infection, infected, uninfected and control APCs were sorted at 1 dpi (details in Chapter 5, section 5.6). RNAs were extracted from all groups of cells (section 2.5.1) and DNase treatments were carried out (section 2.5.1.1).

RNA quantification was carried out using a Qubit RNA Assay Kit (section 2.5.2). A total of 24 RNA samples (infected and control APCs) from 1 dpi were sent for the RNA to be sequenced.

2.8.2 Library preparation and sequencing

RNA sequencing was carried out by Edinburgh Genomics facility (The Roslin Institute). Samples were prepared for mRNA sequencing using total RNA following the Illumina TruSeq RNA Sample Preparation v2 kit protocol. Resulting libraries were quality checked on an Agilent DNA 1000 bioanalyzer (Agilent Technologies, South Queensferry, UK) and then clustered onto a paired end flow cell using the Illumina TruSeq Rapid PE Cluster Kit at a 8 pM concentration. 100 cycle paired-end

sequencing was carried out on an Illumina HiSeq 2500 using an Illumina TruSeq Rapid SBS Kit (Illumina, Little Chesterford, UK). The Illumina HiSeq 2500 platform generated 16.7 -100.2 million RNA-Seq read-pairs per sample, with each read 125 nucleotides in length, resulting in around 75 GB of data.

Raw sequencing data were processed with the software CASAVA 1.8. The quality of the RNA-Seq reads was evaluated using the software FastQC. Adapter sequences were trimmed with using the software Cutadapt and data were provided as FASTQ files.

2.9 Analysing data to reveal differential gene expression

Trimmed reads were analysed with the help of an expert bioinformatician (Richard Kuo, The Roslin Institute) to explore the differentially expressed (DE) genes in MDV-infected and control APCs. The data analysis pipeline included the following steps.

2.9.1 Mapping reads to the reference genome

The short reads were aligned to the chicken genome sequence (Galgal4, Ensembl release 78). The procedures included analysis of data using Bowtie and TopHat. Bowtie (v1.0.0) is an ultrafast short-read aligner that employs a Burrows-Wheeler index and a full-text minute-space (FM) index. Reverse permutation of the characters in text, as in the Burrows-Wheeler algorithm, was applied in Bowtie to allow the large sequencing data to be searched efficiently while keeping the memory footprint small. The FM index is the exact-matching algorithm and Bowtie used two extensions to allow the sequencing errors or genetic variations to be matched. Bowtie formed the basis for analysing data in TopHat.

TopHat (v2.0.13) is a script that aligns RNA-Seq reads to the chicken reference genome in order to identify exon-exon splice junctions. Bowtie cannot align reads that span introns. TopHat was created to address this issue of large gaps in alignments. It uses Bowtie as an alignment tool and breaks up reads into smaller pieces called segments. Many of these segments align contiguously which results in build-up of an index of splice junctions. The goal of mapping was to create an alignment file, also known as a Sequence/Alignment Map (SAM) file for each of the samples that contained, among other details, one line for each of the reads in the sample denoting the reference sequence to which it maps, the position in the reference sequence, and a Phred-scaled quality score of the mapping (Li et al., 2009).

2.9.2 Counting reads using HTSeq-count

Following alignment of the RNA-Seq reads, the data were translated into a quantitative measure of gene expression by counting the number of reads that map to each gene. Reads aligned to annotated coding regions of the chicken reference genome were summarised using HTSeq-count, a tool developed with HTSeq that pre-processes RNA-Seq data for differential expression analysis by counting the overlap of reads with genes (Anders et al., 2015).

2.9.3 Analysis using edgeR

Following summarisation of the total number of reads per gene, the differential gene expression was analysed using the software package edgeR (empirical analysis of digital gene expression in R). edgeR is designed for the analysis of replicated count-based expression data (Robinson and Smyth, 2007; 2008). Differentially expressed genes (DE genes) were filtered at an FDR (False discovery rate) of 0.05.

2.10 Functional analysis of DE gene sets

2.10.1 Analysis with DAVID

DE significant ($p<0.05$) gene lists were submitted to DAVID (Database for Annotation, Visualization and Integrated Discovery) software package version 6.7 (http://david.abcc. ncifcrf.gov/). The analysis classification stringency was set to high level and the resulting annotation clustering was then limited to an enrichment score of >1.00 and FDR for multiple testing was performed by the Benjamin and Hochberg method invoked within DAVID (Huang et al., 2009).

2.10.2 Data analysis using Pathway Express

To determine which biological pathways were involved with genes differentially expressed pre- and post-MDV infection, the Pathway Express software within the Onto-Tools suite (http://vortex.cs.wayne.edu/projects.htm) was used. Genes differentially expressed in the control and MDV-infected APCs ($p<0.05$) were analysed against a reference list of genes. Annotation was based upon the equivalent human genes. In this programme, the analysis was created upon the KEGG (Kyoto Encyclopedia of Genes and Genomes) pathways (Kanehisa and Goto, 2000) and it displayed the altered expression patterns of genes in biological pathways compared to a relevant control. The impact factor analysis included the classical statistics as well as other crucial factors such as the magnitude of each gene's expression change, its type, position and interactions in the given pathways. Significance was determined using the gamma p-value, which is the p-value provided by the impact analysis. Gene networks involved in a particular experimental condition were established using pathway diagrams.

2.10.3 Ingenuity pathway analysis (IPA)

The IPA programme (Ingenuity Systems - http://www.ingenuity.com/) was used to reveal which canonical pathways were inherent in the control APCs and which were switched on following MDV infection in the host. The log p-value was calculated using the right-tailed Fisher Exact Test with a threshold level >1.3 ($p<0.05$). Canonical Pathways can be defined as idealised or generalised pathways that represent common properties of a particular signalling module or pathway.

2.10.4 Analysis using the Expander programme

Genes highly expressed in each of the APC groups in the resistant (6_1) and susceptible (7_2) lines were clustered by similar expression patterns and analysed for enriched gene ontology (GO) terms and transcription factor binding sites using the Expander (v4.1.1) software package (http://acgt.cs.tau.ac.il/expander/expander.html). The enrichment of particular GO terms or transcription factor (TF) binding sites within clusters was carried out by using the TANGO and PRIMA algorithms, respectively, included in the Expander package.

2.10.5 Identification of MDV QTL candidate genes

Genes associated with MD-resistance or susceptibility were identified from the chicken genome sequence (Galgal4, release 78) using the BioMart data mining tool within the Ensembl database (http://www.ensembl.org/biomart/index.html) based on areas of the genome known to be associated with QTL for resistance to MD (as defined in Table S1 on CD). This information was then analysed in conjunction with the gene expression data from the present study to identify potential candidate genes for disease resistance.

Chapter 3:

Developing a *de novo in vitro* MDV infection model of antigen-presenting cells (APCs) in outbred chickens

3.1 Introduction

MDV was primarily described as a lymphotrophic alphaherpesvirus for a long time. Though, apart from immune cells, MDV replicates well *in vitro* in non-lymphoid cells such as fibroblasts, kidney cells and embryonic skin cells (Churchill and Biggs, 1967; Cook and Sears, 1970; Nazerian and Purchase, 1970; Dorange et al., 2000). As described in the well-established 'Cornell model' of MDV infection, the *in vivo* infection takes place by the cell-free virus wrapped in dander (Calnek, 2001) and phagocytic cells from the lungs carry the virus to the spleen and other lymphoid tissues following infection through respiratory tract. Virus was then presumed to pass to the lymphocytes where it caused lytic infection of B lymphocytes and lytic or latent infection in T cells. It was thought that T cells play a crucial role to spread the virus in various visceral organs and also in nerve tissues and that is how pathological lesions emerge after infection. The apparent predominant role of lymphocytes in this disease led scientists to carry out intensive studies on these cells over the years. As a result, B and T lymphocytes can be infected *in vivo* by MDV (Calnek et al., 1984b) and *in vitro* infections of these cells have also been described previously by Calnek et al. (1984a) and more recently by Kaspers (2014). However, the role of innate immune cells, especially APCs, cannot be ignored. APCs are important cells of the innate immune system and play a crucial role at early stages of microbial infection. The early differential viraemia (Burgess and Davison, 2002) and gene expression profiles (Smith et al., 2011) of MDV-infected MD-resistant and susceptible lines support the hypothesis that innate immunity plays a pivotal role in determining resistance to MD. However, very little is known about the early stages of MDV infection. Though it was presumed that phagocytic cells, especially macrophages,

were the carriers of virus from the lungs to the lymphoid organs, it had not been possible to prove that MDV infects macrophages over the years until early 2000s, when Barrow et al. (2003) reported a new cell tropism of MDV by showing *in vivo* infection of macrophages for the first time. But their attempts, like those of others before (Haffer et al., 1979; von Bulow and Klasen, 1983), to infect macrophages *in vitro* were not successful, which led the authors to believe that macrophages require *in vivo* conditions for infection by MDV (Barrow et al., 2003). Therefore, the aim of this Chapter was to establish an *in vitro* model of MDV infection of APCs. Initial experiments focused on culture and characterisation of APCs from outbred J line birds. Following this, conditions for the infection of APCs with MDV were established and finally the MDV-infected APCs were characterised in detail.

3.2 Generation of chicken BMDM and subsequent characterisation

3.2.1 Morphological characterisation

As described in section 2.2.6, bone marrow cells were isolated and processed from outbred J line chickens and cultured in Sterilin single-square plates (non-compartmentalised). Cells were also incubated with zymosan particles to explore their phagocytic properties at day 7 of culture (section 2.2.8).

Chicken bone marrow cells cultured without CSF-1 did not survive (Figure 3.1A). The cell population cultured with CSF-1 was heterogeneous with both loosely and strongly adherent cell types (Figure 3.1B). It has previously been reported that i*n vitro* cultured macrophages show characteristic loosely and strongly adherent cells which are representative of immature and mature cells, respectively (Durban and Boettiger, 1981). Our results are consistent with this. The live cells also

phagocytosed zymosan particles (green beads; Figure 3.1C) which revealed that the cells were phagocytic.

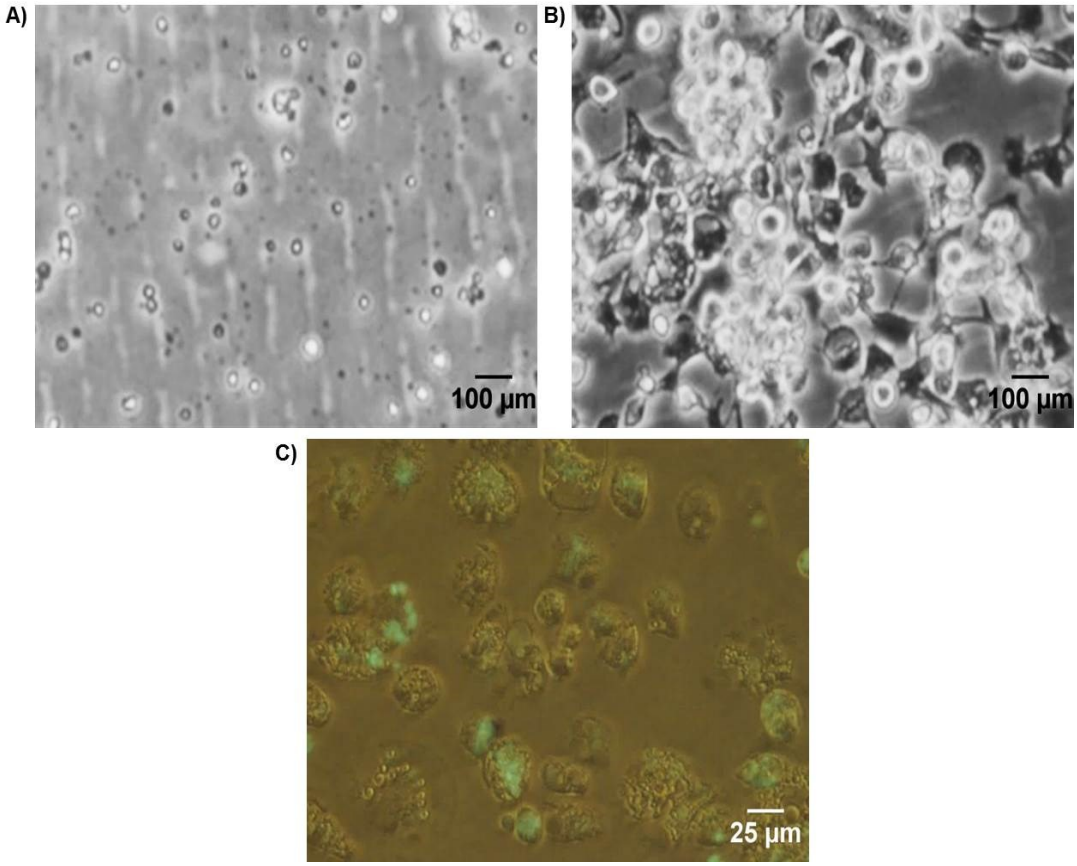

Figure 3.1. *Morphological properties of BMDM cultured from outbred chickens. (A) Cells cultured without recombinant chicken CSF-1 (B) Cells grown with CSF-1(C) Cultured cells engulfed zymosan particles (green beads).*

3.2.2 Characterisation by flow cytometry

To induce maturation, cultured macrophages were stimulated with LPS (100 ng/ml) for 24 h (section 2.2.7), harvested by vigorous pipetting and then stained and examined by flow cytometry to confirm their identity as macrophages. Immunofluorescence staining was carried out following procedures described in section 2.4.2 using fluorescein isothiocyanate (FITC)-labelled antibodies against MHC II, chicken mannose receptor (MRC1L-B) and unconjugated antibodies against

CD11 and ovNKp46. Antibodies and the corresponding antigens are listed in Table 2.1. The antibody, 2G11 (isotype IgG1) binds with chicken MHC class IIβ (B-L) molecules (Kaufman et al., 1990) expressed on the surface of APCs. KUL01 (isotype IgG1) is an antibody for the cells of mononuclear phagocytic system and was recently identified as binding to chicken mannose receptor, MRC1L-B (Staines et al., 2014) and the antibody, 8F2 (isotype IgG1) (kindly provided by Bernd Kaspers, University of Munich) binds with CD11 expressed on chicken mononuclear phagocytes. Gr 13.1 (class IgG1) detects ovNKp46 (kindly provided by Dr. Timothy Connelly, The Roslin Institute) and was used as an isotype control antibody. From now on, the widely used terms for the antibodies and antigens such as MHC II, KUL01, CD11 and Gr 13.1 will be used and designated as 'markers' in this thesis. Macrophages were gated based on forward (FSC) and side scatter (SSC) and at least 20,000 cells were counted for each sample. Analysing the data in SSC/FSC plots, the cultured cells were revealed to be a heterogenous population, as shown in Figure 3.2A. Hence, around 70% of the total cells in both unstimulated and stimulated cells were gated as macrophages on the basis of cell granularity (SSC) and size (FSC). Unstimulated cells showed highest expression of CD11 (99.1%) along with higher expression of MHC II (74.7%) and KUL01 (66.3%) (Figure 3.2B). After LPS-stimulation, no significant variation was observed in the level of surface expression of CD11 (99.4%). However, compared with unstimulated cells, KUL01 expression was increased nearly 15% in stimulated cells, whereas the expression of MHC II was significantly decreased (74.7% to 51.2%) following LPS stimulation (Figure 3.2B). Following flow cytometric characterisation, the two highly expressed markers (CD11

and KUL01) were selected for macrophages to use in the upcoming virus infection experiments.

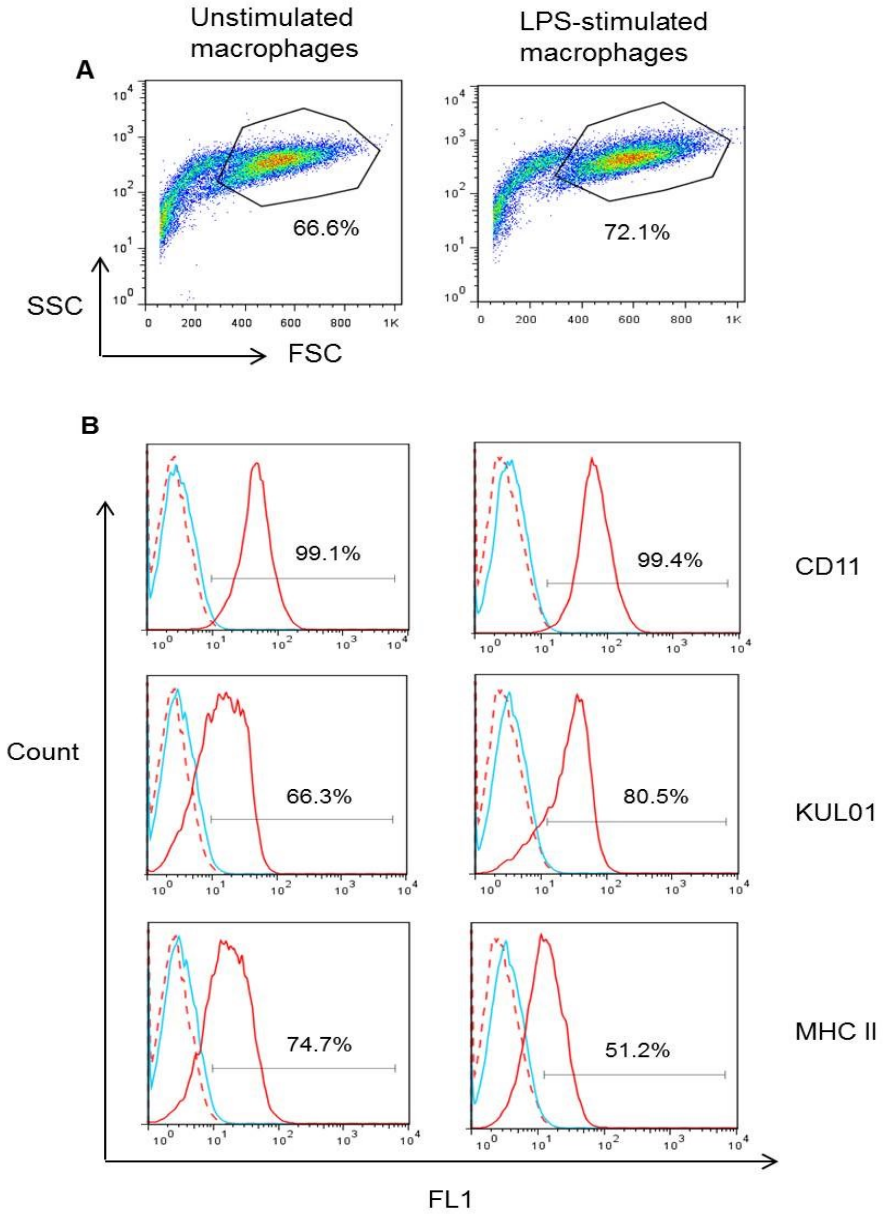

Figure 3.2. *Phenotypic characterisation of BMDM derived from outbred chicken by flow cytometry. Cells were stimulated with LPS (100 ng/ml) on day 7 of culture for 24 h. (A) Unstimulated and LPS-stimulated cells were gated in SSC/FSC plot (B) The staining pattern of gated cells for the surface expression of CD11, KUL01, and MHC II. Red dashed line: unstained control; blue line: isotype control and red solid line: specific mAbs. FL1 shows the fluorescence of FITC. Left panel: unstimulated macrophages and right panel: LPS-stimulated macrophages.*

3.3 Generation of chicken BMDC and subsequent characterisation

3.3.1 Morphological characterisation

Bone marrow cells from outbred J line chickens were aseptically processed as per methods in section 2.2.5 and cultured in 6-well plates.

Chicken BMDC showed cellular aggregates on culture plates at day 6 (Figure 3.3B) which were evident from day 4. These cellular aggregates had the typical morphology of DCs (confirmed by Dr. Zhiguang Wu, personal communication). No cell aggregates were observed when chicken bone marrow cells were cultured under the same conditions but without IL-4 and CSF-2 (Figure 3.3A).

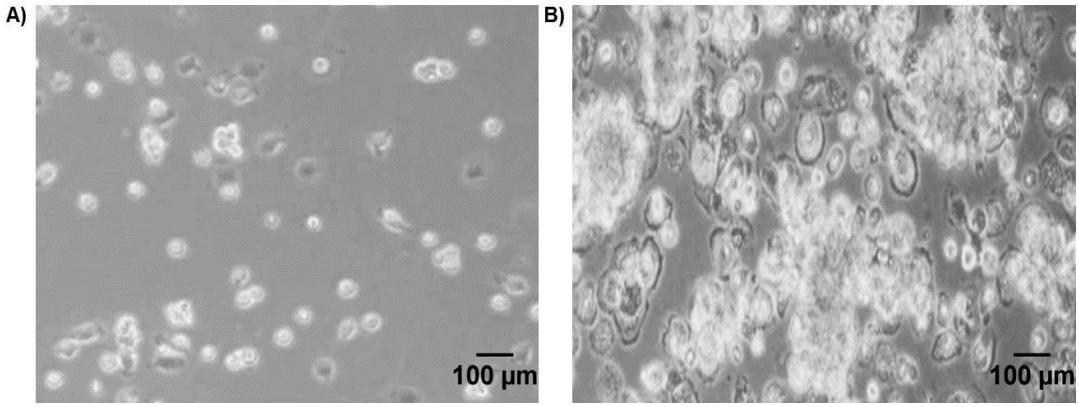

Figure 3.3. *Morphological properties of BMDC cultured from outbred chickens. (A) Cells grown without cytokines (on day 6) did not show any cell aggregation. (B) Cell aggregates were observed at day 6 of culture in the presence of IL-4 and CSF-2.*

3.3.2 Characterisation by Flow cytometry

BMDC from outbred chickens were cultured in 6-well plates, stimulated with LPS (200 ng/ml) on day 6 for 24 h to induce maturation (section 2.2.7) and then harvested by vigorous pipetting. Cells were characterised phenotypically by flow cytometry as per procedures in section 2.4.2.

Cells were stained with FITC-labelled MHC II, KUL01 and non-labelled CD11 and CD40 (detected by antibody AV79, isotype IgG2a). Details of MHC II, KUL01 and CD11 are described in section 3.2.2. CD40 is a molecule from TNF-family expressed on the surface of APCs and also on thrombocytes (Kothlow et al., 2008). IL-A105 binds with boCD8 (class IgG2a) (kindly provided by Dr. Timothy Connelly, The Roslin Institute) and was used as an isotype control antibody for CD40.

Cell surface expression of CD11, MHC II and CD40 was reported previously in cultured DCs (Wu et al., 2010). In this experiment, along with these markers, KUL01 was also tested in order to identify a common highly expressed marker for both macrophages and DCs. The results of single-colour flow cytometry of cultured DCs are shown in Figure 3.4.

DCs were gated based on FSC/SSC pattern and 20,000 cells were counted for each sample. The cultured cells were a heterogenous population, as shown in the SSC/FSC plots (Figure 3.4A). The gated DC population included about 80% of the total cells in unstimulated and 65% in the LPS-stimulated cells (Figure 3.4A). Phenotypic analysis of unstimulated cells showed high surface expression of CD11 (68.7%) and KUL01 (70.2%), moderate expression of MHC II (39.6%) and apparently no expression of CD40 (0.91%) (Figure 3.4B). Compared to unstimulated cells, the expression of CD11 and KUL01 was lower (40.3 and 49.6%, respectively) in LPS-stimulated cells, and MHC II expression was almost identical (34.8%), whereas the pattern of expression of CD40 (0.88%) in stimulated cells followed its unstimulated equivalent (Figure 3.4B).

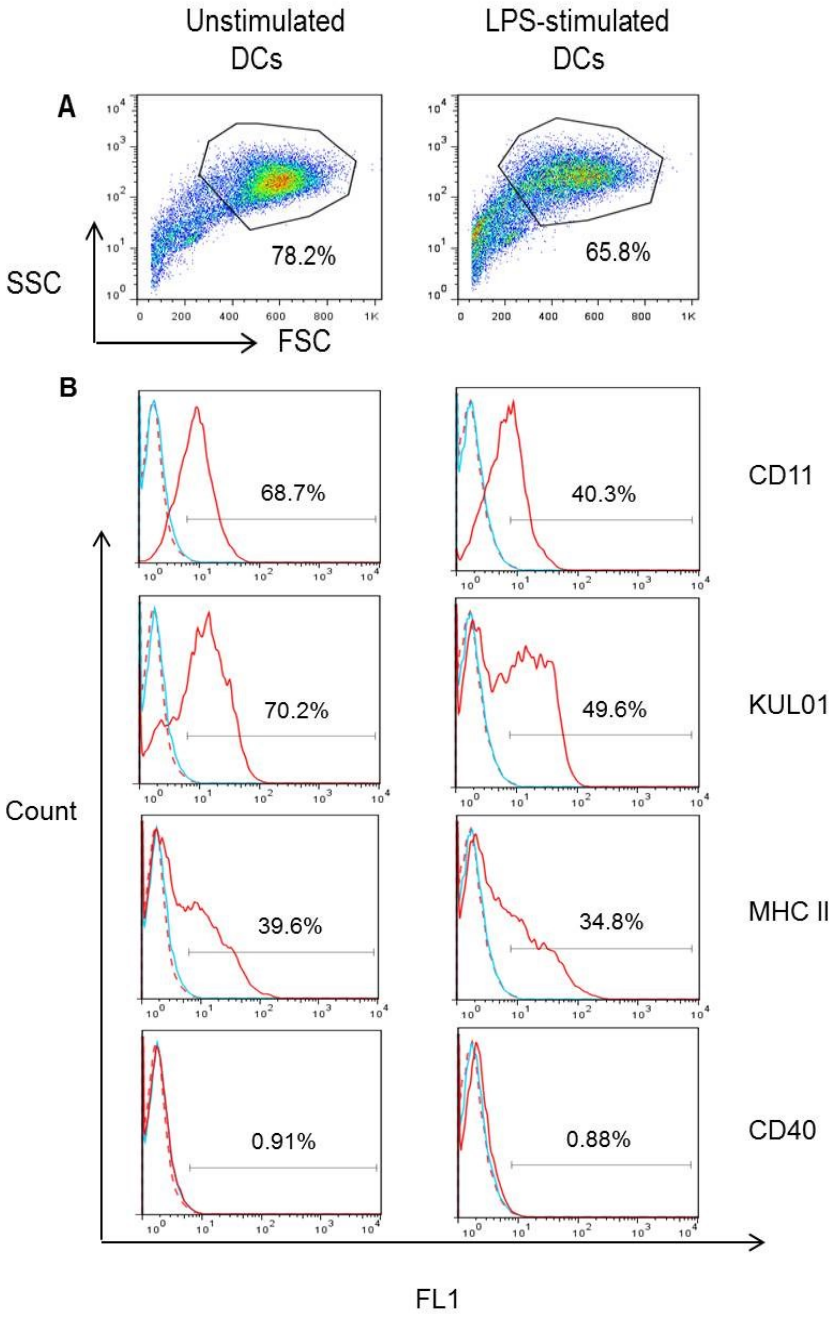

Figure 3.4. *Phenotypic characterisation of BMDC derived from outbred chickens by flow cytometry. Cells were stimulated with LPS (200 ng/ml) on day 6 of culture for 24 h. (A) Unstimulated and LPS-stimulated cells were gated in SSC/FSC plot (B) The staining pattern of gated cells for the surface expression of CD11, KUL01, MHC II and CD40. Red dashed line: unstained control; blue line: isotype control and red solid line: specific mAbs. FL1 shows the fluorescence of FITC. Left panel: unstimulated DCs and right panel: LPS-stimulated DCs.*

As observed in macrophages, CD11 and KUL01 were also found to be highly expressed markers for DCs. However, KUL01 is well-characterised and commercially available, whereas the CD11 antibody is not fully-characterised and is considered as putative CD11c in chickens (Wu et al., 2010) and it is also commercially unavailable. Therefore, KUL01 was chosen as a suitable marker for both macrophages and DCs.

3.4 Growth of virus stocks and infection of APCs

3.4.1 Growth and titration of cell-associated MDV

A GFP-encoded MDV strain was used in this study in order to identify infected cells (green) in culture as well as during flow cytometric analysis. MDV-infected CEFs were grown and plaque assays were carried out to titrate the virus in CEFs as described in section 2.3.3. Plaques were counted under an inverted microscope, but were also visible under bright field (Figure 3.5A) and by fluorescence microscopy (Figure 3.5B).

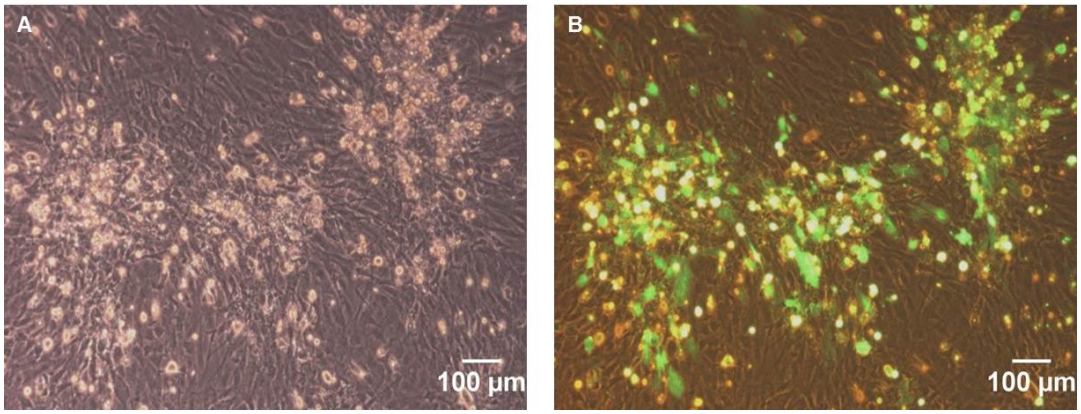

Figure 3.5. *MDV plaques formed in CEFs visualised under (A) bright field and (B) fluorescence microscope.*

The titre of the virus was calculated in plaque-forming units (pfu) per ml, which is a measure of the individual virus particles capable of forming plaques per unit volume.

The pfu was determined by counting the dilution containing the least number of plaques, in other words, the lowest virus concentration at which the cells were infected. The least number of plaques appeared at the dilution of 10^{-3} and the calculated virus titre was 2×10^5 pfu/ml. This virus was constructed from an attenuated vaccine strain (CVI988) and intended for use as a vaccine vector for avian influenza virus antigens (Wasson, 2011) and the required titre for vaccination was 1×10^3 pfu/mL (Landman and Verschuren, 2003). However, this titre was found not high enough to infect APCs as described below.

3.4.2 Infection of macrophages with cell-associated MDV

Macrophages were known to be infected by MDV *in vivo* (Barrow et al., 2003). Therefore, attempts were made to infect macrophages first *in vitro*. Macrophages were cultured in Sterilin square plates (in both single and 25-square plates) as per methods in section 2.2.6.

The optimum level of infection was determined by this formula:

Number of cells to be infected × MOI/ titre of virus.

As for example, according to this formula, to infect 10^6 macrophages with a MOI of 0.2 (2 pfu for 10 macrophages), 1 ml virus was required. This 1 ml virus usually represented MDV-infected CEFs from one T_{75} flask. The total number of CEFs from one T_{75} flask was around 10^7 and it was not possible to accommodate this number of cells with previously cultured 10^6 macrophages per well in 25-square plates.

The Sterilin non-compartmentalised (single-square) plates were thought to be suitable for co-culturing these two types of cells as the plates are spacious. Also from this experiment, macrophages were cultured up to day 4 in these plates (section 2.2.6) as longer culture duration typically lead to more cell death. Prior to the

infection, cells cultured in these plates were tested for their differentiation to macrophages by flow cytometry. Hence, on day 4, macrophages were harvested by vigorous pipetting and then stained with CD45, KUL01 and MHC II as described in section 2.4.2. KUL01 was previously detected as a suitable marker (section 3.3.2). In this experiment, a new marker CD45 and one more (MHC II) from previous studies were used to test their surface expressions on macrophages at day 4. CD45 (detected by antibody AV53, isotype IgG1) was used as a marker for the common leukocyte antigen expressed in all haematopoietic cells.

Flow cytometric analysis revealed that CD45 and KUL01 were the two homogeneous and highly expressed markers compared to cells stained with conjugate control, whereas the pattern of MHC II expression was not uniform in macrophages (Figure 3.6).

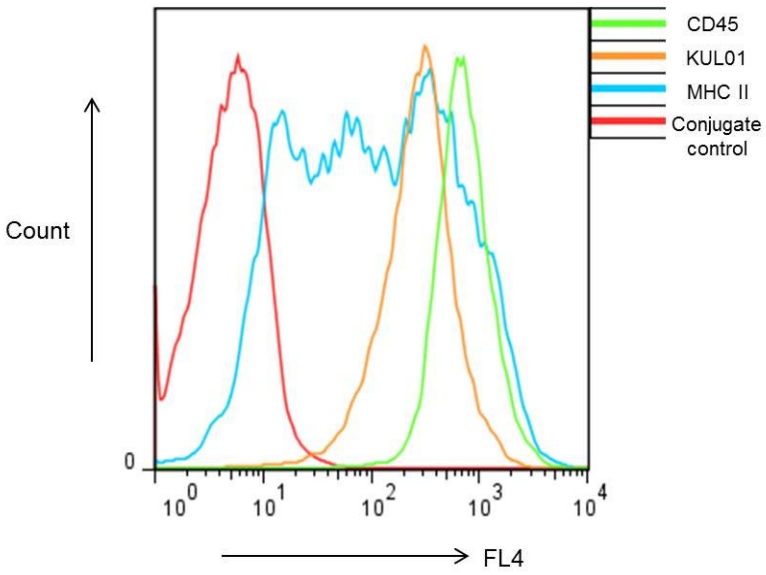

Figure 3.6. *Flow cytometric characterisation of macrophages on day 4 cultured in Sterilin single-square plates. Surface staining of macrophages with CD45, KUL01, and MHC II compared to conjugate control (IgG1 conjugated with Alexa Fluor 647). FL4 shows the fluorescence of Alexa Fluor 647.*

Following culture and characterisation of macrophages in Sterilin single-square plates on day 4, macrophages were co-cultured with cell-associated GFP-MDV in these plates as described in section 2.2.14.

Cells were observed for several hours after incubation and it was found that CEFs were not able to adhere in these plates and remained floating. Cells were in the same condition when examined after 24 h of co-culture. Cells were then harvested by pipetting and analysed by flow cytometry after staining with KUL01, CD45 and Gr 13.1 (isotype control) as per methods in section 2.4.2.

The total number of cells was very low in each tube due to high level of cell death. In flow cytometric analysis, cells were gated first in the SSC/FSC plot (Figure 3.7A) and only 5000 cells per sample were counted.

Analysing cells in the $FL1^{-}FL4^{+}$ channels following staining with KUL01 and CD45 revealed that there were significant proportions of uninfected macrophages (37.2% and 40.3%, respectively) present in the co-cultured cells (Figure 3.7B). However, no infected cells, either CEFs ($FL1^{+}FL4^{-}$) or macrophages ($FL1^{+}FL4^{+}$), were detected in this experiment (Figure 3.7B).

From this co-culture infection experiment, it was clear that CEFs cannot be grown and eventually co-cultured with macrophages in Sterilin square plates. Repeated trials also revealed that these plates do not support cell attachment and growth of CEFs. Hence, a suitable culture plate or flask will be required for co-culturing cells.

It was also noted at this stage that as MDV requires live infected cells to transmit the infection *in vitro*, it would be important to check the frozen stock of MDV-infected CEFs with the cell viability dye to determine the percentage of live cells.

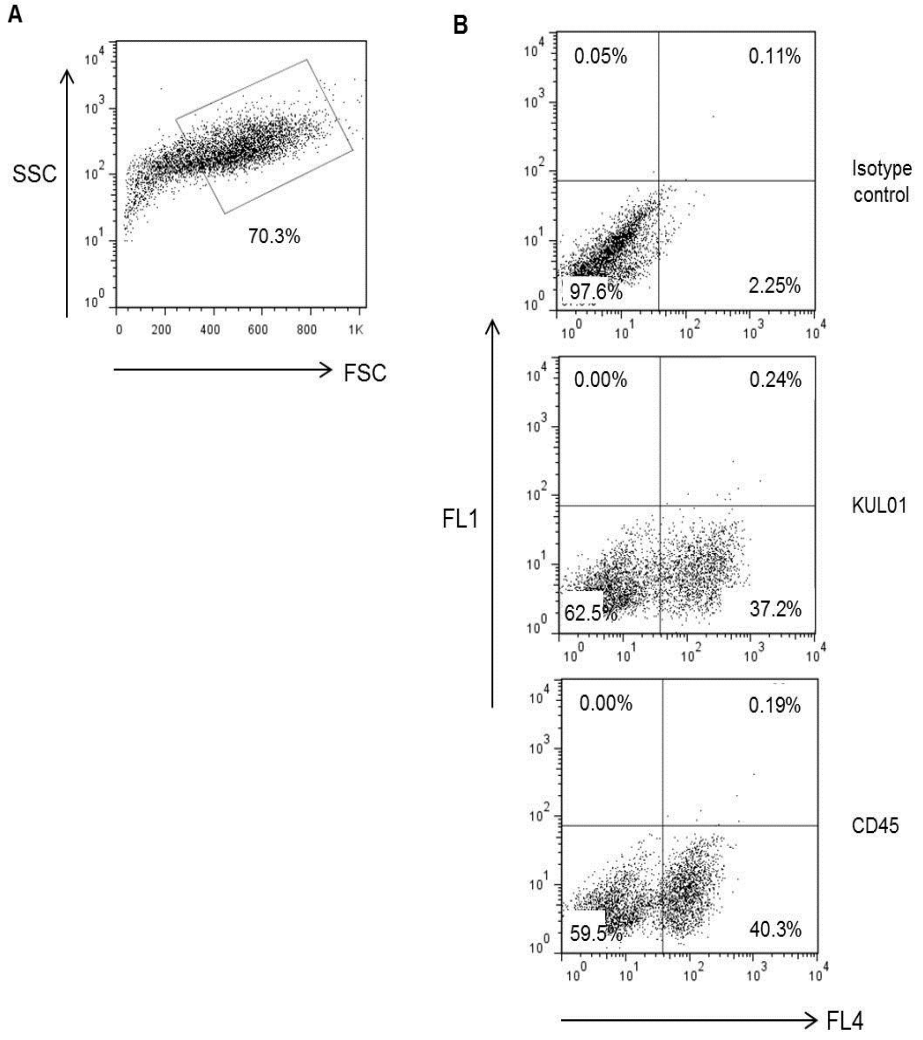

Figure 3.7. *Flow cytometric characterisation of macrophages following co-culture with MDV-infected CEFs in Sterilin single-square plates. (A) Cells were gated in SSC/FSC plot. (B) Gated cells from SSC/FSC plot were analysed in FL1/FL4 dot plots for the surface expression of KUL01 and CD45 in macrophages compared to isotype control (Gr 13.1). FL1 shows the fluorescence of intracellular GFP (green)-encoded MDV and FL4 shows the fluorescence of Alexa Fluor 647 (red) at the surface of the cells. Distribution of cells, $FL1^{-}FL4^{-}$: uninfected CEFs; $FL1^{+}FL4^{-}$: infected CEFs; $FL1^{-}FL4^{+}$: uninfected macrophages and $FL1^{+}FL4^{+}$: infected macrophages.*

3.4.3 Number of live cells in frozen stock of MDV-infected CEFs

MDV-infected CEFs, kept at -80^{o}C for several weeks, were thawed and then stained directly with the cell viability dye, 7-aminoactinomycin D (7-AAD). This dye can penetrate cell membranes in dead cells and then binds DNA while it is not the case if the cells are alive.

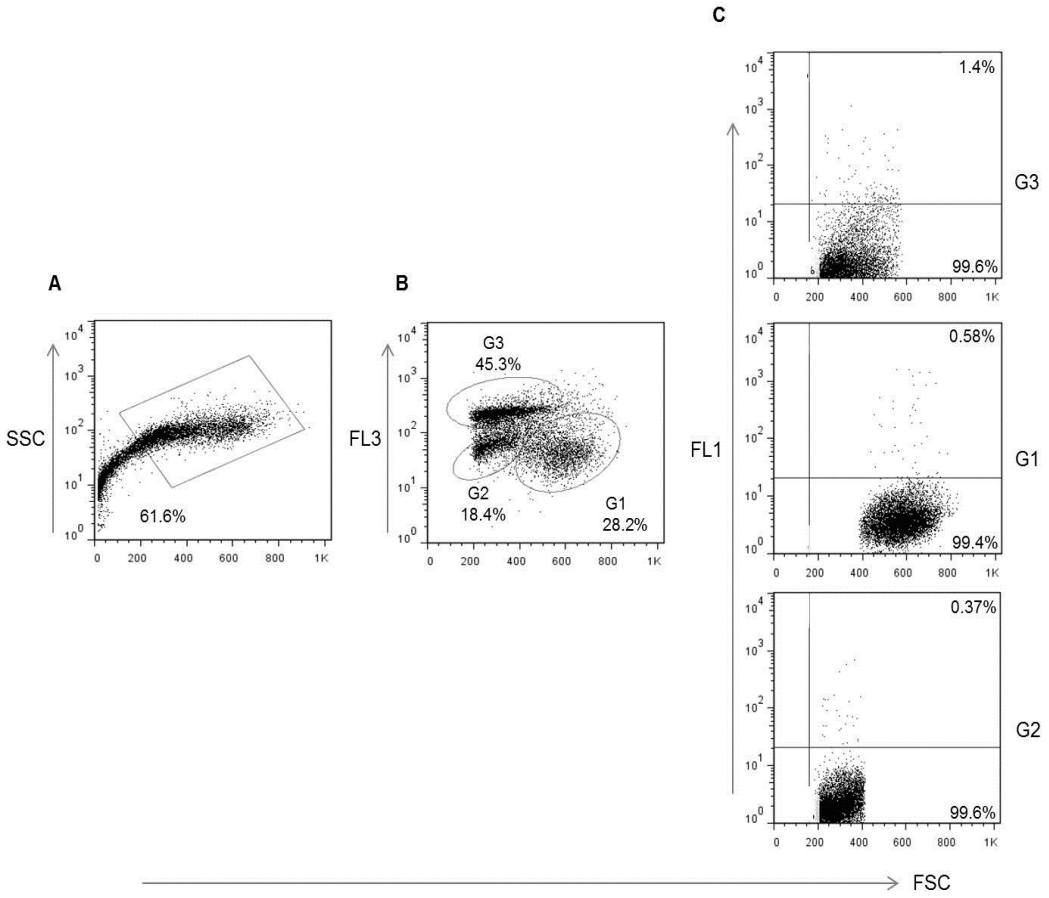

Figure 3.8. *Percentage of viable cells in frozen MDV-infected CEFs. Cells were stored at -80^{o}C for several weeks and then stained with the cell viability dye 7-AAD. (A) Infected CEFs were gated in SSC/FSC plot. (B) SSC/FSC gated cells were analysed in FL3/FSC plot. FL3 shows the fluorescence of 7-AAD while FSC shows cell size. Highly stained cells (G3) are dead, moderately stained cells (G2) are dying and unstained cells (G1) are alive. (C) Live cells from G3, G1 and G2 were plotted in FL1/FSC channel. FL1 shows the fluorescence of intracellular GFP (green)-encoded MDV and FSC shows cell size.*

Flow cytometric analyses revealed that the percentage of live cells was only 28.2% (G1) in frozen MDV-CEFs while the rest of the cells were either dead (G3:45.3%) or dying (G2:18.4%) as these cells were highly stained by 7-AAD (Figure 3.8B). When analysed further in the FL1 channel, only 0.58% cells were found to be GFP^+ within these live CEFs (G1) and rest of the GFP^+ CEFs (G3:1.4% and G2:0.37%) were present in dead and dying CEFs, respectively (Figure 3.8C).

As a substantial number of GFP^+ CEFs were dying in frozen stocks, the follow-up of this was to conduct an experiment with freshly cultured MDV-infected CEFs.

3.4.4 Number of live cells in freshly cultured MDV-infected CEFs

CEFs were cultured in T_{75} flask (section 2.2.12) and once confluent, cells were infected with working cell-associated MDV stock (section 2.3.4). Once plaques formed, CEFs were harvested (section 2.2.10) and stained directly with 7-AAD and then analysed by flow cytometry.

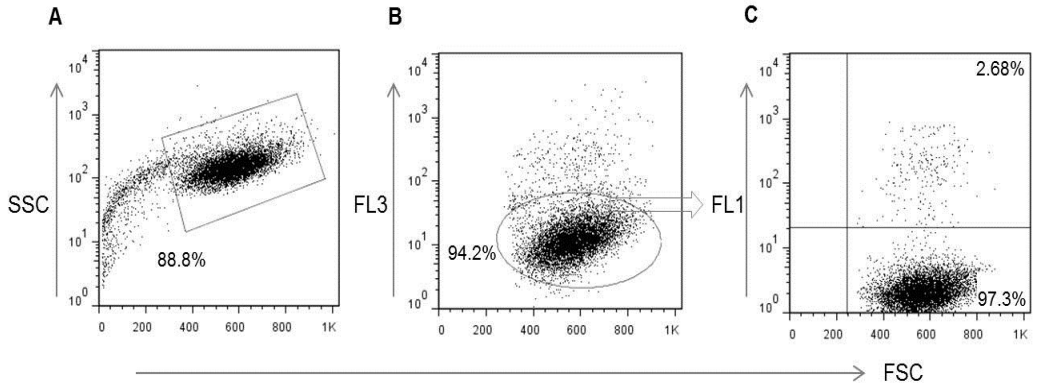

Figure 3.9. *Percentage of viable cells in freshly cultured MDV-infected CEFs. MDV-infected CEFs were cultured for 3 days and then stained with the cell viability dye 7-AAD. (A) Infected CEFs were gated in SSC/FSC plot. (B) SSC/FSC gated cells were analysed in FL3/FSC plot to gate live cells. FL3 shows the fluorescence of 7-AAD while FSC shows cell size. (C) Live cells were plotted in FL1/FSC channel. FL1 shows the fluorescence of intracellular GFP (green)-encoded MDV.*

Flow cytometric analysis revealed that the percentage of live cells was very high 94.2% (Figure 3.9B) compared to those in frozen stock (Figure 3.8B). Analysis of live cells in the FL1 channel also showed that more than 2% of the CEFs were GFP^+ in the freshly cultured cells (Figure 3.9C) in comparison with frozen stock of MDV (0.58%) (Figure 3.8C).

A significant proportion of CEFs were dying in frozen stocks and a higher percentage of GFP^+ CEFs could be found in freshly cultured cells, but still the amount of GFP^+ CEFs (2-3%) (Figure 3.9C) was not enough to conduct the co-culture infection studies efficiently.

Therefore, the next step was to explore techniques to increase the virus titre and at the same time to identify a suitable culture plate or flask to enable adherence of both CEFs and macrophages.

3.4.5 Improvement of the virus titre

MDV is strictly cell-associated *in vitro* and the virus titre so far was not high enough to perform the co-culture infection studies. Therefore, two experiments were carried out to improve the virus titre as described in section 2.3.5. In the first experiment, the virus was titred in infected CEFs harvested from six T_{175} flasks, whereas a total of twelve T_{175} flasks of CEFs were used in the second titration experiment.

Plaque assays revealed that the titre was 5×10^5 pfu/ml in both the experiments which was not much higher compared to the previous titre (2×10^5 pfu/ml). Moreover, the previous virus titre was from the stock of one T_{75} flask of infected CEFs, but this titre contained stocks of infected CEFs from six and twelve T_{175} flasks which made co-culturing of CEFs and macrophages more difficult. Dr. Lorraine-P Smith (The Pirbright Institute, personal communication) advised that the range of titres for BAC-

derived MDV was 2.5×10^3 to 4×10^5 pfu/ml which was also similar to the titre (10^4 to 10^5 pfu/ml) routinely obtained by Prof. Benedikt Kaufer (Institute for Virology, Germany, personal communication).

As the highest MDV titre (10^5 pfu/ml) was not high enough to conduct co-culture infection studies and repeated attempts failed to obtain a high titre, an attempt was made to prepare cell-free MDV from the cultured MDV-infected CEFs.

3.4.6 Infection of macrophages with cell-free MDV

MDV is a highly cell-associated virus and *in vivo* it only becomes cell-free in the feather follicle epithelium (FFE). Fully infectious, cell-free viruses can be processed and purified from FFE and thus used for *in vivo* infection studies; however, the titre is not high enough to work with *in vitro* (Prof. Venugopal Nair, The Pirbright Institute, personal communication). Hence, an attempt was made to isolate cell-free virus from the cultured MDV-infected CEFs. In order to do this, infected CEFs were harvested and processed as per methods used to prepare cell-free murid herpesvirus 4 from infected cells (section 2.3.7). This method involves lysing of infected cells to release infectious virus particles. Cell-free GFP-MDV was prepared from twenty T_{175} flasks of infected CEFs (section 2.3.7) and macrophages were then infected as described in section 2.3.8. Cells were observed daily and GFP expression was rarely seen even after 3-4 days of infection (Figures 3.10A.i and A.ii). This suggested a lack of virus replication and hence no infectivity of cell-free MDV *in vitro*. To confirm MDV was present in the supernatant, a PCR was performed and it indicated presence of MDV DNA (Figure 3.10B) in the suspension buffer (section 2.3.7) containing cell-free virus.

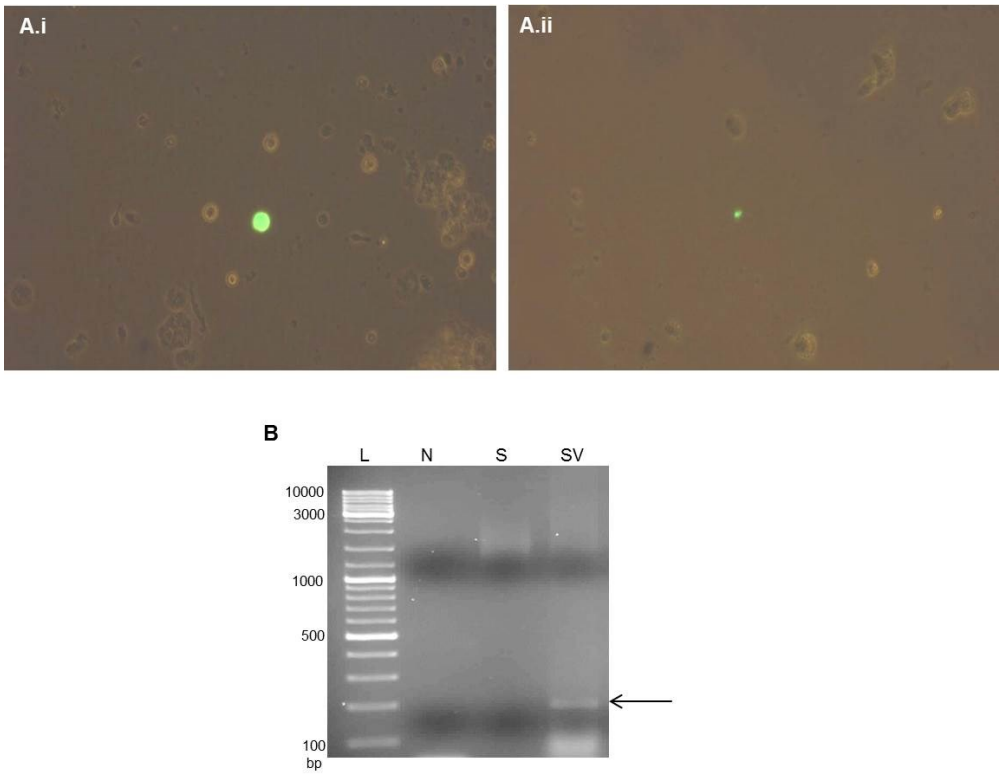

Figure 3.10. *Infection of macrophages with cell-free MDV preparation. (A.i and A.ii) Macrophage cultures on day 7, following infection with cell-free MDV on day 4, showing very few expression of GFP. (B) PCR indicates presence of MDV DNA (L-Meq, 200 bp) in the cell-free virus preparation. L: GeneRuler DNA ladder mix, N: negative control (nuclease-free H_2O). S: suspension buffer, SV: suspension buffer containing cell-free virus.*

As attempts made for improving the virus titre or to make cell-free MDV were not successful, it was then decided to continue work with freshly cultured cell-associated virus with some new concepts. Firstly, to prepare large amounts of viruses for each experiment and secondly, to count high numbers of cells during flow cytometric experiments to obtain a higher number of GFP^+ cells for further analysis. In addition, a suitable culture plate or flask for co-culturing CEFs and macrophages had to be found. Efforts were made to culture macrophages in T_{75} flasks, as CEFs can be grown well in those flasks.

3.4.7 Culture and characterisation of macrophages in T_{75} flasks

To determine whether macrophages could be cultured in T_{75} flasks, chicken bone marrow cells were seeded in T_{75} flasks as described in section 2.2.9. While harvesting cells on day 4 by vigorous pipetting, cells were found to be strongly adherent to the culture flasks. So, macrophages were harvested using 5 ml of trypsin (2.5%)/PBS solution (1:7).

In a separate experiment, cells grown in a T_{75} flask were harvested using 100 mM EDTA (section 2.4.3.2). In both cases, harvested cells were then analysed by flow cytometry to determine the surface expression of KUL01 in macrophages.

To compare the KUL01 expression in both cases, macrophages were also cultured for 4 days in Sterilin square plates and harvested by pipetting only (section 2.2.6).

Flow cytometric analysis indicated that macrophages harvested from T_{75} flasks using trypsin/PBS showed lower expression of KUL01 compared to those harvested by pipetting from square plate (Figure 3.11A), which could also be seen in the difference of their mean KUL01 expression (Figure 3.11A.i). However, this difference disappeared when macrophages from T_{75} flasks were harvested using EDTA as shown in the staining pattern (Figure 3.11B) and also in the mean KUL01 expression (Figure 3.11B.i) compared to those in square plates.

These two experiments showed that macrophages could be cultured and harvested successfully from T_{75} flasks. Therefore, the next step was to determine the phenotypic features of macrophages in T_{75} flasks.

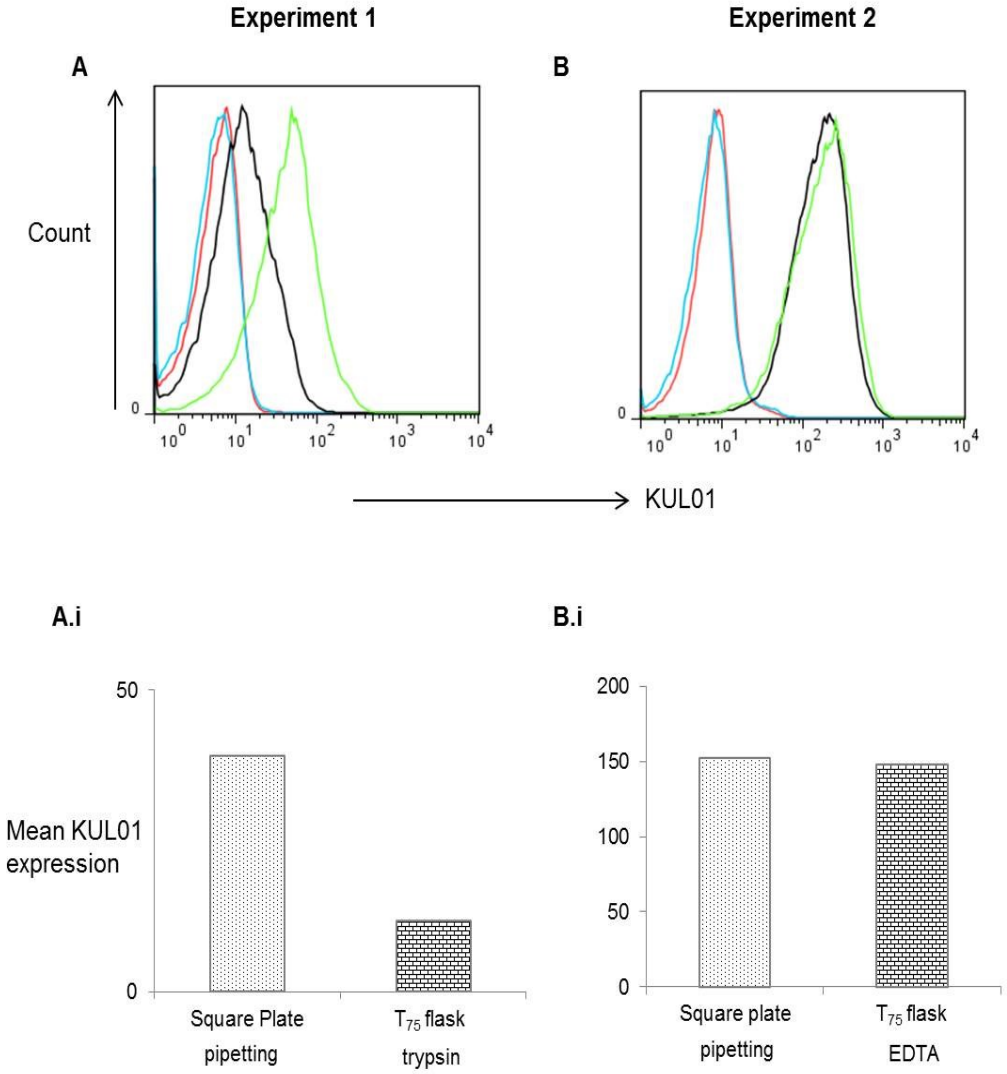

Figure 3.11. *Comparison between macrophages cultured in Sterilin square plates and T_{75} flasks. (A) Surface expression of KUL01 in macrophages harvested from Sterilin square plates (by pipetting) as well as from T_{75} flasks (by trypsin) and (A.i) differences in geometric mean of KUL01 expression. (B) Surface expression of KUL01 in macrophages harvested from Sterilin square plates (by pipetting) as well as from T_{75} flasks (by EDTA) and (B.i) differences in geometric mean of KUL01 expression. Blue line: isotype control in square plate, red line: isotype control in T_{75} flask, green line: KUL01 expression in square plate, black line: KUL01 expression in T_{75} flask. FL4 shows the fluorescence of Alexa Fluor 647 conjugated with KUL01.*

3.4.8 Phenotypic characterisation of macrophages cultured in T_{75} flasks

Macrophages were cultured in T_{75} flasks and harvested with EDTA as described previously (section 2.2.9). Following harvest, cells were stained with KUL01, CD45 and Gr 13.1(isotype control) as described in section 2.4.2 and then analysed by flow cytometry.

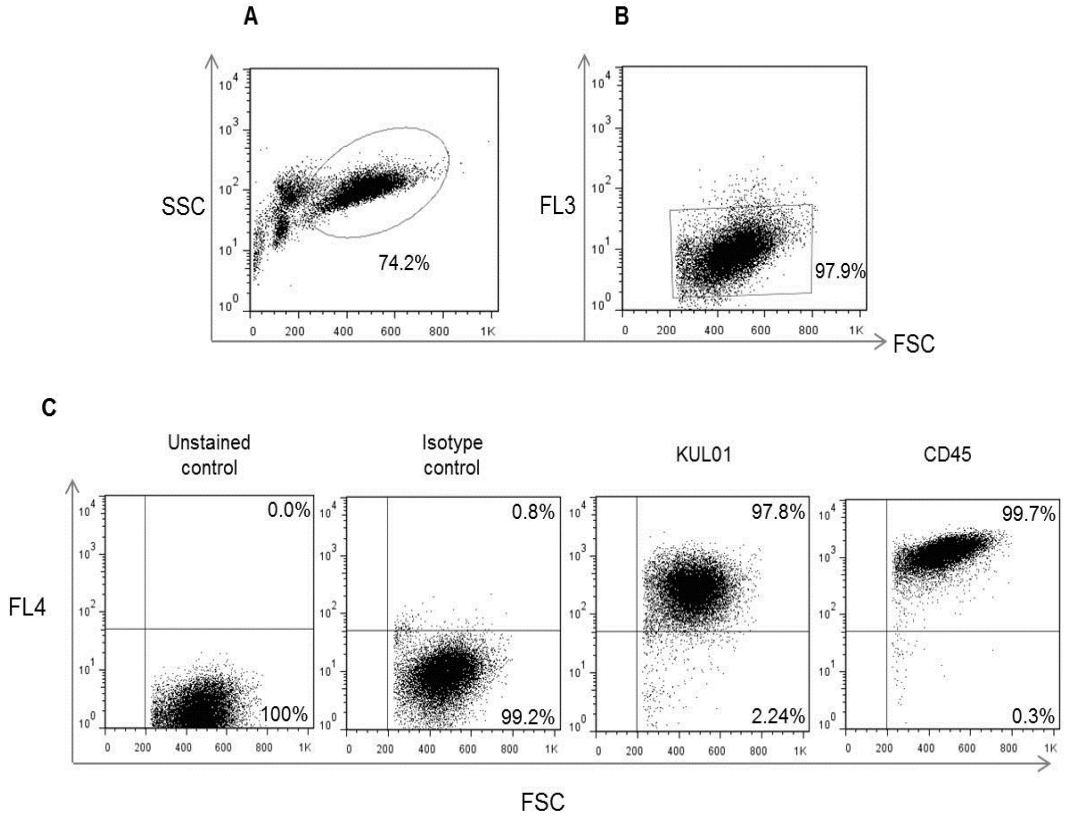

Figure 3.12. *Phenotypic characterisation of macrophages by flow cytometry cultured for 4 days in T_{75} flasks from outbred chickens. (A) Cells were gated in SSC/FSC plot. (B) SSC/FSC gated cells were plotted in FL3/FSC channel to gate live cells. FL3 shows the fluorescence of 7-AAD. (C) Live cells were tested for surface expression of KUL01 and CD45 compared with unstained cells and with cells stained with isotype control antibody (Gr13.1). FL4 shows the fluorescence of Alexa Fluor 647 conjugated with mAbs.*

Cells were first analysed in SSC/FSC plot and more than 70% cells were gated as macrophages for further analysis (Figure 3.12A). Live cells were gated in FL3/FSC channel based on 7-AAD staining (Figure 3.12B). Phenotypic analyses of live cells showed that the surface expression of both KUL01 and CD45 was homogenous and very high (97.8% and 99.7%, respectively) in macrophages cultured in T_{75} flasks (Figure 3.12C).

In this experiment, macrophages were successfully cultured and characterised in T_{75} flasks. Therefore, the next step was to infect macrophages with cell-associated MDV in T_{75} flasks.

3.4.9 Co-culture infection of macrophages with GFP-MDV CEFs

BMDM from outbred chickens were cultured in T_{75} flasks for 4 days (section 2.2.9). Meanwhile, MDV-infected CEFs were grown in two T_{75} flasks following procedures in section 2.3.4. The CEF culture and infection procedures were planned such that fully formed and confluent plaques were visible on the day of macrophage infection (day 4 of macrophage culture).

On day 4 of macrophage culture, infected CEFs from one T_{75} flask were added to one T_{75} flask of macrophage culture as per methods in section 2.2.15. One T_{75} flask of uninfected CEFs was also grown and added to one separate T_{75} flask of cultured macrophages as control.

Cells were observed daily and it was found that a very thick cell monolayer was formed in both control and infected flasks at 2 dpi. These thick cell sheets spontaneously detached from the flasks at around 60 h post-infection. Therefore, cells were harvested by disrupting the monolayers in PBS with vigorous pipetting.

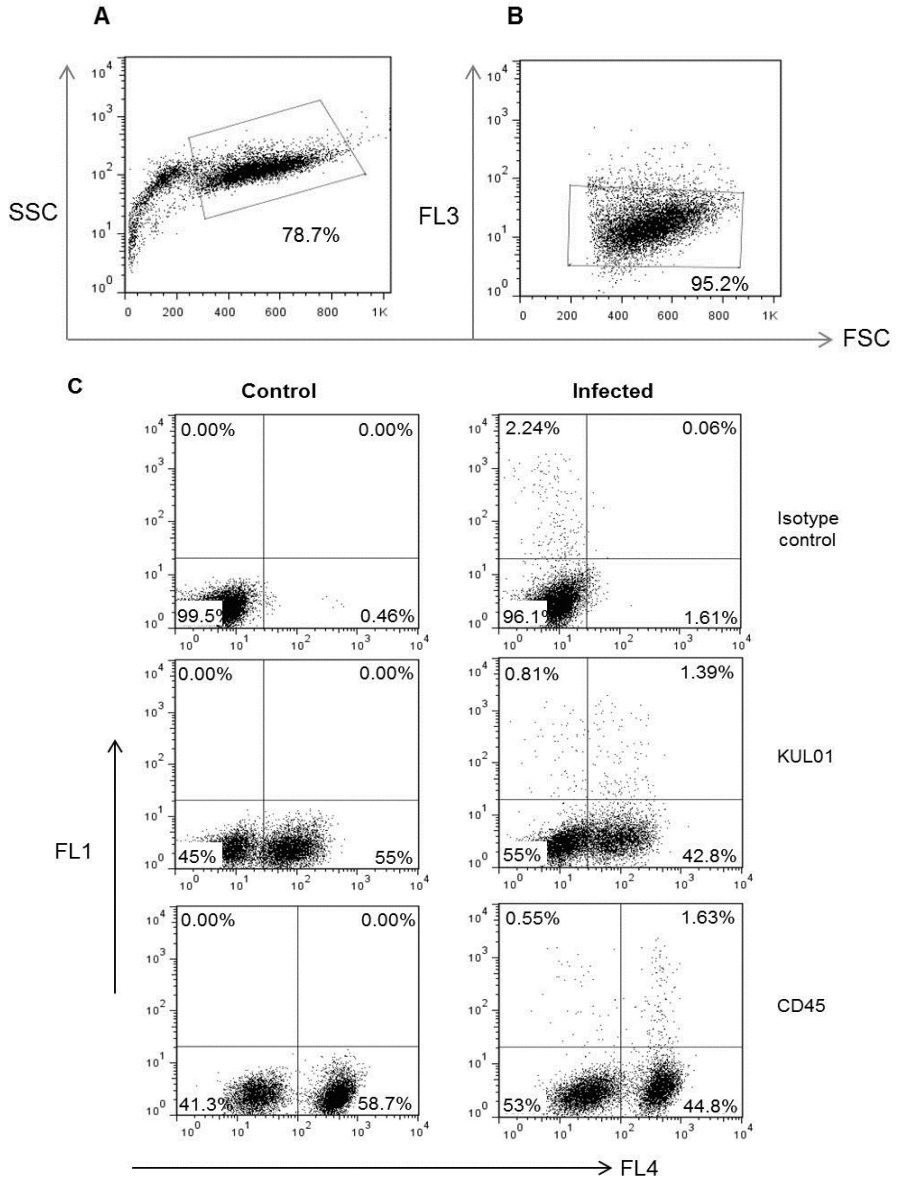

Figure 3.13. *Co-culture infection of macrophages with MDV-infected CEFs. (A) Cells were gated in SSC/FSC plot on the basis of cell granularity (SSC) and size (FSC). (B) SSC/FSC gated cells were plotted in FL3/FSC channel to gate live cells. FL3 shows the fluorescence of 7-AAD. (C) Gated cells from FL3/FSC plot were analysed in FL1/FL4 dot plots for the surface expression of KUL01 and CD45 in macrophages compared to isotype control (Gr 13.1) in both control and infected cells. FL1 shows the fluorescence of intracellular GFP (green)-encoded MDV and FL4 shows the fluorescence of Alexa Fluor 647 (red) at the surface of the cells. Distribution of cells, $FL1^{-}FL4^{-}$: uninfected CEFs; $FL1^{+}FL4^{-}$: infected CEFs; $FL1^{-}FL4^{+}$: uninfected macrophages and $FL1^{+}FL4^{+}$: infected macrophages.*

Cells were stained with KUL01, CD45 and Gr 13.1 following procedures in section 2.4.2 and then analysed by flow cytometry.

Phenotypic analysis revealed that co-cultured CEFs and macrophages had uniform cell granularity and size as shown in SSC/FSC plot (Figure 3.13A) and around 80% cells were gated to analyse in the FL3/FSC channels. Of these, more than 95% cells were found alive as they remained unstained with 7-AAD (Figure 3.13B).

Flow cytometric analyses of live cells in both control and infected groups for the surface expression of KUL01 and CD45 are shown in Figure 3.13C. It was shown that CEFs and macrophages could be distinguished as separate cell populations in KUL01 and CD45 staining (Figure 3.13C). These figures also indicating infected CEFs ($FL1^{+}FL4^{-}$) and more importantly, for the first time infected cells were stained with KUL01 and CD45 ($FL1^{+}FL4^{+}$), which were most likely MDV-infected macrophages.

Though these infected cell percentages were not high (1.39% and 1.63% for KUL01 and CD45, respectively) (Figure 3.13C), a count of 2×10^{6} cells per tube revealed that around 20,000 infected cells could be sorted from each of the antibody-stained FACS tubes, which in total would be almost 10^{5} cells/T_{75} flask. A clear demarcation between CEFs and macrophages was observed after staining with CD45 in both control and infected group (Figure 3.13C) and therefore, CD45 marker was selected for the downstream cell sorting experiments.

The results of this experiment were the first evidence that macrophages can be infected by MDV in an *in vitro* co-culture study. However, this method was found not to be sustainable, as it was not possible to maintain co-cultured cells more than

2.5 days and there was always a concern that cell monolayers could come off from the plastic at any time.

One more concern that arose at this stage was that as macrophages appear in chicken embryo at the very early stage (3-4 days) of embryonic development (Cuadros et al., 1993) and CEFs in this study were collected from 9-11 days old embryos, it was not clear whether or not these infected macrophages (Figure 3.13C) were derived from MDV-infected CEF cultures.

To test this, freshly cultured CEFs and MDV-infected CEFs were tested for the presence of macrophages with KUL01 staining in the next experiment.

3.4.10 Testing CEFs and MDV-infected CEFs for the presence of macrophages

CEFs and MDV-infected CEFs were grown in T_{75} flasks as per the methods in section 2.3.5. Cells were harvested, stained with KUL01 and Gr 13.1 and then analysed by flow cytometry (section 2.4.2).

Uninfected CEFs (Figure 3.14A) contained a significant amount of $KUL01^+$ macrophages (12%). A similar proportion of cells (8%) was also observed in MDV-infected CEFs and there were a few infected macrophages (0.07%) as well (Figure 3.14B).

It was discovered from this experiment that macrophages are present in uninfected and infected CEF cultures and so, the infected macrophages in previous experiment (section 3.4.9) could be derived from MDV-infected CEF cultures. As a consequence, an attempt was made to sort only GFP^+ CEFs by FACS after staining MDV-infected CEFs with CD45 and then to infect macrophages with these pre-sorted GFP^+ CEFs.

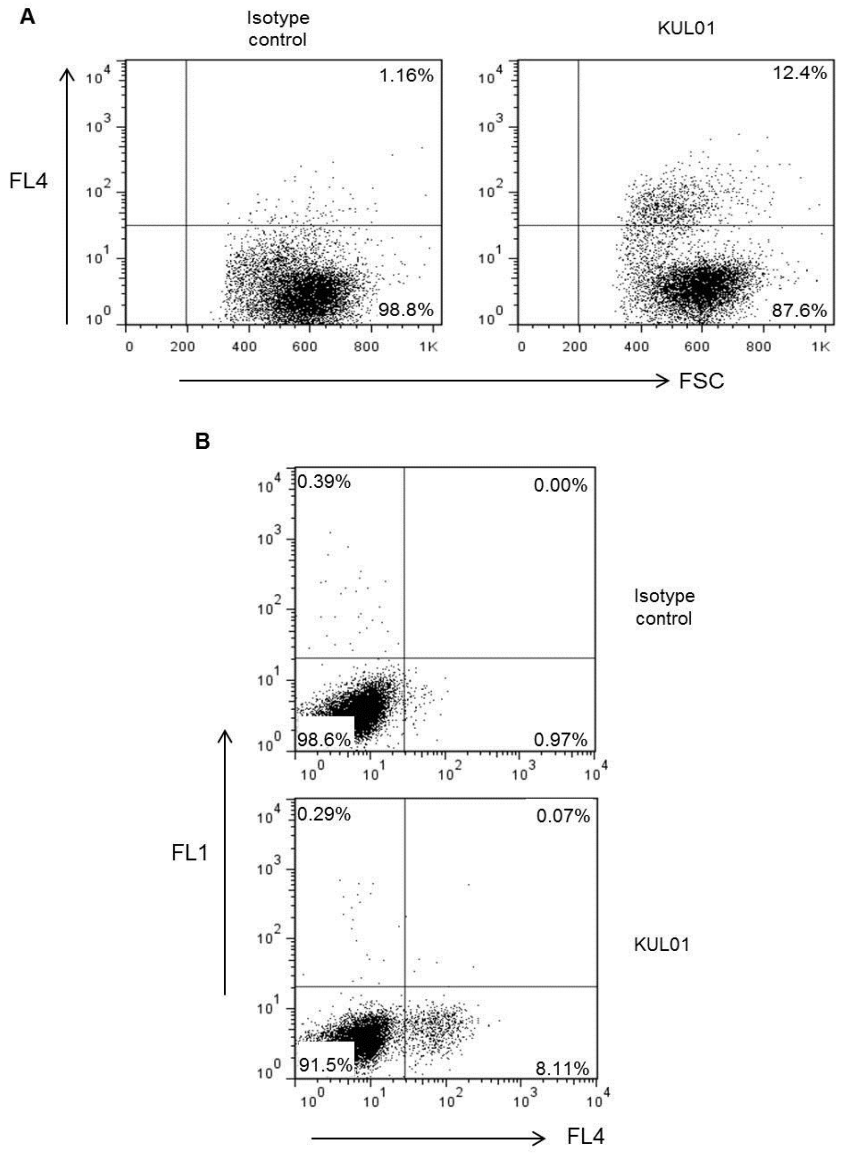

Figure 3.14. *Flow cytometric analyses showing presence of macrophages in CEFs and MDV-infected CEFs. KUL01$^+$ cells in (A) CEFs and in (B) MDV-infected CEFs while comparing with cells stained with isotype control (Gr 13.1). FL4 shows the fluorescence of Alexa Fluor 647 conjugated with KUL01. FSC represents cell size and FL1 shows the fluorescence of GFP-encoded MDV.*

3.4.11 Sorting GFP$^+$ CEFs and subsequent infection of macrophages

Macrophages were grown in T_{75} flasks for 4 days as described previously (section 2.2.9).

MDV-infected CEFs were cultured in 5 T_{175} flasks according to procedures in section 2.3.4. On the day of macrophage infection, infected CEFs from all the flasks were harvested and prepared for sorting as described in section 2.4.3.1. Prior to the sort, MDV-infected CEFs were stained with CD45 to distinguish macrophage populations from CEFs as shown in Figure 3.15 (Q2 and Q4). A total of 4.5×10^6 GFP$^+$ CEFs (Q1) were sorted from 5 T_{175} flasks of MDV-infected CEFs (Figure 3.15).

Sorted GFP$^+$ CEFs were then added to one T_{75} flask of cultured macrophages (1×10^7 cells) at an infection ratio of around 1:2 (CEF:macrophage) as per methods in section 2.2.15 and incubated for 3 days. Cells were then harvested using EDTA (section 2.4.3.2) and analysed by flow cytometry (section 2.4.2) after staining with KUL01 and CD45.

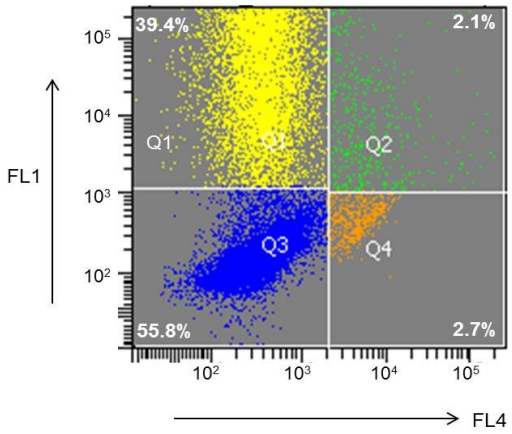

Figure 3.15. *Sorting GFP$^+$ CEFs prior to co-culture with macrophages. On the day of macrophage infection, MDV-infected CEF cultures were stained with CD45 and then GFP$^+$ CEFs (Q1) were sorted by FACS. Distribution of cells, FL1$^-$FL4$^-$: uninfected CEFs (Q3); FL1$^+$FL4$^-$: infected CEFs (Q1); FL1$^-$FL4$^+$: uninfected macrophages (Q4) and FL1$^+$FL4$^+$: infected macrophages (Q2).*

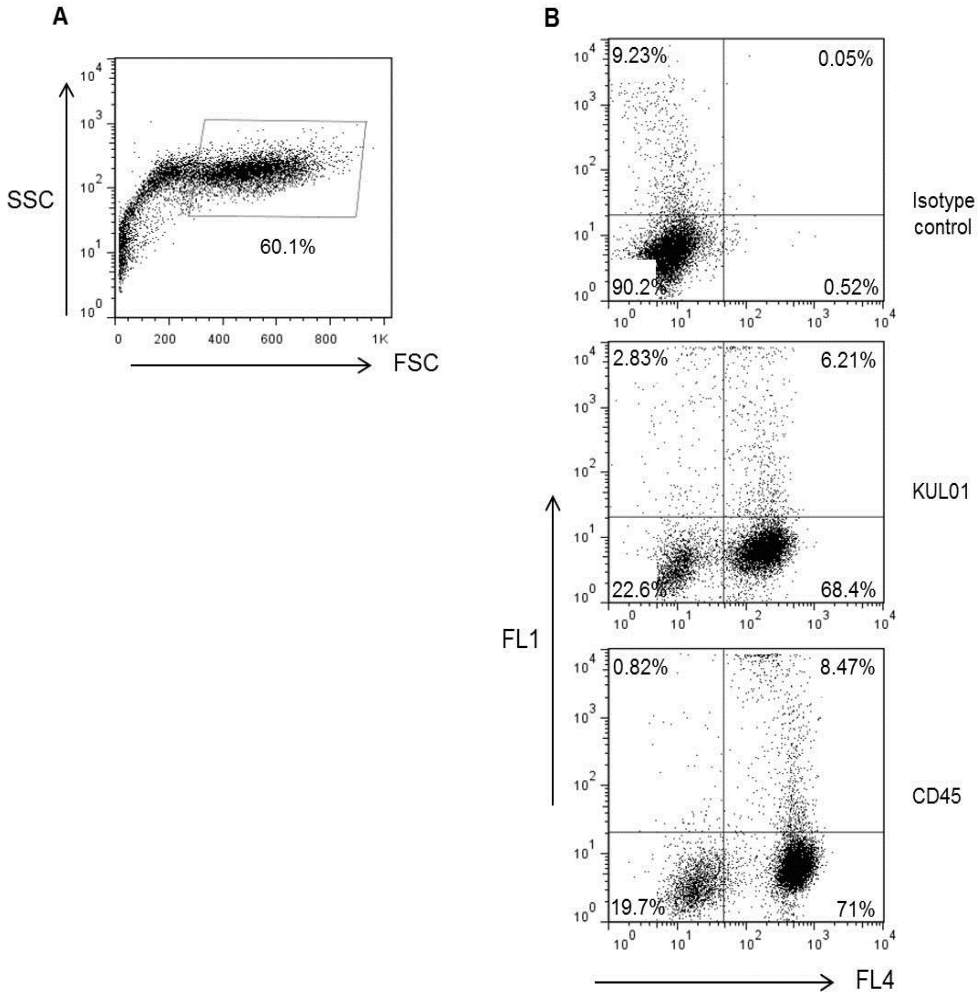

Figure 3.16. *Characterisation of macrophages by flow cytometry following infection with pre-sorted MDV-infected GFP$^+$ CEFs. (A) Cells were gated in SSC/FSC plot on the basis of cell granularity (SSC) and size (FSC). (B) Gated cells from SSC/FSC plot were analysed in FL1/FL4 dot plots for the surface expression of KUL01 and CD45 in macrophages compared with isotype control (Gr 13.1). FL1 shows the fluorescence of intracellular GFP (green)-encoded MDV and FL4 shows the fluorescence of Alexa Fluor 647 (red) at the surface of the cells. Distribution of cells in KUL01 and CD45 staining, FL1$^-$FL4$^-$: uninfected CEFs; FL1$^+$FL4$^-$: infected CEFs; FL1$^-$FL4$^+$: uninfected macrophages and FL1$^+$FL4$^+$: infected macrophages.*

In a SSC/FSC plot, cells were gated based on cell granularity and size (60%) (Figure 3.16A). Flow cytometric analyses for the surface expression of KUL01 and CD45 revealed 6-9% double positive cells, indicating infected macrophages (Figure 3.16B). A significant proportion of uninfected CEFs ($FL1^-FL4^-$ cells: 19-23%) were also evident in these figures (Figure 3.16B) which could be due to the presence of contaminating uninfected CEFs during sorting of infected CEFs, as revealed in the purity check in a later experiment (Figure 3.17). These contaminant uninfected CEFs (12%) (Q3) had grown rapidly with co-culture media containing 10% FBS. So, lower serum concentrations (2-5%) might be useful to prevent growth of CEFs.

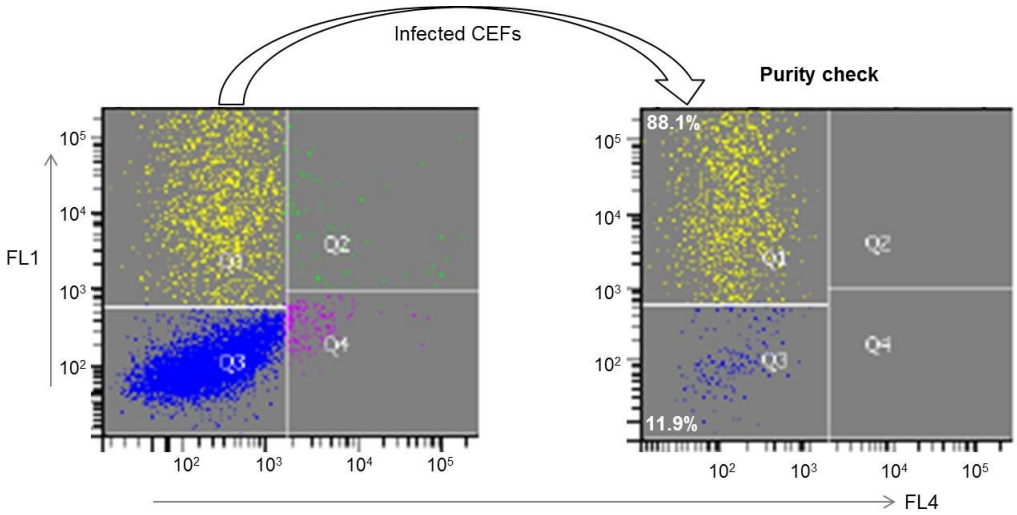

Figure 3.17. *Purity check of the sorted GFP^+ CEFs. Distribution of cells, $FL1^-FL4^-$: uninfected CEFs (Q3); $FL1^+FL4^-$: infected CEFs (Q1); $FL1^-FL4^+$: uninfected macrophages (Q4) and $FL1^+FL4^+$: infected macrophages (Q2). FL1 shows the fluorescence of intracellular GFP (green)-encoded MDV and FL4 shows the fluorescence of Alexa Fluor 647 (red) at the surface of the cells.*

This experiment indicated for the first time that macrophages could be infected *in vitro* with MDV, although as mentioned later (section 3.5.2), the presence of small numbers of contaminating infected CEFs still needs to be considered. It was

practically not feasible to generate large amounts of cell-associated viruses for the purpose of sorting around 5×10^6 GFP^+ CEFs to use at an infection ratio of 1:2 (CEF:macrophage) in each experiment. Therefore, it was decided to carry out experiments with a lower infection ratio and hence in the next experiment, macrophages were infected with pre-sorted MDV-CEFs at a ratio of 1:5.

3.4.12 Infection of macrophages with pre-sorted GFP^+ CEFs at a ratio of 1:5

MDV-infected CEFs were sorted from 2 T_{175} flasks as described in section 3.4.11 and 2×10^6 GFP^+ CEFs were added to one T_{75} flask of macrophage culture with co-culture media containing 5% FBS (section 2.2.15) at an infection ratio of 1:5 (Figure 3.18A). Following infection, cells were incubated for 3 days (Figure 3.18B), harvested and then analysed by flow cytometry after staining with KUL01 and CD45. At least 10^6 cells were counted from each sample.

In flow cytometric analysis, more than 80% cells were gated on the basis of cell granularity and size (Figure 3.19A). Of these, 96% cells were found to be alive after staining with 7-AAD (Figure 3.19B).

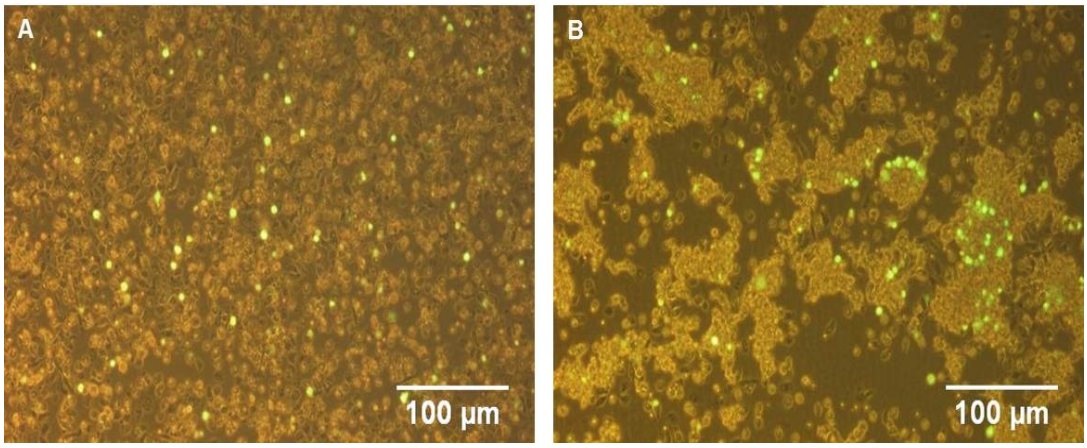

Figure 3.18. *Infection of macrophage with pre-sorted GFP^+ CEFs. The ratio of infection was 1:5 (CEF:macrophage). (A) On the day of infection. (B) On 3 dpi.*

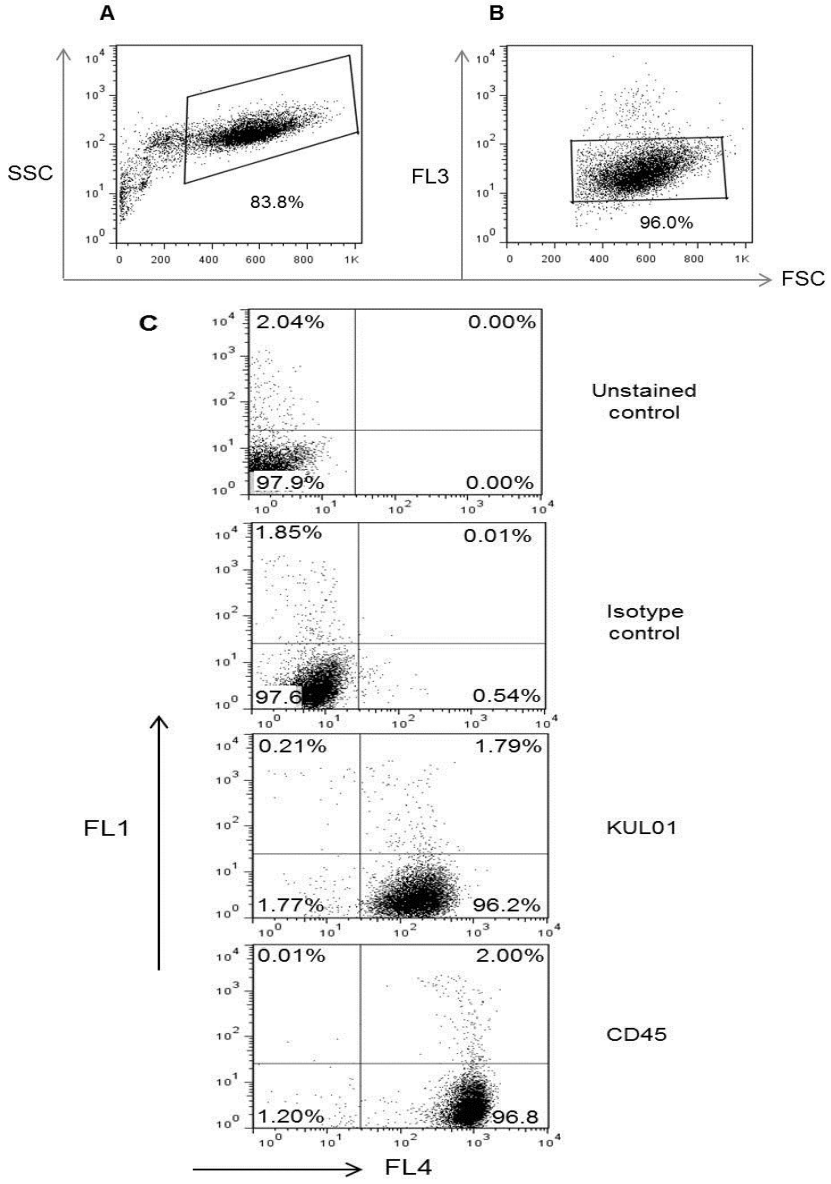

Figure 3.19. *Infection of macrophages with pre-sorted GFP$^+$ CEFs at 1:5 ratios (CEF:macrophage). (A) Cells were gated in SSC/FSC plot. (B) SSC/FSC gated cells were analysed in FL3/FSC plot to identify live cells after staining with 7-AAD. (C) Live cells from FL3/FSC plot were analysed in FL1/FL4 dot plots to detect KUL01$^+$ and CD45$^+$ macrophages compared to unstained control and isotype control (Gr 13.1). FL1 shows the fluorescence of intracellular GFP (green)-encoded MDV and FL4 shows the fluorescence of Alexa Fluor 647 (red) at the surface of the cells. Distribution of cells in KUL01 and CD45 staining, FL1$^-$FL4$^-$: uninfected CEFs; FL1$^+$FL4$^-$: infected CEFs; FL1$^-$FL4$^+$: uninfected macrophages and FL1$^+$FL4$^+$: infected macrophages.*

Live cells were then analysed in FL1/FL4 dot plots to detect MDV-infected macrophages. The proportion of infected macrophages, as shown by KUL01 and CD45 staining ($FL1^+FL4^+$), was 1.79% and 2%, respectively and very few uninfected CEFs ($FL1^-FL4^-$) were observed (Figure 3.19C). A count of 10^6 cells per tube revealed that at least 10^5 infected macrophages could be sorted from one T_{75} flask in the downstream cell-sorting experiments. A repeat of this experiment resulted in similar figures.

As macrophages from outbred chickens were successfully infected in this experiment, attempts were then made to culture and infect DCs with MDV-infected CEFs in T_{75} flasks.

3.4.13 Culture and characterisation of BMDC in T_{75} flasks

Following the successful development of a method for culturing and infecting macrophages *in vitro* with MDV-infected CEFs, the method was adapted for cultured DCs.

The phenotypic properties of DCs cultured in T_{75} flasks were determined first by flow cytometry. DCs were grown in T_{75} flasks (section 2.2.9) and harvested as described previously (section 2.4.3.2) and then analysed by flow cytometry after staining with KUL01, CD45 and Gr 13.1(isotype control) (section 2.4.2).

Around 70% cells were gated as DCs in SSC/FSC plot on the basis of cell granularity and size (Figure 3.20A). Analysis of these cells in the FL3/FSC plot after staining with 7-AAD revealed that 97.5% cells were alive (Figure 3.20B). Phenotypic analyses of live cells showed that CD45 was expressed on a higher (99.1%) percentage of DCs than KUL01 (76%) (Figure 3.20C).

DCs were successfully cultured in T_{75} flasks and characterised by flow cytometry in this experiment. Therefore, the next step was to infect DCs with MDV-infected CEFs in T_{75} flasks.

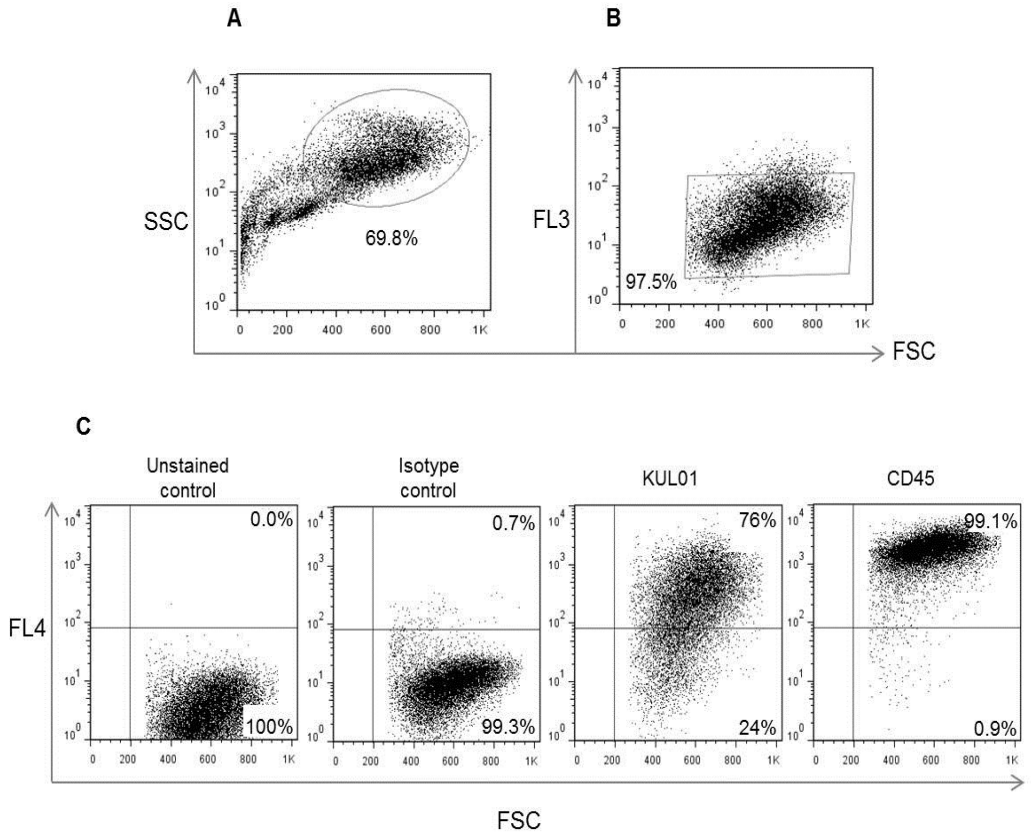

Figure 3.20. *Phenotypic characterisation of DCs by flow cytometry cultured in T_{75} flasks from outbred chickens. On day 4, cells were harvested using EDTA. (A) Cells were gated in SSC/FSC plot. (B) SSC/FSC gated cells were plotted in FL3/FSC channel to gate live cells. FL3 shows the fluorescence of 7-AAD. (C) Live cells were tested for surface expression of KUL01 and CD45 compared with unstained cells and also with cells stained with isotype control antibody (Gr 13.1). FL4 shows the fluorescence of Alexa Fluor 647 conjugated with mAbs.*

3.4.14 Infection of DCs with pre-sorted GFP$^+$ CEFs at a ratio of 1:5

BMDC were infected in T_{75} flasks with pre-sorted 2×10^6 GFP$^+$ CEFs at a ratio of 1:5 (CEF:DCs) as described previously (section 3.4.12). Following infection (Figure 3.21A), cells were incubated for 3 days as described in section 2.2.14. It was observed that the number of GFP$^+$ cells was highly reduced (Figure 3.21B) in DC culture on 3 dpi compared to those in macrophages (Figure 3.18B). Cells were harvested, stained with KUL01 and CD45 and then analysed by flow cytometry (section 2.4.2). At least 10^6 cells were counted for each sample.

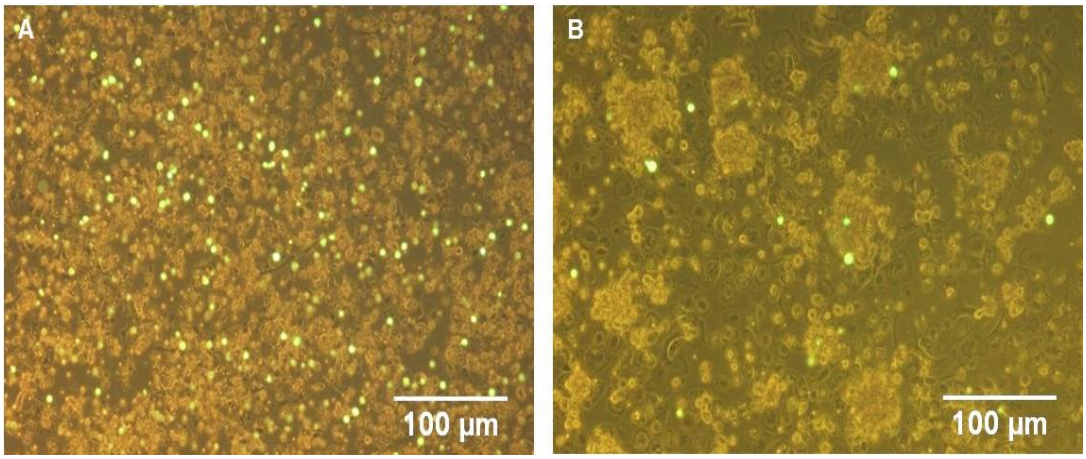

Figure 3.21. *Infection of DCs with pre-sorted GFP$^+$ CEFs. The ratio of infection was 1:5 (CEF:DC). (A) On the day of infection. (B) On 3 dpi.*

When analysed by flow cytometry, 63% cells were gated on the basis of cell granularity (SSC) and size (FSC) (Figure 3.22A). Of these, 98% cells were found alive after staining with 7-AAD (Figure 3.22B).

Flow cytometric analyses of live cells in FL1/FL4 dot plots revealed that the proportions of infected DCs, based on KUL01 and CD45 staining (FL1$^+$FL4$^+$), was 0.45% and 0.57%, respectively (Figure 3.22C).

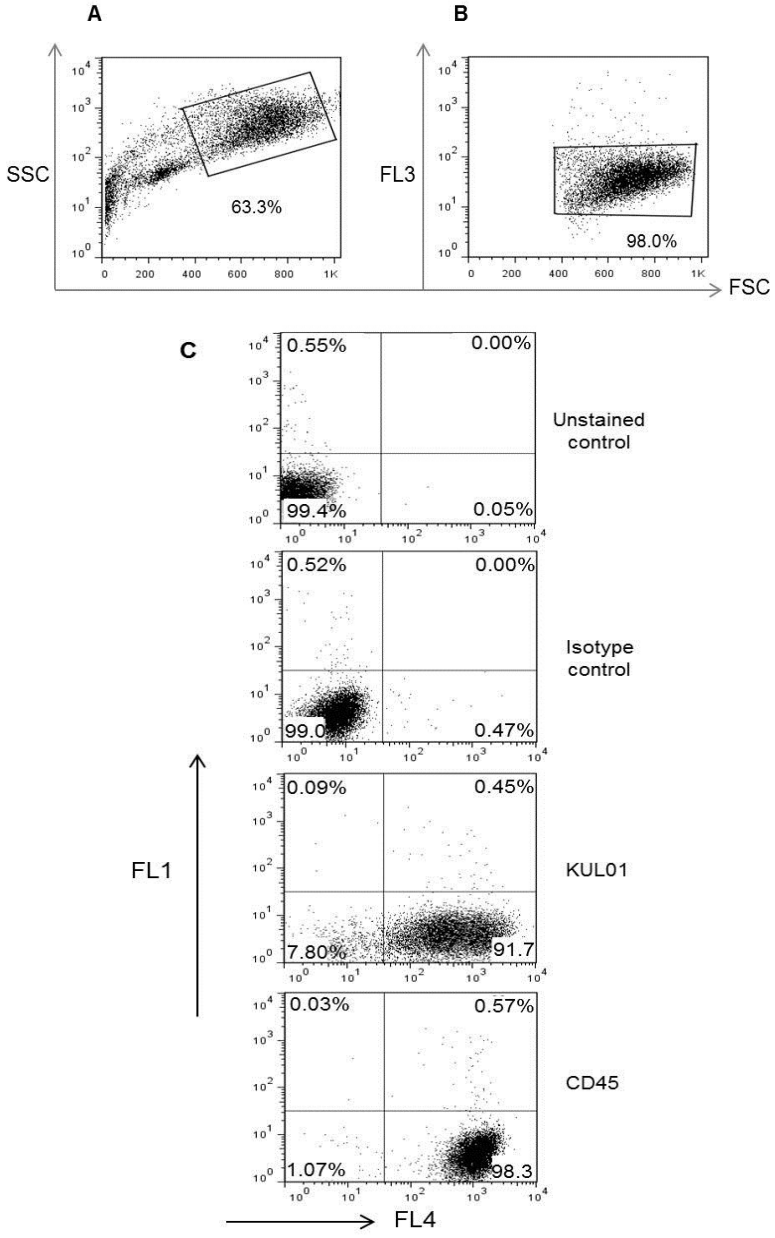

Figure 3.22. *Infection of DCs with pre-sorted GFP$^+$ CEFs at 1:5 ratios (CEF:DC). (A) Cells were gated in SSC/FSC plot. (B) SSC/FSC gated cells were analysed in FL3/FSC plot to gate live cells. (C) Live cells from FL3/FSC plot were analysed in FL1/FL4 dot plots for the surface expression of KUL01 and CD45 in DCs compared with unstained control and isotype control (Gr 13.1). FL1 shows the fluorescence of intracellular GFP (green)-encoded MDV and FL4 shows the fluorescence of Alexa Fluor 647 (red) at the surface of the cells. Distribution of cells in KUL01 and CD45 staining, FL1$^-$FL4$^-$: uninfected CEFs; FL1$^+$FL4$^-$: infected CEFs; FL1$^-$FL4$^+$: uninfected DCs and FL1$^+$FL4$^+$: infected DCs.*

A count of 10^6 cells per tube revealed that it would be possible to sort at least 2.5×10^4 infected DCs from one T_{75} flask in future cell-sorting experiments. A repeat experiment also showed similar results.

As co-culture infection experiments with macrophages and DCs in outbred chickens and their characterisation by flow cytometry were successful, attempts were then made to further characterise infected and uninfected APCs using various techniques.

3.5 Further characterisation of APCs following MDV infection

3.5.1 Live cell confocal microscopy

As described in section 2.6.1, infected and uninfected macrophages and DCs (Figures 3.23A and B, respectively) were sorted by FACS on day 3 post-MDV infection.

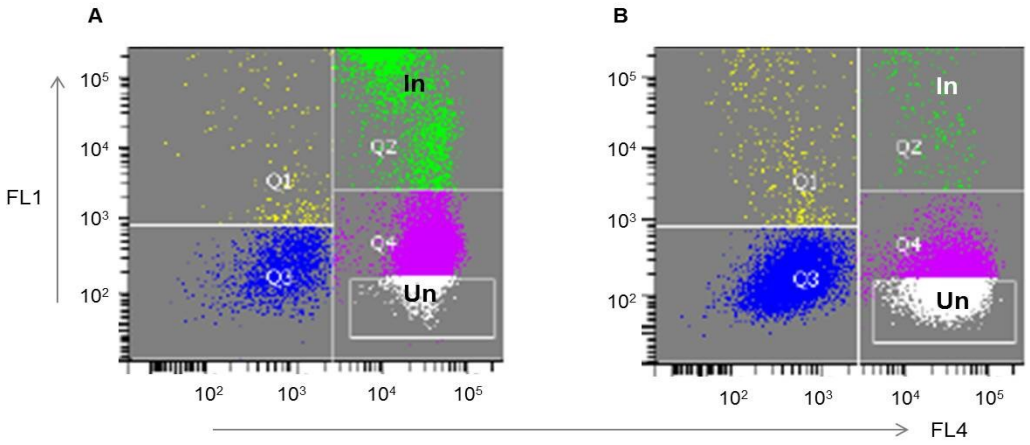

Figure 3.23. *Cell sorting for live cell confocal microscopy. Sorting infected (In) and uninfected (Un) (A) macrophages and (B) DCs on 3 dpi. FL1 shows the fluorescence of intracellular GFP (green)-encoded MDV and FL4 shows the fluorescence of Alexa Fluor 647 (red) at the surface of the cells. Distribution of cells, $FL1^-FL4^-$: uninfected CEFs (Q3); $FL1^+FL4^-$: infected CEFs (Q1); $FL1^-FL4^+$: uninfected macrophages or DCs (Q4) and $FL1^+FL4^+$: infected macrophages or DCs (Q2).*

Infected and uninfected live macrophages and DCs were examined under a confocal microscope to determine the detailed morphology of cells. GFP was encoded by MDV, so green-coloured cells (GFP^+) will indicate the presence of virus. The appearance of $CD45^+$ cells will be red at the surface as it was labelled with Alexa Fluor 647. Cells were also examined to detect whether the expression of GFP was from the surface of the cells, as GFP^+ MDV-infected CEFs could be adherent to APCs which can indicate virus infection of APCs in the cell sorter.

Examination of infected macrophages revealed that there were intracellular vacuole-like structures surrounding the nucleus (N) (Figures 3.24A.i and A.ii), which are most likely a feature of activated macrophages (Petricevich et al., 2008). GFP expression was in the cytoplasm and also in the nucleus, indicating MDV infection of these cells (Figures 3.24A.i and A.ii). Presence of GFP only in the cytoplasm could be an indication of phagocytosis of virus but not infection. Uninfected macrophages only showed the expression of CD45 (Figure 3.24B).

The confocal pictures of both infected and uninfected DCs showed cells with dendrites, a feature which is characteristic of dendritic cells (Figure 3.25). Like macrophages, GFP was present in the nucleus (N) as well as in the cytoplasm of DCs, indicating MDV infection of DCs (Figures 3.25A.i and A.ii), whereas uninfected DC only showed the expression of CD45 (Figure 3.25B).

Though CD45 expression was expected to be from the cell surface only, some intracellular expression was also observed in both infected and uninfected macrophages and DCs. These cells were stressed due to sorting that might have led to the disintegration of cell membranes, which in turn probably caused internalisation of CD45.

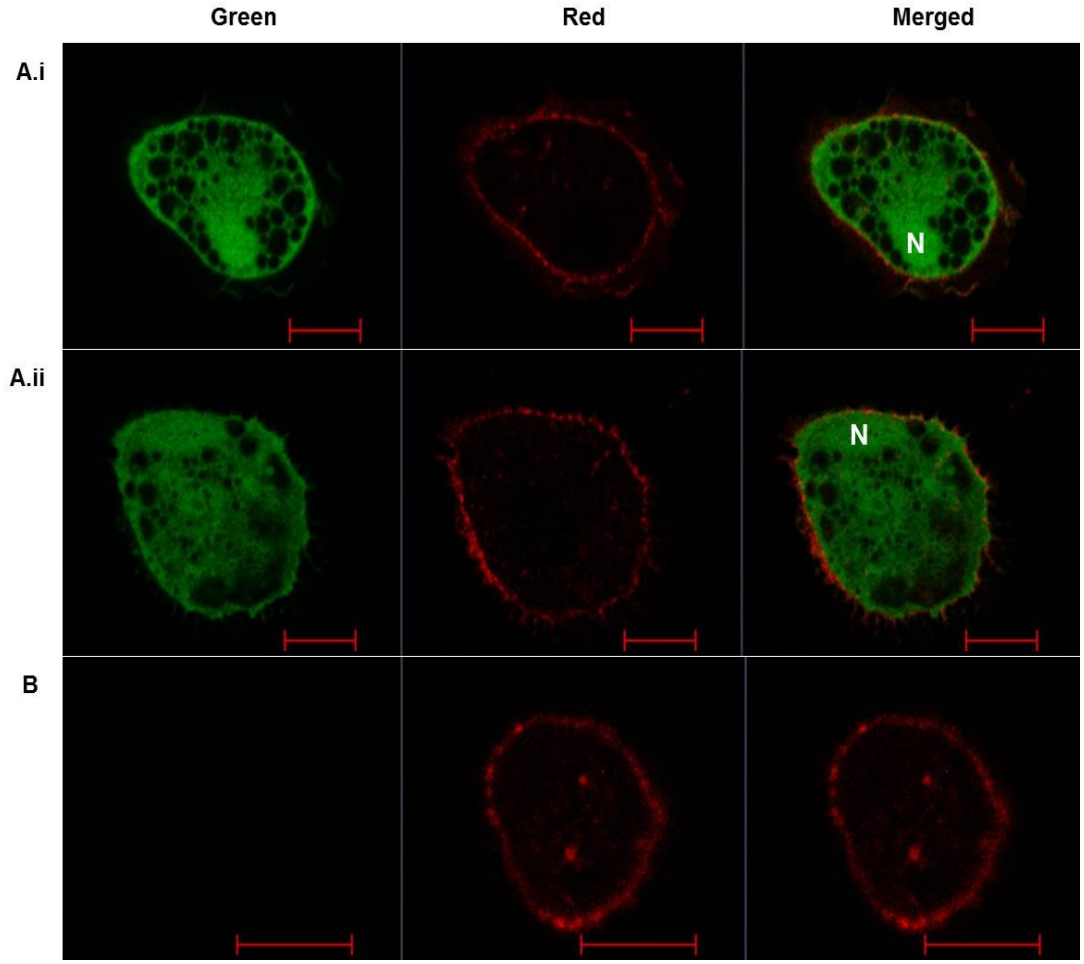

Figure 3.24. *Visualisation of infected and uninfected macrophages using confocal microscopy. On day 3 post-MDV infection, cells were sorted and examined for (A.i and A.ii) infected macrophages and (B) uninfected macrophage. Green channel: cells examined for the expression of GFP-encoded MDV, red channel: cells examined for the expression of CD45 conjugated with Alexa Fluor 647 (red), merged channel: cells examined for combined expression of green and red. N: nucleus. Scale bar: 10 µm. Microscope: LSM710 Confocal AxioObserver with objective ×63/1.40 Oil DIC.*

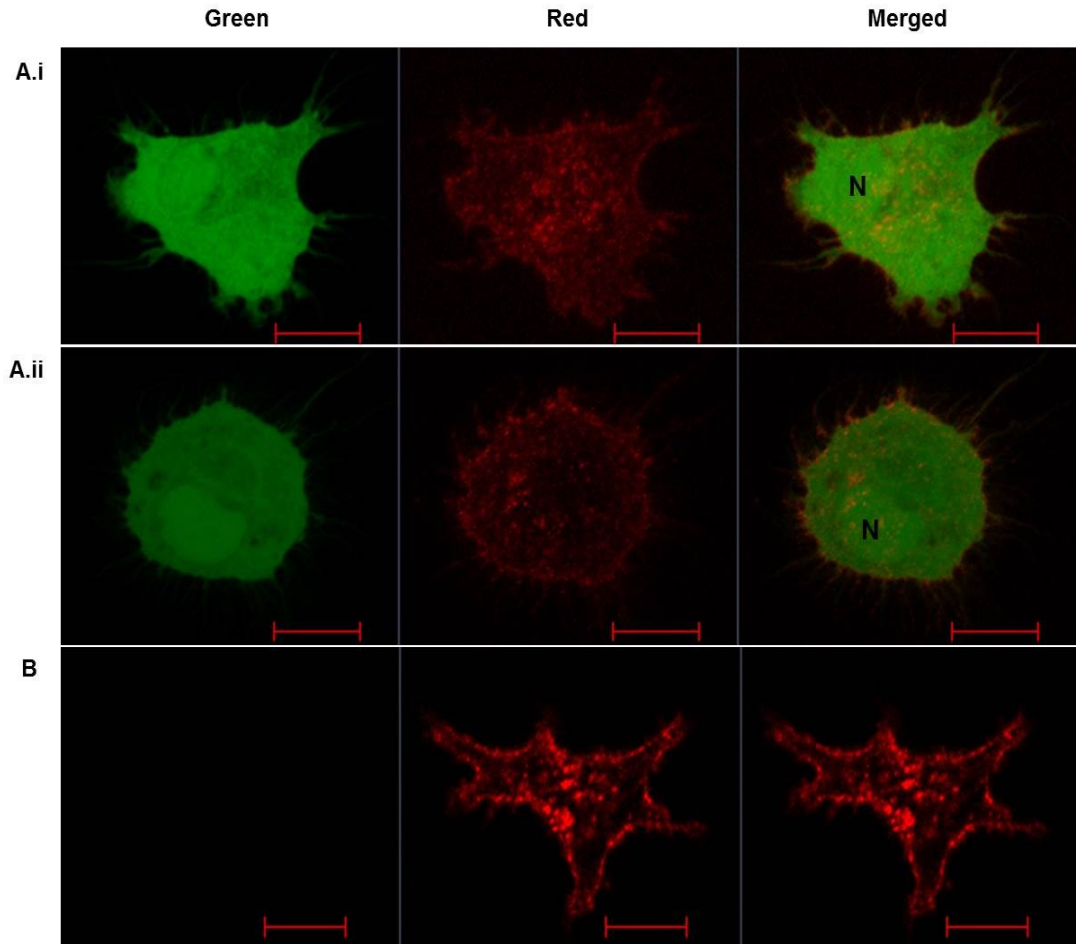

Figure 3.25. *Visualisation of infected and uninfected DCs using confocal microscopy. On day 3 post-MDV infection, cells were sorted and examined for (A.i and A.ii) infected DCs and (B) uninfected DC. Green channel: cells examined for the expression of GFP-encoded MDV, red channel: cells examined for the expression of CD45 conjugated with Alexa Fluor 647 (red), merged channel: cells examined for combined expression of green and red. N: nucleus. Scale bar: 10 µm. Microscope: LSM710 Confocal AxioObserver with objective ×63/1.40 Oil DIC.*

3.5.2 Characterisation of MDV-infected cells by RT-PCR

RT-PCR was performed to define the transcription of virus genes in MDV-infected CEFs, macrophages and DCs following procedures described in sections 2.5.3 and 2.5.5.

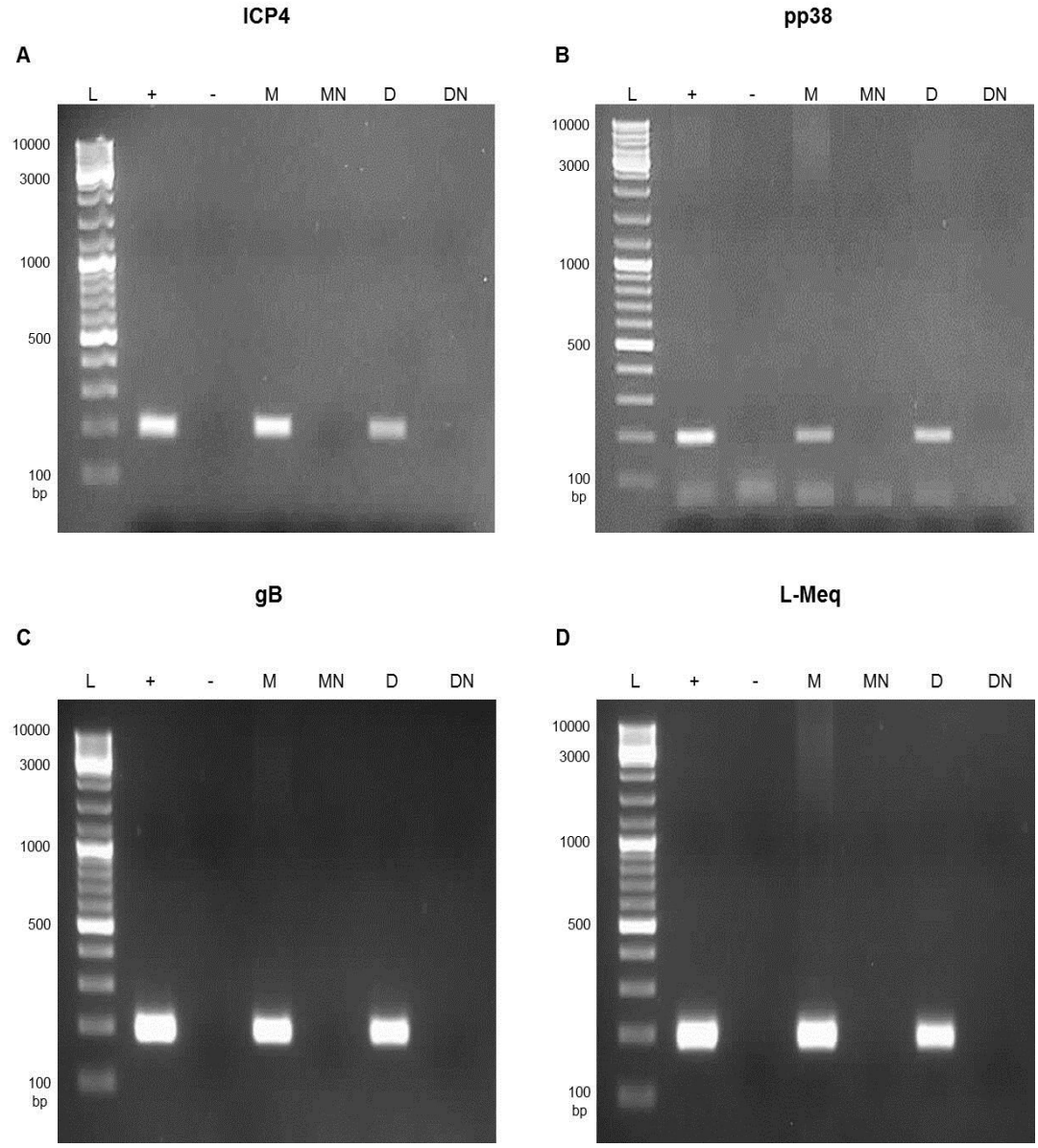

Figure 3.26. *RT-PCR showing transcription of virus genes in MDV-infected cells. Figures showing expression of herpesvirus specific (A) immediate early, ICP4 (200 bp) (B) early, pp38 (198 bp) (C) late, gB (193 bp) genes and MDV specific (D) oncogene, L-Meq (200 bp). L = GeneRuler DNA Ladder Mix (Thermo Scientific), + = positive control: MDV-infected CEFs, - = negative control: nuclease-free H_2O, M = infected macrophage (cDNA), MN = infected macrophage no-RT control (DNase treated RNA), D = infected DC (cDNA), DN = infected DC no-RT control (DNase treated RNA).*

Herpesvirus specific immediate early (ICP4), early (pp38) and late (gB) genes as well as the MDV-specific oncogene (L-Meq) were expressed (Figures 3.26A, B, C and D, respectively), in MDV-infected macrophages and DCs.

Transcription of all virus genes in MDV-infected macrophages and DCs was compared with those in virus infected CEFs, which were used as a positive control. DNase treated RNA from both infected macrophages and DCs was used in PCRs as no-RT controls and no bands in these lanes (MN and DN) confirmed the transcription of all the virus genes in MDV-infected macrophages and DCs (Figures 3.26A, B, C and D). However, these infected macrophages and DCs were not 100% pure but contained nearly 2% contaminant infected CEFs as revealed later when the cell purity was checked (section 3.5.4; Figure 3.30).

3.5.3 Time-lapse confocal video microscopy

To determine the possible mechanism(s) of MDV infection of macrophages, time-lapse confocal video microscopy was carried out on the day of MDV infection as described in section 2.6.2. Images from an approximately 10 min long experiment were compressed to create a movie. Movies are provided herewith on a CD and two still pictures from movies A and B are shown in Figures 3.27 and 3.28, respectively. MDV is strictly cell-associated *in vitro*. The transmission of MDV between cells should therefore occur in a cell to cell mode. However, as discussed in Chapter 1 (section 1.9), it is not exactly known yet how the virus transmits between cells. Moreover, as a phagocyte, macrophages might also engulf the MDV-infected CEFs and subsequently get infected.

Analysis of movie A shows cells containing vacuoles which are characteristic of activated macrophages that might construct phagolysosomal compartments by fusing

phagosomes with lysosomes (Petricevich et al., 2008). GFP particles can also be seen moving around within these vacuoles (as shown by arrows in Figure 3.27), indicating presence of virus. Presence of virus within these phagolysosomes might be an indication of phagocytosis of MDV-infected cells by macrophages which later could potentially turn into infection of cells.

Possible cell-to-cell mode of transmission of MDV could be more clearly explained in the second video. Movie B illustrates a large infected macrophage-like cell (green nucleus indicating virus infection) showing intercellular connections with two other small-sized or apoptotic cells and also green cellular processes emerging from the maccrophages (arrows in Figure 3.28).

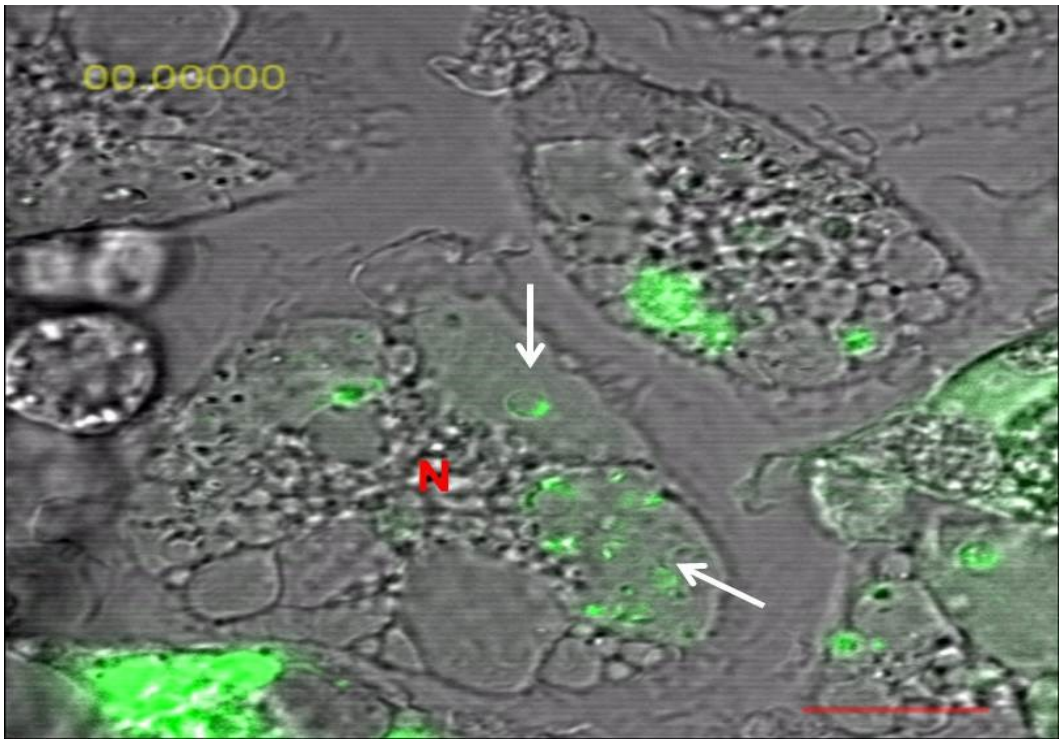

Figure 3.27. *A still picture from movie A. Figure showing possible mode of infection of macrophages by phagocytosis. Arrows indicate presence of GFP within the phagolysosome-like structures of cell. N: nucleus. Scale bar: 10 µm. Microscope: LSM710 Confocal AxioObserver with objective ×63/1.40 Oil DIC.*

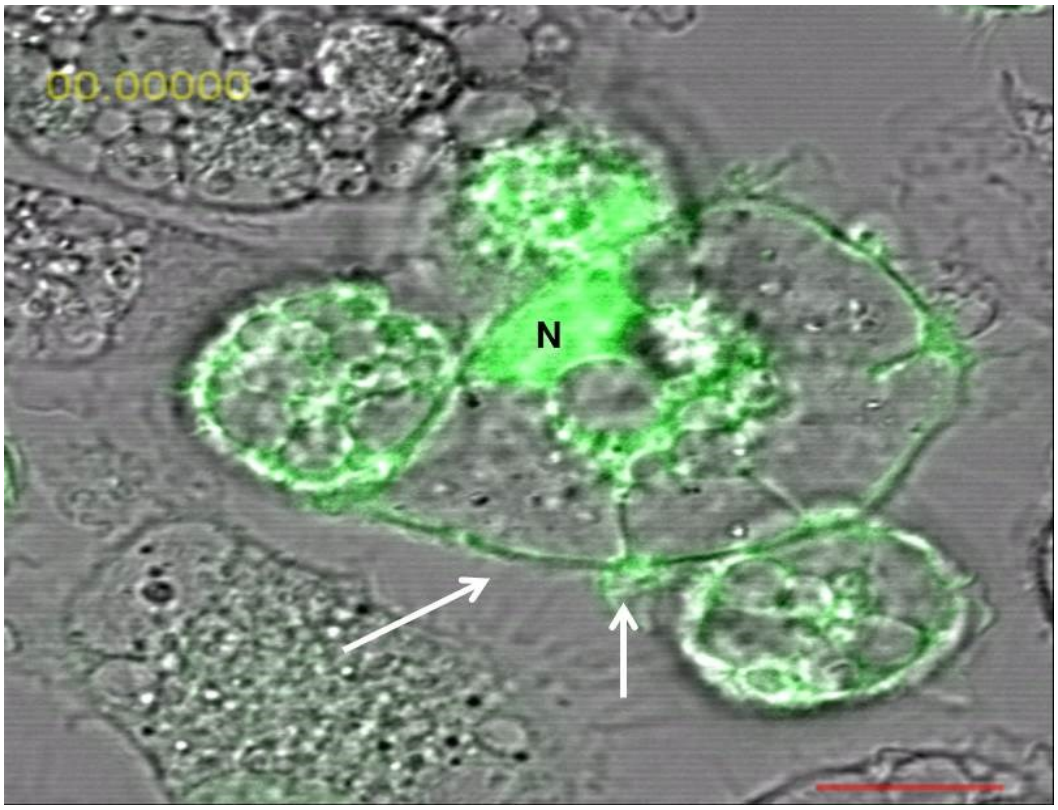

Figure 3.28. *A still picture from movie B. Figure showing possible cell to cell mode of transmission of MDV through cellular processes. Arrows indicate presence of green cellular projections from and between cells. N = nucleus. Scale bar: 10 µm. Microscope: LSM710 Confocal AxioObserver with objective ×63/1.40 Oil DIC.*

3.5.4 Re-infection of CEFs with MDV-infected macrophages

To determine whether the *in vitro* MDV-APC infection is productive or abortive, CEFs were 're-infected' with MDV-infected macrophages. The term 're-infection' is used as virus infection was initially transmitted to macrophages from CEFs. Macrophages were used for infecting CEFs because it was possible to obtain more MDV-infected macrophages during cell sorting as the percentages of infected macrophages were higher than that of DCs (Figures 3.19C and 3.22C, respectively).

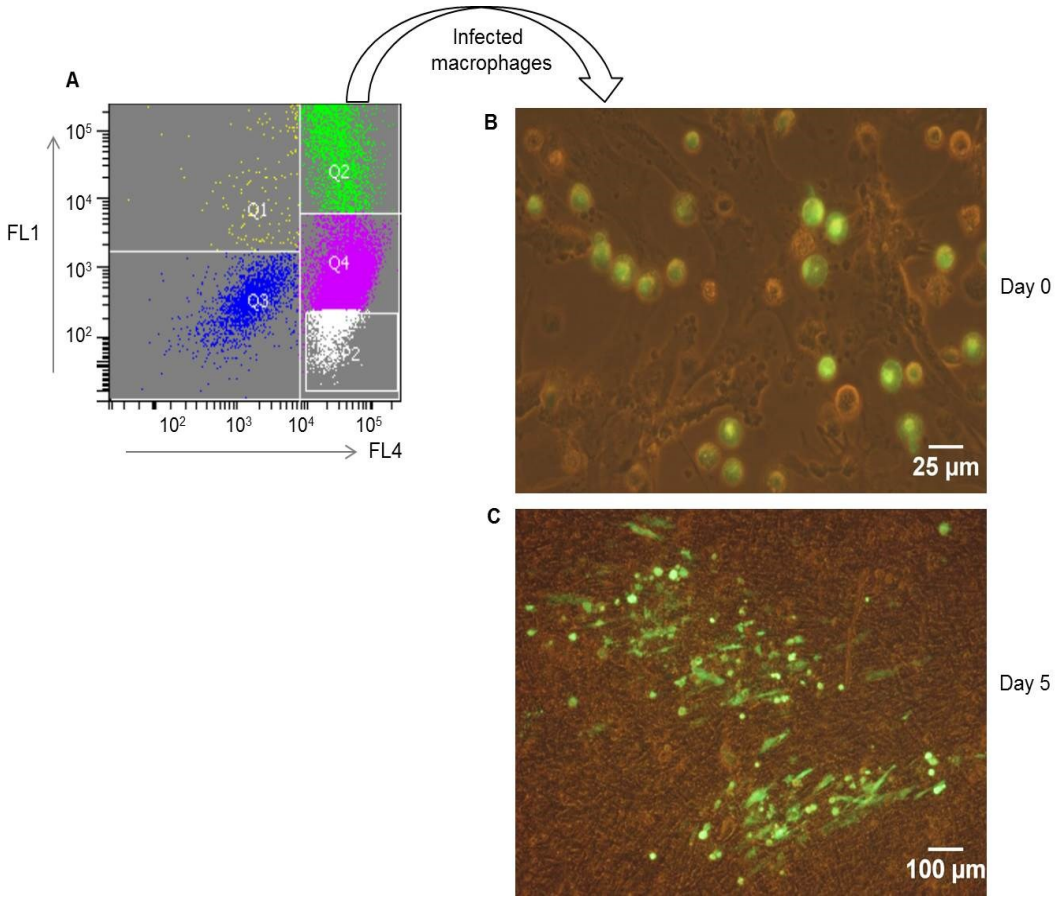

Figure 3.29. *Re-infection of CEFs with MDV-infected macrophages. (A) MDV-infected macrophages were sorted and (B) added to CEF culture, day 0 (on the day of infection). (C) Fully-formed plaques in CEF culture on 5 dpi. FL1 shows the fluorescence of intracellular GFP (green)-encoded MDV and FL4 shows the fluorescence of Alexa Fluor 647 (red) at the surface of the cells. Distribution of cells in sorting plot, $FL1^{-}FL4^{-}$: uninfected CEFs (Q3); $FL1^{+}FL4^{-}$: infected CEFs (Q1); $FL1^{-}FL4^{+}$: uninfected macrophages (Q4) and $FL1^{+}FL4^{+}$: infected macrophages (Q4).*

As described in section 2.2.19, CEFs were cultured in 6-well plates 2-3 days prior to the infection. MDV-infected macrophages were sorted on 3 dpi (Figure 3.29A) and added to the CEF culture (Figure 3.29B).

After co-culturing of GFP^{+} macrophages with uninfected CEFs, plaque formation started from 2 dpi and fully formed plaques were observed at 5 dpi (Figure 3.29C).

Formation of plaques in CEF cultures following infection with MDV-infected macrophages was an indication that MDV-macrophage infection is productive. However, in a repeat experiment the purity of the infected macrophages was checked by placing 1000 sorted cells in the same sorting plot and it was revealed that there were nearly 2% contaminant infected CEFs within the infected macrophages (Figure 3.30). That means, within 10^5 infected macrophages there would be 2000 contaminant infected CEFs.

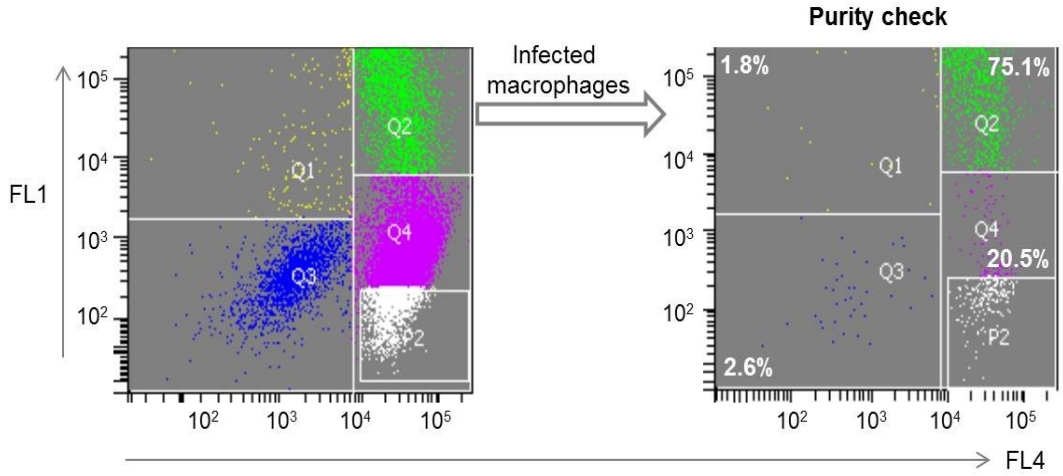

Figure 3.30. *Purity check of the infected macrophages. Contaminant cells were present from all sections with nearly 2% infected CEFs (Q1). FL1 shows the fluorescence of intracellular GFP (green)-encoded MDV and FL4 shows the fluorescence of Alexa Fluor 647 (red) at the surface of the cells. Distribution of cells in sorting plots, $FL1^-FL4^-$: uninfected CEFs (Q3); $FL1^+FL4^-$: infected CEFs (Q1); $FL1^-FL4^+$: uninfected macrophages (Q4) and $FL1^+FL4^+$: infected macrophages (Q2).*

In a separate experiment, freshly cultured CEFs were infected with pre-sorted MDV-infected CEFs at low numbers to determine the least number of infected CEFs required for producing one plaque and it was observed that around 10 infected CEFs could form one plaque.

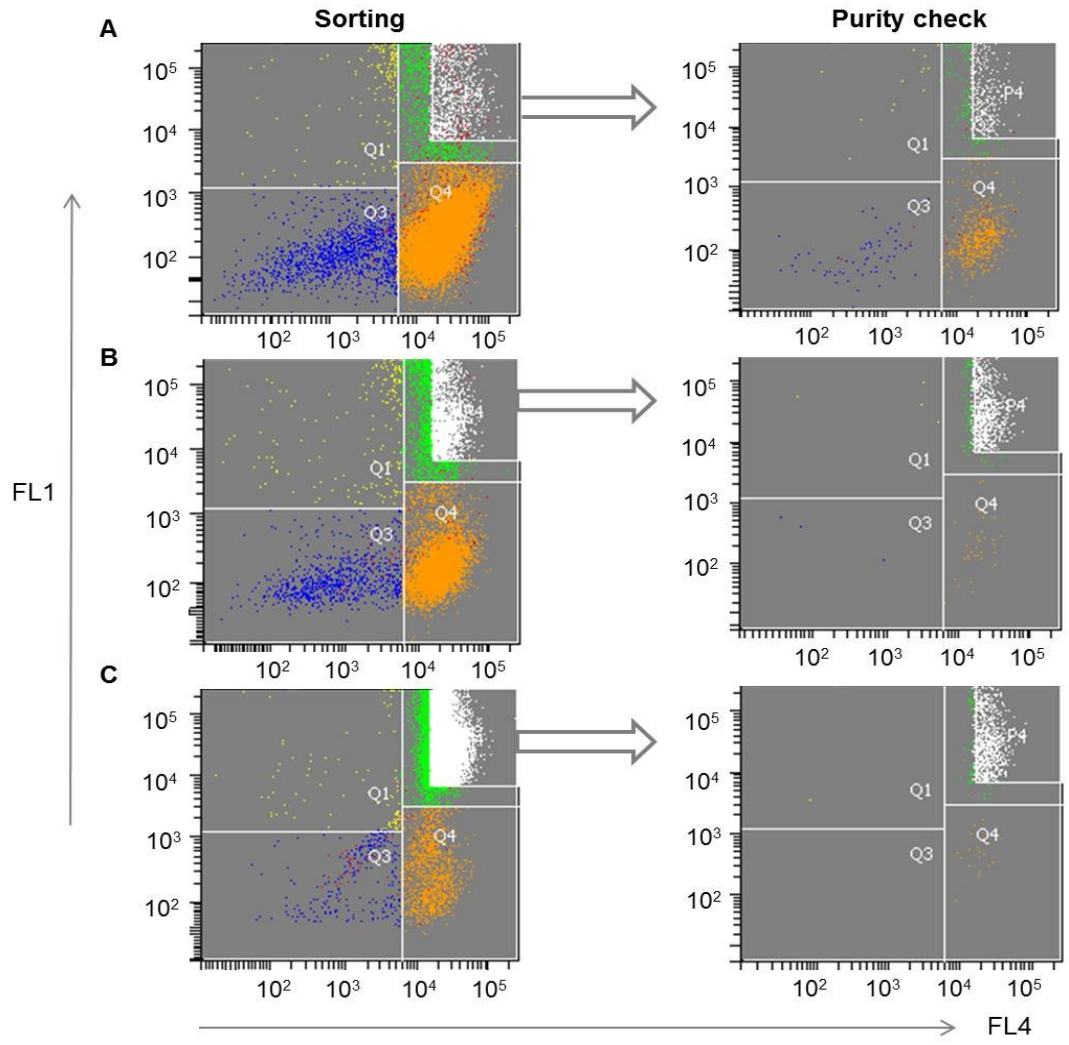

Figure 3.31. *Triple-sorting of MDV-infected macrophages with corresponding purity check. (A) In the first sort, 1.28×10^6 cells were sorted and the purity check revealed presence of lots of contaminant cells (B) Sorted cells were re-sorted and there were 4 contaminant infected CEFs (Q1) per 1000 infected macrophages (C) After sorting macrophages for the third time, the purity check shows one infected CEF (Q1) per 1000 infected macrophages with a total of 87,789 cells remaining at the end. FL1 shows the fluorescence of intracellular GFP (green)-encoded MDV and FL4 shows the fluorescence of Alexa Fluor 647 (red) at the surface of the cells. Distribution of cells in sorting plots, $FL1^-FL4^-$: uninfected CEFs (Q3); $FL1^+FL4^-$: infected CEFs (Q1); $FL1^-FL4^+$: uninfected macrophages (Q4) and $FL1^+FL4^+$: infected macrophages (Q2).*

Therefore, plaques observed in the previous experiment (Figure 3.29C) could perhaps be derived from contaminant infected CEFs. Therefore, it was then decided to re-sort infected macrophages prior to infect CEFs.

3.5.4.1 Re-infection of CEFs with re-sorted MDV-infected macrophages

MDV-infected macrophages were re-sorted to remove contaminant infected CEFs. As shown in Figure 3.31A, 1.28×10^6 infected macrophages were sorted first time and the purity check revealed that there were many contaminant infected CEFs (Q1). So, cells were sorted for a second time (Figure 3.31B) and 2×10^5 infected macrophages were sorted with 4 contaminant infected CEFs (Q1) per 1000 infected macrophages. These cells were sorted one more time (Figure 3.31C) and nearly 90,000 cells were sorted in the final sort. However, still one contaminant infected CEF (Q1) was noticed per 1000 infected macrophages when the purity was checked.

These triple-sorted MDV-infected macrphages were then added to the CEF culture as per methods in section 2.2.18.

Following infection, cells were observed daily under fluorescence microscope. Plaques were detected in CEF monolayers from day 3 onwards and a total of around 50 plaques were counted on 5 dpi from a co-culture of CEFs with nearly 90,000 infected macrophages. The majority of the plaques were fully-formed (Figures 3.32A.i and A.ii). The infected macrophages contained contaminant infected CEFs and as mentioned previously (section 3.5.4), at least 10 infected CEFs were required to form one plaque. These 90,000 infected macrophages contained 90 contaminant infected CEFs and therefore, out of 50, at most 10 plaques could be derived from 90 contaminant infected CEFs, while rest of the plaques were most likely formed from infected macrophages. So, according to this calculation, MDV-macrophage infection

seemed to be a productive infection. Though out of these 50 plaques, a considerable number of plaques (10-12 plaques) were not fully formed as revealed simply by the focal infection of CEFs (Figures 3.32B.i and B.ii).

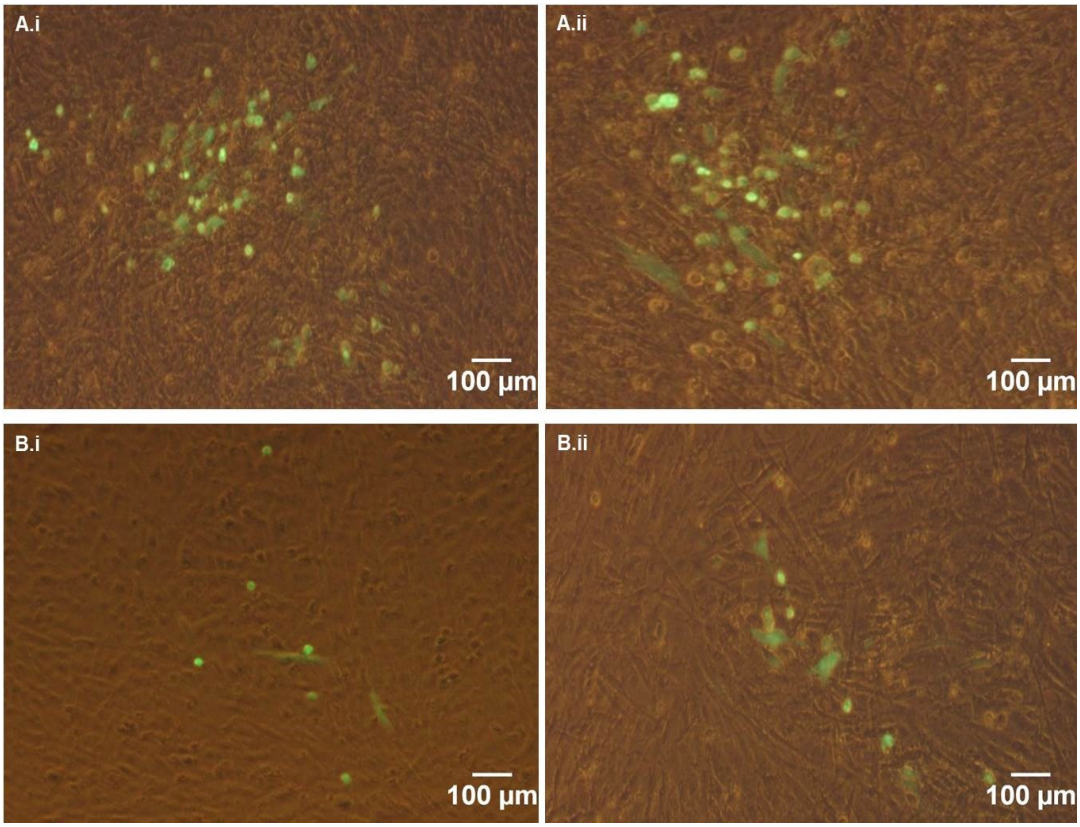

Figure 3.32. *Visualisation of plaques using fluorescence microscope formed in the CEF cultures on 5 dpi. CEFs were infected with triple-sorted MDV-infected macrophages. (A.i and A.ii) Fully-formed plaques. (B.i and B.ii) Appearance of plaque that was not fully-formed.*

3.6 Discussion

The goal of this Chapter was to develop an *in vitro* model of MDV infection of APCs. To date there has been no *in vitro* model for MDV infection of APCs. Repeated efforts, carried out over a course of time, have not been successful (Haffer et al., 1979; von Bulow and Klasen, 1983; Barrow et al., 2003). Therefore, the priority was to solve this enigma which would make it possible to study the role of

APCs in resistance or susceptibility to MD in the inbred chicken lines. In this Chapter, attempts were made to establish and subsequently characterise an *in vitro* model of MDV infection of APCs in outbred J line chickens. For this, chicken bone marrow cells were first cultured and characterised and then infected with MDV.

3.6.1 Culture and characterisation of APCs in outbred chickens

Chicken bone marrow cells cultured with CSF-1 for 7 days displayed typical morphology of macrophages (Figure 3.1B) as shown in Garceau et al. (2010). Cultured macrophages were also phagocytic (Figure 3.1C) as revealed by the uptake of zymosan particles in a widely used *in vitro* phagocytosis assay (Reis e Sousa et al., 1993). Macrophages grown in Sterilin single-square plates were verified phenotypically (CD11, KUL01, MHC II and CD45) by flow cytometry for the surface expression of various molecules to confirm their identity and also to select suitable antibodies for the downstream virus infection experiments. CD11 is a type 1 transmembrane protein that is expressed on a wide variety of cells of myeloid lineage both *in vivo* and *in vitro* (Kansas et al., 1990; Hume, 2008; Wu et al., 2010; Hu et al., 2012; Campisano et al., 2013). In the present study, chicken bone marrow-derived macrophages (both unstimulated and stimulated) showed very high surface expression of CD11 (Figure 3.2B). KUL01 is a widely used chicken macrophage and monocyte marker (Mast et al., 1998) which has recently been identified as a mannose receptor (Staines et al., 2014). High expression of KUL01 was observed in cells before LPS stimulation though it was increased after LPS-stimulation (Figure 3.2B). In contrast, the expression of MHC class II was high in unstimulated cells while it declined in LPS-stimulated macrophages (Figure 3.2B). MHC class II molecules are normally expressed on APCs that play a crucial role in activating $CD4^+$ T cells. Bone

marrow cells cultured for 4 days in T_{75} flasks showed very high surface expression of KUL01 and CD45 (Figure 3.12C), indicating their differentiation to macrophages as early as day 4 of culture. CD45 is a pan-leukocyte marker, which was used in this study as it clearly distinguished macrophages from CEFs in flow cytometric analysis (Figure 3.13C).

DCs were cultured from chicken bone marrow cells in 6-well plates with IL-4 and CSF-2 and then induced maturation with LPS. Cultured DCs can be matured by LPS in humans (Buelens et al., 1997) and this is also the case in chickens (Wu et al., 2010). DCs showed typical cellular aggregates in culture (Figure 3.3B) as reported previously (Wu et al., 2010).

Phenotypic characteristics of chicken bone marrow-derived DCs were determined by flow cytometry for the cell surface expression of CD11, MHC II, CD40 and KUL01. An elevated surface expression of CD11, MHC II and moderate expression of CD40 in immature (unstimulated) DCs was reported previously (Wu et al., 2010). In this study, high surface expression of CD11 was observed in unstimulated DCs whereas, MHC II expressed moderately and apparently no expression of CD40 was noticed (Figure 3.4B). LPS inhalation induces maturation and hence caused up-regulation of MHC II in lung dendritic cells in mammals (Alexis et al., 2005) and also in chickens (de Geus et al., 2012). The surface expression of CD11, MHC II and CD40 was reported to be elevated in LPS-stimulated DCs (Wu et al., 2010). In contrast, in this study, CD11 and MHC II expressed moderately in LPS-stimulated cells with no expression of CD40 (Figure 3.4B). A moderate expression of MHC II (around 40%) and very low expression of CD40 (2-3%) was also observed in the splenic lymphocytes (data not shown) of outbred J line chickens, suggesting that MHC II

expresses at moderate levels in immune cells of vaccinated, outbred chickens and CD40 shows very low surface expression in all types of immune cells of these birds. However, in the absence of a positive control, the functional activity of the antibodies, especially for CD40, needs to be tested in future studies.

A significant percentage of unstimulated and stimulated DCs showed high surface expression of KUL01 (Figure 3.4B), suggesting that KUL01 is also a surface marker for DCs. Expression of KUL01 was also reported in chicken epidermal dendritic cells (Igyártó et al., 2006). Characterising DCs cultured in T_{75} flasks for 4 days by flow cytometry indicated that they were fully differentiated as shown by high expression of KUL01 and CD45 (Figure 3.20C). In the present study, KUL01 was used as a common marker for both macrophages and DCs and there was no specific marker (such as DEC-205) to differentiate DCs from macrophages. Therefore, the difference between the two cell types was primarily based on the morphology (section 3.5.1) and hence there was a chance of potential overlap between the two cell types in the flow cytometry experiments.

3.6.2 Attempts made to infect macrophages by MDV

After culture and characterisation of APCs in outbred chickens, attempts were made to infect them with MDV. Macrophages were selected first for the *in vitro* infection because *in vivo* MDV-macrophage infection was reported previously (Barrow et al., 2003). MDV remains firmly cell-associated in all cultured cells and unlike other herpesviruses, its infectivity cannot be recovered from supernatants or even from cell lysates (reviewed in Denesvre, 2013). However, an attempt was made to isolate and stock cell-free viruses from cultured cell-associated MDV, but infection of macrophages with a cell-free virus preparation was not successful (Figure 3.10). *In*

vitro MDV infections require co-culture of naïve cells with live infected cells. Thus, establishing a co-culture infection model was crucial but difficult to set up when it was revealed that both CEFs and macrophages are adherent to cell culture plates which made co-culturing of cells very problematic. The virus titre was also very low and thus, an average MDV titre of 10^5 pfu/ml was not sufficient to cause infection of macrophages. Repeated experiments to increase virus titre were not successful and caused an increase of CEF numbers which made co-culture infection experiments more difficult (section 3.4.5). Furthermore, Sterilin square plates, which are suitable for macrophage growth and differentiation, were found not to be supportive for cell attachment and growth of CEFs. As a result, macrophages were cultured in T_{75} flasks and then characterised phenotypically by flow cytometry (Figure 3.18).

A significant number of MDV-infected CEFs died during storage and thawing of virus stocks (Figure 3.8), which led to the use of freshly cultured MDV-infected CEFs (Figure 3.9) in the co-culture infection experiments. This brought about an apparent success in MDV-macrophage infection (Figure 3.13), but it had not been possible to incubate co-cultured cells more than 2.5 days and those infected macrophages (section 3.4.9) could also be derived from MDV-infected CEF cultures as discussed below.

CEFs used in this study were collected from 9-11 day old embryos (section 2.2.10). Embryonic macrophages appear in chickens as early as 2.5-4.5 days and their number increases gradually (Cuadros et al., 1993). They play a crucial role during embryonic development by phagocytosing apoptotic cells (Shepard and Zon, 2000). Macrophages also release soluble factors, such as nitric oxide (NO), which is produced by the increased activity of iNOS (indicible nitric oxide synthase). The

production of iNOS in CEF cultures was observed by Xing and Schat (2000), which is also an indication of the presence of macrophage-like cells in CEF cultures. Likewise, the presence of $KUL01^+$ cells was observed in this study in both uninfected and infected CEFs (Figure 3.14). As a widely recognised marker for macrophages, $KUL01^+$ cells thus confirmed the presence of macrophages in CEFs. However, it was not possible to completely segregate macrophages from CEFs with KUL01 staining during sorting as shown in Figure 3.13 and hence CD45 was used to stain and then remove these contaminating macrophages by FACS. For this, MDV-infected CEFs were stained with CD45 on the day of infection of APCs and only GFP^+ CEFs were sorted (Figure 3.15) and thus successful MDV-infection of APCs was established.

3.6.3 Infection of APCs with pre-sorted MDV-CEFs and subsequent characterisation

For the first time, macrophages were successfully infected with MDV *in vitro*, as shown in flow cytometric analyses (Figure 3.19C), in contrast to the previous attempts (Haffer et al., 1979; von Bulow and Klasen, 1983; Barrow et al., 2003). Following the same procedures, DCs were infected and it was shown that DCs could also be infected by MDV *in vitro* (Figure 3.22C). MDV infection of DCs, either *in vivo* or *in vitro*, has not been reported previously. This is the first demonstration of MDV infection of DCs. The infection ratio was the same (1:5) in both co-culture studies with macrophages and DCs, but the number of MDV-infected DCs was approximately 4 times less compared to those of macrophages (Figures 3.22C and 3.19C, respectively). However, one factor should be considered here. DCs were cultured with IL-4 and CSF-2/GM-CSF. IL-4 is an anti-inflammatory cytokine.

Despite the removal of the cytokine containing medium on the day of infection, differentiation of DCs with IL-4 might play a role in preventing MDV infection. The potential role of anti-inflammatory cytokines (such as, IL-10) during viral pathogenesis has been reported previously. For example, excessive or poorly timed IL-10 production in plasma may allow dengue virus (DENV) to escape from immune surveillance during its pathogenesis, whereas DENV induced IL-10 production might lead to immunosuppression and thus enhance viral replication (Tsai et al., 2013). On the other hand, GM-CSF (CSF-2) has been reported to cause inhibition of HIV-1(Human immunodeficiency virus-1) replication in monocyte-derived macrophages (MDM) *in vitro* (Kedzierska et al., 2000). Therefore, as the role of IL-4 and CSF-2 on MDV replication in DCs has not been studied yet, no conclusion can be drawn regarding the lower MDV infection of DCs compared to macrophages.

The confocal microscopic view of live cells revealed the characteristic morphology of macrophages and DCs with or without MDV infection (Figures 3.24 and 3.25, respectively). Cells have empty vacuoles which most likely occurred due to activation by MDV (Figure 3.24). Macrophages might become activated when they contact a foreign particle or sense any specific stimulus (Janeway and Medzhitov, 2002) which in turn causes formation of vacuoles in the cytoplasm (Petricevich et al., 2008). These vacuoles play a role in taking up extracellular particles, and fusion of lysosomal compartments with vacuoles is a fundamental mechanism by which macrophages kill pathogens (Luzio et al., 2003). Lysosomal compartments are perhaps better adapted for digestion of internalised material and thus, the clearance of invading microorganisms, which is a major function for macrophages in innate immunity (Aderem and Underhill, 1999; Lauber et al., 2004). Confocal pictures also

revealed projections or dendrites from the surface of the cells which are characteristic of DCs (Figure 3.25). Dendrites enable DCs to interact with T cells (Banchereau and Steinman, 1998; Hugues et al., 2004). On 3 dpi, macrophages and DCs were infected with MDV as indicated by the emission of GFP from the nucleus of cells (Figures 3.24 and 3.25, respectively). Phagocytic cells would rapidly degrade any virus antigens present in phagosomes, and hence their antigenicity will be lost (reviewed by Aderem and Underhill, 1999). So, if MDV-infected CEFs are phagocytosed by macrophages, there will be no GFP expression in the nucleus or if it emits, it will only be from the cytoplasm unless MDV can evade lysosomal degradation. Herpesviruses can exploit endocytic pathways during entry to the cells (Clement et al., 2006). There are different forms of endocytosis, such as phagocytosis, macropinocytosis, caveolae mediated endocytosis, and clathrin-mediated endocytosis (CME) and many viruses can hijack the CME machinery in order to be internalized into host cells (Doherty and McMahon, 2009). Phagocytosis is a clathrin-independent method of engulfing large extracellular particles and it most likely requires actin rearrangement and dynamin assembly and is regulated by signalling pathways that apparently involve action of RhoA GTPase and may also involve tyrosine kinases (Clement et al., 2006). HSV-1 (herpes simplex virus-1) infects cells by exploiting the endocytic pathway of cells with mimicking many features of phagocytosis, a feature which is common for other herpesviruses as well, such as CMV (cytomegalovirus) and HHV-8 (human herpesvirus-8) (Clement et al., 2006; Tiwari and Shukla, 2012).

MDV expresses herpesvirus specific immediate early (ICP4), early (pp38) and late (gB) genes and the presence of ICP4 in the nucleus of *in vivo* infected KUL01^{+} cells

confirmed the infection of macrophages by MDV (Barrow et al., 2003). In this study, the transcription of herpesvirus specific ICP4, pp38 and gB and MDV-specific L-Meq was observed in MDV-infected macrophages and DCs (Figure 3.26), which is also a demonstration of virus infection. However, detection of viral antigens, including structural and non-structural proteins needs to be performed in future studies to confirm virus replication in APCs.

Confocal video microscopy gives an indication of the possible modes of MDV transmission to macrophages on the day of infection. Movie A (also in Figure 3.27) illustrates GFP particles inside the intracellular vacuoles of macrophages, indicating internalisation of virus most likely by phagocytosis. Though it is not clear from this movie, as MDV is a cell-associated virus *in vitro*, phagocytosis of virus should therefore have occurred by phagocytosis of MDV-infected apoptotic cells by macrophages. Following internalisation, virus particles could either be destroyed within phagolysosomal compartments or cells can be infected by the viruses as herpesviruses have evolved mechanisms to escape lysosomal degradation by inhibiting autophagy. Autophagy is a cellular housekeeping process that delivers aged or unnecessary cytoplasmic organelles for lysosomal degradation, and thus facilitates pathogen degradation and pathogen fragment loading onto MHC molecules for antigen presentation to T cells (Mizushima et al., 2008). As for example, HSV-1 counteracts the induction of autophagy via ICP34.5 by antagonising autophagy-stimulating PKR (protein kinase RNA-activated) signalling (Orvedahl et al., 2007). Movie B (also in Figure 3.28) provides supportive evidence of cell-to-cell transmission of MDV to macrophages. MDV remains strictly cell-associated *in vitro* and hence, possible cell-to-cell transmission of viruses could be predicted. The cell-

to-cell mode of virus transmission has only been described for enveloped viruses and it has been adopted by many animal virus families including herpesviruses as a potential way of evasion of humoral immunity (Sattentau, 2008). Alphaherpesviruses can transmit between cells by inducing syncytium formation and express a range of glycoproteins, gB, gD and gH-gL on the virus infected cell that have a role in cell-to-cell fusion (Campadelli-Fiume et al., 2007; Reske et al., 2007). This video shows potential cellular connections with green cellular projections from and between cells, which are most likely actins (Caroline Denesvre, personal communication). During HSV-1 and PRV (pseudorabies virus) entry, rearrangement of the actin cytoskeleton associated with projection of plasma membrane took place, which was then followed by trafficking of virions in phagosome-like vesicles (La Boissiere et al., 2004; Favoreel et al., 2005; Clement et al., 2006). Schumacher et al. (2005) also reported that polymerisation of the actin cytoskeleton is required for the effective cell-to-cell spread of MDV in chicken embryo cells *in vitro*. To date, very little is known about MDV transmission to APCs *in vitro*, but as a herpesvirus this method could also be suggestive for MDV entry as it co-relates with the method described by Clement et al. (2006) in which the author mentioned that herpesviruses can induce actin or tubulin containing structures by which virions project towards adjacent cells (Figure 1.6d). However, advanced imaging research is required to discover the exact mode of transmission of MDV to APCs.

In order to determine the type of MDV-macrophage infection, attempts were made to re-infect CEFs with GFP^+ macrophages *in vitro*. Barrow et al. (2003) reported that the *in vivo* MDV-macrophage infection is an abortive infection as infected macrophages failed to produce plaques in CEF cultures. In the present study, plaques

were observed in CEF cultures in the first experiment (Figure 3.29), indicating the productive nature of MDV-macrophage infection. However, this conclusion came under suspicion due to presence of contaminant infected CEFs within the infected macrophages (Figure 3.30). MDV is strictly cell-associated *in vitro* and as shown previously, virus transmission could take place between cells fused together with intercellular bridges (Movie B). These 'fused' cells form doublets and by this way contaminant infected CEFs could perhaps be present in the sorted infected macrophage populations. For this reason, a separate gate was created in all the cell sorting experiments to keep these doublet cells out of the analysis, but surprisingly there were still contaminant cells in every sorting of infected cells (Figure 3.30). Infected macrophages were therefore sorted for three times to remove the contaminant infected CEFs though it was not possible to sort a fully pure population of infected macrophages (Figure 3.31C). However, infection of CEFs with around 90,000 MDV-infected macrophages resulted in formation of approximately 50 plaques in the CEF cultures (Figures 3.32A.i and A.ii), with considering the inclusion of at best 10 plaques which were, perhaps, formed from the contaminant infected CEFs. Among the plaques, not all were fully formed (Figures 3.32B.i and B.ii), but it needs to be considered that these infected macrophages were triple-sorted and hence severely stressed, which might have hindered the ability to produce fully-formed plaques. However, further studies are required to clarify this.

Following establishment of *in vitro* MDV-APC infection, B and T cells were co-cultured with infected macrophages to determine if MDV infection could transfer from macrophages to these cells. All the results are presented and discussed in Chapter 4.

Chapter 4:

In vitro MDV infection of B and T lymphocytes in outbred chickens

4.1 Introduction

During *in vivo* infection, MDV is thought to be engulfed by phagocytes in the chicken lungs and carried to the lymphoid tissues where they initially infect B lymphocytes and subsequently infect activated T lymphocytes. Both B and T cells can be infected *in vitro* with MDV-infected CEFs (Kaspers, 2014) and an *in vitro* MDV-APC infection model has also been developed in the present study (Chapter 3). It has been proposed that *in vivo* the virus infection transmits from macrophages to B cells via the ellipsoid-associated reticular cells (EARCs) (Baigent and Davison, 2004). In the spleen, EARCs, which border capillaries, are closely surrounded by B cells. These EARCs are phagocytic and MDV antigens could readily be identified in splenic EARCs (Jeurissen et al., 1989), a feature which suggests why B cells are the main targets for acute cytolytic infection of MDV (Baigent and Davison, 2004). However, it has not yet been reported *in vitro* that the virus infection could transfer from APCs to B and T cells. Barrow et al. (2003) first reported that MDV antigens can be detected in splenic macrophages *in vivo*, but at the same time this MDV-macrophage infection was reported as a possible abortive infection because infected macrophages were not able to produce plaques in CEF cultures, suggesting that MDV infection cannot be transmitted from macrophages to other cells. However, in this thesis *in vitro* MDV-infected macrophages were able to form plaques in CEF cultures (Chapter 3), which suggests that MDV infection could possibly be transferred from macrophages to B or T cells. Therefore, the aim of this Chapter was to mimic this virus transmission process *in vitro*. Experiments were carried out using cells from outbred chickens by co-culturing B cells or splenocytes with MDV-

infected macrophages. Cells were then analysed by flow cytometry for the presence of MDV.

4.2 Positive sorting and subsequent characterisation of B cells from spleen

To determine whether MDV could be transferred from macrophages to B cells, B lymphocytes were co-cultured with *in vitro* infected macrophages. MDV-infected macrophages were chosen because co-culture studies showed that higher numbers of macrophages were infected than DCs (Figures 3.19 and 3.22, respectively).

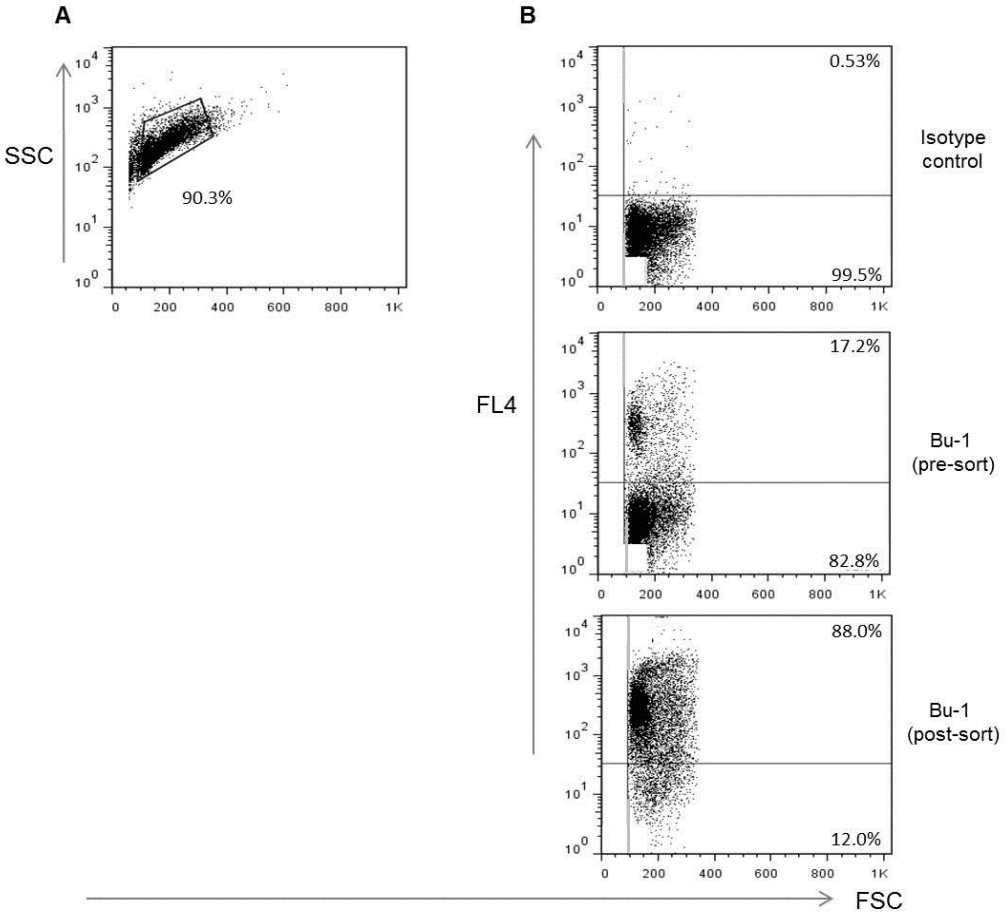

Figure 4.1. *Flow cytometric characterisation of pre- and post-sort B lymphocytes. (A) Cells were analysed in SSC/FSC gate (B) Surface staining of B cells with Bu-1 compared to isotype control antibody (Gr 13.1) in FL4/FSC plots. FL4 shows the fluorescence of Alexa Fluor 647.*

Prior to the infection, B cells were positively sorted from the spleen (section 2.4.4) and phenotypically characterised by flow cytometry as described in section 2.4.2 after staining with Bu-1 and Gr 13.1(isotype control). Bu-1 (clone AV20, subclass IgG1) is expressed on B cells from bursa, spleen, thymus and peripheral blood lymphocytes (Rothwell et al., 1996).

Cells from both pre- and post-sort tubes were analysed by flow cytometry to check the staining pattern of Bu-1. Flow cytometric analyses revealed that 88% cells were stained with Bu-1 after sorting, while prior to the sort, only 17.2% cells were Bu-1^{+} (Figure 4.1B).

Following characterisation of positively sorted B cells, cells were infected with pre-sorted MDV-infected macrophages.

4.2.1 Infection of positively sorted B cells with MDV-infected macrophages

Positively sorted B lymphocytes were co-cultured with MDV-infected macrophages as per methods in section 2.2.18 to determine if infected macrophages could infect B cells. As described in section 2.2.18, B cells were infected at an infection ratio of 1:5 (infected macrophages:positively sorted B cells). After 2.5 days of infection, cells were stained with Bu-1 and Gr 13.1(isotype control) and characterised by flow cytometry (section 2.4.2).

While running samples in the flow cytometer, cells were mistakenly acquired in the log phase of SSC instead of linear phase. However, around 95% of the SSC/FSC gated cells were found alive when analysed in FL3/FSC plot based on 7-AAD staining (Figure 4.2A). As revealed by the Bu-1 staining, there were apparently no

infected B cells ($FL1^+FL4^+$) following co-cultured with MDV-infected macrophages, though there were more than 60% uninfected B cells (Figure 4.2B).

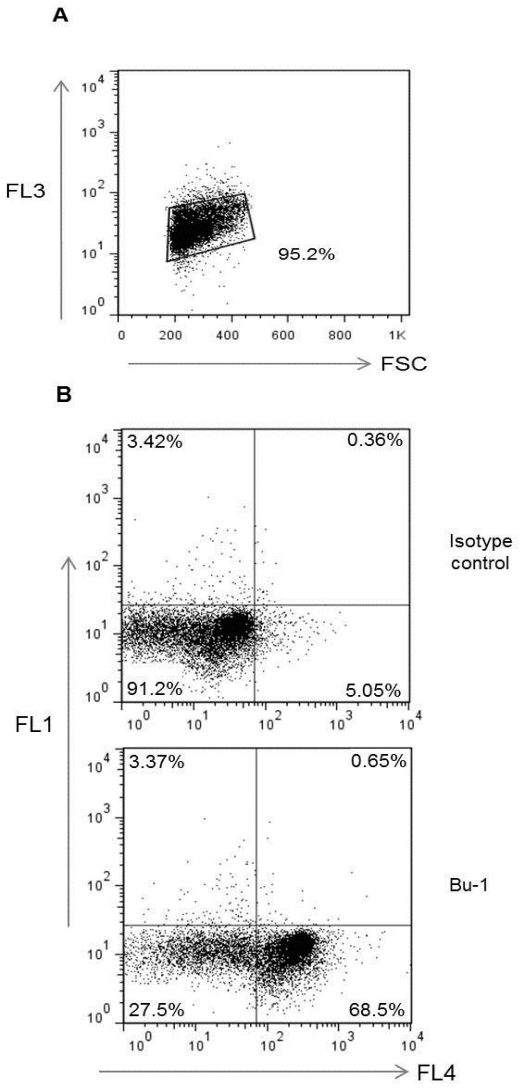

Figure 4.2. *Infection of positively sorted B lymphocytes with MDV-infected macrophages. Cells were infected at 1:20 ratios (infected macrophage:B cell). (A) SSC/FSC gated cells were analysed in FL3/FSC plot to gate live cells. FL3 shows the fluorescence of 7-AAD. (B) Live cells were analysed in FL1/FL4 dot plots to detect Bu-1^+ cells compared to isotype control antibody (Gr 13.1). FL1 shows the fluorescence of intracellular GFP (green)-encoded MDV and FL4 shows the fluorescence of Alexa Fluor 647 (red) at the surface of the cells. Distribution of cells in Bu-1 staining, $FL1^-FL4^-$: uninfected splenocytes; $FL1^+FL4^-$: infected splenocytes; $FL1^-FL4^+$: uninfected B cells and $FL1^+FL4^+$: infected B cells.*

Co-culture of positively sorted B cells with MDV-infected macrophages did not result in infection of B cells (Figure 4.2B). Positive sorting of B cells may act as a stimulus which perhaps caused cell death as the cell numbers in each tube were very low. Therefore, the next step was to infect negatively sorted B cells with MDV-infected macrophages.

4.2.2 Infection of negatively sorted B cells with MDV-infected macrophages

B lymphocytes were negatively sorted from spleens as positive sorting might cause increased cell death or alter the cell phenotype. Negatively sorted cells, containing B cells and other splenic non-T cells were collected as per methods in section 2.4.4 and co-cultured with pre-sorted MDV-infected macrophages at an infection ratio of 1:5 (infected macrophages:negatively sorted B cells) (section 2.2.18). In this experiment, cells were incubated for 1 day after infection because incubation for a longer time could also be a cause of increased cell death. Cells were analysed by flow cytometry after staining with Bu-1 and Gr 13.1(isotype control) as described in section 2.4.2. Around 45% cells were gated in the SSC/FSC plot (Figure 4.3A) and of these, 65% cells were selected as live cells (Figure 4.3B).

Flow cytometric analyses of live cells in the FL1/FL4 plot revealed that there were no infected B cells ($FL1^{+}FL4^{+}$), though 22% of live cells remained as uninfected B cells (Figure 4.3C).

As repeated efforts to infect B cells with MDV-infected macrophages were not successful, attempts were then made to determine if splenocytes could be infected by MDV-infected macrophages.

4.3 Isolation of splenocytes and subsequent flow cytometric characterisation

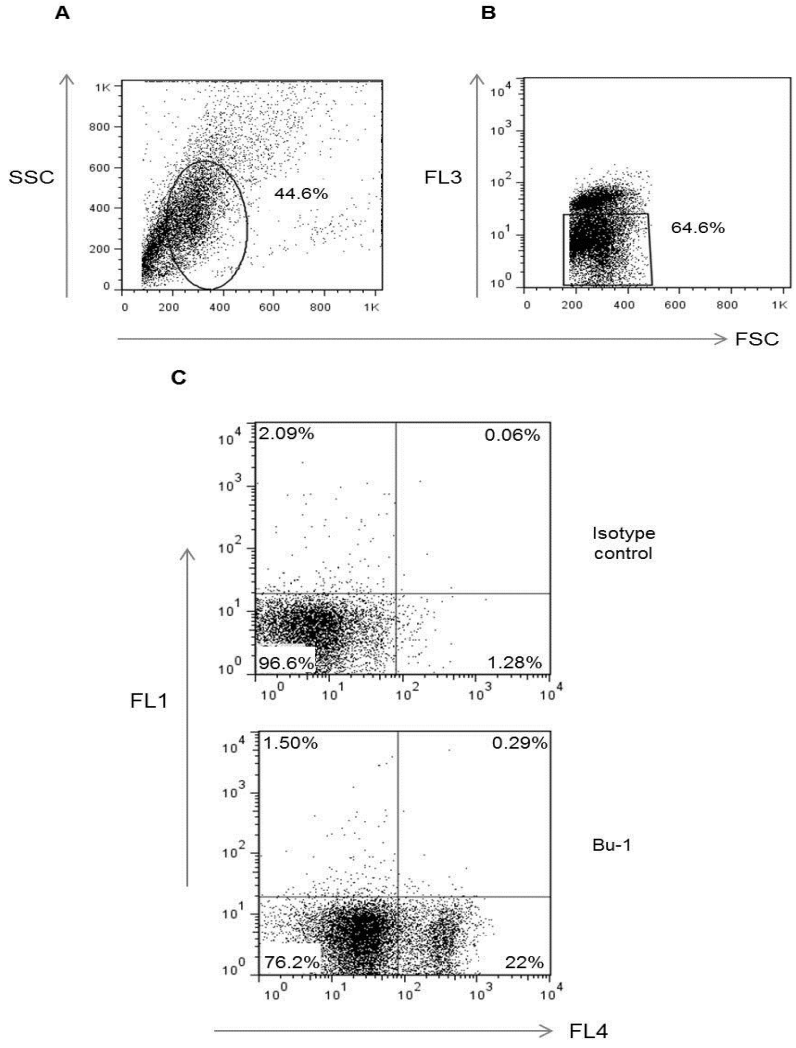

Figure 4.3. *Infection of negatively sorted B lymphocytes with MDV-infected macrophages. Cells were infected at 1:5 ratios (infected macrophage:B cells). (A) Cells were gated in SSC/FSC plot. (B) SSC/FSC gated cells were analysed in FL3/FSC plot to gate live cells. FL3 shows the fluorescence of 7-AAD. (C) Live cells were analysed in FL1/FL4 dot plots to detect Bu-1$^+$ cells compared to isotype control antibody (Gr 13.1). FL1 shows the fluorescence of intracellular GFP (green)-encoded MDV and FL4 shows the fluorescence of Alexa Fluor 647 (red) at the surface of the cells. Distribution of cells in Bu-1 staining, FL1$^-$FL4$^-$: uninfected splenocytes; FL1$^+$FL4$^-$: infected splenocytes; FL1$^-$FL4$^+$: uninfected B cells and FL1$^+$FL4$^+$: infected B cells.*

Co-culture infection experiments were carried out to test if splenocytes could be infected with MDV-infected macrophages. Prior to the infection, splenocytes were characterised phenotypically by flow cytometry.Splenocytes were isolated and cultured in T_{75} flasks for 1 day as described in section 2.2.16. Single colour immunofluorescence staining was carried out with Bu-1, CD3 and Gr 13.1 (isotype control) using procedures in section 2.4.2. CD3 (antibody CT-3, class IgG1) was used as a pan-T lymphocyte marker (Chen et al., 1986).

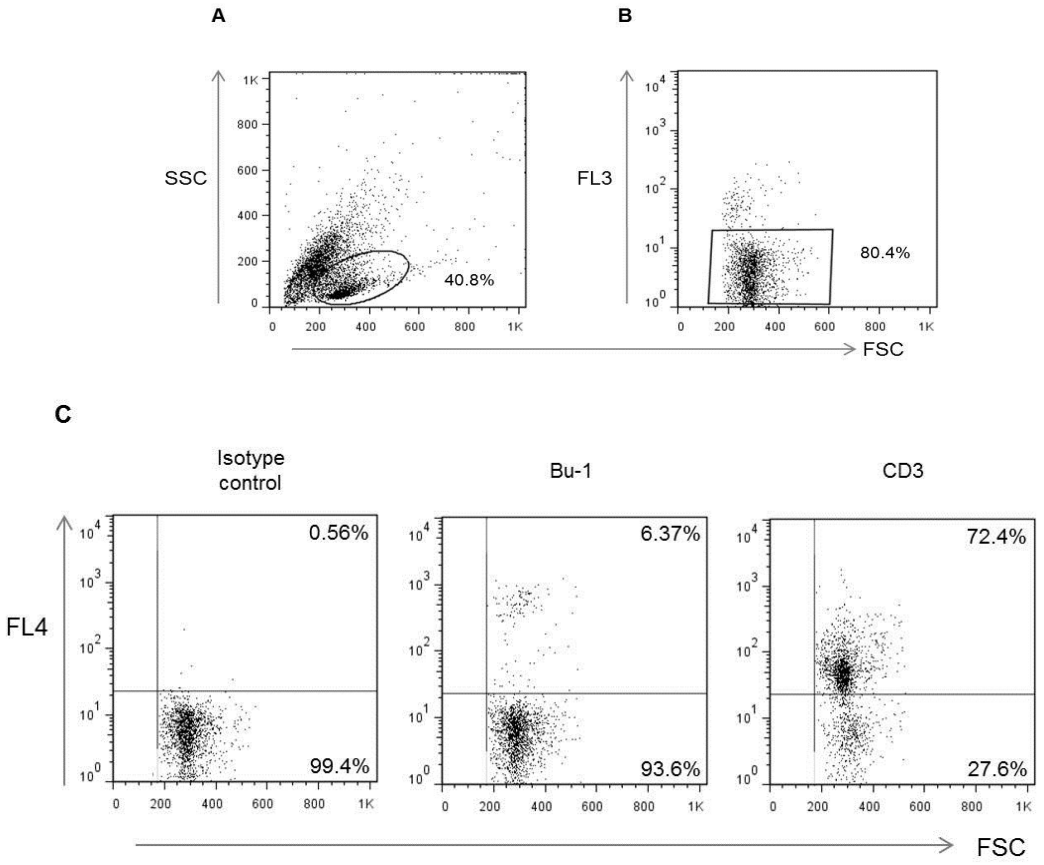

Figure 4.4. *Phenotypic characterisation of splenocytes on day 1 of culture by flow cytometry. (A) Cells were gated in SSC/FSC plot. (B) SSC/FSC gated cells were plotted in FL3/FSC plot to gate live cells. FL3 shows the fluorescence of 7-AAD. (C) Live cells were tested for surface expression of Bu-1 and CD3 compared with cells stained with isotype control antibody (Gr 13.1). FL4 shows the fluorescence of Alexa Fluor 647.*

Approximately 40% cells were gated as live lymphocytes in the SSC/FSC plot (Figure 4.4A). Analysis of these cells in the FL3/FSC plot revealed that 80% cells were live (Figure 4.4B). Phenotypic analyses of live cells showed that 6% cells were Bu-1$^+$, whereas more than 70% were CD3$^+$ T cells (Figure 4.4C).

It was suggested that in the *in vivo* MDV infection the virus is transmitted from macrophages to B cells in the spleen (Calnek, 2001). The ultimate target in this Chapter is to mimic this infection *in vitro* by co-culturing MDV-infected macrophages with splenocytes. Prior to this, an experiment was carried out to test if B and T cells can be infected with MDV-infected CEFs. Though *in vitro* infection of B and T cells has been described previously (Kaspers, 2014), this experiment was done to check whether it can be repeated under the existing experimental conditions.

4.3.1 Infection of splenocytes with MDV-infected CEFs

Splenocytes were co-cultured with MDV-infected CEFs to determine whether MDV infection could be transmitted from CEFs to B and if possible, T lymphocytes. Following isolation of splenocytes (section 2.2.16), cells were infected with pre-sorted MDV-infected CEFs at a ratio of 1:5 (CEF:splenocyte) in T_{75} flask as per methods in section 2.2.17.

Following infection, cells were incubated for 2 days as a substantial numbers of GFP$^+$ cells were visible when examined under fluorescence microscope. At 2 dpi, cells were analysed by flow cytometry after staining with Bu-1, CD3 and Gr 13.1 (isotype control) as described previously (section 2.4.2).

Around 13% cells were gated as live lymphocytes in the SSC/FSC plot (Figure 4.5A). Nearly 70% of the lymphocytes were found to be alive after staining with 7-AAD (Figure 4.5B).

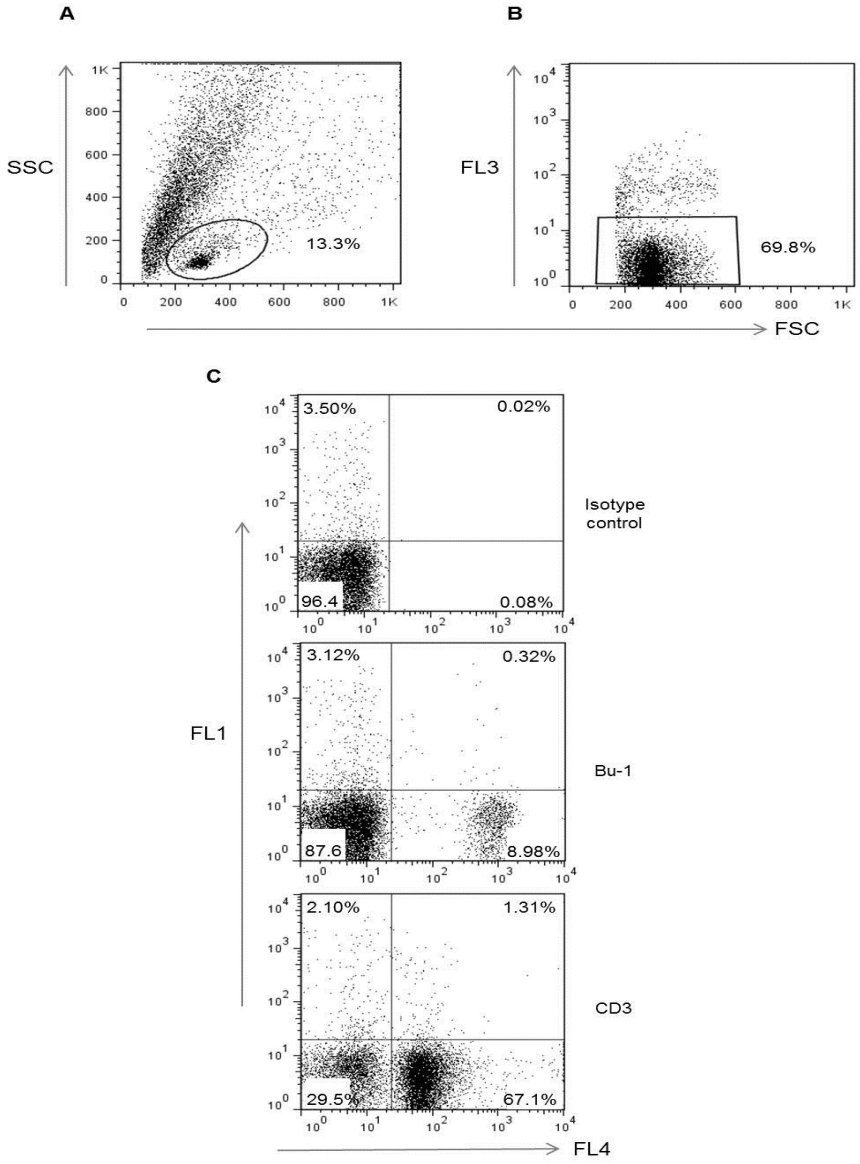

Figure 4.5. *Flow cytometric characterisation of splenocytes following infection with pre-sorted MDV-infected CEFs. Cells were infected at 1:5 ratios (infected CEF:splenocyte). (A) Cells were gated in SSC/FSC plot. (B) SSC/FSC gated cells were analysed in FL3/FSC plot to gate live cells. FL3 shows the fluorescence of 7-AAD. (C) Live cells from FL3/FSC plot were analysed in FL1/FL4 to detect Bu-1$^+$ and CD3$^+$ splenocytes compared to isotype control (Gr 13.1). FL1 shows the fluorescence of GFP (green)-encoded MDV and FL4 shows the fluorescence of Alexa Fluor 647 (red) at the surface of the cells. Distribution of cells in Bu-1 and CD3 staining, FL1$^-$FL4$^-$: uninfected splenocytes; FL1$^+$FL4$^-$: infected splenocytes; FL1$^-$FL4$^+$: uninfected B/T cells and FL1$^+$FL4$^+$: infected B/T cells.*

Flow cytometric analyses of live cells in FL1/FL4 dot plots revealed that the proportion of infected B cells, as shown by Bu-1 staining, was 0.32%. On the other hand, the number of infected T cells ($CD3^+$) was 1.31% (Figure 4.5C).

It was clear from this experiment that MDV infection could be transmitted from infected CEFs to B and T cells *in vitro* in the present experimental conditions. Hence in the next experiment, an attempt was made to explore whether virus transmission could take place from MDV-infected macrophages to B or T cells.

4.3.2 Infection of splenocytes with MDV-infected macrophages

Following infection of B and T cells *in vitro* by MDV-infected CEFs, MDV-infected macrophages were co-cultured with splenocytes.

Sorting large numbers of MDV-infected macrophages on 3 dpi was very challenging and in the first attempt (data not shown), 2.5×10^6 splenocytes were infected with 0.5×10^6 infected macrophages in 6-well plates at 1:5 ratios (infected macrophage:splenocyte) as per methods in section 2.2.18. This experiment was not successful as GFP^+ cells were not detected after 24 h of infection using flow cytometry.

An attempt was then made to sort infected macrophages on 1 dpi. In this experiment, 5×10^6 MDV-infected macrophages were sorted on 1 dpi and 2.5×10^7 splenocytes were infected at a ratio of 1:5 (infected macrophage:splenocyte) in T_{75} flask according to the procedures in section 2.2.18. Following infection, it was observed that the number of GFP^+ cells was rapidly declining from the culture flask. Thus on 1 dpi, cells were harvested by pipetting and subsequently analysed by flow cytometry after staining with Bu-1, CD3 and Gr 13.1 (isotype control) as per methods in section 2.4.2.

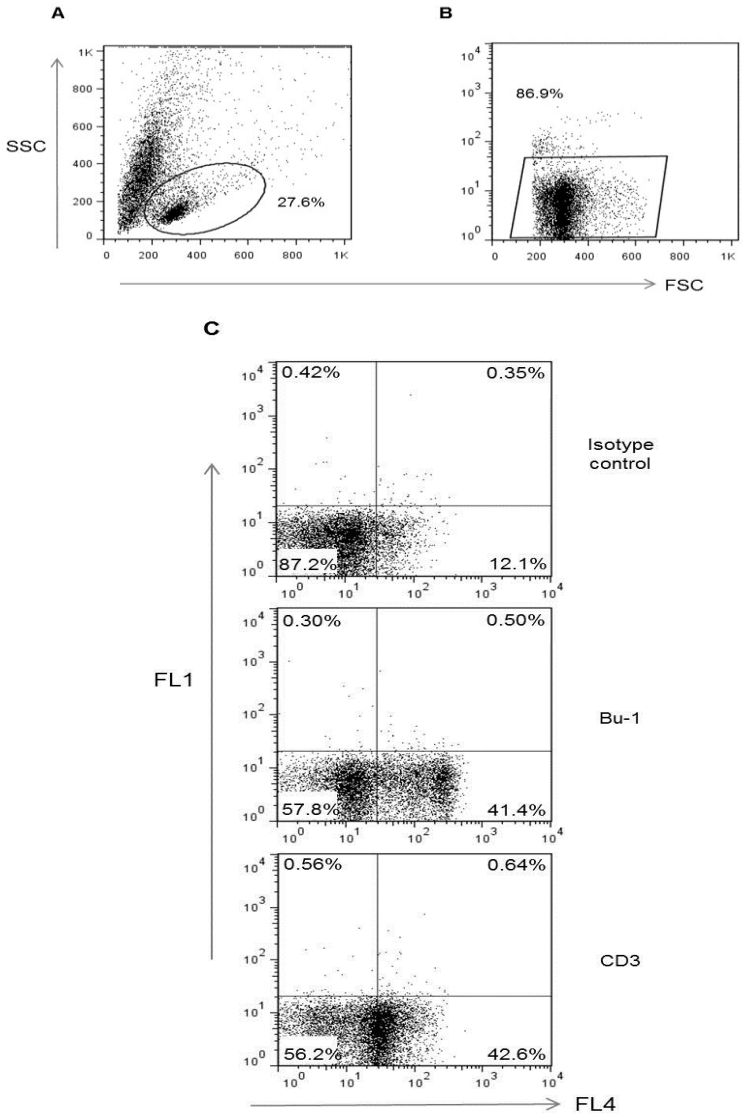

Figure 4.6. *Flow cytometric characterisation of splenocytes following infection with pre-sorted MDV-infected macrophages on 1 dpi. Cells were infected at 1:5 ratios (infected macrophage:splenocytes). (A) Cells were gated in SSC/FSC plot (B) SSC/FSC gated cells were analysed in FL3/FSC plot to gate live cells. FL3 shows the fluorescence of 7-AAD. (C) Live cells were analysed in FL1/FL4 dot plots to detect Bu-1$^+$ and CD3$^+$ splenocytes compared to isotype control (Gr 13.1). FL1 shows the fluorescence of GFP (green)-encoded MDV and FL4 shows the fluorescence of Alexa Fluor 647 (red) at the surface of the cells. Distribution of cells in Bu-1 and CD3 staining, FL1$^-$FL4$^-$: uninfected splenocytes; FL1$^+$FL4$^-$: infected splenocytes; FL1$^-$FL4$^+$: uninfected B/T cells and FL1$^+$FL4$^+$: infected B/T cells.*

In the SSC/FSC plot, around 28% cells were gated as lymphocytes (Figure 4.6A) and nearly 90% of these cells were found to be alive after staining with 7-AAD (Figure 4.6B).

Analysis of live cells in FL1/FL4 dot plots revealed that there were apparently no infected B or T cells as shown by Bu-1 and CD3 staining ($FL1^{+}FL4^{+}$) (Figure 4.6C). Hence, attempts to infect splenocytes with MDV-infected macrophages were not successful.

4.4 Discussion

Splenic B and T cells or whole splenocytes were co-cultured with MDV-infected macrophages to determine whether the infection could transfer from macrophages to B or T cells. In the previous Chapter, MDV-infected macrophages produced plaques in CEF cultures, indicating that MDV-macrophage infection is a productive type of infection. During *in vivo* infection, MDV infection presumably transmits from macrophages to B cells possibly through EARCs in the lymphoid tissues. To mimic this process, several attempts were made to infect B and T cells with MDV-infected macrophages *in vitro*.

Efforts were initially made by co-culturing sorted B lymphocytes with MDV-infected macrophages. In the first experiment, B cells were positively sorted from spleen and subsequently co-cultured with MDV-infected macrophages, but there were no detectable infected B cells (Figure 4.2C). In the second experiment, B cells were negatively sorted as positive sorting might cause alteration of B cell-phenotype in culture. However, this co-culture infection experiment was also not successful as there were no measurable infected Bu-1^{+} cells (Figure 4.3C).

It was then tested whether B and T cells could be infected *in vitro* with MDV-infected CEFs in the present experimental conditions. Although the number of infected cells were very low, it has been observed that both B and T cells could be infected in a single experiment where splenocytes were co-cultured with MDV-infected CEFs (Figure 4.5C). In contrast, B and T cells were not infected after co-culture with MDV-infected macrophages (Figure 4.6C).

It was observed that, unlike MDV-infected CEFs, MDV-infected macrophages were very difficult to work with because they were found to die quickly after sorting as observed by the rapid disappearance of GFP^+ cells in culture, a feature which most likely caused downstream experiments unsuccessful.

Due to the strict cell-associated nature of MDV, it requires live cells to cause infection to other cells. In the experiments where CEFs were infected with sorted MDV-infected macrophages (Chapter 3), it was possible to incubate cells for a long time after infection due to high longevity of cultured CEFs. Infected macrophages also died in those experiments at 2-3 dpi but MDV infection was harboured in CEFs and gradually re-emerged by forming plaques from 3-5 dpi, a feature which was absent in B cell infections. Specific growth factors or activating ligands (such as CD40L) that promote growth and activation of B cells (Kothlow et al., 2008) were not used for B cell cultures in this study. This probably accounts for the observed rapid death of B cells and the failure to infect these cells with MDV.

Although these experiments were not successful, it is still too early to draw the conclusion about the ability to infect of B and T cells *in vitro* with MDV-infected macrophages. Viral plaques were formed in CEF cultures co-cultured with infected macrophages (Chapter 3), indicating MDV infection can be transmitted from

macrophages to other cells. Further experiments are required to determine whether infection can be established in suitably activated B and T cells.

Following establishment and characterisation of the *in vitro* MDV-APC infection model in outbred chickens, this model was then applied to APCs of inbred MD-resistant (6_1) and susceptible (7_2) chicken lines. The results will be presented in Chapter 5.

Chapter 5:

In vitro MDV infection of APCs in inbred chicken lines

5.1 Introduction

MDV is primarily a lymphotrophic alphaherpesvirus though it also infects APCs in its life cycle. However, the cell or cells involved in resistance or susceptibility to MD are yet to be explored. Genetic resistance to MD is a complex trait, as genes from the MHC and also from outside of the MHC are involved. However, two chicken inbred lines, 6_1 and 7_2 which are highly resistant and susceptible to MD, respectively, are MHC-congenic (Cole, 1968), which shows that the resistance to MD is largely determined by genes outside of the MHC. Research has been carried out to determine the basis of resistance or susceptibility between the two lines, such as differences in the virus titre (10-fold higher in susceptible compared to resistant birds) in splenocytes (Lee et al., 1981) and differential cytokine expression in splenocytes (IL-6 and IL-18 were expressed in susceptible but not in resistant birds) (Kaiser et al., 2003) during the cytolytic phase of MDV infection. However, an in-depth study of the role of any specific immune cell population in resistance or susceptibility has not been carried out. Differential gene expression was observed in splenocytes of these two lines as early as 3 dpi (Smith et al., 2011) and by this time, MDV infection occurs in APCs, B and activated T cells. Therefore, any or all of these cells could be involved in determining resistance to MD. In this study, the hypothesis was tested that the resistance mechanism is expressed at the early phase of infection when MDV encounters APCs. To study the MDV infection of APCs in MD-resistant and susceptible birds, a *de novo in vitro* MDV-APC infection model has been developed (Chapter 3). In this Chapter, the model was applied to the APCs of these two inbred lines and the aims were to characterise infected and uninfected cells by flow cytometry and also to measure the cytokine responses in APCs between two lines by

qRT-PCR. APCs were first cultured and characterised phenotypically from the two lines and then infected with MDV-infected CEFs.

5.2 Culture and characterisation of BMDM from the chicken inbred lines 6_1 and 7_2

5.2.1 Morphological characterisation

Chicken bone marrow cells from inbred lines 6_1 and 7_2 were cultured in T_{75} flasks for 4 days following procedures described previously (section 2.2.9). In both cases, cultured macrophages showed a heterogeneous population containing loosely and strongly adherent spindle shaped cells (Figures 5.1A and B).

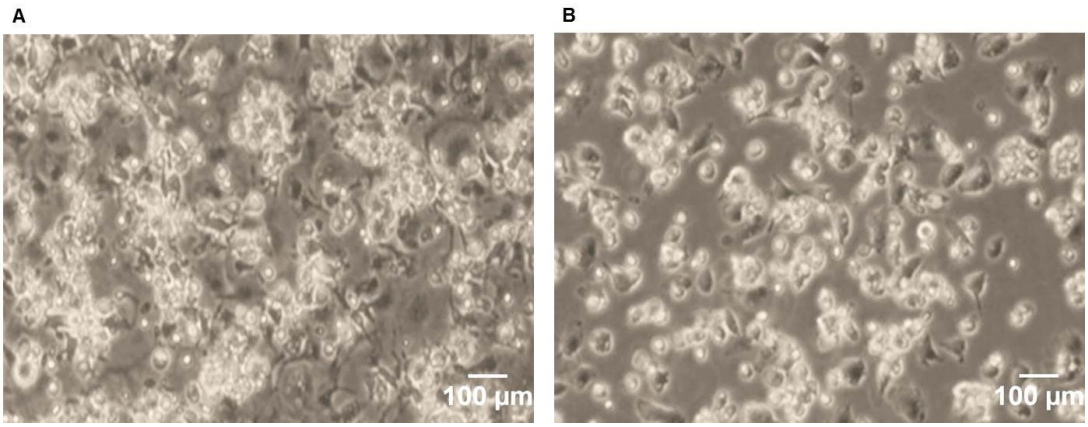

Figure 5.1. *Morphological properties on day 4 of BMDM cultured from inbred chickens. (A) Cells cultured from line 6_1 birds. (B) Cells grown from line 7_2 birds.*

5.2.2 Characterisation by flow cytometry

Macrophages from two inbred lines were cultured in T_{75} flasks (section 2.2.9). On day 4, cells were analysed by flow cytometry after staining with KUL01, CD45 and Gr 13.1 (isotype control) as described in section 2.4.2.

Around 48% and 72% cells were gated in SSC/FSC plots as macrophages for further analysis in lines 6_1 and 7_2, respectively (Figure 5.2A). Live cells were then gated in FL3/FSC plot based on 7-AAD staining (Figure 5.2B).

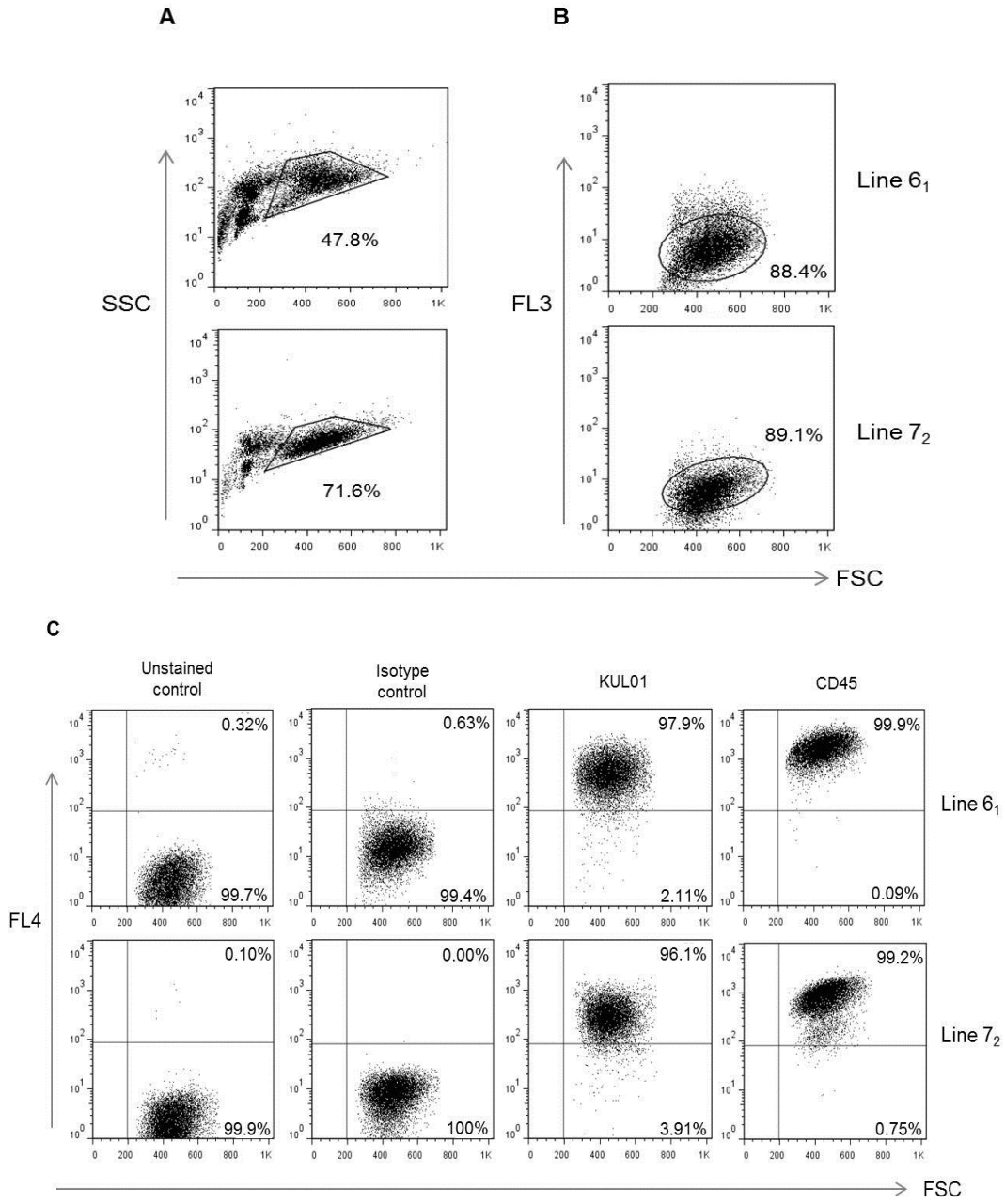

Figure 5.2. *Phenotypic characterisation of BMDM by flow cytometry from inbred chickens. (A) Cells from line 6_1 and 7_2 were gated in SSC/FSC plot. (B) SSC/FSC gated cells from both lines were plotted in FL3/FSC channel to gate live cells. FL3 shows the fluorescence of 7-AAD. (C) Live cells from line 6_1 and 7_2 were tested for surface expression of KUL01 and CD45 and compared with unstained cells and cells stained with the isotype control antibody (Gr 13.1). FL4 shows the fluorescence of Alexa Fluor 647.*

Phenotypic analyses of live cells revealed that the mean fluorescent intensity (MFI) of CD45 staining was higher than that of KUL01, though both were expressed on most macrophages (more than 95%) and there was no difference regarding KUL01 and CD45 expression between two inbred lines (Figure 5.2C).

Following culture and characterisation of macrophages in inbred lines, the next step was to repeat this experiment in DCs from lines 6_1 and 7_2 birds.

5.3 Culture and characterisation of BMDC from the chicken inbred lines 6_1 and 7_2

5.3.1 Morphological characterisation

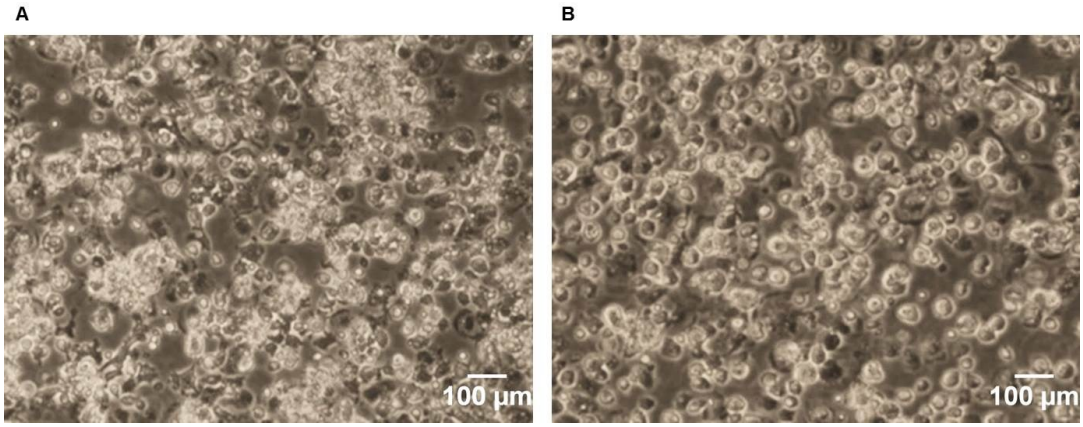

Figure 5.3. *Morphological properties of BMDC on day 4 cultured from inbred chickens. (A) Cells cultured from line 6_1 birds. (B) Cells grown from line 7_2 birds.*

DCs were cultured from lines 6_1 and 7_2 following isolation and processing of bone marrow cells and seeded in T_{75} flasks for 4 days (section 2.2.9). Cellular aggregates were observed in the culture flasks at day 4 in both the inbred lines (Figures 5.3A and B).

5.3.2 Characterisation by flow cytometry

BMDC from inbred lines were grown in T_{75} flasks for 4 days as described in section 2.2.9.

Immunofluorescence staining was carried out on day 4 with KUL01, CD45 and Gr 13.1(isotype control) and cells were then analysed by flow cytometry (section 2.4.2).

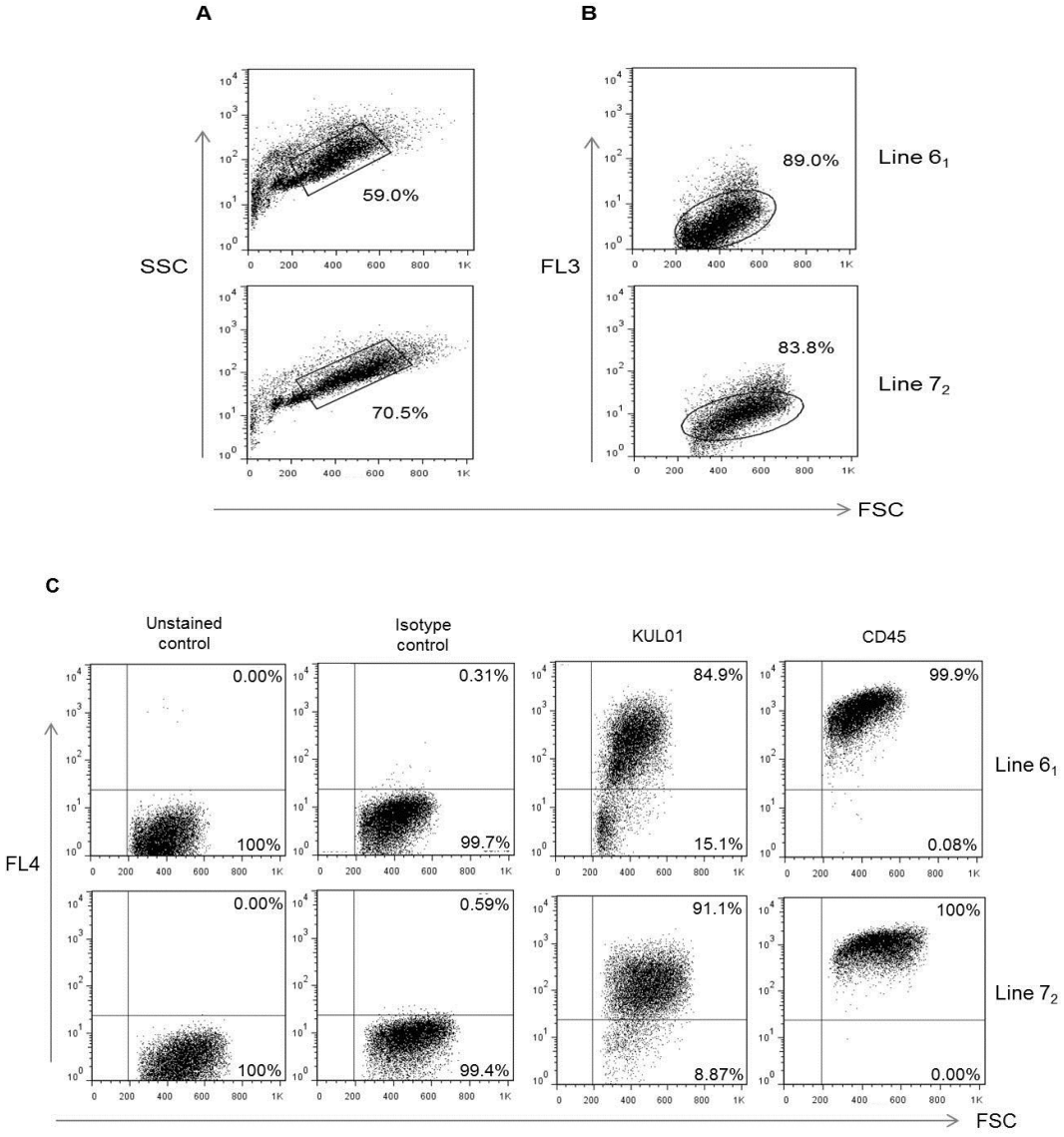

Figure 5.4. *Phenotypic characterisation of BMDC by flow cytometry from inbred chickens. (A) Cells from lines 6_1 and 7_2 were gated in SSC/FSC plots. (B) SSC/FSC gated cells from both lines were plotted in FL3/FSC plots to gate live cells. FL3 shows the fluorescence of 7-AAD. (C) Live cells from lines 6_1 and 7_2 were tested for surface expression of KUL01 and CD45 and compared with unstained cells and cells stained with the isotype control antibody (Gr 13.1). FL4 shows the fluorescence of Alexa Fluor 647.*

Around 60% and 70% cells were gated as DCs in SSC/FSC plots in lines 6_1 and 7_2 birds, respectively (Figure 5.4A). Analysis of these cells in FL3/FSC plots with the staining of cell viability dye revealed that more than 80% of SSC/FSC gated cells were live in both the lines (Figure 5.4B). Phenotypic analyses of live cells revealed that the MFI of CD45 was higher than that of KUL01. CD45 was also expressed on a higher number (100%) of DCs compared to KUL01 (around 90%) in both the lines (Figure 5.4C).

Following characterisation of macrophages and DCs in inbred lines, these cells were infected with pre-sorted MDV-infected CEFs in the next two experiments and subsequently characterised by flow cytometry.

5.4 Infection and subsequent flow cytometric characterisation of BMDM from the inbred lines

Chicken BMDM from lines 6_1 and 7_2 were grown in T_{75} flasks as described in section 2.2.9. Three T_{75} flasks of macrophages were cultured separately from each of the two inbred lines to carry out flow cytometric experiments on 1, 3 and 5 dpi. Meanwhile, MDV-infected CEFs were grown in two T_{175} flasks for each experiment as per methods in section 2.3.4. On day 4 of culture, macrophages were infected with pre-sorted GFP^+ CEFs at an infection ratio of 1:5 (CEF:macrophage) as described in section 3.4.1.

Following infection, cells were observed daily under the fluorescence microscope and it was noted that the number of GFP^+ cells was gradually reduced as the time progressed (Figure 5.5).

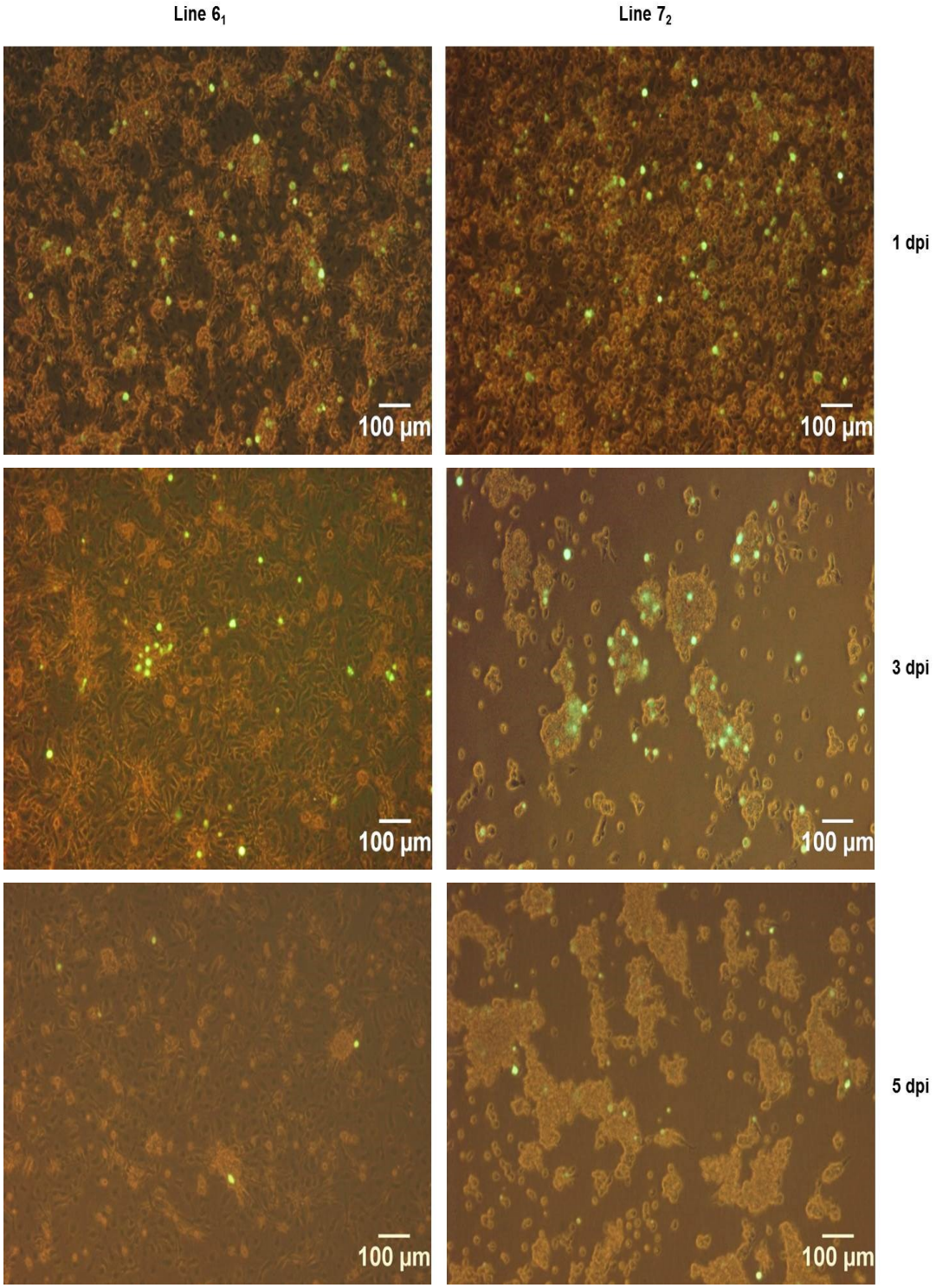

Figure 5.5. *Infection of macrophages with pre-sorted GFP$^+$ CEFs in inbred lines. The ratio of infection was 1:5 (CEF:macrophage). Left panel: Line 6$_1$ macrophages on 1, 3 and 5 dpi. Right panel: Line 7$_2$ macrophages on 1, 3 and 5 dpi.*

Cells were harvested on 1, 3, and 5 dpi from both lines (Figure 5.5) for flow cytometric analyses after staining with KUL01, CD45 and Gr 13.1 (isotype control) as described in section 2.4.2. At least 10^6 viable cells were counted from each sample.

On 1 dpi, around 88% of the SSC/FSC gated cells in line 6_1 and 75% of the SSC/FSC gated cells in line 7_2 were found alive after staining with 7-AAD (Figure 5.6B). Flow cytometric analyses of live cells in FL1/FL4 dot plots, as shown in KUL01 and CD45 staining ($FL1^+FL4^+$), revealed that the proportion of infected macrophages was around 3 times higher in line 7_2 (36%), which is susceptible to MD, compared to those in line 6_1 (12%), which is resistant to MD (Figure 5.6C). These experiments were also repeated four times at the same infection ratio (1:5) with macrophages of two inbred lines for cell sorting purposes (section 5.6) on 1 dpi and the data were analysed using different software (FACSDiva instead of FlowJo). However, the percentages of infected macrophages in line 6_1 were 20.5%, 10%, 13.5% and 7.8% (average 12.5%), whereas in line 7_2 macrophages the percentages were 30.5%, 27.7%, 45.8% and 13.7% (average 29.45%), still denoting a higher susceptibily of macrophages in line 7_2, though the mean difference between the two lines was not statistically significant (Figure 5.6D).

More than 90% of the SSC/FSC gated cells were found alive on 3 dpi after staining with cell viability dye in both the lines (Figure 5.7B). The number of infected macrophages on 3 dpi, as observed in KUL01 and CD45 staining, was reduced in both line 6_1 (4%) and line 7_2 (10%) when compared to those on 1 dpi (Figure 5.6C), though there was still a large difference (2.5 times) between two lines (Figure 5.7C).

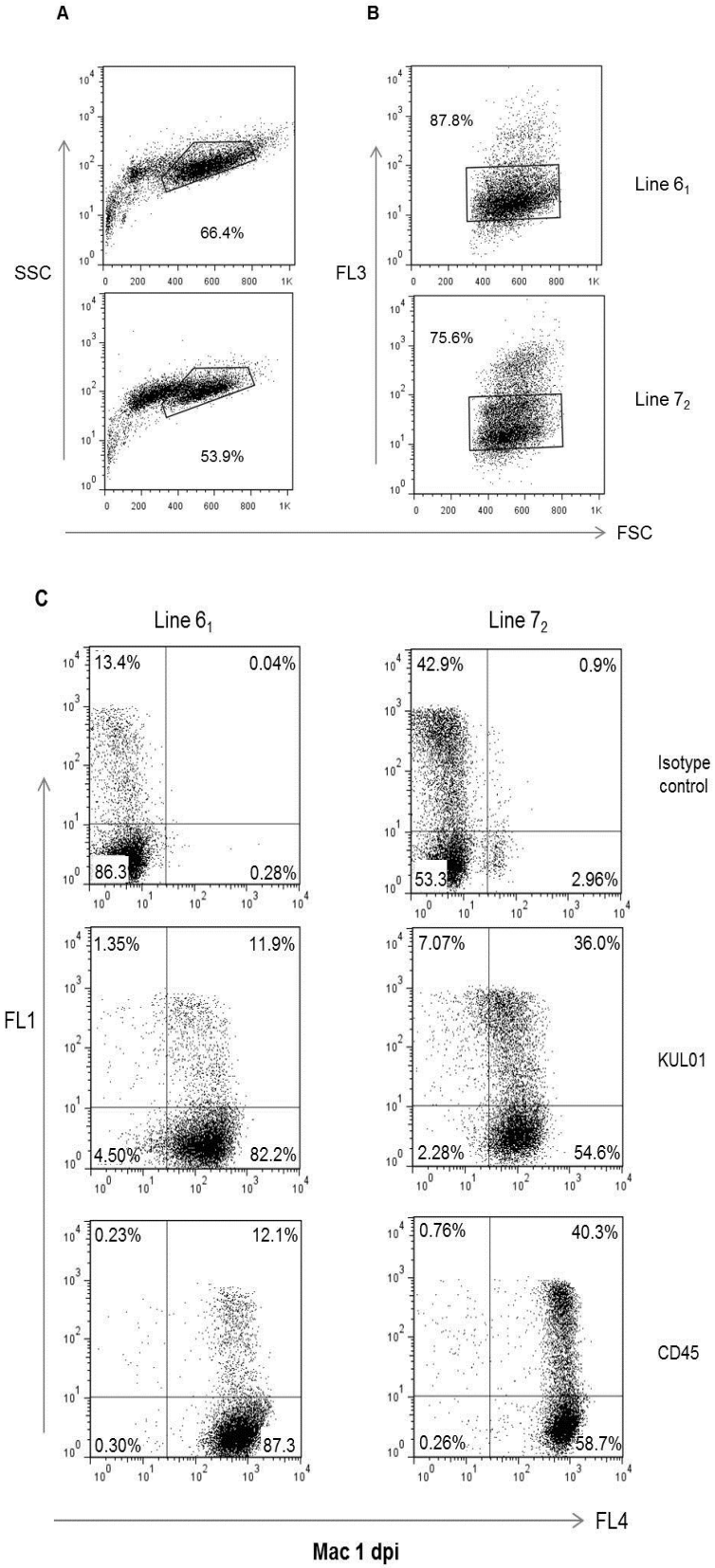
A
B
SSC
FL3
66.4%
53.9%
87.8%
75.6%
Line 6$_1$
Line 7$_2$
FSC
C
Line 6$_1$
Line 7$_2$
13.4%
0.04%
86.3%
0.28%
42.9%
0.9%
53.3%
2.96%
Isotype control
1.35%
11.9%
4.50%
82.2%
7.07%
36.0%
2.28%
54.6%
KUL01
FL1
0.23%
12.1%
0.30%
87.3%
0.76%
40.3%
0.26%
58.7%
CD45
FL4
Mac 1 dpi

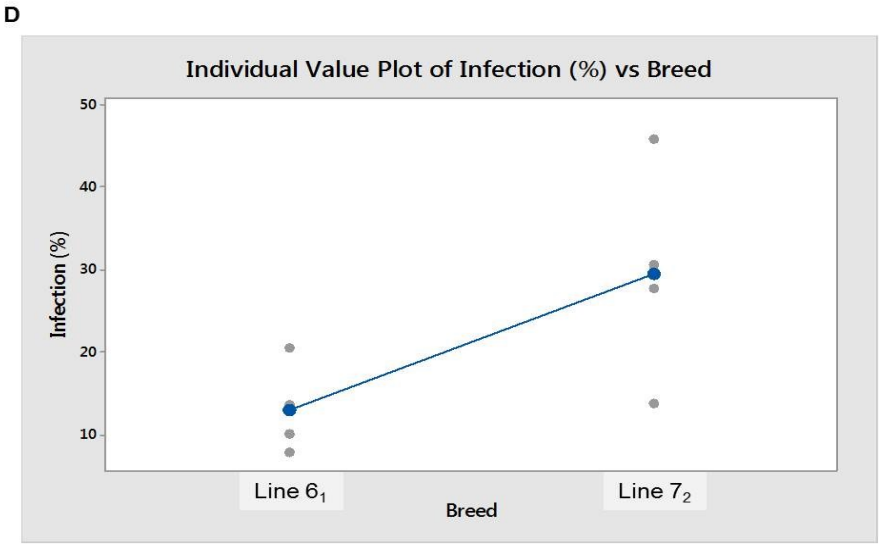

Figure 5.6. *Characterisation of macrophages (Mac) by flow cytometry and during cell sorting following co-culture with MDV-infected CEFs in two inbred lines on 1 dpi. Macrophages were infected with pre-sorted MDV-infected GFP$^+$ CEFs at 1:5 ratio (CEF:macrophage) (A) Cells were gated in SSC/FSC plots. (B) SSC/FSC gated cells were analysed in FL3/FSC plots to identify live cells. (C) Live cells were analysed in FL1/FL4 dot plots to detect KUL01$^+$ and CD45$^+$ macrophages compared to isotype control (Gr 13.1). (D) The percentages of infection of macrophages and the mean difference between the two inbred lines during cell sorting experiments. Statistical difference was measured with 2-sample T-test (95% confidence interval) using Minitab 16 software. FL1 shows the fluorescence of GFP (green)-encoded MDV and FL4 shows the fluorescence of Alexa Fluor 647 (red) at the surface of the cells. Distribution of cells in antibody stained plots, FL1$^-$FL4$^-$: uninfected CEFs; FL1$^+$FL4$^-$: infected CEFs; FL1$^-$FL4$^+$: uninfected macrophages and FL1$^+$FL4$^+$: infected macrophages.*

On 5 dpi, more than 90% of the SSC/FSC gated cells in both lines were identified as live cells in FL3/FSC plots (Figure 4.8B). Flow cytometric analyses of live cells following KUL01 and CD45 staining revealed that the number of infected macrophages was very few (around 0.6%) in the resistant line (6_1) compared to its susceptible counterpart (line 7_2, 5.5%) (Figure 5.8C).

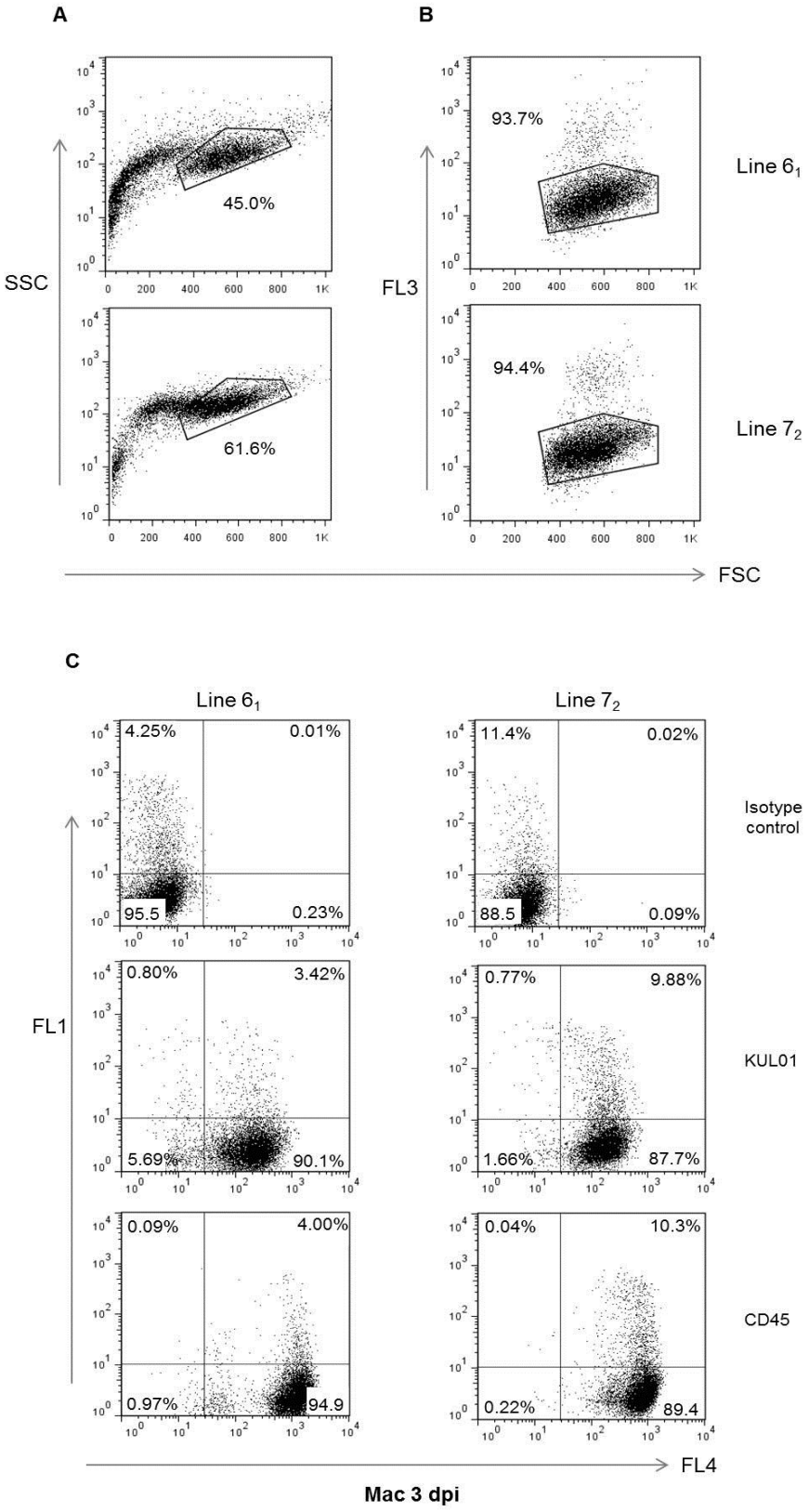
A
B
SSC
FL3
45.0%
61.6%
93.7%
94.4%
Line 6$_1$
Line 7$_2$
FSC
C
Line 6$_1$
Line 7$_2$
4.25%
0.01%
95.5
0.23%
11.4%
0.02%
88.5
0.09%
Isotype control
FL1
0.80%
3.42%
5.69%
90.1%
0.77%
9.88%
1.66%
87.7%
KUL01
0.09%
4.00%
0.97%
94.9
0.04%
10.3%
0.22%
89.4
CD45
FL4
Mac 3 dpi

Figure 5.7. *Flow cytometric characterisation of macrophages (Mac) following co-culture with MDV-infected CEFs in two inbred lines on 3 dpi. Macrophages were infected with pre-sorted MDV-infected GFP$^+$ CEFs at 1:5 ratio (CEF:macrophage) (A) Cells were gated in SSC/FSC plots. (B) SSC/FSC gated cells were analysed in FL3/FSC plots to identify live cells. (C) Live cells were analysed in FL1/FL4 dot plots to detect KUL01$^+$ and CD45$^+$ macrophages compared to isotype control (Gr 13.1). FL1 shows the fluorescence of GFP (green)-encoded MDV and FL4 shows the fluorescence of Alexa Fluor 647 (red) at the surface of the cells. Distribution of cells in antibody stained plots, FL1$^-$FL4$^-$: uninfected CEFs; FL1$^+$FL4$^-$: infected CEFs; FL1$^-$FL4$^+$: uninfected macrophages and FL1$^+$FL4$^+$: infected macrophages.*

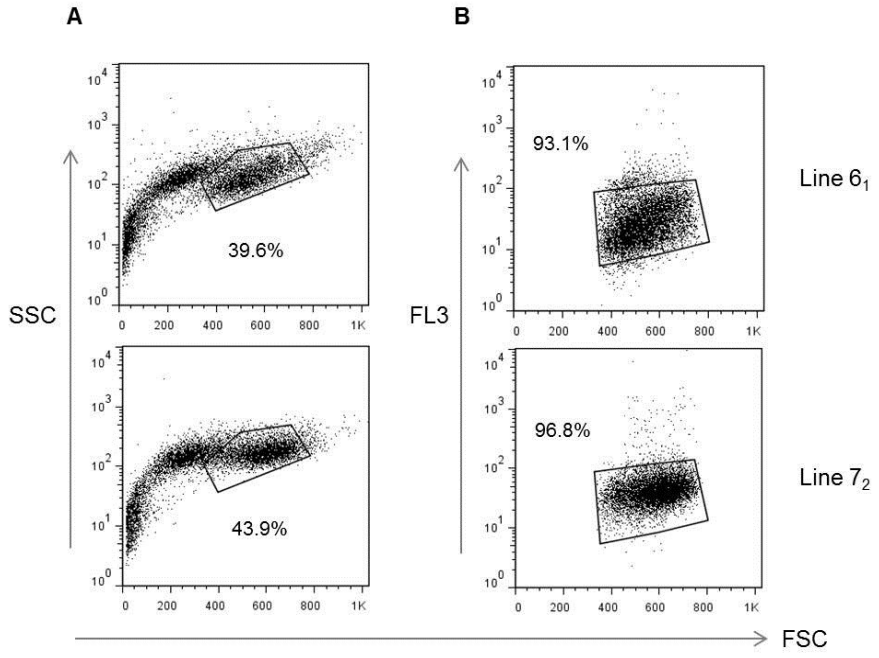

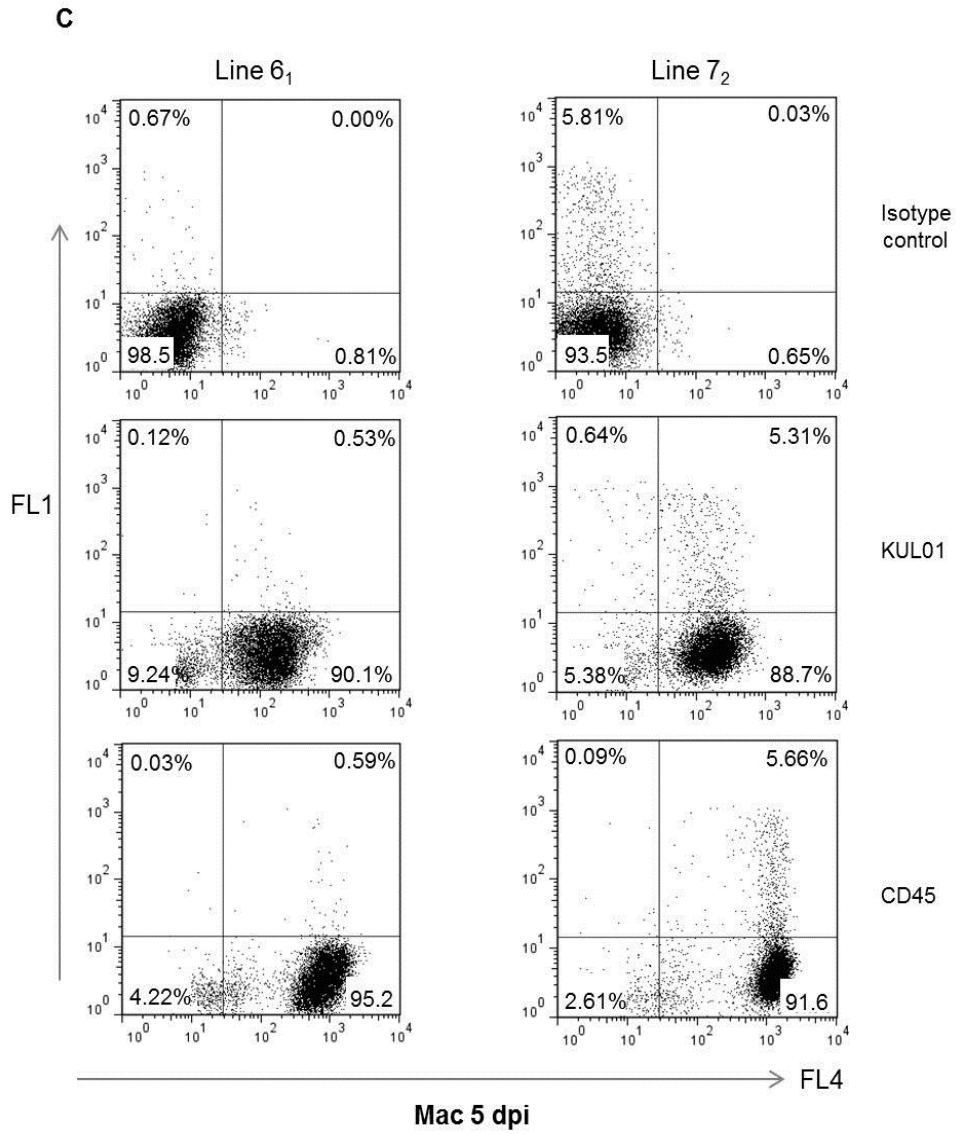

Figure 5.8. *Flow cytometric characterisation of macrophages (Mac) following co-culture with MDV-infected CEFs in two inbred lines on 5 dpi. Macrophages were infected with pre-sorted MDV-infected GFP$^+$ CEFs at 1:5 ratio (CEF:macrophage) (A) Cells were gated in SSC/FSC plots. (B) SSC/FSC gated cells were analysed in FL3/FSC plots to identify live cells. (C) Live cells were analysed in FL1/FL4 dot plots to detect KUL01$^+$ and CD45$^+$ macrophages compared to isotype control (Gr 13.1). FL1 shows the fluorescence of GFP (green)-encoded MDV and FL4 shows the fluorescence of Alexa Fluor 647 (red) at the surface of the cells. Distribution of cells in antibody stained plots, FL1$^-$FL4$^-$: uninfected CEFs; FL1$^+$FL4$^-$: infected CEFs; FL1$^-$FL4$^+$: uninfected macrophages and FL1$^+$FL4$^+$: infected macrophages.*

5.5 Infection and subsequent flow cytometric characterisation of BMDC from the inbred lines

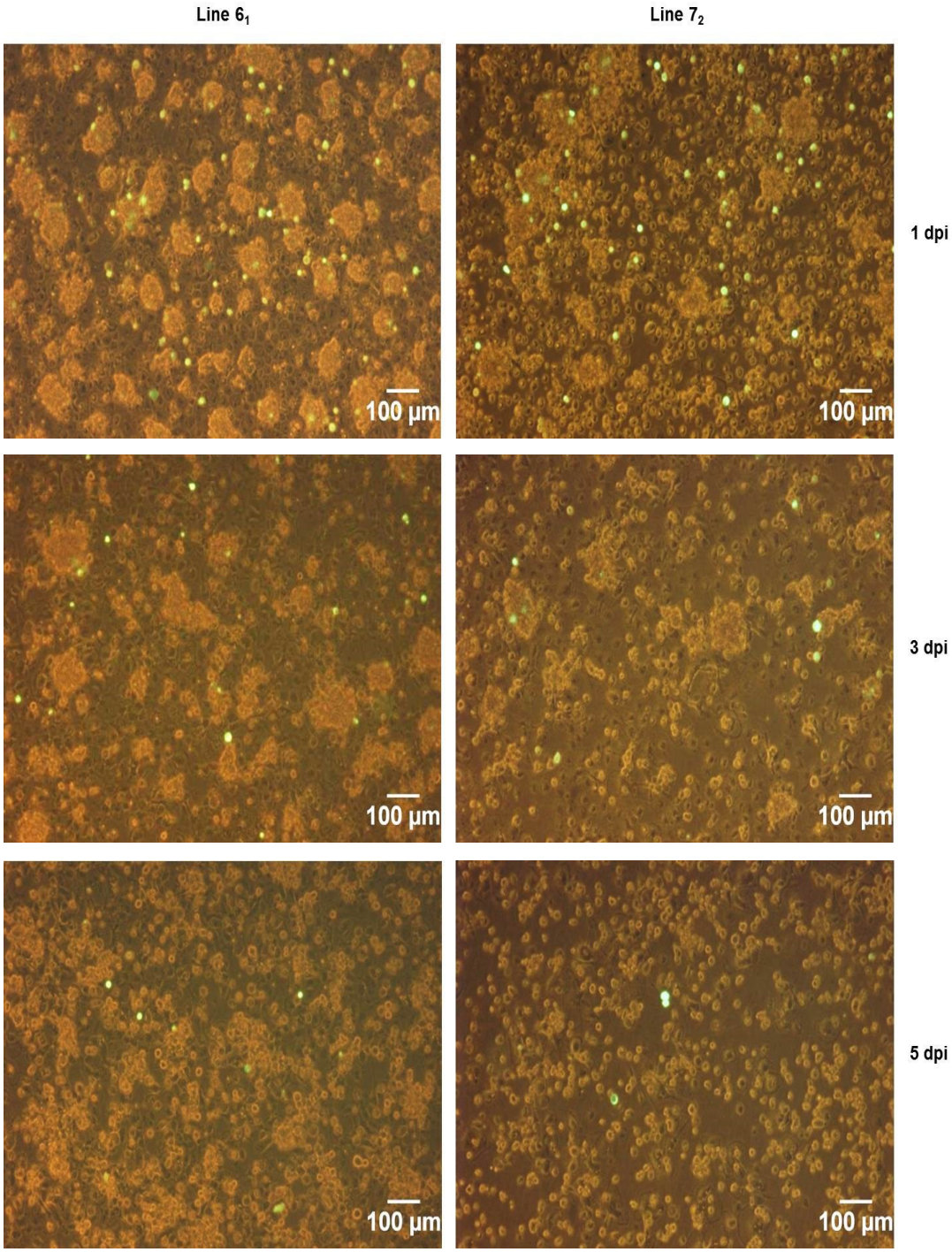

Figure 5.9. *Infection of BMDC with pre-sorted GFP$^+$ CEFs in inbred lines. The ratio of infection was 1:5 (CEF:DC). Left panel: Line 6_1 DCs on 1, 3 and 5 dpi. Right panel: Line 7_2 DCs on 1, 3 and 5 dpi.*

Chicken BMDC were cultured in three separate T_{75} flasks from each of the two inbred lines as per methods in section 2.2.9 to carry out flow cytometric experiments on 1, 3 and 5 dpi.

In parallel, MDV-infected CEFs were also grown in two T_{175} flasks for each experiment (section 2.3.4) and DCs were infected with pre-sorted GFP^+ CEFs at a ratio of 1:5 (CEF:DC) (section 3.4.11). It was observed that the number of GFP^+ cells was sharply reduced at the later days of infection (Figure 5.9). Flow cytometric analyses were carried out on 1, 3 and 5 dpi (Figure 5.9) after staining with KUL01, CD45 and Gr 13.1 (isotype control), according to procedures in section 2.4.2 and at least 10^6 viable cells were counted from each sample.

On 1 dpi, around 85% of the SSC/FSC gated cells were found alive in FL3/FSC gating in both lines after staining with 7-AAD (Figure 5.10B). Live cells were placed in FL1/FL4 dot plots and the analyses of KUL01 and CD45 staining revealed that the proportion of infected DCs ($FL1^+FL4^+$) was almost identical in both the MD-resistant (6_1) (6%) and MD-susceptible line (7_2) (around 5.5%) (Figure 5.10C).

Over 90% of the SSC/FSC gated cells were identified as viable cells in FL3/FSC plots in both lines on 3 dpi (Figure 5.11B). Live cells were then analysed in FL1/FL4 plots to detect the $KUL01^+$ and $CD45^+$ DCs. As for 1 dpi, no major difference was observed, in terms of the percentage of infected DCs, between two lines on 3 dpi, though the infected cell numbers were decreased (Figure 5.11C) compared to those on 1 dpi (Figure 5.10C).

On 5 dpi, more than 90% of the SSC/FSC gated cells were found alive in FL3/FSC plots in both lines (Figure 5.12B). The KUL01 and CD45 staining revealed that the number of infected DCs was very few (around 0.5%) and as observed previously on

1 and 3 dpi, there was no difference between resistant (6_1) and susceptible line (7_2) (Figure 5.12C).

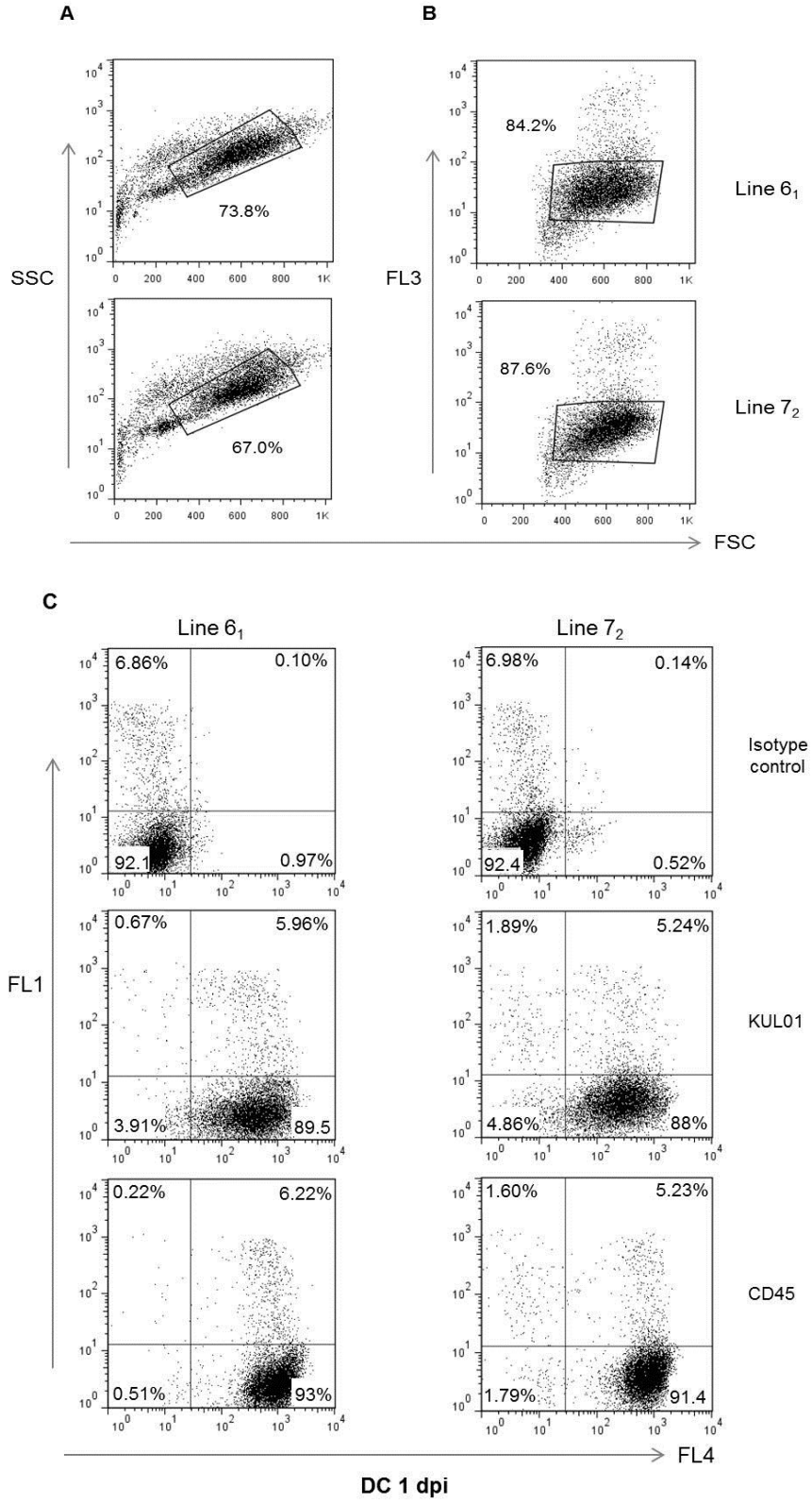

Figure 5.10. *Flow cytometric characterisation of DCs following co-culture with MDV-infected CEFs in two inbred lines on 1 dpi. DCs were infected with pre-sorted MDV-infected GFP$^+$ CEFs at 1:5 ratio (CEF:DC) (A) Cells were gated in SSC/FSC plots. (B) SSC/FSC gated cells were analysed in FL3/FSC plots to gate live cells. (C) Live cells were analysed in FL1/FL4 dot plots to detect KUL01$^+$ and CD45$^+$ DCs compared to isotype control (Gr 13.1). FL1 shows the fluorescence of GFP (green)-encoded MDV and FL4 shows the fluorescence of Alexa Fluor 647 (red) at the surface of the cells. Distribution of cells in antibody stained plots, FL1$^-$FL4$^-$: uninfected CEFs; FL1$^+$FL4$^-$: infected CEFs; FL1$^-$FL4$^+$: uninfected DCs and FL1$^+$FL4$^+$: infected DCs.*

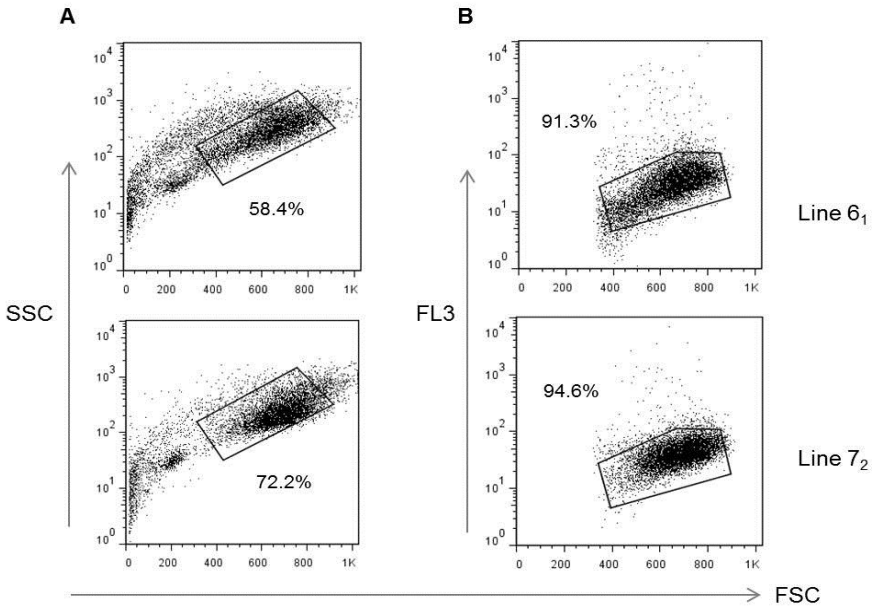

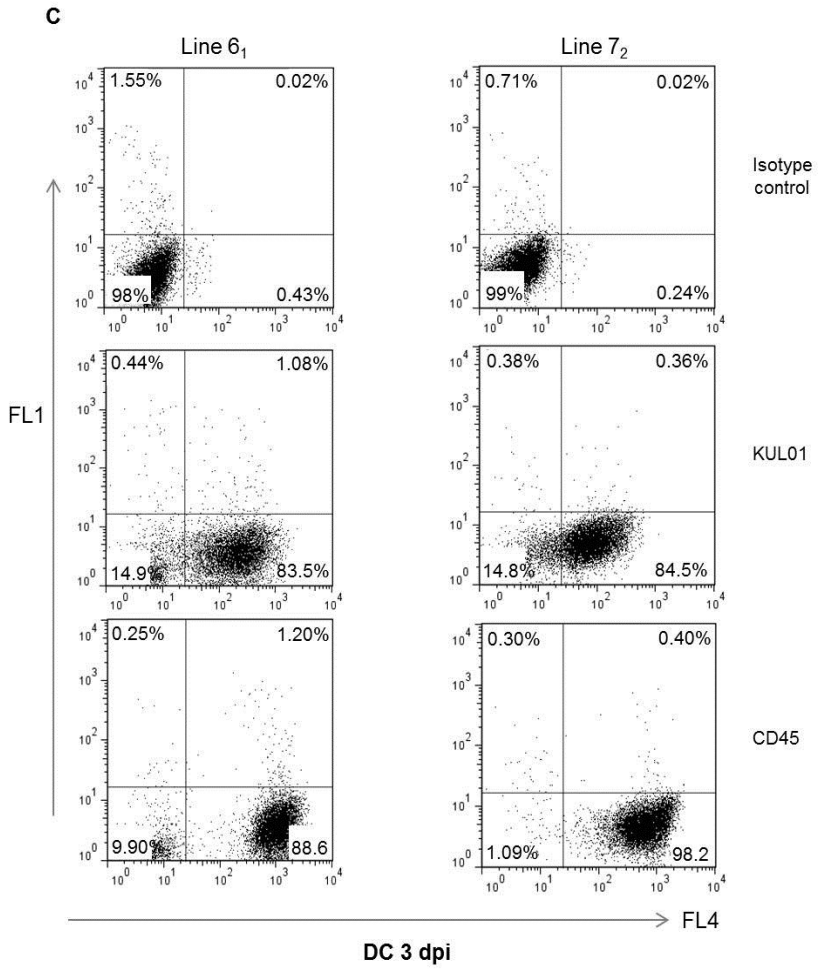

Figure 5.11. *Flow cytometric characterisation of DCs following co-culture with MDV-infected CEFs in two inbred lines on 3 dpi. DCs were infected with pre-sorted MDV-infected GFP$^+$ CEFs at 1:5 ratio (CEF:DC) (A) Cells were gated in SSC/FSC plots. (B) SSC/FSC gated cells were analysed in FL3/FSC plots to gate live cells. (C) Live cells were analysed in FL1/FL4 dot plots to detect KUL01$^+$ and CD45$^+$ DCs compared to isotype control (Gr 13.1). FL1 shows the fluorescence of GFP (green)-encoded MDV and FL4 shows the fluorescence of Alexa Fluor 647 (red) at the surface of the cells. Distribution of cells in antibody stained plots, FL1$^-$FL4$^-$: uninfected CEFs; FL1$^+$FL4$^-$: infected CEFs; FL1$^-$FL4$^+$: uninfected DCs and FL1$^+$FL4$^+$: infected DCs.*

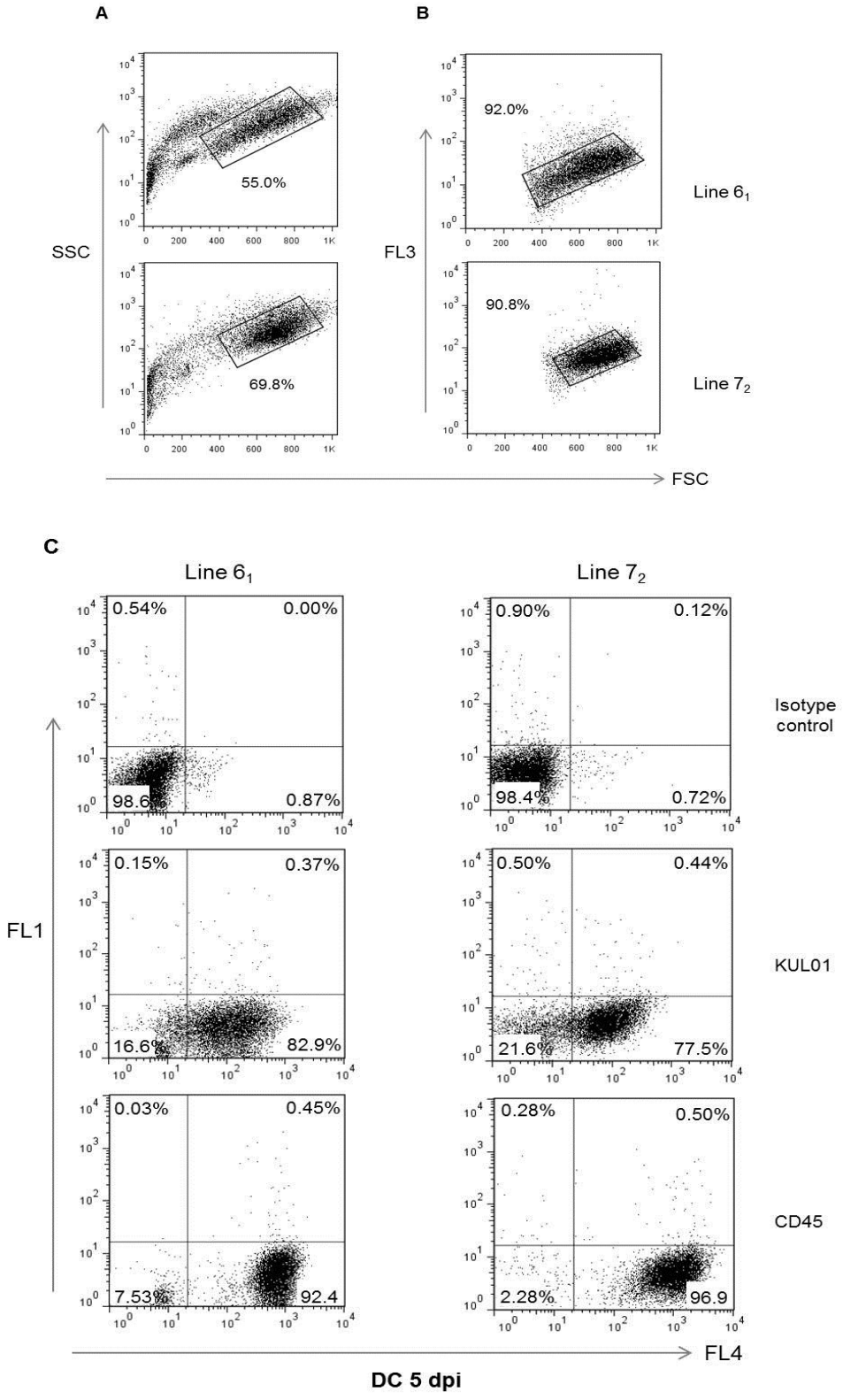
A
B
SSC
FL3
55.0%
69.8%
92.0%
90.8%
Line 6$_1$
Line 7$_2$
FSC
C
Line 6$_1$
Line 7$_2$
0.54%
0.00%
98.6%
0.87%
0.90%
0.12%
98.4%
0.72%
Isotype control
0.15%
0.37%
16.6%
82.9%
0.50%
0.44%
21.6%
77.5%
KUL01
0.03%
0.45%
7.53%
92.4
0.28%
0.50%
2.28%
96.9
CD45
FL1
FL4
DC 5 dpi

Figure 5.12. *Flow cytometric characterisation of DCs following co-culture with MDV-infected CEFs in two inbred lines on 5 dpi. DCs were infected with pre-sorted MDV-infected GFP$^+$ CEFs at 1:5 ratio (CEF:DC) (A) Cells were gated in SSC/FSC plots. (B) SSC/FSC gated cells were analysed in FL3/FSC plots to gate live cells. (C) Live cells were analysed in FL1/FL4 dot plots to detect KUL01$^+$ and CD45$^+$ DCs compared to isotype control (Gr 13.1). FL1 shows the fluorescence of GFP (green)-encoded MDV and FL4 shows the fluorescence of Alexa Fluor 647 (red) at the surface of the cells. Distribution of cells in antibody stained plots, FL1$^-$FL4$^-$: uninfected CEFs; FL1$^+$FL4$^-$: infected CEFs; FL1$^-$FL4$^+$: uninfected DCs and FL1$^+$FL4$^+$: infected DCs.*

5.6 Sorting macrophages and DCs following MDV infection in inbred lines

In order to explore the cellular basis of resistance to MD, GFP$^+$ APCs were sorted following infection with MDV *in vitro* and RNA samples were sent for RNA-Seq. Macrophages and DCs from inbred lines 6_1 and 7_2 were cultured and infected with MDV as per methods in section 5.4 (for macrophages) and in section 5.5 (for DCs). Cell sorting was carried out on 1 and 3 dpi. The infection ratios varied because the number of infected cells was not consistent between macrophages and DCs during sorting. A higher number of cells (macrophages or DCs) were infected on 1 dpi than on 3 dpi and in general, the percentages of infected macrophages were higher than those of DCs (sections 5.4 and 5.5, respectively). Therefore, to obtain the optimum number of infected cells during sorting, higher infection ratios (1:2 or 1:2.5, CEF:APCs) were used for DCs and also for the sorting experiments on 3 dpi. In all other cases, an infection ratio of 1:5 was used. Prior to the sort, cells were harvested and prepared for sorting as described in section 2.4.3.1 (for CEFs) and in section 2.4.3.2 (for APCs). As shown in Figure 5.13A, infected and uninfected macrophages

and DCs were sorted on 1 and 3 dpi. The 'uninfected' cells were sorted from the same flask as the infected cells were sorted and therefore, the uninfected cells were exposed to virus. Hence to obtain control APCs, sort-stressed uninfected CEFs were added to one separate T_{75} flask of macrophage or DC culture at 1:5 ratios on the day of infection of APCs in each experiment and 'control' macrophages or DCs that have been exposed to CEFs but not to MDV were then sorted on 1 and 3 dpi after staining cells with CD45 (Figure 5.13B).

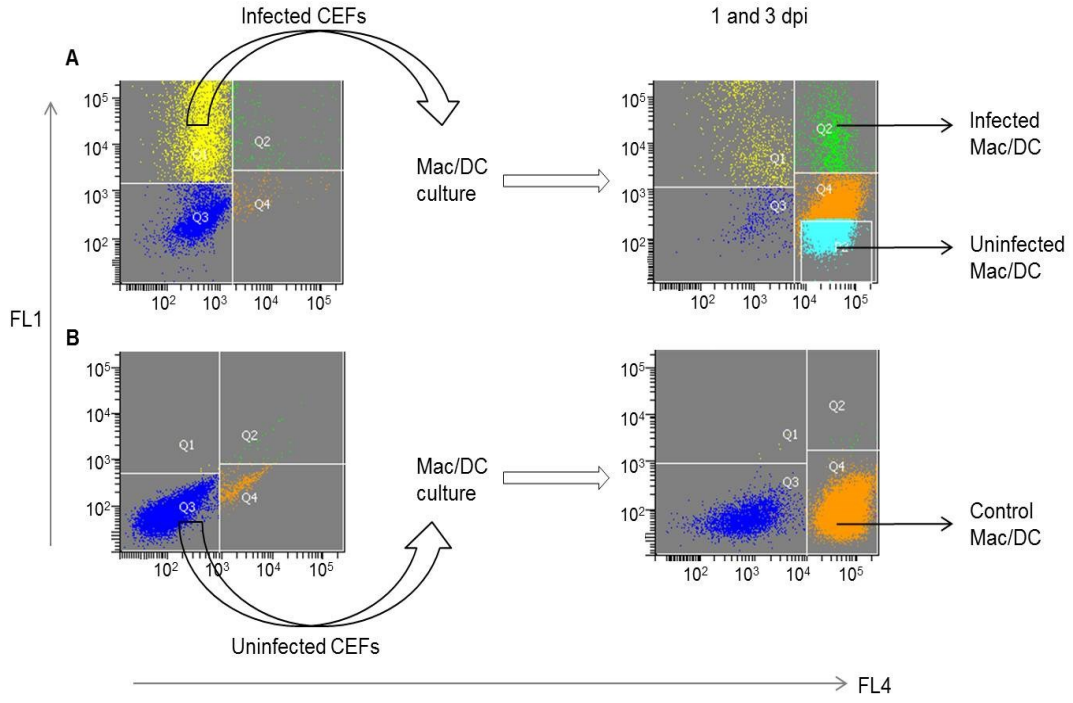

Figure 5.13. *The overall model of cell sorting. On the day of infection, (A) GFP$^+$ CEFs were sorted and added to macrophage (Mac) or DC culture and infected and uninfected macrophages or DCs were sorted subsequently on 1 and 3 dpi, (B) sort-stressed uninfected CEFs were added to macrophage or DC culture followed by the sorting of control macrophages or DCs on the same days. FL1 shows the fluorescence of GFP (green)-encoded MDV and FL4 shows the fluorescence of Alexa Fluor 647 (red) at the surface of the cells. Distribution of cells in sorting plots, FL1$^-$FL4$^-$: uninfected CEFs (Q3); FL1$^+$FL4$^-$: infected CEFs (Q1); FL1$^-$FL4$^+$: uninfected APCs (Q4) and FL1$^+$FL4$^+$: infected APCs (Q2).*

After sorting, the purity of infected and uninfected APCs was checked (Figures 5.14B and C, respectively) by placing 1000 sorted cells into the same sorting plot and it was shown that the uninfected APCs were a pure population, but infected APCs were not. Though a separate gate was created in each cell sorting experiment to keep the doublet cells out of the analysis, there were contaminating cells in the infected cell-group from each of the remaining three quarter (Q1, Q3 and Q4) (Figure 5.14B).

These sorting experiments were repeated 4 times with APCs from inbred lines 6_1 and 7_2.

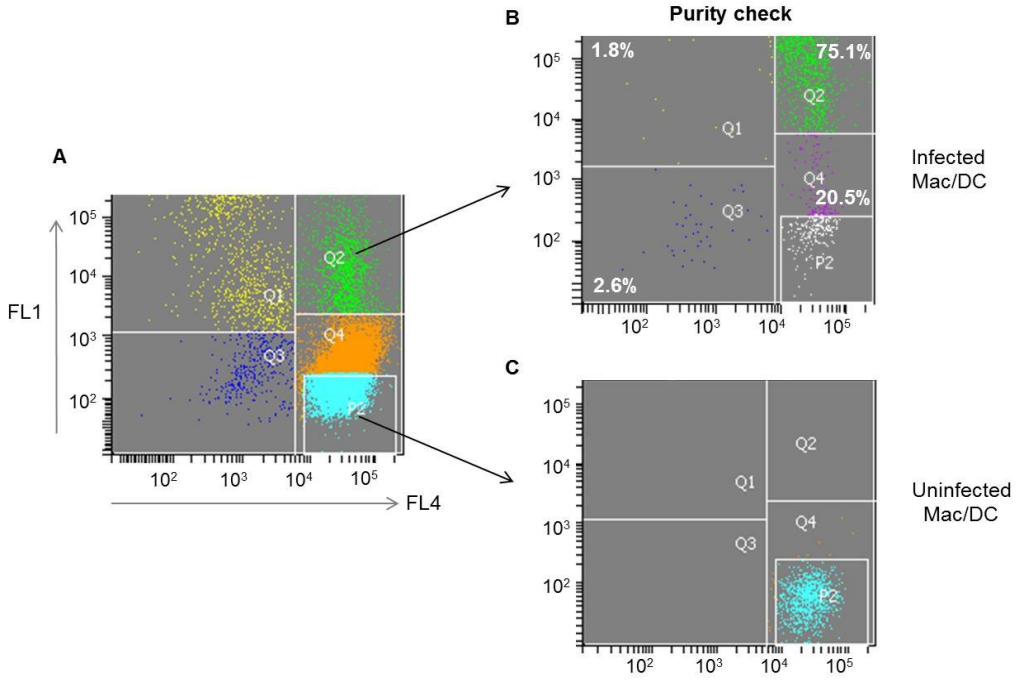

Figure 5.14. *Checking purity of the sorted cells. On 1 and 3 dpi, (A) infected and uninfected APCs were sorted and (B) the purity of infected and (C) uninfected macrophages (Mac) or DCs was checked. FL1 shows the fluorescence of GFP (green)-encoded MDV and FL4 shows the fluorescence of Alexa Fluor 647 (red) at the surface of the cells. Distribution of cells in sorting plots, $FL1^{-}FL4^{-}$: uninfected CEFs (Q3); $FL1^{+}FL4^{-}$: infected CEFs (Q1); $FL1^{-}FL4^{+}$: uninfected APCs (Q4) and $FL1^{+}FL4^{+}$: infected APCs (Q2).*

5.7 Characterisation of APCs from inbred lines after MDV infection by qRT-PCR

BMDM and BMDC from the two inbred chicken lines 6_1 and 7_2 were infected with MDV and infected, uninfected and control APCs were sorted on 1 and 3 dpi (section 5.6). Total RNA was extracted from all the groups (control, infected and uninfected) as described in section 2.5.1 and DNase treatment of RNAs was carried out (section 2.5.1.1). The mRNA expression levels of two pro-inflammatory cytokines, IL-6 and IL-18 were then measured on 1 dpi in MDV-infected, uninfected and control macrophages and DCs from the two inbred lines using TaqMan qRT-PCR as described in section 2.5.4. The results are expressed as corrected 40-Ct and shown in Figures 5.15 and 5.16.

No statistically significant difference ($p>0.05$) was observed in the mean IL-6 mRNA expression of all macrophage and DC groups in the two inbred lines (Figures 5.15A and B, respectively). IL-18 expression level was higher in all line 6_1 macrophages compared to the expression in line 7_2. In infected macrophages, IL-18 mRNA expression was significantly higher in line 6_1 compared to line 7_2 ($p<0.05$) (Figure 5.16A). There was no statistically significant difference ($p>0.05$) in IL-18 mRNA expression of three DC groups between two inbred lines (Figure 5.16B).

5.8 Discussion

To explore the cellular basis of resistance to MD, APCs from two inbred lines 6_1 and 7_2 were infected with MDV-infected CEFs using a previously developed infection model (Chapter 3) and subsequently characterised by flow cytometry and qRT-PCR. Despite sharing the same MHC genes, the chicken inbred line 6_1 is highly resistant and line 7_2 is highly susceptible to MD.

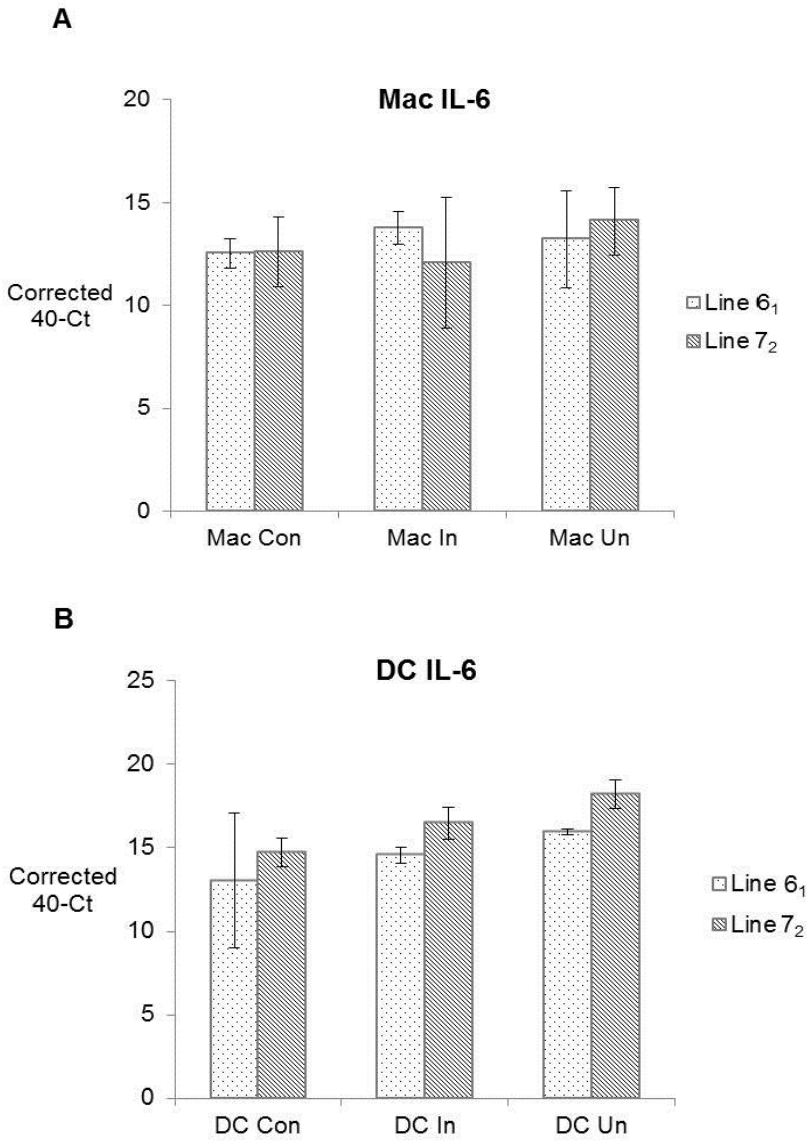

Figure 5.15. *Quantification of IL-6 mRNA expression level in (A) macrophages and (B) DCs derived from inbred chicken lines on 1 dpi. Results are shown as corrected 40-Ct for the expression of IL-6 in infected, uninfected and control macrophages (Mac) and DCs. The 40-Ct figures show means and standard deviations of three biological replicates from each line except for the line 7_2 uninfected macrophage group where values from two replicates were counted. Pairwise statistical comparisons between means in three groups of the two inbred chicken lines were carried out with a General linear model with Tukey (95% confidence interval) using Minitab 16 software. Con - control; In - infected; Un - uninfected.*

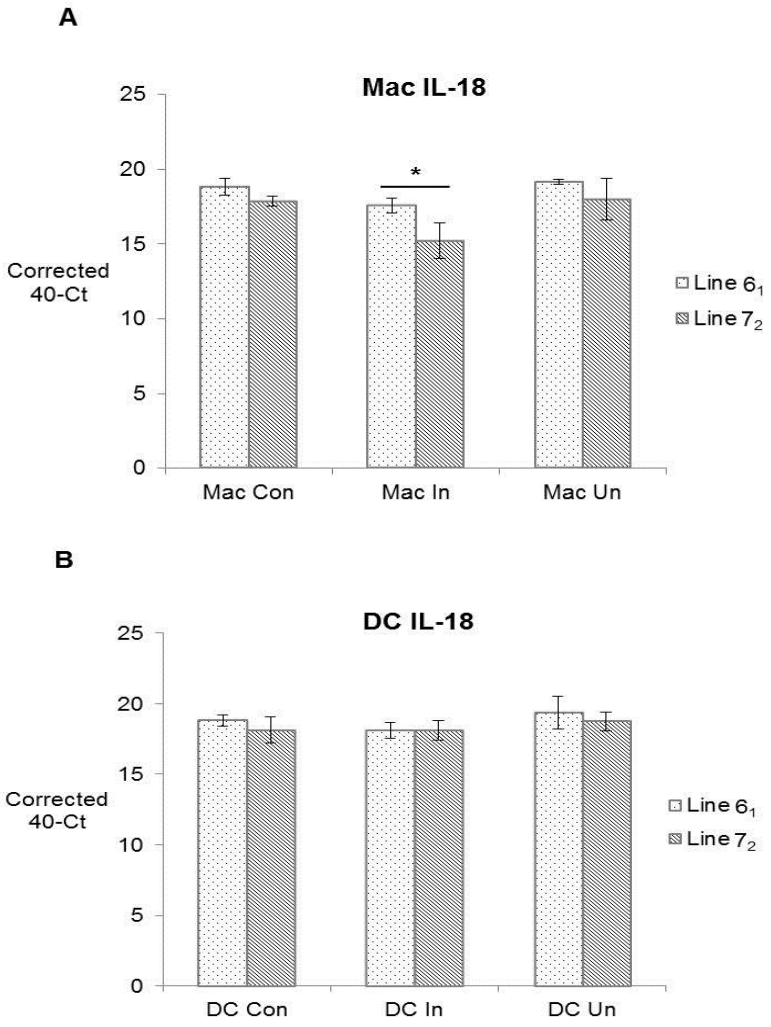

Figure 5.16. *Quantification of IL-18 mRNA expression level in (A) macrophages and (B) DCs derived from inbred chickens on 1 dpi. Results are shown as corrected 40-Ct for the expression of IL-18 in infected and uninfected macrophages (Mac) and DC compared to those in controls. The 40-Ct figures show means and standard deviations of three biological replicates from each line. Pairwise statistical comparisons between means in three groups of the two inbred chicken lines were carried out with a General linear model with Tukey (95% confidence interval) using Minitab 16 software. * = $p<0.05$. Con- control; In- infected; Un- uninfected.*

The chicken inbred lines (6_1 and 7_2) show differences in viraemia level and gene expression profiles in splenocytes from the very early stages of MDV infection (Lee et al., 1981; Smith et al., 2011), suggesting that the inherent difference between two

lines is due to differential responses of the innate immune system (Bumstead and Kaufman, 2004). The cells of the innate immune system, especially macrophages, play a crucial role during MDV infection. For example, peritoneal macrophages isolated from MDV-infected chickens inhibited the formation of MDV plaques *in vitro* (Kodama et al., 1979). Peritoneal macrophages also showed more phagocytic activity and plaque-inhibiting activity following MDV infection in susceptible than those of resistant chickens (Powell et al., 1983). In the present study, APCs from MD resistant (6_1) and susceptible (7_2) lines were infected with MDV *in vitro* for the first time.

It was observed in the flow cytometric analyses that on 1 dpi, line 6_1 macrophages were approximately 3 times less infected than those of line 7_2 (Figure 5.6C). As mentioned before (section 5.4), these experiments were repeated four times at an infection ratio of 1:5 with macrophages of two inbred lines for cell sorting purposes and the data were analysed using a different software (FACSDiva instead of FlowJo) The mean diference of percentages of infection between two lines also denotes a higher susceptibily of macrophages in line 7_2 (Figure 5.6D).

On 3 and 5 dpi, the numbers of infected macrophages gradually reduced in both the lines but line 7_2 macrophages were still infected higher in numbers (more than 2.5 times) than line 6_1 macrophages (Figures 5.7C and 5.8C, respectively).

The numbers of infected DCs were almost identical between two lines on 1, 3 and 5 dpi (Figures 5.10C, 5.11C and 5.12C, respectively). The experiments on 1 dpi were also repeated four times using a higher infection ratio (1:2 or 1:2.5) in the cell sorting experiments to obtain optimum number of infected DCs (data were not shown). Therefore, those results are not compared with flow cytometry data (which were

carried out at 1:5 infection ratio), but it was observed that a high infection ratio can produce increased number of infected DCs.

The overall flow cytometric results revealed that, irrespective of lines and the days-post infection, with a fixed infection ratio (1:5) a higher percentage of macrophages were infected than DCs. Moreover, a higher proportion of macrophages from susceptible line (7_2) were infected compared to the resistant line (6_1) but no apparent difference was observed in the number of infected DCs between two lines. This might be an indication that macrophages play a more important role to exert resistance or susceptibility to MD than DCs. Among the immune cells, macrophages are well-known to exert resistance to herpesvirus infections. For example, a macrophage-dependent and T-cell independent resistance to systemic HSV-1 infection was demonstrated in mice where a selective reduction of macrophage function by silica treatment increased the susceptibility to HSV-1, but the reduction of thymic function by the aging process or by the combined effect of adult thymectomy and ATS (anti-mouse thymocyte serum) did not increase the susceptibility to HSV-1(Schlabach et al., 1979).

Macrophages are thought to inhibit MDV replication as they release NO (nitric oxide) through the increased activity of iNOS. NO is presumed to be crucial for inhibiting MDV replication during the cytolylic and latent phases of infection *in vivo* as an increased level of NO was observed in splenocyte cultures of MDV-infected MD-resistant chickens (Xing and Chat, 2000).

As an APC, DCs might be expected to infect at similar level to macrophages, but it was not the case. However, one factor should also be considered here. As in outbred chickens (Chapter 3), the standard media for culturing DCs from inbred lines also

contained the cytokines IL-4 and GM-CSF (CSF-2) as growth promoting factors. Though no studies have been performed yet regarding MDV infection, the inhibitory role of IL-4 and GM-CSF might be crucial in MDV replication and hence low infection to DCs (Kedzierska et al., 2000; Tsai et al., 2013). But if only the difference in inbred lines is considered, it can be said that no apparent variation was observed between MD-resistant and susceptible lines in the context of MDV-DC infection, suggesting that, like macrophages, DCs are infected by MDV but act only as a carrier of the virus to the lymphoid tissues and perhaps do not play a role in determining resistance to MD.

However, the level of *in vitro* virus infection may vary within APCs. For example, Vatter and Brinton (2014) reported a higher number of SHFV (simian haemorragic fever virus) infected macrophages than those of DCs in macaque and baboons *in vitro*. Analysing the transcriptomic signatures of infected macrophages and DCs by RNA-Seq will be helpful to clarify this question.

The mRNA expression levels of two pro-inflammatory cytokines, IL-6 and IL-18, in MDV infected APCs, were measured on 1 dpi in the three groups (infected, uninfected and control) of two inbred lines using Taqman qRT-PCR. Among the three groups, infected cells were sorted from the MDV-infected culture flask, while control cells were sorted from a separate flask which was not exposed to virus. A group of cells was also sorted as 'uninfected' APCs from the same MDV-infected flask (Figure 5.13) to study the pattern of cytokine expression in these virus exposed, but not infected, cells.

The term 'pro-inflammation' is a widely used and has an association with stress (patho) physiology (Dinarello, 2000). Pro-inflammatory cytokines are associated

with pathological lesions following MDV infection. For example, an elevated expression of IL-6 and IL-18 was measured in the brain tissues of chickens infected with a vvMDV strain that caused transient paralysis in chickens (Abdul-Careem et al., 2006). Pro-inflammatory cytokines may also play a role in determining resistance to MD. Recently, Haunshi and Cheng (2014) reported a differential expression of IL-6 and IL-8 along with TLR3, between CEFs from resistant and susceptible lines, suggesting an important role for these cytokines in MD resistance. In a previous *in vivo* MDV infection study (Kaiser et al., 2003), the role of two pro-inflammatory cytokines, IL-6 and IL-18 was reported crucial regarding resistance or susceptibility to MD. Both cytokines were found to be expressed in the splenocytes of susceptible birds (lines 7_2 and P) and the authors suggested that it might lead to lymphoma formation in these birds, whereas in MD-resistant chickens (lines 6_1 and N) neither of the transcripts was expressed which was thought to be critical for promoting and maintaining latency in these chicken lines.

In contrast to the previous study, IL-6 expression was observed here in both resistant (6_1) and susceptible (7_2) lines, though exact comparison cannot be made as previous expression was measured in splenocytes (Kaiser et al., 2003). In this study, no significant differences were observed in IL-6 expression levels within three groups in macrophages and DCs of both lines (Figures 5.15A and B, respectively).

IL-18, which is also pro-inflammatory in nature (Okamura et al., 1995), induces production of IFN-γ in NK and T cells and a range of cells, including macrophages or monocytes and DCs produce this cytokine. As shown in Figure 5.16A, the IL-18 expression level was significantly higher in infected macrophages of the resistant line

(6_1) than in macrophages of the susceptible line (7_2), but no difference was observed in infected DCs between the two lines (Figure 5.16B).

An elevated expression of pro-inflammatory cytokines during the cytolytic phase is most likely related to increased pathology in susceptible chickens (Kaiser et al., 2003), which is also in agreement with a recent study where higher expression of IL-18 was reported in caecal tonsils of MD-susceptible chickens (line 7_2) compared to MD-resistant chickens (line 6_3) at 6 and 14 dpi (Heidari et al., 2014), but the scenario is contradictory in this study where an elevated expression of IL-6 (Figure 5.15A) and IL-18 (Figure 5.16A) was measured in the infected macrophages of MD-resistant line (6_1), though a higher number of infected macrophages was found in the MD-susceptible line (7_2) than the MD-resistant line (6_1) (Figure 5.6C). However, an increased expression of pro-inflammatory cytokines might lead to IFN-γ production in macrophages of MD-resistant (6_1) chickens which in turn may play an inhibitory role on MDV replication in these birds (Xing and Schat, 2000). Measuring other cytokine expression levels in APCs between the two inbred lines will be helpful to get a comprehensive idea regarding resistance to MD, which was not possible at this stage due to shortage of RNA. In future, an evaluation of viral transcripts in infected cells (from transcriptomic data generated in studies described in Chapter 6) could also be helpful both to confirm viral replication and to determine whether the pattern of transcription differs between cells from the two chicken lines.

Following MDV infection of APCs in inbred chickens lines, RNA samples from 1 dpi were sent for RNA-Seq to explore the differentially expressed (DE) genes in control and MDV-infected APCs of two inbred lines. Funtional analyses of those DE genes will be described in next Chapter.

Chapter 6:

Functional analysis of differentially expressed genes pre- and post-MDV infection of APCs in inbred chicken lines

6.1 Introduction

Resistance to MD is multifaceted, as many features, including host genetics, virus and environmental factors, constitutively determine this mechanism. Again, within the host, various genes from inside and outside of the MHC are interrelated. The two MHC-homozygous inbred chicken lines (6_1 and 7_2) have differential resistance to infection with MDV, which suggests that resistance in these lines is mainly exerted by the genes outside of the MHC. Variation in gene expression is a major determinant of phenotypic variation and differences in MD genetic resistance are most likely due to variation in the transcriptional regulation of genes (Cheng et al., 2013). Several potential non-MHC candidate genes for MD resistance or susceptibility have been identified so far in various cell types, such as TLR3 in CEFs (Haunshi and Cheng, 2014), GH and Ly6E in splenocytes (Liu et al., 2001; Liu et al., 2003) and IRG1 in splenocytes (Smith et al., 2011), but it remains to be established specifically in which cell types this resistance signature is expressed. Immune cells, such as APCs, B and T cells are involved in MDV pathogenesis. In order to explore the resistance phenotype in innate immune cells, APCs from lines 6_1 and 7_2 were infected with MDV using a newly developed *in vitro* MDV-APC infection model (Chapter 5) and RNA samples were sent for transcriptomic analysis to determine differentially expressed (DE) genes in the two chicken lines pre- and post-MDV infection of APCs, by RNA-Seq. The aim of this Chapter was to carry out the functional analysis of these DE gene sets to explore the biological pathway(s) associated with resistance or susceptibility and also to identify genes(s) involved in these mechanisms.

6.2 Differential gene expression in APCs pre- and post-MDV infection

Analysis of RNA-Seq data was carried out with the help of a skilled bioinformatician (Richard Kuo, The Roslin Institute) to explore various categories of DE genes in infected and control APCs of the two inbred lines as described in section 2.9. As shown in Figure 6.1, the expression of genes was compared within the APCs of infected and control birds of lines 6_1 and 7_2. As mentioned before (section 5.6), infected and control APCs were obtained from separate flasks after co-culturing with infected and uninfected CEFs, respectively. In the top level of comparison, gene expression of infected vs control cells of each line was measured and compared. In the lower level comparisons, differential expression of genes was compared within infected and control cells of each of the two inbred lines. DE genes from lower level comparisons are presented here.

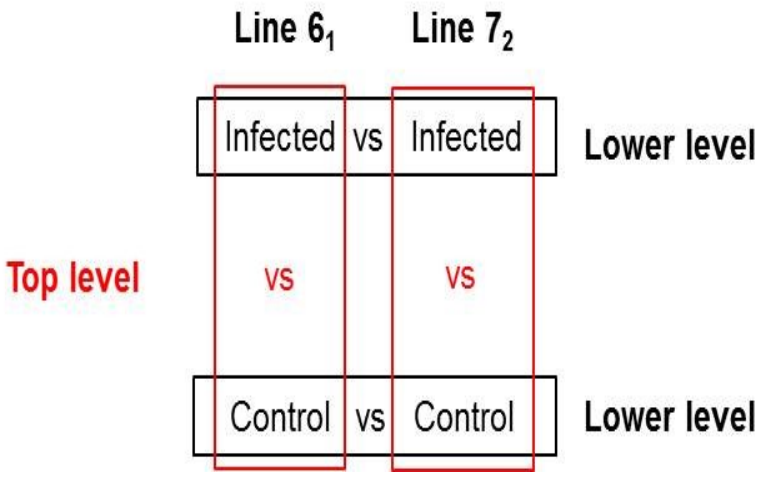

Figure 6.1. *Levels of comparison to explore DE genes in infected and control groups of two inbred chicken lines.*

Various categories of differentially expressed genes were revealed by these analyses, such as up- or down-regulation in the control or infected group only, up- or down-

regulation in both the control and infected groups, up-regulation in the control group but down-regulation in the infected group, and vice versa. In this Chapter, functional analysis of DE genes in the control (no expression of these genes in the infected group) and infected (no expression of these genes in the control group) groups was carried out using several software programmes. The comparative analysis was based on line 6_1, which means genes up-regulated in line 6_1 represent genes highly expressed in line 6_1 compared to line 7_2 and genes down-regulated in line 6_1 indicate genes highly expressed in line 7_2 compared to line 6_1.

From the lists of DE genes, a subset of genes were selected in each category based on their fold changes (>2). The DE gene numbers that were used for functional analysis using various software packages are given in Table 6.1. The full lists of DE genes in macrophages and DCs are provided in Appendix 2 (Table S2.1 to Table S2.4 for macrophages and Table S2.5 to Table S2.8 for DCs).

Category ⟹	Up-regulated in line 6_1 (compared to line 7_2)	Down-regulated in line 6_1 (compared to line 7_2)
Terms used in this Chapter ⟹	Highly expressed in line 6_1	Highly expressed in line 7_2
Macrophage control	173	263
Macrophage infected	261	236
DC control	183	234
DC infected	401	122

Table 6.1. *The DE gene numbers (fold change >2) used for functional analysis.*

6.3 Analysis of DE genes using DAVID software package

DE genes from each category were analysed using several software packages to reveal their involvement in various biological pathways. Analysis in DAVID was carried out to identify gene clusters with enriched biological terms in control and infected APCs as described in section 2.10.1. The enrichment score was calculated with a set of input genes highly associated with certain biological terms, which was statistically measured by a Fisher Exact test in the DAVID system. Usually a p-value equal to or smaller than 0.05 was considered to be strongly enriched in the annotation categories. The overall enrichment score for the group was based on the p-value of each term member. The higher the score, the more enriched it is; usually the threshold is >1.

6.3.1 Analysing genes highly expressed in control and infected macrophages

Genes highly expressed in line 6_1 control macrophages clustered in functions related to the regulation of apoptosis and cell death (Table 6.2), whereas highly expressed genes in line 7_2 control macrophages clustered mainly with growth and structural maintenance factors such as collagen, hydoxylysine and EGF (epidermal growth factor) (Table 6.3).

Following MDV infection, the highly enriched gene clusters in line 6_1 macrophages were those engaged in immune responses such as cytokine and chemokine activity and JAK-STAT (Janus Kinase (JAK)-Signal transducers and activators of transcription (STAT)) signalling pathways (Table 6.4), but genes in line 7_2 macrophages clustered in biological processes e.g. dephosphorylation and also with cellular components such as lipoprotein (Table 6.5). The JAK-STAT pathway is the

principal signalling mechanism for a wide array of cytokines and growth factors resulting in cell proliferation, differentiation, cell migration and apoptosis. A diverse array of ligands (e.g. cytokines, interferons, growth factors) and their receptors stimulate the JAK-STAT pathway (Vignais et al., 1996). An activation of JAK-STAT signalling pathway was reported in splenocytes of broilers and layers following MDV-infection (Perumbakkam et al., 2013). Smith et al. (2011) also observed an increased activity of JAK-STAT pathway in the splenocytes of MDV-infected chickens.

Annotation cluster/ Enrichment score	Term	Gene count	Percentage	p-value
1/1.88	Regulation of apoptosis	7	5	1.20E-02
	Regulation of cell death	7	5	1.40E-02

Table 6.2. *DAVID analysis of genes highly expressed in line 6$_1$ control macrophages ($p<0.05$).*

Annotation cluster/ Enrichment score	Term	Gene count	Percentage	p-value
1/2.08	Hydroxylysine	3	1.3	2.30E-03
	Collagen triple helix repeat	4	1.7	9.70E-03
	VWA	3	1.3	2.90E-02
	von Willebrand factor, type A	3	1.3	2.90E-02
	Extracellular matrix	4	1.7	8.70E-02
2/1.51	Transmembrane receptor Protein serine/threonine kinase signalling pathway	4	1.7	2.40E-02
3/1.32	Mesoderm formation	3	1.3	2.80E-02
4/1.29	Purine nucleotide binding	23	10	3.40E-02
	EGF	4	1.7	2.90E-02

5/1.14	EGF-like domain	4	1.7	5.70E-02
	EGF	4	1.7	6.10E-02

Table 6.3. *DAVID analysis of genes highly expressed in line 7_2 control macrophages ($p<0.05$).*

Annotation cluster/ Enrichment score	Term	Gene count	Percentage	p-value
1/2.62	Chemokine activity	4	2	6.50E-04
	SCY	3	1.5	2.60E-03
	Small chemokine, interleukin-8-like	3	1.5	4.10E-03
	Immune response	7	3.6	6.30E-03
	Cytokine activity	4	2	1.70E-02
2/1.76	Cytokine receptor activity	4	2	6.10E-03
	JAK-STAT signalling pathway	5	2.6	3.10E-02

Table 6.4. *DAVID analysis of genes highly expressed in line 6_1 infected macrophages ($p<0.05$).*

Annotation cluster/ Enrichment score	Term	Gene count	Percentage	p-value
1/1.11	Protein tyrosine phosphatase activity	4	1.9	4.50E-02
	Dephosphorylation	4	1.9	1.10E-01
2/1.09	Propeptide: Removed in mature form	3	1.4	8.00E-02
	Anchored to membrane	3	1.4	1.10E-01
	Lipoprotein	4	1.9	1.40E-01
3/1.07	Transmembrane region	8	3.8	2.80E-01

Table 6.5. *DAVID analysis of genes highly expressed in line 7_2 infected macrophages ($p<0.05$).*

6.3.2 Analysis of genes highly expressed in control and infected DCs

The genes which showed high expression in line 6_1 control DCs clustered in biological processes such as activation, proliferation and differentiation of T cells (Table 6.6), but no high enrichment (>1) of gene clusters was observed in line 7_2 control DCs.

In line 6_1 infected DCs, DAVID analysis revealed various annotation clusters of genes in which top scored clusters were associated with growth and structural terms such as extracellular matrix and hydroxylysine and low scored gene clusters were involved in immune activities like innate immune response and chemotaxis (Table 6.7). Genes highly expressed in line 7_2 infected DCs showed enrichment with the biological term signal peptide (Table 6.8) which is a short (5-30 amino acids long) peptide present at the N-terminus of the majority of newly synthesised secretory proteins (Blobel and Dobberstein, 1975).

Annotation cluster/ Enrichment score	Term	Gene count	Percentage	p-value
1/1.24	Alpha-beta T cell activation	3	1.9	1.70E-03
	Lymphocyte proliferation	3	1.9	1.10E-02
	T cell differentiation	3	1.9	4.50E-02
	Immune system development	3	1.9	3.30E-01

Table 6.6. *DAVID analysis of genes highly expressed in line 6_1 control DCs ($p<0.05$).*

Annotation cluster/ Enrichment score	Term	Gene count	Percentage	p-value
1/6.95	Extracellular matrix	19	6.1	3.00E-08
2/5.67	Collagen triple helix repeat	8	2.6	1.80E-06
	Collagen	8	2.6	2.80E-06
3/5.43	Carbohydrate binding	12	3.9	1.90E-06
4/3.09	Hydroxyline	4	1.3	1.50E-04
	von Willebrand factor, type A	5	1.6	4.50E-04
	VWA	5	1.6	1.40E-03
	Sarcolemma	4	1.3	5.00E-03
5/2.75	Fibrillar collagen, C-terminal	4	1.3	2.10E-04
	COLFI	4	1.3	5.60E-03
	Collagen	4	1.3	1.80E-02
6/2.36	domain:Ig-like C2-type 1,2,3	5	1.6	2.80E-03
7/2.19	IGc2	7	2.3	4.70E-03
	Immunoglobulin domain	7	2.3	5.60E-03
8/1.77	Serine-type endopeptidase inhibitor activity	5	1.6	1.10E-02
9/1.57	Immunoglobulin-like	8	2.6	2.40E-02
	IG	6	1.9	1.30E-01
10/1.44	Fibronection, type III	6	1.9	2.40E-02
	FN3	6	1.9	7.10E-02
11/1.43	Endopeptidase activity	10	3.2	1.50E-02
	Proteolysis	12	3.9	1.60E-01
12/1.29	Chemotaxis	4	1.3	2.20E-02
13/1.25	Toll-Interleukin receptor	3	1	4.90E-02
	TIR	3	1	8.30E-02
	Innate immune response	3	1	1.00E-01

Table 6.7. *DAVID analysis of genes highly expressed in line 6_1 infected DCs ($p<0.05$).*

Annotation cluster/ Enrichment score	Term	Gene count	Percentage	p-value
1/1.12	Signal peptide	8	8.2	4.70E-02
	Glycoprotein	6	6.2	1.40E-01

Table 6.8. *DAVID analysis of genes highly expressed in line 7_2 infected DCs ($p<0.05$).*

6.4 Pathway Express analysis of DE genes

Following DAVID analysis, which identified gene clusters with enriched biological terms, the DE gene sets were analysed using the Pathway Express software package (Draghici et al., 2007) in order to determine biological pathways associated with genes in control APCs and their potential alterations after MDV infection. As described in section 2.10.2, the analysis was based upon the KEGG pathways and significantly affected pathways (FDR-corrected gamma p value of <0.05) pre- and post-MDV infection of APCs in the two inbred lines are shown in Table 6.9 to Table 6.16. The p-value was determined based on the impact analysis of each gene's expression and interactions in a given pathway (section 2.10.2). Immune pathways previously known and relevant to this study are highlighted in red in both control and infected APCs.

6.4.1 Analysis of genes highly expressed in control and infected macrophages

No apparent difference was observed between control macrophages in the context of activated biological pathways in two lines. TGF-β signalling was the common immune pathway in lines 6_1 and 7_2 control macrophages (Tables 6.9 and 6.10, respectively). TGF-β signalling pathway is involved in many cellular processes including cell growth, cell differentiation and apoptosis (Miyazawa et al., 2002). An

important involvement of this pathway was reported in MDV-infected cells where MDV-1-miR-M3 blocked the protein level expression of Smad2 (a crucial element of the TGF-β signalling pathway), resulting in a cellular environment suitable for viral latency and oncogenesis (Xu et al., 2011).

Following MDV infection, the JAK-STAT signalling pathway along with the cytokine-cytokine receptor interaction were significantly activated in line 6_1 macrophages (Table 6.11), whereas in line 7_2 infected macrophages, natural killer cell mediated cytotoxicity pathway was the only immune pathway activated (Table 6.12). As mentioned in section 6.3.1, the JAK-STAT pathway was reported to be activated in MDV-infected cells (Smith et al., 2011; Perumbakkam et al., 2013). An increased activity of cytokine-cytokine receptor interaction was also observed in splenocytes after MDV infection (Smith et al., 2011; Perumbakkam et al., 2013). NK cell cytotoxicity is a receptor mediated killing of virus-infected or tumour cells (Terunuma et al., 2008) and an activation of this pathway could be an indication of NK-cell involvement in response to MDV infection. The cytotoxic activity of NK cells was increased in MD-resistant chickens (6_1) compared to MD-susceptible chickens (7_2) following MDV infection (Garcia-Camacho et al., 2003) which is in contrast to present observation.

6.4.2 Analysis of genes highly expressed in control and infected DCs

Control DCs of the two inbred lines showed almost identical immune activities. TGF-β and JAK-STAT signalling were the two known immune pathways significantly activated in lines 6_1 and 7_2 control DCs (Tables 6.13 and 6.14, respectively).

Following MDV infection, more immune pathways were activated in line 6_1 DCs compared to line 7_2. While a significant activation of JAK-STAT signalling pathway, cytokine-cytokine receptor interaction, antigen processing and presentation, and MAPK (mitogen activated protein kinase) signalling pathway was observed in line 6_1 infected DCs (Table 6.15), genes highly expressed in line 7_2 infected DCs were only involved with cytokine-cytokine receptor interaction mechanisms (Table 6.16). Processing of antigen and its presentation on the surface in the context of MHC is a characteristic feature of APCs (Blum et al., 2013).

Rank	Pathway Name	Impact Factor	Input Genes/ Genes in the Pathway	Corrected gamma p-value
1	Melanoma	7.342	1/71	0.005403562
2	TGF-beta signalling pathway	6.702	2/87	0.009461541
3	Pathways in cancer	5.679	2/330	0.022821967
4	B cell receptor signalling pathway	5.172	2/65	0.035015059
5	Regulation of actin cytoskeleton	5.152	5/217	0.035606653
6	Type II diabetes mellitus	4.623	1/45	0.055236314

Table 6.9. *Pathway express analysis of genes highly expressed in line 6_1 control macrophages. Immune pathways are shown in red.*

Rank	Pathway Name	Impact Factor	Input Genes/ Genes in the Pathway	Corrected gamma p-value
1	ECM-receptor interaction	12.468	9/84	5.18E-05
2	Focal adhesion	10.735	11/203	2.55E-04
3	Neuroactive ligand-receptor interaction	9.451	7/256	8.22E-04
4	TGF-beta signalling pathway	4.952	4/87	0.042076
5	Small cell lung cancer	4.626	5/86	0.0551

Table 6.10. *Pathway express analysis of genes highly expressed in line 7_2 control macrophages. Immune pathways are shown in red.*

The role of MAPKs is very critical for cellular homeostasis, and loss of fine control of MAPK regulation due to mutation or changes in the expression of proteins regulating MAPK signalling, may contribute to cancer (Dhanasekaran and Johnson, 2007). The MDV oncogene, Meq, was shown to transcriptionally regulate many genes in the MAPK and JAK-STAT signalling pathways, which are crucial for oncogenesis and/or include signalling mediators involved in apoptosis (Subramaniam et al., 2013).

Rank	Pathway Name	Impact Factor	Input Genes/ Genes in the Pathway	Corrected gamma p-value
1	Phosphatidylinositol signalling system	27.679	2/76	2.73E-11
2	Cytokine-cytokine receptor interaction	16.043	13/263	1.84E-06
3	Adherens junction	9.76	1/78	6.21E-04
4	JAK-STAT signalling pathway	9.506	7/155	7.82E-04
5	Basal cell carcinoma	7.313	3/55	0.005543222
6	Axon guidance	7.281	5/129	0.005701441

Table 6.11. *Pathway express analysis of genes highly expressed in line 6_1 infected macrophages. Immune pathways are shown in red.*

Rank	Pathway Name	Impact Factor	Input Genes/ Genes in the Pathway	Corrected gamma p-value
1	Phosphatidylinositol signalling system	26.737	1/76	6.78E-11
2	Adherens junction	14.571	3/78	7.31E-06
3	Cell adhesion molecules (CAMs)	9.57	6/134	7.38E-04
4	Gap junction	6.358	1/96	0.012750155
5	Natural killer cell mediated cytotoxicity	6.062	4/135	0.016452601
6	Melanoma	6.029	1/71	0.016925134
7	Focal adhesion	5.645	6/203	0.023491061
8	Tight junction	5.363	4/135	0.029822264

Table 6.12. *Pathway express analysis of genes highly expressed in line 7_2 infected macrophages. Immune pathways are shown in red.*

Rank	Pathway Name	Impact Factor	Input Genes/ Genes in the Pathway	Corrected gamma p-value
1	Phosphatidylinositol signalling system	24.953	1/76	3.78E-10
2	TGF-beta signalling pathway	12.746	1/87	4.01E-05
3	Basal cell carcinoma	8.158	1/55	0.002623169
4	Adherens junction	6.915	1/78	0.007857865
5	Leukocyte transendothelial migration	6.321	4/119	0.013164216
6	Axon guidance	5.502	4/129	0.026519097
7	Adipocytokine signalling pathway	5.117	1/67	0.036665163

Table 6.13. *Pathway express analysis of genes highly expressed in line 6_1 control DCs. Immune pathways are shown in red.*

Rank	Pathway Name	Impact Factor	Input Genes/ Genes in the Pathway	Corrected gamma p-value
1	Phosphatidylinositol signalling system	22.839	5/76	2.87E-09
2	Small cell lung cancer	11.359	8/86	1.44E-04
3	Adherens junction	9.055	1/78	0.001174
4	Hematopoietic cell lineage	9.039	4/87	0.001192
5	Melanoma	8.575	3/71	0.001807
6	Cell adhesion molecules (CAMs)	8.424	2/134	0.002069
7	Pathways in cancer	7.587	11/330	0.004354
8	JAK-STAT signalling pathway	6.013	5/155	0.017159
9	Focal adhesion	5.705	7/203	0.022323
10	Renal cell carcinoma	5.516	4/69	0.026207

Table 6.14. *Pathway express analysis of genes highly expressed in line 7_2 control DCs. Immune pathways are shown in red.*

Rank	Pathway Name	Impact Factor	Input Genes/ Genes in the Pathway	Corrected gamma p-value
1	Phosphatidylinositol signalling system	25.802	2/76	1.67E-10
2	ECM-receptor interaction	20.707	14/84	2.21E-08
3	Cytokine-cytokine receptor interaction	18.371	18/263	2.04E-07
4	Focal adhesion	16.312	18/203	1.43E-06
5	JAK-STAT signalling pathway	8.966	10/155	0.001272438
6	Regulation of actin cytoskeleton	8.373	10/217	0.002165364
7	Pathways in cancer	6.816	15/330	0.008567091
8	Prostate cancer	6.453	5/90	0.011744346
9	Calcium signalling pathway	6.415	9/182	0.01213702
10	Complement and coagulation cascades	5.872	5/69	0.019360027
11	TGF-beta signalling pathway	5.846	6/87	0.019794811
12	Melanoma	5.837	3/71	0.01994751
13	Antigen processing and presentation	5.605	3/89	0.024302573
14	MAPK signalling pathway	5.588	9/272	0.024655626
15	Adherens junction	5.554	3/78	0.025376685
16	Pancreatic cancer	5.381	4/72	0.029373124
17	Graft-versus-host disease	5.144	2/42	0.035845975
18	Glioma	4.851	3/65	0.045758056

Table 6.15. *Pathway express analysis of genes highly expressed in line 6_1 infected DCs. Immune pathways are shown in red.*

Rank	Pathway Name	Impact Factor	Input Genes/ Genes in the Pathway	Corrected gamma p-value
1	Adherens junction	36.087	2/78	7.89E-15
2	Tight junction	9.05	1/135	0.00118
3	Cytokine-cytokine receptor interaction	6.673	1/263	0.009703
4	Basal cell carcinoma	5.967	2/55	0.017849
5	Prostate cancer	4.784	3/90	0.048369

Table 6.16. *Pathway express analysis of genes highly expressed in line 7_2 infected DCs. Immune pathways are shown in red.*

6.5 Analysis of DE genes using IPA

Complementary to the findings from Pathway Express, use of the IPA program (Ingenuity Systems) (section 2.10.3) revealed which canonical pathways were inherently expressed in control APCs and which were up-regulated following MDV infection of APCs. The p-value was calculated using the right-tailed Fisher Exact Test. By default, IPA applies a -log (p-value) cut-off of 1.3 ($p<0.05$), that means pathways with a p-value equal to or greater than 0.05 are not shown.

6.5.1 Analysing genes highly expressed in control and infected macrophages

A higher number of immune pathways were inherently expressed in line 7_2 control macrophages than in line 6_1. For instance, the cytotoxic T lymphocyte (CTL) mediated apoptosis of target cell was the only immune pathway in line 6_1 control macrophages (Figure 6.2A), but LPS/IL-1 mediated inhibition of RXR (retinoid X receptor) function, role of PKR (protein kinase RNA-activated) in interferon induction and antiviral response and SAPK /JNK signalling pathways were involved with genes highly expressed in line 7_2 control DCs (Figure 6.2B).

LPS/IL-1 mediated inhibition of RXR function leads to decreased nuclear RXRα levels and reduced nuclear DNA binding and transcriptional activity (Zimmerman et al., 2006). An activation of this pathway was observed in the splenocytes of MDV-infected chickens (Smith et al., 2011).

PKR belongs to the family of pattern-recognition receptors (PRRs) which is in the centre of cellular response to different stress signals such as pathogens, lack of nutrients, cytokines, irradiation, mechanical stress or stress of endoplasmic reticulum. PKR can be induced by IFNs and is activated by dsRNA from viral

sources. PKR pathway leads to stress response through activation of other stress pathways such as JNK, p38, NF-κB, PP2α (protein phosphatase 2α) and phosphorylated eIF-2α (eukaryotic translation initiation factor 2α) (Hotamisligil, 2010). By catalysing the phosphorylation of eIF-2α, PKR leads to an inhibition of the initiation of protein synthesis (Meurs et al., 1990). In this study, an activation of PKR signalling in control macrophages may be due to the stress induced by culture conditions.

Stress-activated protein kinases (SAPKs), also referred to as c-Jun N-terminal kinases (JNKs), play an important role in the regulation of key cellular processes, including survival and death (Bhoumik et al., 2007).

More immune pathways were activated in macrophages from resistant birds (6_1) compared to susceptible birds (7_2) following MDV infection. The canonical immune pathways significantly induced by MDV infection in line 6_1 macrophages were JAK-STAT signalling and eNOS signalling (Figure 6.3A), whereas in line 7_2 macrophages no immune pathway was activated following infection (Figure 6.3B).

An involvement of JAK-STAT signalling pathway in MDV-infected cells was described previously. eNOS signalling is involved in synthesis of nitric oxide (NO) which is a short-lived free radical involved in varieties of physiological and pathological processes. NO is produced along with L-Citrulline by the oxidation of L-Arginine in the reaction catalysed by three different isoforms of NOS (nitric oxide synthase). Of them, neuronal (nNOS) and endothelial (eNOS) isoforms are $Ca2^{+}$ dependent for their enzyme activity and inducible NOS (iNOS) is $Ca2^{+}$-independent (García-Cardeña et al., 1996). eNOS plays a crucial role in the state of blood vessel vasodilation and hence blood pressure regulation (Liu et al., 1996). Abnormalities in

vascular NO production are thought to contribute to the pathogenesis of certain vascular disorders such as atherosclerosis. Infection with MDV is sometimes associated with atherosclerosis in large arteries (Minick et al., 1979).

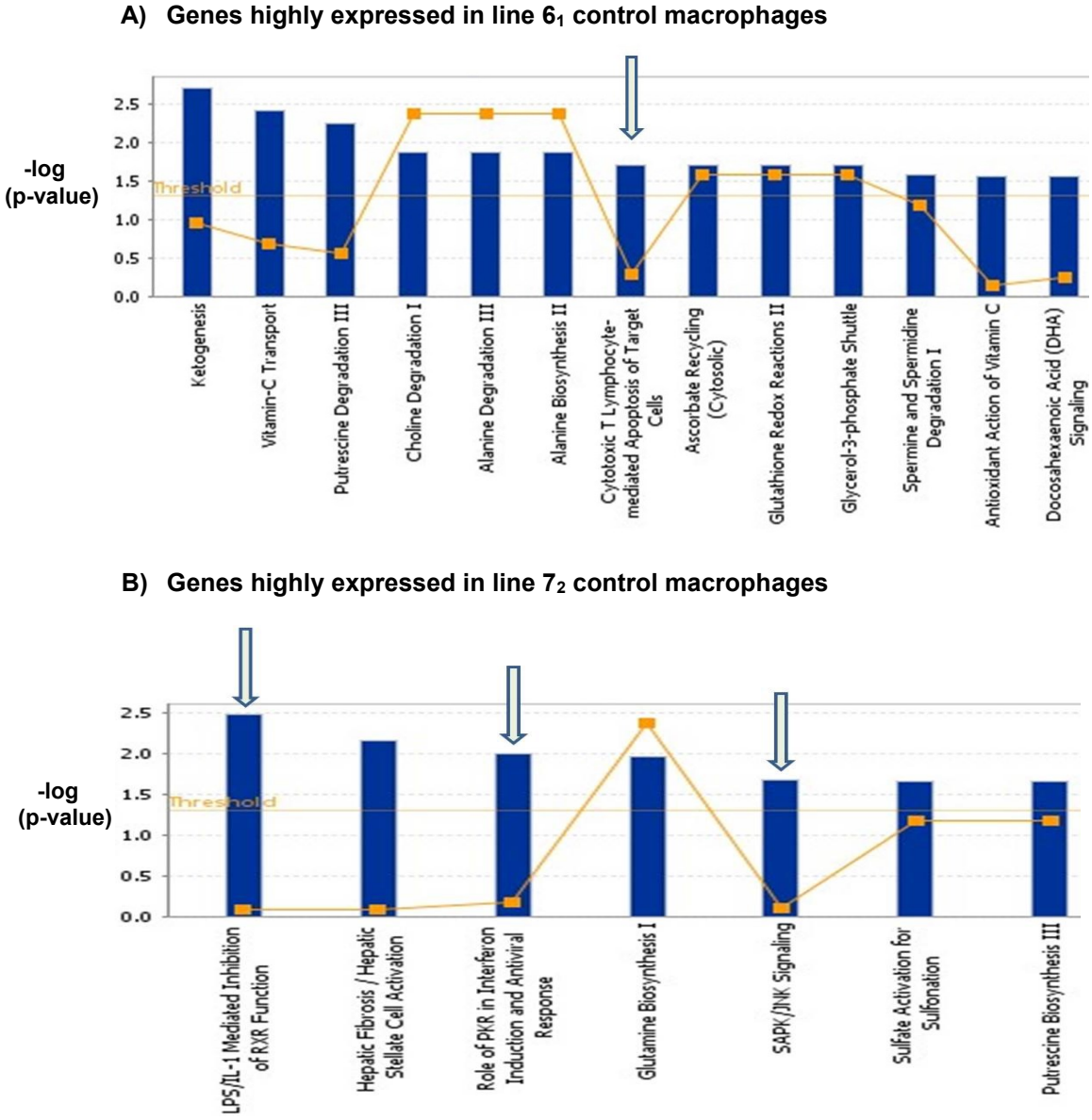

Figure 6.2. *Ingenuity pathway analysis showing the most highly represented canonical pathways that genes highly expressed in (A) line 6_1 and (B) line 7_2 control macrophages are involved with. Arrows indicate the pathways related to immune mechanisms. The yellow line represents the ratio of the number of genes represented within each pathway to the total number of genes in the pathway. The threshold line showing pathways that have a p-value <0.05.*

A) Genes highly expressed in line 6_1 infected macrophages

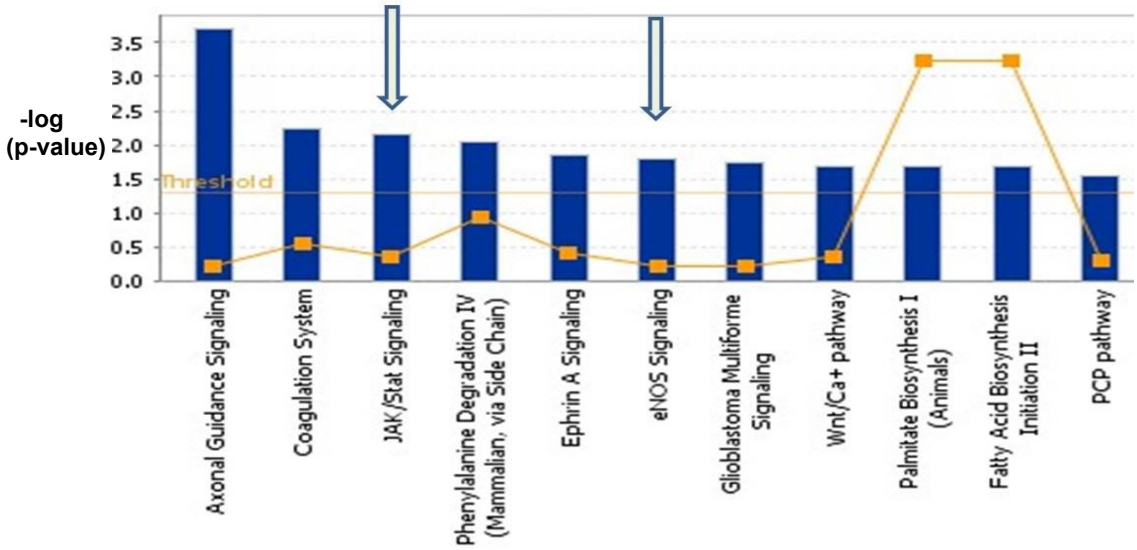

B) Genes highly expressed in line 7_2 infected macrophages

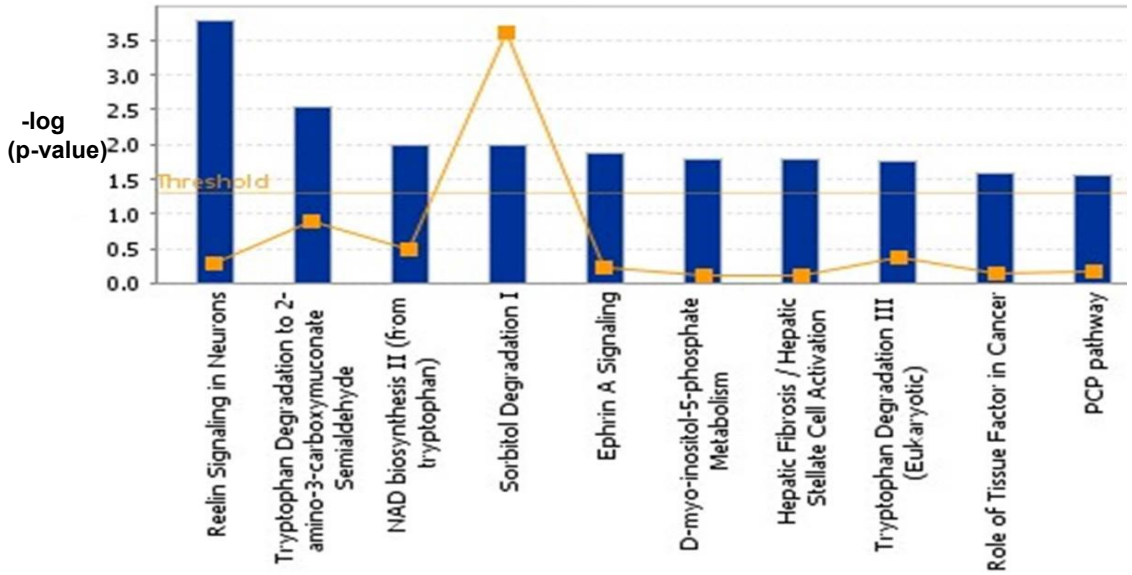

Figure 6.3. *Ingenuity pathway analysis showing the most highly represented canonical pathways that genes highly expressed in (A) line 6_1 and (B) line 7_2 infected macrophages are involved with. Arrows indicate the pathways related to immune mechanism. The yellow line represents the ratio of the number of genes represented within each pathway to the total number of genes in the pathway. The threshold line showing pathways that have a p-value <0.05.*

6.5.2 Analysing genes highly expressed in control and infected DCs

Before MDV infection, more immune pathways were involved with genes highly expressed in DCs of susceptible birds (7_2) (Figure 6.4B) than the resistant birds (6_1) (Figure 6.4A). In line 6_1 control DCs, the immune related canonical pathways were LPS/IL-1 mediated inhibition of RXR function, CTL mediated apoptosis of target cells and IL-15 signalling (Figure 6.4A). IL-15 plays an important role as an inducer of immune response by activating various signalling pathways including the JAK-STAT, MAPK, and NF-κB (nuclear factor kappa-light-chain-enhancer of activated B cells) pathways to control cell growth and differentiation, enhance phagocytosis and increase the inflammatory response (Jakobisiak et al., 2011; Perera et al., 2012).

In line 7_2 control DCs, significantly expressed inherent immune pathways were CD40 signalling, p53 signalling, lymphotoxin β receptor (LT-βR) signalling, role of PKR in interferon induction and antiviral response and IL-4 signalling (Figure 6.4B).

CD40-mediated signal transduction induces the transcription of a large number of genes implicated in host defence against pathogens. This is accomplished by the activation of multiple pathways including NF-κB, MAPK and STAT3 (Chatzigeorgiou et al., 2009). CD40-CD40L ligation on the surface of dendritic cells regulates production of pro-inflammatory cytokines such as IL-8 and IL-12. Ligation of CD40 on monocytes is important in stimulating production of IL-1α, IL-1β, IL-6, and IL-8, as well as in the rescue of circulating monocytes from apoptosis (Sakata et al., 1995).

The p53 pathway is composed of a network of genes and transcriptional regulators that monitor key cellular processes such as DNA replication, chromosome

segregation and cell division (Vogelstein et al., 2000). In response to a stress signal, the p53 protein is activated in a specific manner by post-translational modifications, and this leads to either cell cycle arrest, a programme that induces cell senescence or cellular apoptosis (Jin and Levine, 2001).

Signalling through the LT-βR pathway is a crucial element in the organisation of secondary lymphoid tissues. LT-βR activates multiple signalling pathways including transcriptional factor NF-κB, and cell death (Remouchamps et al., 2011).

IL-4 binding to its receptor activates JAK/TYK2 followed by phosphorylation and dimerization of STAT6. The transcriptional regulator STAT6 is able to induce various genes that are involved immune function like IgE and MHC II (Bhattacharjee et al., 2013).

Following MDV infection, line 6_1 DCs showed greater immune activity (Figure 6.5A) than the DCs of line 7_2 (Figure 6.5B). The immune pathways significantly induced in line 6_1 DCs were STAT3 pathway, IL-6 signalling, DC maturation, PRR recognition of bacteria and viruses, JAK-STAT signalling, IL-15 production and NF-κB signalling (Figure 6.5A).

STAT3 mediates the expression of a variety of genes in response to cell stimuli, and thus plays a key role in many cellular processes such as cell growth and apoptosis (Yang et al., 2007).

IL-6 is considered as a regulator of acute-phase responses and a lymphocyte stimulatory factor. The central role of IL-6 in inflammation makes it an important target for the management of infectious and inflammatory diseases. IL-6 and associated cytokines utilise JAK-STAT family members as major mediators of signal transduction (Heinrich et al., 2003). A significant up-regulation of IL-6 was observed

in the splenocytes of susceptible chickens but not in resistant lines following MDV infection (Kaiser et al., 2003).

A) Genes highly expressed in line 6_1 control DCs

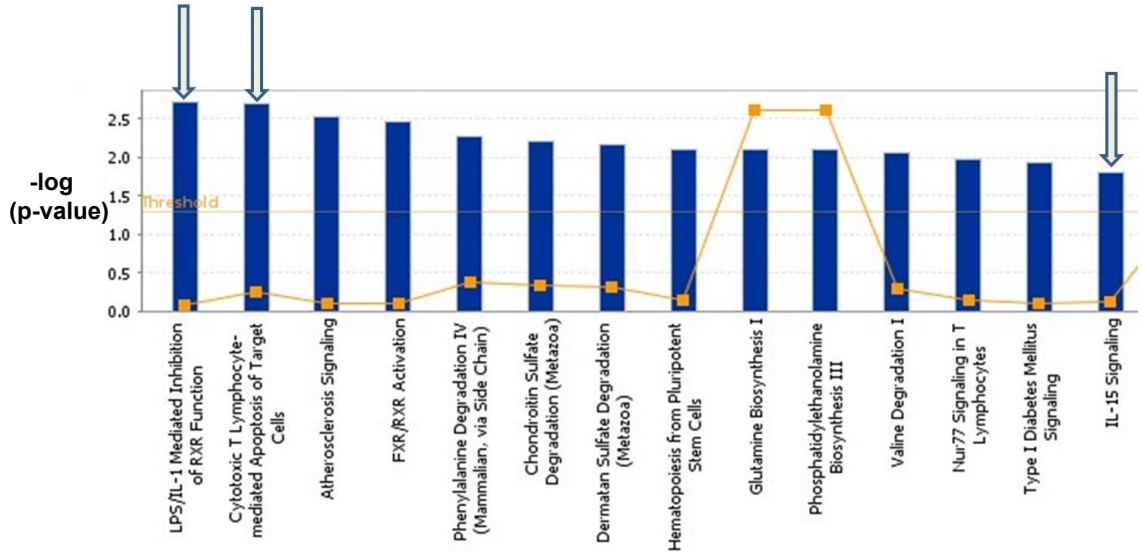

B) Genes highly expressed in line 7_2 control DCs

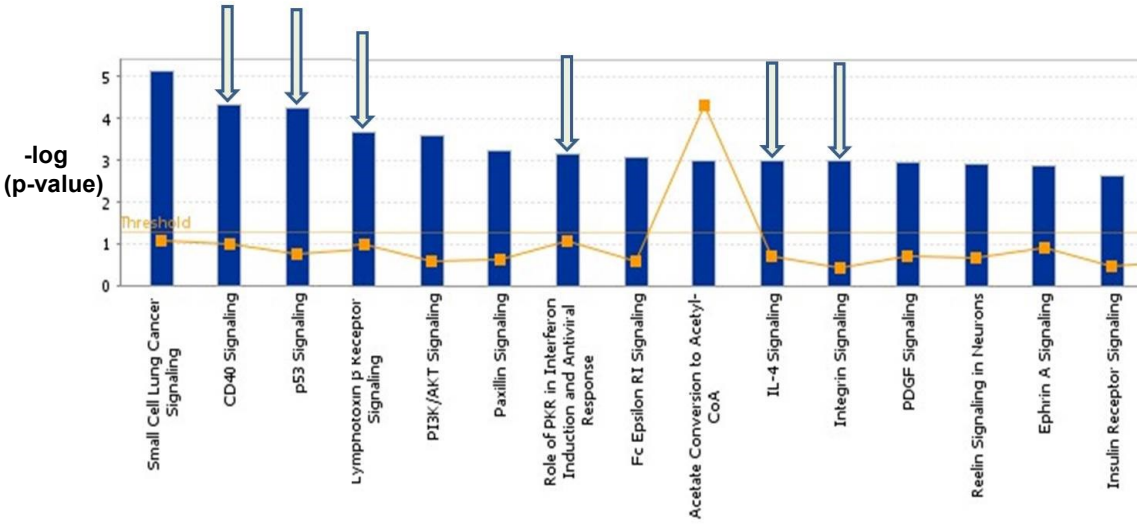

Figure 6.4. *Ingenuity pathway analysis showing the most highly represented canonical pathways that genes highly expressed in (A) line 6_1 and (B) line 7_2 control DCs are involved with. Arrows indicate the pathways related to immune mechanism. The yellow line represents the ratio of the number of genes represented within each pathway to the total number of genes in the pathway. The threshold line showing pathways that have a p-value <0.05.*

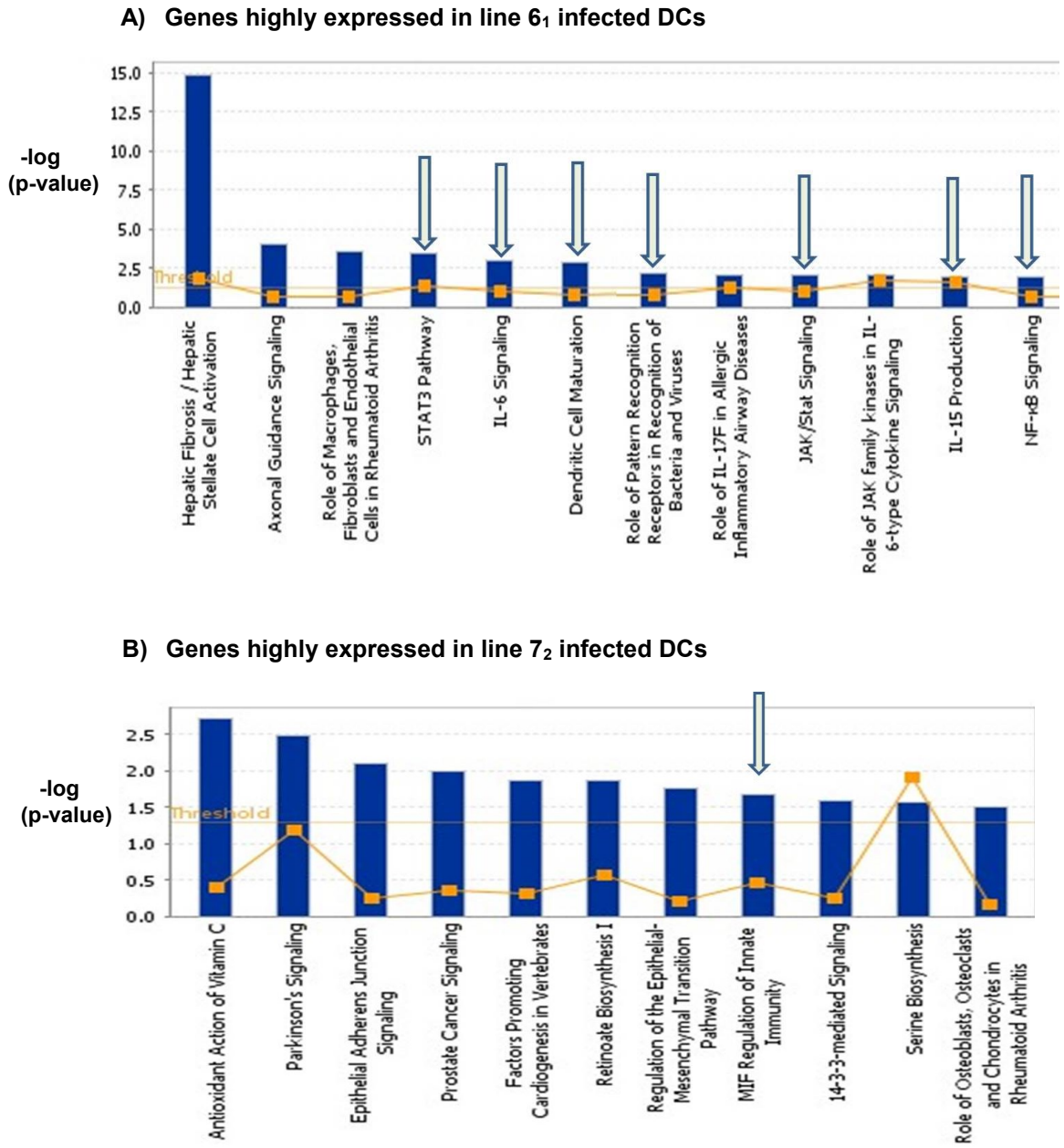

Figure 6.5. *Ingenuity pathway analysis showing the most highly represented canonical pathways that genes highly expressed in (A) line 6_1 and (B) line 7_2 infected DCs are involved with. Arrows indicate the pathways related to immune mechanism. The yellow line represents the ratio of the number of genes represented within each pathway to the total number of genes in the pathway. The threshold line showing pathways that have a p-value <0.05.*

Maturation of DCs leads to the up-regulation of MHC class I and II as well as co-stimulatory molecules such as CD80, CD83 and CD86, leading to an enhanced antigen presentation function in DCs. Several factors trigger the maturation of DCs, including microbes, cytokines and other cells of the immune system. They also up-regulate CCR7 (Wu et al., 2011), a chemotactic receptor that induces the dendritic cell to travel through the blood stream to the spleen or through the lymphatic system to lymphoid tissues. Mature DCs may also drive T cells to an antiviral Th1 immunity and an anti-MDV Th1 response was also suggested by Smith et al. (2011).

Role of PRR in recognition of bacteria and viruses is an innate immune pathway which was also reported to be activated in MDV-infected splenocytes (Smith et al., 2011).

The NF-κB signalling is a key mediator in controlling both innate and adaptive immunity. After activation by a large number of inducers, NF-κB proteins regulate the transcription of a large number of genes, including antimicrobial peptides, cytokines, chemokines, stress-response proteins and anti-apoptotic proteins (Li and Verma, 2002). NF-κB was shown to involve in MDV-induced neoplastic transformation of lymphocytes *in vivo* (Kumar et al., 2012).

In line 7_2 DCs, only MIF (macrophage migration inhibitory factor) regulation of innate immunity was activated after MDV infection (Figure 6.5B). MIF is primarily a regulator of innate immune responses to endotoxin and gram-negative bacteria (Meng and Lowell, 1997). It is an integral component of the host antimicrobial alarm system and stress response that promotes the pro-inflammatory functions of immune cells (Calandra and Roger, 2003).

6.6 The JAK-STAT signalling pathway

Analysing data using three software packages revealed that JAK-STAT was the common signalling pathway involved with genes highly expressed in line 6_1 infected macrophages and DCs. Therefore to get insight into the function of the molecules involved in this pathway, an illustrated diagram is provided in Figure 6.6 (for macrophages) and in Figure 6.7 (for DCs).

The genes involved in line 6_1 infected macrophages include CSF3, IL-2Rα, IL-13Rα2, IL-20Rα, IL-23R, STAT2 and STAT4 (Figure 6.6) and in line 6_1 infected DCs the genes were IL-6, IL-22Rα, JAK3, SOCS1, SOCS3 and CISH (CIS) (Figure 6.7).

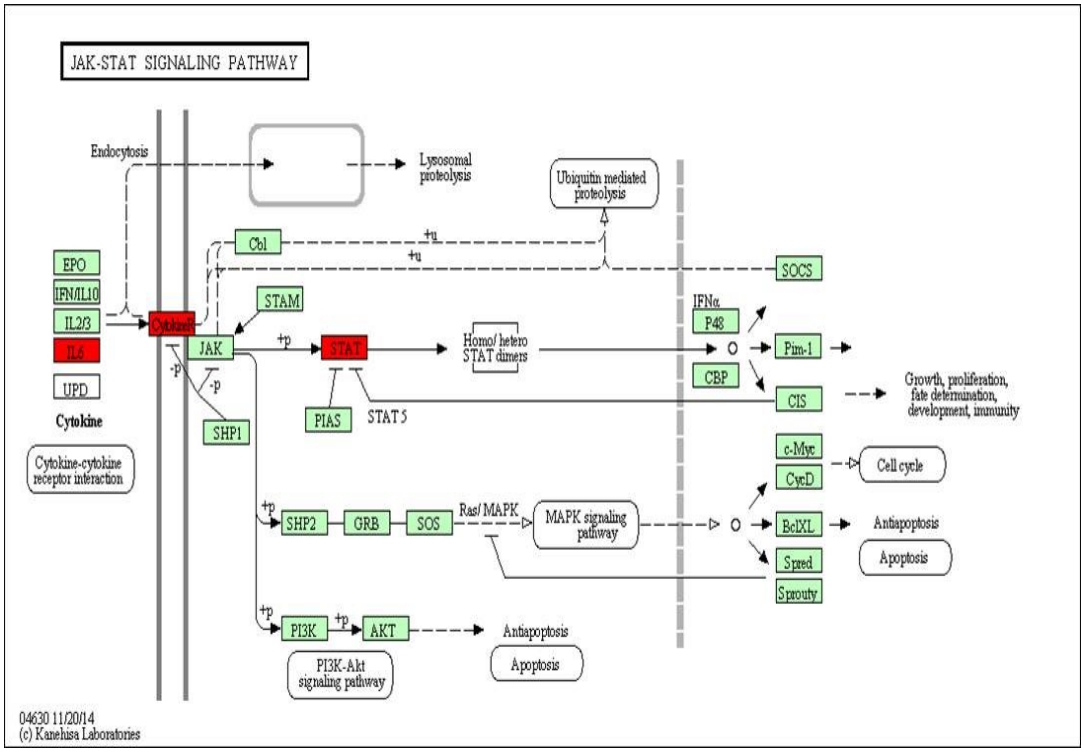

Figure 6.6. *JAK-STAT signalling pathway shows involvement of genes (red) highly expressed in line 6_1 infected macrophages.*

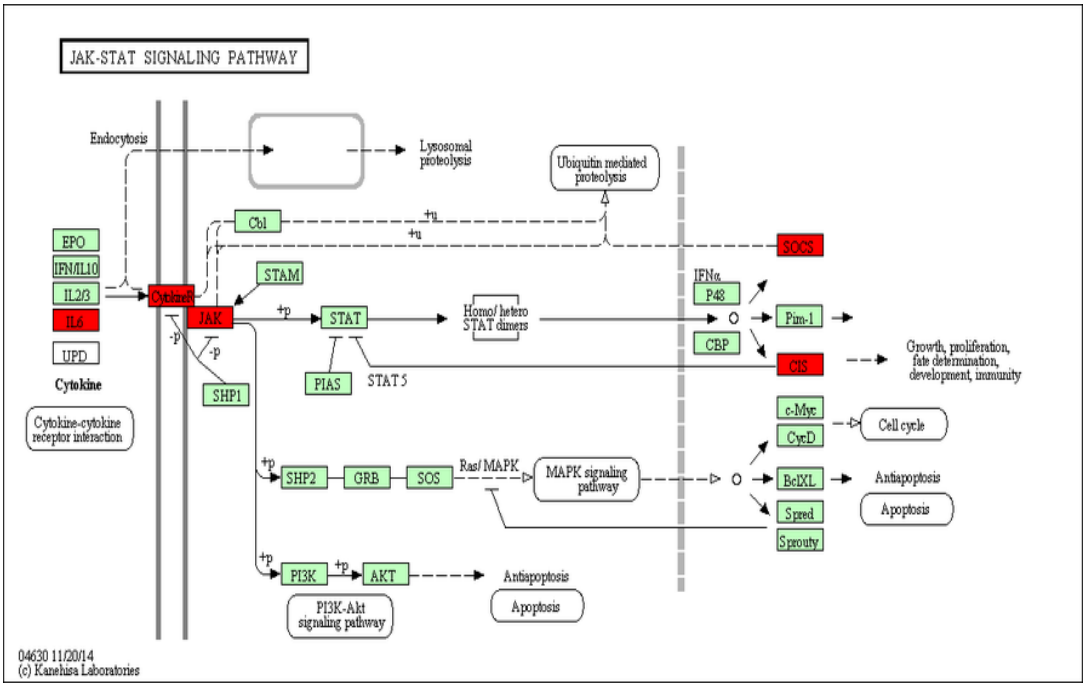

Figure 6.7. *JAK-STAT signalling pathway shows involvement of genes (red) highly expressed in line 6_1 infected DCs.*

Type	Ligand	Complex	Receptors		Downstream Pathways			Functions
Antiviral	IFNα	Type I IFNR	IFNαR1	IFNαR2	Jak1, Tyk2	Stat1,2,3,5	Socs1, Socs3	Antiviral
	IFNβ							
	IFNκ							
	IFNω							
	IFNε							
	IFNγ	Type II IFNR	IFNγR2	IFNγR1	Jak1, Jak2	Stat1,3,5	Socs1, Socs3	Antivirial, pro-inflammatory
	IFN-λ1	IFN-λR	IFNλR1		Jak1, Tyk2	Stat1,2,3,5		Antiviral
	IFN-λ2							
	IFN-λ3							
Non-antiviral	IL-10	IL-10R	IL-10R1	IL-10R2		Stat1,3,5		Anti-inflammatory
	IL-26	Type III IL-20R	IL-20R1					Immune response
	IL-22	IL-22R	IL-22R1					Pro-inflammatory
	IL-19	Type I IL-20R	IL-20R1	IL-20R2				
	IL-20							Keratinocyte proliferation
	IL-24							Anti-tumour
	IL-20	Type II IL-20R	IL-22R1					Keratinocyte proliferation
	IL-24							Anti-tumour
	IL-22	IL-22 Decoy	IL-22BP					IL-22 antagonist
	FVIIa	TF	TF					Clotting cascade

Structure
Ligand Binding
Accessory

Table 6.17. *Various physiological and pathological functions accomplished by molecules involved in JAK-STAT signalling pathway. Adapted and modified from O'Sullivan et al. (2007) with permission from Elsevier.*

Interleukins, IFNs and haematopoietic growth factors activate JAK-STAT pathway (O'Shea et al., 2002) and SOCS1, SOCS3 and CISH (CIS) are negative regulators of JAK-STAT signalling pathway (Tamiya et al., 2011). The interactive functions between molecules involved in this pathway may play role in various physiological and pathological processes. As shown in Table 6.17, IFN-mediated activation of JAK-STAT pathway play crucial role in anti-viral immunity.

6.7 Analyses using Expander programme

The Expander programme was used to analyse the gene ontology (GO) functional annotations (section 2.10.4) to determine the functions of the genes highly expressed in control and MDV-infected APCs of lines 6_1 and 7_2, The transcriptional factor (TF) binding sites were also determined using the Expander software. Significance was determined as Bonferroni corrected p-values lower than 1.0E-4, which is the default value of the Expander programme.

6.7.1 Analysis of genes in control and infected macrophages

In line 6_1 control macrophages, genes were significantly involved in oxidoreductase activity (Figure 6.8), but no specific TF binding sites were identified.

In line 7_2 control macrophages, significantly enriched gene functions were protein binding and anatomical structure formation (Figure 6.9A) and the genes had a higher proportion of IRF-7 (interferon regulatory factor -7) TF binding sites (Figure 6.9B). The frequency ratio (frequency in set divided by frequency in background) was 2 (Figure 6.9B), which means presence of twice as many IRF-7 sites than would be expected by chance.

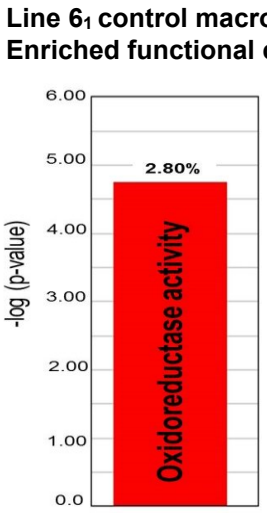

Figure 6.8. *Expander programme showing the overrepresentation analysis of genes highly expressed in line 6_1 control macrophages. The GO biological process which is significantly enriched and the frequency of genes of the functional class within the examined set described as a percentage of the total.*

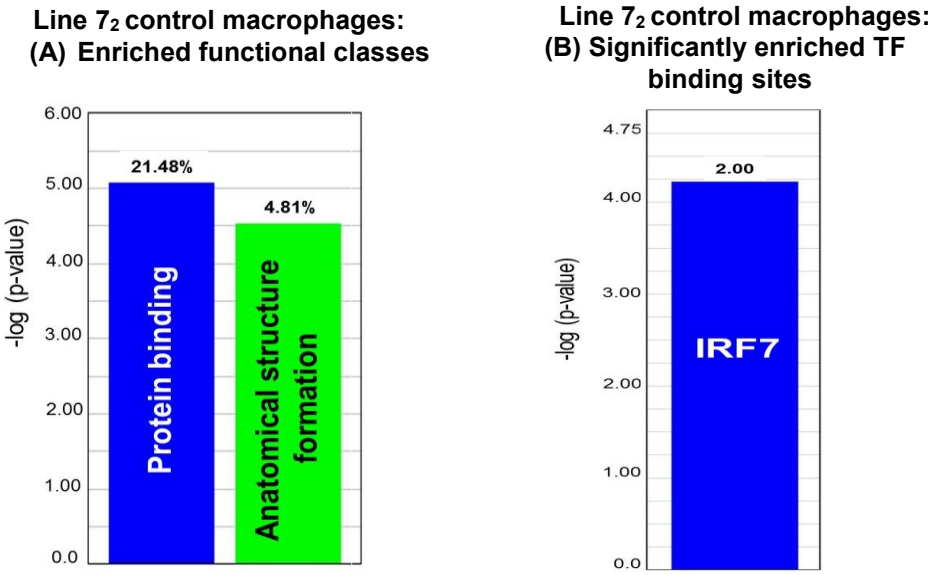

Figure 6.9. *Expander programme showing the overrepresentation analyses of genes highly expressed in line 7_2 control macrophages. (A) The GO biological processes which are significantly enriched. The frequency of genes of a functional class within the examined set is described as a percentage of the total. (B) Genes showing significantly enriched IRF-7 TF binding sites. The frequency ratio (frequency of the set divided by the frequency of the background) is shown.*

Line 6_1 infected macrophages:
(B) Enriched functional classes

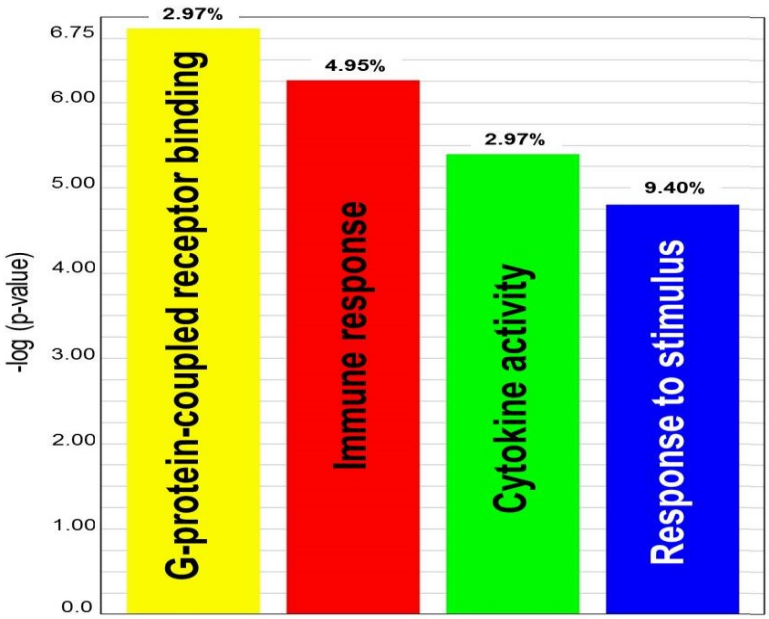

Line 6_1 infected macrophages:
(B) Significantly enriched TF binding sites

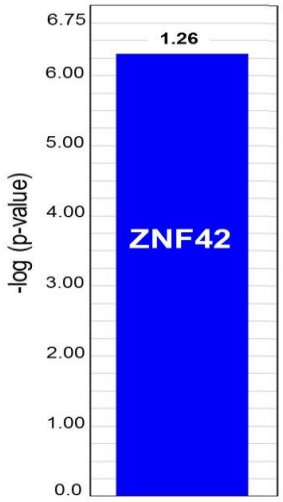

Figure 6.10. *Expander programme showing the overrepresentation analyses of genes highly expressed in in line 6_1 infected macrophages. (A) The GO biological processes which are significantly enriched. The frequency of genes of a functional class within the examined set is described as a percentage of the total. (B) Genes showing significantly enriched ZNF42 TF binding sites. The frequency ratio (frequency of the set divided by the frequency of the background) is shown.*

The functions of genes changed in infected macrophages compared with controls as could be predicted. Significantly enriched functional gene clusters in line 6_1 infected macrophages showed involvement in immune activities such as response to stimulus, immune response and cytokine activity (Figure 6.10A). A substantial number of these genes (list in Table S4.1 in Appendix 4) had ZNF42 (zinc finger protein 42) TF binding sites (frequency ratio 1.26) in their promoter regions (Figure 6.10B). ZNF42, also known as MZF1 (myloid zinc finger 1), is a putative tumour suppressor protein (Peterson et al., 2006; Mudduluru et al., 2010). No significantly enriched functional cluster of genes or TF binding sites was identified in line 7_2 infected macrophages.

6.7.2 Analysis of genes in control and infected DCs

Genes highly expressed in line 6_1 control DCs showed significantly enriched oxidoreductase activity (Figure 6.11) but no enriched TF binding sites was detected and in line 7_2 control DCs, no functional classes or TF binding sites was identified.

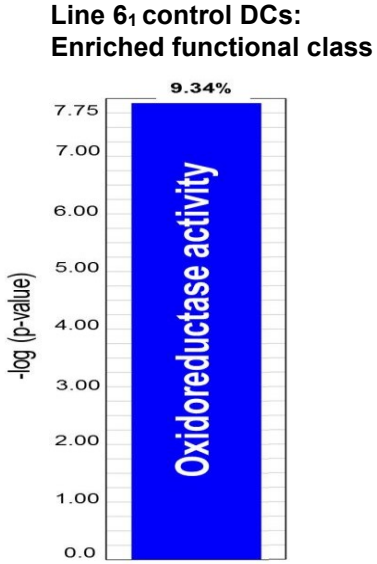

Figure 6.11. *Expander programme showing the overrepresentation analysis of genes highly expressed in line 6_1 control DCs. The GO biological process which is significantly enriched and the frequency of genes of the functional class within the examined set described as a percentage of the total.*

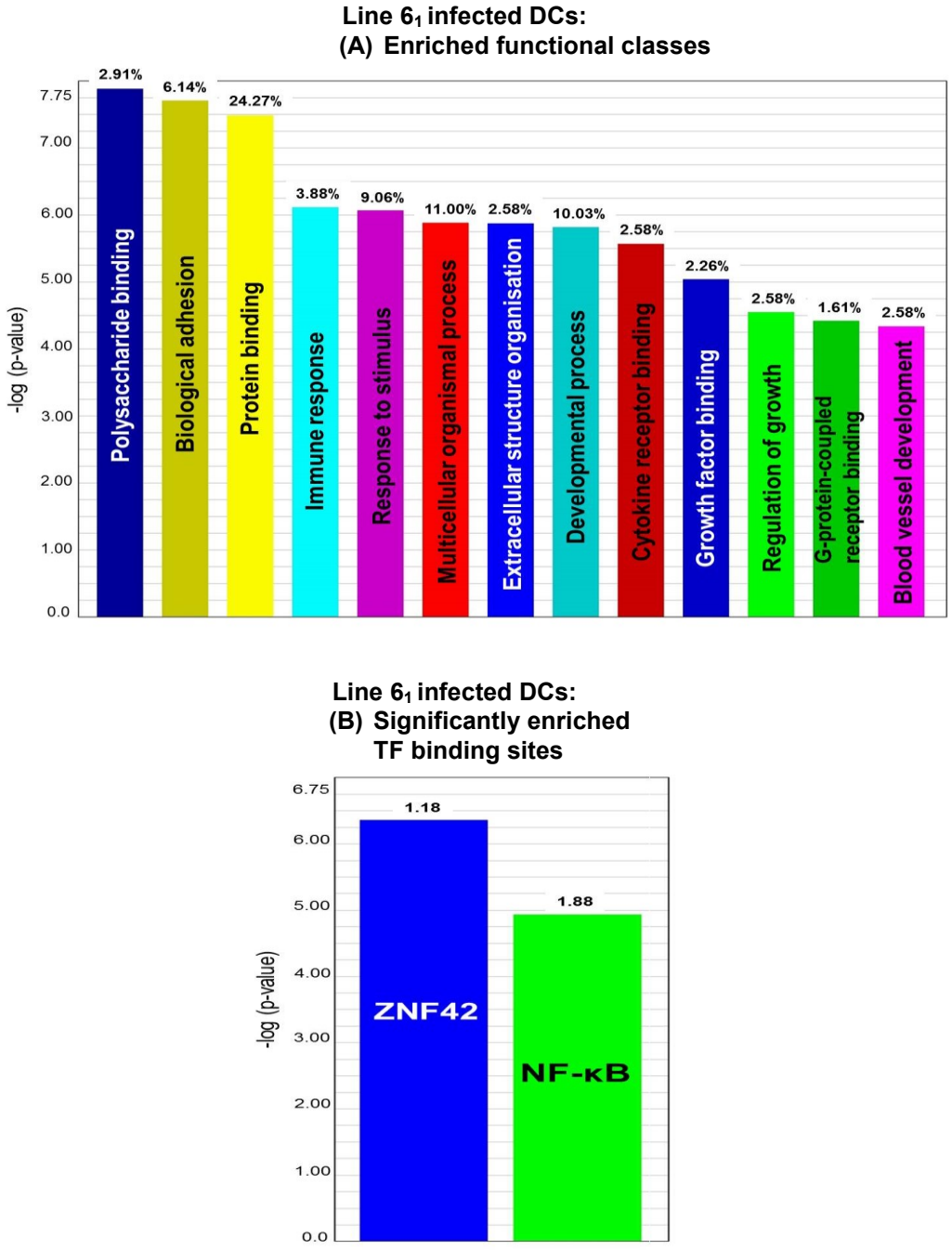

Figure 6.12. *Expander programme showing the overrepresentation analyses of genes highly expressed in in line 6_1 infected DCs. (A) The GO biological processes which are significantly enriched. The frequency of genes of a functional class within the examined set is described as a percentage of the total. (B) Genes showing significantly enriched ZNF42 and NF-kB TF binding sites. The frequency ratio (frequency of the set divided by the frequency of the background) is shown.*

Highly expressed genes in line 6_1 infected DCs showed many functionally enriched clusters related to physiological processes, such as polysaccharide binding, biological adhesion and defensive processes, such as immune response, response to stimulus (Figure 6.12A). A subset of these genes also showed enriched TF binding sites for ZNF42 (list in Table S4.2 in Appendix 4) and NF-κB in their promoter regions (Figure 6.12B). As mentioned before, ZNF42 acts as a putative tumour suppressor. The NF-κB family of transcription factors play crucial roles in inflammation, immunity, cell proliferation, differentiation, and survival (Oeckinghaus and Ghosh, 2009).

In line 7_2 infected DCs, no functional enrichment or TF binding sites was identified.

6.8 Determining MDV QTL candidate genes

The BioMart data mining tool within the Ensembl database was used (section 2.10.5) to identify genes involved in MD resistance or susceptibility based on previously identifined MDV QTLs (Vallejo et al., 1998; Yonash et al., 1999; McElroy et al., 2005) (Table S1 on CD). Genes inherently different between control macrophages and DCs of lines 6_1 and 7_2 were also identified. A subset of genes from each group is given here (Table 6.18 to Table 6.21) which were selected based on high fold change and genes related to immune functions. In the case of infected APCs of lines 6_1 and 7_2, two more selection criteria, namely previous reports and genes enriched with ZNF42 TF binding sites (lists in Tables S4.1 and S4.2 in Appendix 4), were also included. Full lists of MDV QTL candidate genes are provided in Appendix 3. Among the listed genes, previously reported putative candidate genes for MD-resistance or susceptibility were CXCL13L2, FN1, LIPA, IL-15, IFITM5 (Smith et al., 2011), K60 (Heidari et al., 2010) and GZMA (Sarson et al., 2006). Of these

genes, CXCL13L2 and IFITM5 were also in the lists of genes identified in this study with enriched ZNF42 TF binding sites in line 6_1 infected macrophages and DCs, respectively.

(A) Line 6_1 control macrophages

Gene	QTL	Chr.	Fold Change	Ensembl Gene ID
BCL2	MD16-17	2	4	ENSGALG00000012885
BLNK	MD22	6	2	ENSGALG00000006973
CD247	MD1	1	3	ENSGALG00000015441
ITGA1	MD25-30	Z	3	ENSGALG00000014891
MLPH	MD10	7	5	ENSGALG00000003904
PPP4R4	MD19-21	5	10	ENSGALG00000010950

(B) Line 7_2 control macrophages

Gene	QTL	Chr.	Fold Change	Ensembl Gene ID
ELOVL7	MD25-30	Z	8	ENSGALG00000014730
FN1	MD10	7	2	ENSGALG00000003578
IRG1	MD2	1	4	ENSGALG00000016919
ISG12(2)	MD16-17	2	10	ENSGALG00000013575
MAPK8IP1	MD19-21	5	7	ENSGALG00000008430
RGSL1	MD23	8	8	ENSGALG00000003671
SORCS3	MD22	6	97	ENSGALG00000008434
TJP2	MD25-30	Z	10	ENSGALG00000015109
Uncharacterised	MD22	6	16	ENSGALG00000004653
Uncharacterised	MD13	12	13	ENSGALG00000006325

Table 6.18. *A subset of genes inherently expressed differently in (A) line 6_1 and (B) line 7_2 control macrophages. QTL = Quantitative Trait Loci, Chr. = Chromosome.*

(A) Line 6_1 infected macrophages

Gene	QTL	Chr.	Fold Change	Ensembl Gene ID
AMIGO3	MD13	12	2	ENSGALG00000028339
BATF*	MD19-21	5	3	ENSGALG00000010323
BEST4	MD23	8	11	ENSGALG00000010126
CXCL13L2*†	MD8	4	3	ENSGALG00000010338
GRIP2	MD13	12	24	ENSGALG00000006449
IGSF3*	MD1	1	2	ENSGALG00000015469
IL-23R	MD23	8	7	ENSGALG00000011212
IRF-4	MD16-17	2	9	ENSGALG00000012830
K60†	MD7	4	3	ENSGALG00000011668
LEPR	MD23	8	3	ENSGALG00000011058
Uncharacterised	MD2	1	12	ENSGALG00000022751

(B) Line 7_2 infected macrophages

Gene	QTL	Chr.	Fold Change	Ensembl Gene ID
CD274	MD25-30	Z	2	ENSGALG00000015032
CHANK3	MD22	6	6	ENSGALG00000003135
CLCN4	MD2	1	5	ENSGALG00000016607
GALNTL4	MD19-21	5	10	ENSGALG00000005584
IL-15†	MD8	4	2	ENSGALG00000009870
STS	MD2	1	57	ENSGALG00000016622
TCEANC	MD2	1	6	ENSGALG00000016581
TFPI	MD10	7	11	ENSGALG00000002594
TMEM61	MD23	8	5	ENSGALG00000010801
Uncharacterised	MD5	4	5	ENSGALG00000027201

Table 6.19. *A subset of genes differentially expressed in (A) line 6_1 and (B) line 7_2 infected macrophages. QTL = Quantitative Trait Loci, Chr. = Chromosome.* = gene with enriched ZNF42 TF binding sites, † = previously reported.*

(A) Line 6_1 control DCs

Gene	QTL	Chr.	Fold Change	Ensembl Gene ID
BCL2	MD16-17	2	3	ENSGALG00000012885
CD247	MD1	1	3	ENSGALG00000015441
IL-15	MD8	4	3	ENSGALG00000009870
IL-1R2	MD2	1	4	ENSGALG00000016782
MYO16	MD2	1	32	ENSGALG00000016837
PPARGC1A	MD5	4	19	ENSGALG00000014398
SRGAP3	MD13	12	7	ENSGALG00000008378
TESC	MD24	15	19	ENSGALG00000008206
TLR7	MD2	1	3	ENSGALG00000016590
TMEM116	MD24	15	6	ENSGALG00000004760
TNN	MD23	8	7	ENSGALG00000004538
Uncharacterised	MD24	15	12	ENSGALG00000020975

(B) Line 7_2 control DCs

Gene	QTL	Chr.	Fold Change	Ensembl Gene ID
APOBEC4	MD23	8	9	ENSGALG00000020926
AVD	MD25-30	Z	7	ENSGALG00000023622
BAFF	MD2	1	2	ENSGALG00000016852
CD2	MD1	1	90	ENSGALG00000015463
FGF14	MD2	1	16	ENSGALG00000016866
IRG1	MD2	1	9	ENSGALG00000016919
ISG12(2)	MD16-17	2	3	ENSGALG00000013575
ITGA2	MD25-30	Z	5	ENSGALG00000014903
MAPK8IP1	MD19-21	5	5	ENSGALG00000008430
MX	MD2	1	21	ENSGALG00000016142
PTGS2	MD12	8	8	ENSGALG00000005069
SH3PXD2A	MD22	6	8	ENSGALG00000008293
TRAF3	MD19-21	5	2	ENSGALG00000011389
TRAIP	MD13	12	3	ENSGALG00000002908

Table 6.20. *A subset of genes inherently different in (A) line 6_1 and (B) line 7_2 control DCs. QTL = Quantitative Trait Loci, Chr. = Chromosome.*

(A) Line 6_1 infected DCs

Gene	QTL	Chr.	Fold Change	Ensembl Gene ID
BDKRB2*	MD19-21	5	3	ENSGALG00000011080
CD72*	MD25-30	Z	4	ENSGALG00000002383
CERCAM*	MD14	17	4	ENSGALG00000004986
CHB1	MD25-30	Z	7	ENSGALG00000005194
COL25A1*	MD8	4	4	ENSGALG00000010521
COL3A1*	MD10	7	4	ENSGALG00000002552
COL6A3*	MD10	7	4	ENSGALG00000003923
COL7A1	MD13	12	8	ENSGALG00000005811
CXCL12*	MD22	6	2	ENSGALG00000028136
F2RL2*	MD25-30	Z	2	ENSGALG00000023379
FN1†	MD10	7	3	ENSGALG00000003578
GZMA†	MD25-30	Z	31	ENSGALG00000013548
HTRA3*	MD5	4	3	ENSGALG00000015575
IFITM5*†	MD19-21	5	2	ENSGALG00000004239
IL-1RL1*	MD2	1	4	ENSGALG00000016785
IRF-3	MD19-21	5	2	ENSGALG00000014297
ITGB5	MD9	7	2	ENSGALG00000011778
LAMC2*	MD23	8	2	ENSGALG00000004627
LIF*	MD24	15	2	ENSGALG00000008028
LIPA†	MD22	6	2	ENSGALG00000006378
LMCD1*	MD13	12	3	ENSGALG00000008349
NFKBIZ*	MD1	1	2	ENSGALG00000015346
NR4A3*	MD16-17	2	3	ENSGALG00000013568
PAPPA2*	MD23	8	11	ENSGALG00000004487
PRRX2*	MD14	17	4	ENSGALG00000028236
RSFR*	MD22	6	2	ENSGALG00000027165
TBX3*	MD24	15	3	ENSGALG00000008250
TLR2B	MD8	4	2	ENSGALG00000009239
TMEM119*	MD24	15	3	ENSGALG00000004893
TMEM26*	MD22	6	3	ENSGALG00000025862
TSPAN15*	MD22	6	3	ENSGALG00000004257
WSCD2*	MD24	15	3	ENSGALG00000004849
Uncharacterised	MD2	1	66	ENSGALG00000013985

(B) Line 7_2 infected DCs

Gene	QTL	Chr.	Fold Change	Ensembl gene ID
GALNTL4	MD19-21	5	4	ENSGALG00000005584
LGI2	MD5	4	6	ENSGALG00000028945
NEGR1	MD23	8	5	ENSGALG00000011350
SLC44A5	MD23	8	4	ENSGALG00000011379
STS	MD2	1	18	ENSGALG00000016622
Uncharacterised	MD19-21	5	8	ENSGALG00000025939
Uncharacterised	MD19-21	5	5	ENSGALG00000026584

Table 6.21. *A subset of genes differentially expressed in (A) line 6_1 and (B) line 7_2 infected DCs. QTL = Quantitative Trait Loci, Chr. = Chromosome,* = gene with enriched ZNF42 TF binding sites, † = previously reported.*

6.9 Discussion

Functional analyses of DE genes pre- and post-MDV infection of APCs from lines 6_1 and 7_2 were carried out in this Chapter. The overall analyses in the three software packages revealed that, before infection immune activities were higher in APCs of the susceptible line (7_2) than those of resistant line (6_1), but this pattern reversed following MDV infection when APCs from line 6_1 exhibited a more strong immune response to MDV than the APCs of line 7_2, suggesting a potential role of APCs in determining resistance to MD in line 6_1 chickens.

Expression of only a few TLRs was increased after MDV infection, specifically TLR2B in line 7_2 infected macrophages (Table S2.4 in Appendix 2) and TLR2B and TLR21 in line 6_1 infected DCs (Table S2.7 in Appendix 2). TLR21 is the avian equivalent of mammalian TLR9 and recognises pathogen CpG DNA (Brownlie et al., 2009; Keestra et al., 2010), suggesting a potential role for this PRR in MDV infection. It is interesting that TLR2B, which recognises bacterial cell surface peptidoglycan (Higuchi et al., 2008), was also highly expressed after MDV infection,

though it could be due to a positive feedback loop to drive innate anti-viral immunity.

Host cells have developed multiple strategies to restrict viral infection. The expression of many of these restriction factors is subject to transcriptional regulation by IFN (Horner, 2014). Viral DNA or RNA is first recognised by cellular PRRs, which in turn recruit the PRR-mediated adaptor proteins and activate downstream signalling leading to production of IFNs (Kawai and Akira, 2006; Horner, 2014). IFNs bind to their receptor complex (IFNAR) present on the cell surface and trigger the JAK-STAT pathway to drive the synthesis of over 300 IFN-stimulated genes (ISGs), which can block virus replication at different phases of the replication cycle (Saito and Gale, 2008; Lemon, 2010; Horner, 2014). In this study, the expression of certain genes involved in controlling IFN response, such as BATF, BATF3, STAT 2 and STAT4, was up-regulated in line 6_1 infected macrophages (Table S2.3 in Appendix 2), suggesting a role for these genes in IFN-mediated anti-MDV immunity in macrophages of MD-resistant chickens.

The most highlighted immune pathway identified by three distinct software packages was the JAK-STAT signalling pathway. JAK-STAT is an important cellular pathway which has been linked to the genetic basis of MD resistance (MacEachern et al., 2011; Perumbakkam et al., 2013). It is most likely to be involved in the innate immune response (Smith et al., 2011). Following MDV infection, a transcriptional up-regulation of the JAK-STAT and MAPK pathways was observed in the CEFs of the susceptible line but not in the resistant line, suggesting a role for these pathways in the expression of genes involved in cell survival and proliferation which might lead to MDV-induced transformation of cells in susceptible lines (Subramaniam et

al., 2013). However, the JAK-STAT pathway may play a reverse role in MD-resistant line as type I IFN mediated activation of JAK-STAT signalling pathway can induce apoptosis in virally infected cells resulting in limiting the spread of virus (Tanaka et al., 1998). A higher expression of STAT2 in MD-resistant birds was observed in splenic tissues at 4 dpi as compared to MD-susceptible birds, suggesting an activated host defence against MDV presumably by the IFN-mediated pathway in resistant birds (Sarson et al., 2008b).The signal transduction molecules, STAT2 and 4 were up-regulated in this study only in line 6_1 infected macrophages (Figure 6.6). STAT1 and 2, together with IFN regulatory factor (IRF)-9, are involved in type I IFN signalling (Stark et al., 1998; Figure 6.13). Type I IFNs and the JAK-STAT pathway are exclusively related to anti-viral responses. For example, mice with deficiencies in the induction of type I IFNs and their receptors, or cytokine induced JAK-STAT signal transduction pathways are vulnerable to WNV (West Nile virus) and DENV (Dengue) infections (Samuel and Diamond, 2005; Shresta et al., 2005; Perry et al., 2009). A type I IFN-mediated activation of JAK-STAT signalling was found to be a key component of host defence mechanisms that consist of pathways regulating apoptosis against reovirus infection in the mouse brain (Goody et al., 2007). In humans, expression of STAT1, STAT2, STAT3 and STAT5A has been observed during the latent phase of infection with EBV (Zhang et al., 2004). JAK-STAT signalling pathways also regulate iNOS expression and NO production in macrophages (Sareila et al., 2006) and NO has an inhibitory effect on MDV replication (Xing and Schat, 2000; Djeraba et al., 2002a).

STAT4 is involved in IL-12 mediated Th1 cell differentiation and proliferation (Nishikomori et al., 2002; Figure 6.13). In this study, an elevated expression of

STAT4 in line 6_1 infected macrophages suggests a role for macrophages in induction of an anti-MDV Th1 response, as described by Kaiser et al. (2003) and Smith et al. (2011). However, Th2 (Heidari et al., 2008a) or Treg (Buza and Burgess, 2007) mediated immune responses have also been described following MDV infection.

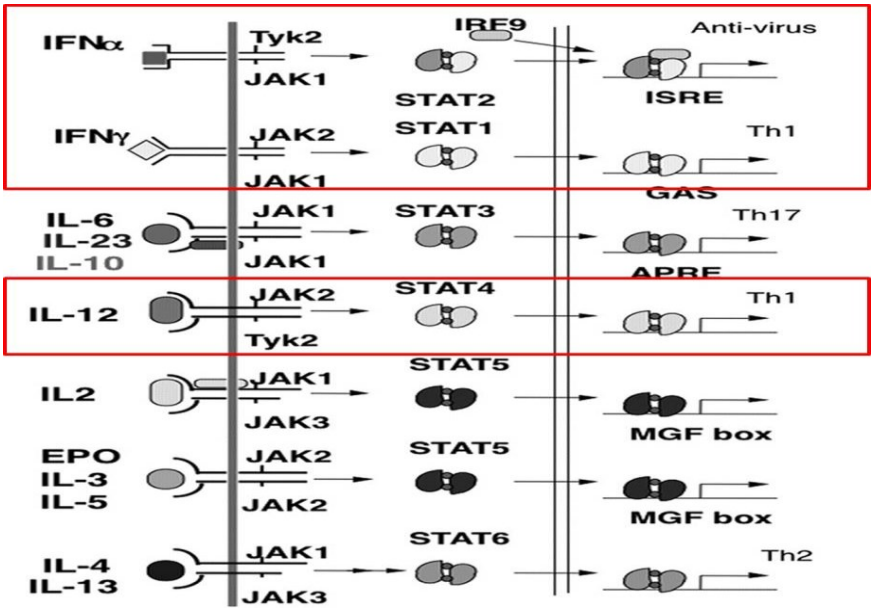

Figure 6.13. *Anti-viral and Th1 responses mediated by activated JAK-STAT pathway. Adapted and modified from Tamiya et al. (2011) with permission from Wolters Kluwer Health.*

Genes highly expressed in line 6_1 infected DCs were also involved in the JAK-STAT pathway. The genes include SOCS1 (suppressor of cytokine signalling 1), SOCS3 and CISH (Cytokine-inducible SH2-containing protein, also known as CIS) (Figure 6.7), which are potent suppressors of JAK-STAT signalling (Tamiya et al., 2011). Both SOCS1 and SOCS3 can directly inhibit JAK tyrosine kinase activity through their kinase inhibitory regions (KIR), a pseudosubstrate essential for the suppression of cytokine signals (Figure 6.14). SOCS3 also inhibits IL-12-induced STAT4 activation by binding through its SH2 domain (Yamamoto et al., 2003), indicating a doubtful role for DCs in the Th1 mediated anti-viral immunity to MDV.

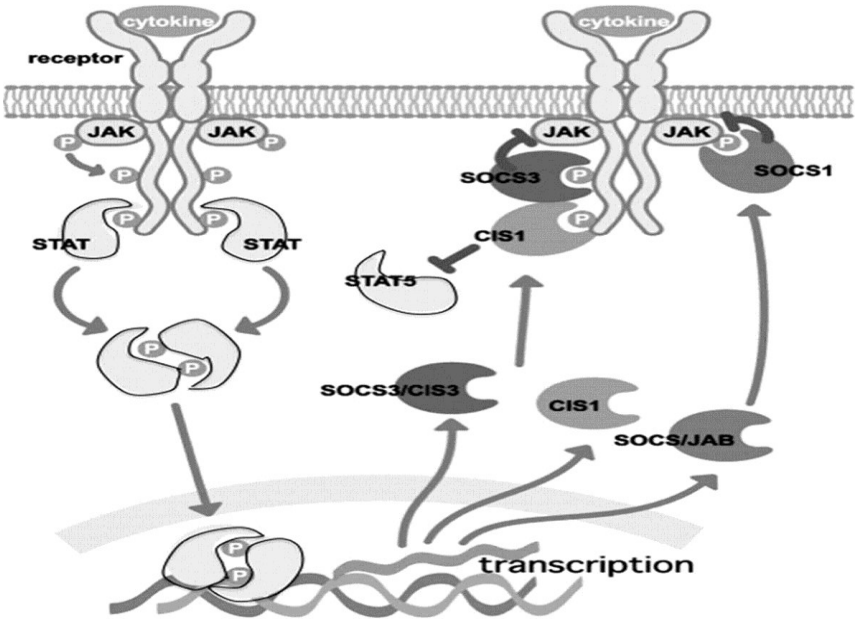

Figure 6.14. *Mechanism of suppression of JAK-STAT pathway by CIS, SOCS1, and SOCS3. All of these are induced by cytokine stimulation. CIS binds to the STAT5 activating receptors, thereby suppressing further activation of STAT5, and induces degradation of the receptor. SOCS1 binds to JAKs, and SOCS3 binds to the receptor through the SH2 domain, but both inhibit JAK activity through the KIR. Adapted and modified from Tamiya et al. (2011) with permission from Wolters Kluwer Health.*

Genes highly expressed in line 6_1 control macrophages and line 7_2 control DCs were also involved in the JAK-STAT pathway, though in line 6_1 only one negative regulator gene (SOCS2) and in line 7_2 three cytokine receptors (IL-13Rα1, IL-13Rα2 and IL-20Rα) were identified. However, following MDV infection this pathway was not activated in line 7_2 macrophages or DCs, suggesting a potential anti-viral role for the JAK-STAT signalling pathway only in line 6_1 (MD-resistant) chickens in response to MDV infection.

A group of genes highly expressed in line 6_1 infected macrophages and DCs showed significantly enriched ZNF42 TF binding sites in their promoter regions (Tables S4.1 and S4.2, respectively, in Appendix 4). ZNF42, commonly known as myeloid zinc

finger protein 1 (MZF1), is a zinc finger TF preferentially expressed in haematopoietic stem cells, myeloid progenitor cells, and in differentiated myeloid cells (Bavisotto et al., 1991; Morris et al., 1995). MZF1 is associated with haematopoiesis (Morris et al., 1995) and is also critical to the regulation of cell proliferation and apoptosis (Hromas et al., 1996; Robertson et al., 1998). Several reports suggest a contradictory role of MZF1 in tumourigenesis influencing cell migration and invasion. For example, a decreased expression of MZF-1 inhibited the expression of protein kinase C alpha (PKCα), which is an important family of signalling molecules that regulate cell proliferation, differentiation, transformation, and apoptosis, and thus reduced cell migration and invasion in human hepatocellular carcinoma (HCC) (Hsieh et al., 2006). In contrast, HCC cells transfected with antisense oligonucleotide of MZF-1 showed an inhibitory effect on tumour growth and prolonged time for tumour formation (Hsieh et al., 2007). Gaboli et al. (2001) reported that inactivation of MZF-1 in mice resulted in a striking increase in haematopoietic progenitors, with the eventual development of lethal myeloid neoplasias, suggesting a role of MZF-1 protein as tumour suppressor. Recently, Chen et al. (2014) reported that increased MZF-1 expression led to high ferroportin concentration, resulting in reduced iron-related cellular activities and decreased growth of human prostate tumour cells. From these perspectives, it can be said that MZF-1 has bi-functional transcriptional regulatory properties depending on the cellular environment.

To date, the role of MZF1 TF binding sites in genes highly expressed during MDV infection has not been evaluated, though MZF1 was considered to have a repressive function in one MDV infection study. Tian et al. (2012) reported that MDV infection

influenced the methylation status of CR1 (Chicken Repeat 1, the transposable elements located upstream of genes near the promoters) levels of IL-12α, which might have reduced the binding affinity of two transcriptional repressors, MZF1 and E47 (Yang et al., 2004; Yan et al., 2006), resulting in higher mRNA expression level of IL-12α in line 6_3 (MD-resistant) than line 7_2 (MD-susceptible) chickens. Smith et al. (2011) observed enriched HIC1 (hypermethylated in cancer 1, a tumour suppressor) TF binding sites in the genes down-regulated in MDV-infected splenocytes at 4 dpi, and hence suggested that MDV infection could block an anti-tumour mechanism long before the MDV oncogene (Meq) is expressed. In the present study, a putative tumour suppressor TF binding sites (MZF1) was detected in genes highly expressed in APCs of the MD-resistant line (6_1) at 1 dpi, but not in the susceptible line (7_2). Takahashi et al. (2005) reported that transcriptional repression by MZF-1 required FHL3 (four and a half LIM domain protein 3) as a cofactor. On the other hand, FHL3 can also recruit a C-type binding protein (CtBP) as a co-repressor by which they regulate gene expression (Turner et al., 2003). The interaction of CtBP with oncogene Meq plays a crucial role in MDV-induced lymphomas (Brown et al., 2006) and it was also speculated that by recruiting CtBP and its co-repressors, Meq might function in tumourigenesis and/or the establishment of latency in T cells (Brown et al., 2006). MDV induces T cell latency in resistant lines, whereas it induces latency and lymphoma formation in susceptible lines. Therefore, further studies will be required to explore the exact role of MZF1 in MD-resistant chickens.

The expression of several previously reported potential candidate genes for MD resistance or susceptibility was also observed in the present study. Ly6E (Liu et al.,

2003) and GZMA (Sarson et al., 2006) were highly expressed in line 7_2 and line 6_1 infected DCs. An elevated expression of IRG1 was reported in splenocytes of MDV-infected susceptible line (Smith et al., 2011). In this study, its expression was observed in control APCs of susceptible line, but not after infection.

Two putative MD resistance genes (CXCL13L2 and IFITM5) had enriched ZNF42 TF binding sites in their promoter regions (Tables 6.19A and 6.21A, respectively). The chicken CXCL13 chemokines are grouped as homeostatic chemokines like mammals though they may have inflammatory roles as well (Kaiser, 2012). Humans and mice have a single copy of CXCL13, but the chicken genome has three genes at the same locus (CXCL13L1, CXCL13L2 and CXCL13L3). Two of them, CXCL13L1 and CXCL13L2, interact with the receptor, CXCR5 (reviewed in Kaiser, 2012). CXCR5 is involved in ligand mediated B-cell chemoattraction (Legler et al., 1998; Chan et al., 2013) as well as providing essential signals for immunoglobulin production to B cells functioning together with $CD4^+$ T cells (Breitfeld et al., 2000). During *in vivo* infection, MDV presumably passes from macrophages to B cells in the lymphoid tissues. An elevated expression of CXCL13L2 in MDV-infected macrophages in this study supports this hypothesis. Heidari et al. (2010) also reported a higher expression of CXCL13 at 5 dpi in splenocytes of chickens infected with a vv^+ strain of MDV.

The interferon-induced transmembrane protein 5 (IFITM5) was another putative MD resistance gene highly expressed in line 6_1 infected DCs. IFITM proteins are anti-viral IFN-stimulated genes (ISGs) that disrupt distinct steps of the viral replication cycle (Brass et al., 2009). IFITM proteins effectively inhibit human RSV (respiratory syncytial virus) infection mainly by interfering with both virus entry and the

subsequent replication steps (Zhang et al., 2015). Though IFITM5 was primarily recognised as a protein involved in bone mineralisation (Moffatt et al., 2008), later work identified it as a stimulator of the expression of interferon-induced genes (Hanagata and Li, 2011). Recently, IFITM5 was identified as a highly expressed gene in IBDV-susceptible chickens, suggesting an important role for this gene in resistance or susceptibility to virus infection (Smith et al., 2015). The chicken IFITM5 effectively restricted filovirus $GP_{1,2}$ proteins-mediated entry, but had little or no effect on influenza A virus haemagglutinin-mediated entry (Huang et al., 2011). To date no report is available on the effect of IFITM5 during MDV infection, therefore further study is required to investigate the role of this gene in MD resistance.

Although these functional analyses provide a broad picture of the transcriptional changes in infected cells and the differences between the chicken lines, no validation of DE genes has been carried out in this study due to the shortage of RNA. Therefore, further work is required to fully verify the findings. However, the data generated in this Chapter support the hypothesis that the resistance signature to MD is most likely determined at the APC level, as macrophages from line 6_1 showed greater activity of immune response genes compared to line 7_2. This is consistant with the findings reported in Chapter 5 and suggests differential activation of JAK-STAT signalling is at least one pathway by which this mechanism is exerted.

Chapter 7:

General discussion

7.1 Overall perspective of this study

The aim of this project was to explore the cellular basis of resistance to MD. Many studies have been carried out to explore the genes involved in resistance to MD, but it is not yet exactly known in which cell type resistance is expressed. *In vivo*, MDV infects several immune cells, including APCs, B and activated T cells. The hypothesis of this project was that the resistance is expressed at the very early stage of MDV infection, when the virus encounters APCs. In order to infect these cells *in vitro* with MDV, it was first necessary to develop an *in vitro* model of MDV infection of APCs because several previous attempts to establish an *in vitro* MDV-macrophage infection model had not been successful (Haffer et al., 1979; von Bulow and Klasen, 1983; Barrow et al., 2003). Therefore, the major initial challenge was to develop a new *in vitro* MDV-APC infection model. Chicken bone marrow-derived macrophages and DCs were used for MDV-infection experiments and following establishment of an *in vitro* infection model, the model was applied to infect APCs of two inbred lines which provided an experimental means of investigating the cellular basis of resistance to MD *in vitro* rather than *in vivo*.

7.2 Establishment of a *de novo in vitro* MDV infection model of APCs and subsequent characterisation

The techniques involved in the development of a new MDV-APC infection model and the subsequent characterisation infected APCs were described in Chapter 3. The virus used was a recombinant CEF-associated construct of the vaccine strain (CVI988) of MDV, in which the host shut-off gene (UL41) was replaced with GFP. The encoded GFP was therefore helpful to determine the presence of the virus in infected cells.

As mentioned before, MDV is highly cell-associated and it never becomes cell-free *in vitro* (reviewed in Denesvre, 2013). Therefore, MDV-infected CEFs were co-cultured with macrophages. The first problem encountered was that both CEFs and macrophages were adherent to culture plates and hence it was not possible to co-culture an optimal amount of infected CEFs with macrophages. At the same time, the virus titre was found to be very low (section 3.4.5), and not sufficient to initiate infection of macrophages. Moreover, the culture plates (Sterilin square plates), which are suitable for macrophage growth and differentiation, did not support cell attachment and growth of CEFs (Figure 3.7). A substantial number of the infected CEFs were also dying during attempts to freeze MDV-infected CEFs (Figure 3.8), but MDV requires live cells to pass infection to other cells. Therefore, it was decided to use freshly infected MDV-infected CEFs in each experiment.

All of the above-mentioned problems were almost completely overcome by co-culturing fresh infected CEFs and macrophages in T_{75} flasks. A proportion of infected macrophages were detected by flow cytometric analysis of these cells after MDV infection (section 3.4.9). However, this success quickly came under suspicion as it was realised that those infected macrophages could also be derived from MDV-infected CEF cultures as macrophages appear in chicken embryos as early as 2.5-4.5 days (Cuadros et al., 1993). To overcome this, infected macrophages in CEF cultures were excluded by FACS after the culture cells were stained with an anti-CD45 mAb. Pre-sorted MDV-infected CEFs were then added to macrophage cultures and MDV-infected macrophages were detected by flow cytometric analysis on 3 dpi (Figure 3.19), which established a successful *in vitro* MDV-infection model of macrophages. This has therefore provided evidence that macrophages can be infected *in vitro*, even

though they had been uninfectable in previous studies (Haffer et al., 1979; von Bulow and Klasen, 1983; Barrow et al., 2003), probably due to the lack of a suitable co-culture method. Though, as described later, the infectivity of macrophages for other cell types such as B and T cells remains to be fully investigated, this provided model system could be helpful to study the effects of the virus on the responses of the APCs.

Using this model, DCs from outbred chickens were also infected *in vitro* with MDV. The studies revealed that the cultured macrophages used in these studies were infected at higher numbers than cultured DCs (approximately 4 times higher) (Figures 3.19C and 3.22C, respectively).

Infected APCs were then characterised using confocal microscopy and RT-PCR. Confocal microscopic views indicated the presence of infection in macrophages and DCs (Figures 3.24 and 3.25, respectively) by the presence of GFP in the nucleus. Although expression of herpesvirus specific genes was detected by RT-PCR (Figure 3.26), the presence of 2% contaminant infected CEFs in these experiments means that these experiments need to be repeated.

Confocal video microscopy was used to investigate the possible modes of MDV transmission to macrophages. Movies A and B illustrate possible phagocytosis-like and cell-to-cell mode of spread of MDV, respectively. In movie A (Figure 3.27), GFP can be seen interior to the vacuoles of a macrophage-like cell, suggesting entry of MDV into the macrophages through phagocytosis, though the exact mechanism could not be explained from this video. Therefore, advanced imaging techniques will be required to investigate this feature.

A potential route of cell-to-cell transmission of MDV can be proposed based on images from movie B (Figure 3.28).This video shows actin-like intercellular projections; the green colour of those could be an indication of the transportation of virus particles between cells.

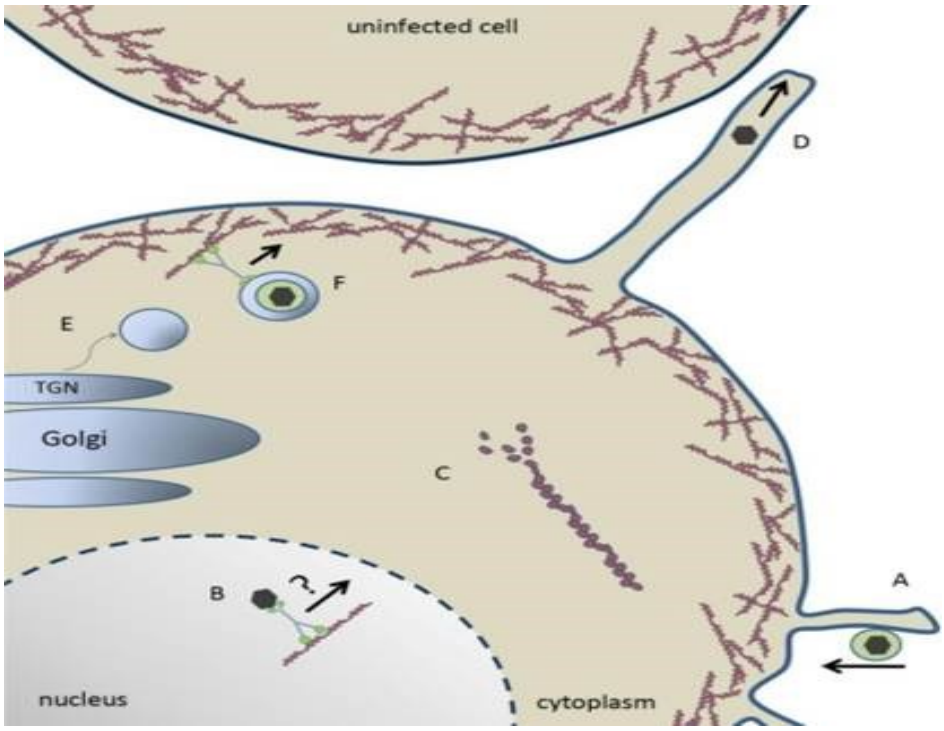

Figure 7.1. *Model of herpesvirus entry, maturation and egress. (A) Herpes virion "surfing" towards the plasma membrane along membrane protrusions for entry. (B) Capsid trafficking toward the nuclear periphery for budding via a myosin motor on F-actin. (C) US3-mediated depolymerisation of actin stress fibres. (D) US3-mediated generation of membrane projection and cell to cell spread of herpesvirus. (E) Myosin IIA- and Rab6-dependent fission of nascent vesicles from the Golgi body. (F) Enveloped virion within a TGN* (*trans-Golgi network)-derived vesicle trafficking through cortical actin via myosin Va toward the plasma membrane for secretion. Adapted from Roberts and Baines (2011).*

Actin is a highly dynamic protein with two basic forms, monomeric or globular actin (G-actin) and filamentous actin (F-actin), which are involved in a wide variety of

cellular processes, such as cell division, adherence, migration and transport of intra and extracellular materials (Roberts and Baines, 2011). Like all viruses, herpesviruses depend on host machinery to replicate and spread, and actin plays a crucial and diverse role in maintaining these functions.

The importance of polymerisation of the actin cytoskeleton and the role of US3 orthologue of MDV was reported previously for the effective cell-to-cell spread of MDV in chicken embryo cells *in vitro* (Schumacher et al., 2005). Figure 7.1 shows the role of actin in US3-mediated spread of herpesvirus. Therefore, it is more likely possible for MDV to spread between macrophages via actin-mediated cellular cytoskeletal protrusions.

To determine if MDV-macrophage infection is productive or abortive in nature, CEFs were infected with MDV-infected macrophages (section 3.5.4) and triple-sorted infected macrophages were to shown to form plaques were CEF culture (Figures 3.32A.i and A.ii), indicating the productive nature of MDV-macrophage infection which was in contrast to what was reported by Barrow et al. (2003).

7.3 Infection of B and T cells

In Chapter 4, attempts were made to infect B and T cells with MDV *in vitro*. MDV is believed to transmit from macrophages to B cells in the lymphoid tissues *in vivo* (Baigent and Davison, 2004). In order to mimic this process, several attempts were made to infect B and T cells with MDV-infected macrophages *in vitro*. However, none of these experiments was successful, probably because of the lack of growth factors in the B and T cell cultures to stimulate activation and retain cell viability. In addition, sorting of MDV-infected macrophages leads to them being in a very

stressed condition, which in turn causes early death of these cells in culture. Using a macrophage cell line could be a useful alternative to overcome this problem.

7.4 Determining the cellular basis of resistance to MD in APCs of inbred chickens

The newly developed *in vitro* MDV infection model was extended to infect APCs of MHC-identical inbred MD-resistant (line 6_1) and MD-susceptible (line 7_2) chickens (Chapter 5). Flow cytometric analyses showed that, at a fixed infection ratio (1:5), macrophages from line 7_2 were infected in greater numbers than those from line 6_1 (section 5.4). DCs were infected at lower numbers than macrophages but there was no apparent difference between the two lines in the context of MDV-DC infections (Section 5.5). As mentioned before, DCs were also infected at lower numbers in outbred chickens. This lower infection of DCs in both outbred and inbred lines could be due to the different culture conditions used to generate the two cell types, in particular the addition to the DC cultures of IL-4 and CSF-2 (GM-CSF), which can have immunomodulatory activities (Kedzierska et al., 2000; Tsai et al., 2013).

The lower infection of macrophages in resistant line 6_1 and higher infection in susceptible line 7_2 in this study suggests that macrophages play a critical role in exerting resistance to MD. Differential susceptibility or resistance in MHC-congenic chicken lines was also reported in the infection of macrophages with another alphaherpesvirus, ILTV (infectious laryngotracheitis virus) (Loudovaris et al., 1991a). Moreover, the crucial involvement of macrophages in resistant chicken lines has been suggested in recovery from infection with ILTV. In an *in vitro* study, Loudovaris et al. (1991b) detected higher percentages of ILTV antigen-positive macrophages in genetically resistant chickens over levels in susceptible chickens,

indicating that the macrophages from resistant chickens might be better able to process viral antigen and present it to the immune system, which in turn results in clearance of the infection.

Macrophages are well-known to induce cellular resistance against MCMV (murine cytomegalovirus) (Selgrade and Osborn, 1974). Macrophages show intrinsic resistance to HSV infection by phagocytic and degradative functions, leading to presentation of viral antigens, as well as inhibition of virus replication (Sarmiento, 1988).

The mRNA expression levels of two pro-inflammatory cytokines (IL-6 and IL-18) were measured by Taqman qRT-PCR. Only IL-18 expression was significantly up-regulated in line 6_1 infected macrophages compared to those from line 7_2 (Figure 5.16A). Increased expression of pro-inflammatory cytokine in the resistant line was in contrast to previous reports where an elevated expression of pro-inflammatory cytokines was measured in susceptible chickens (Kaiser et al., 2003; Heidari et al., 2014), though differences in experimental conditions between two studies need to be considered.

Functional analyses of differentially expressed (DE) genes identified from RNA-Seq in MDV-infected and control APCs of the two inbred lines were carried out in Chapter 6. The JAK-STAT signalling appeared as a common pathway in the infected APCs of MD-resistant chickens (line 6_1). Activation of the JAK-STAT signalling pathway was previously reported in MDV-infected CEFs, but in MD-susceptible birds where it was considered to be most likely involved in the transformation of cells (Subramanium et al., 2013). Inappropriate and defective functioning of the JAK-STAT signalling pathway may be associated with several disorders, including

cancer (Boudny and Kovarik, 2002). However, the JAK-STAT pathway, when activated by IFNs, can play a crucial role in anti-viral responses. Improta and Pine (1997) stated that susceptibility to virus infection could be determined by the cell's ability to respond to the autocrine effect of IFN by the STAT-mediated pathway of gene induction. The JAK-STAT pathway is involved in blocking replication of HSV-1 in DCs and macrophages in mice (Mott et al., 2009). IFN-mediated recruitment of TNK1 (tyrosine kinase, non-receptor, 1) causes activation of the JAK-STAT signalling pathway, which in turn leads to inhibition of HCV (hepatitis C virus) replication in hepatocytes (Ooi et al., 2014). JAK-STAT activation not only has the potential to affect infection in the infected cells but also indirectly by altering the infected cell's ability to generate an adaptive immune response. Down-regulation of key genes in the JAK-STAT signalling pathway in lung cells led to severe HPAIV (H5N1) infection at 24 h in chickens, but not in ducks, where expression of the same genes was either up-regulated or unchanged (Kuchipudi et al., 2014).

Apoptosis of virus-infected cells can also be a strategy of host cells to limit virus transmission and thus confer resistance. In this study, higher apoptotic death of infected cultured line 6_1 macrophages was observed following MDV infection than line 7_2 (Figure 5.5). As mentioned before, type I IFN-mediated JAK-STAT signalling may induce apoptosis in virus-infected cells (Tanaka et al., 1998). Figure 7.2 illustrates the mechanism of apoptosis of host cells following virus infection. Viral dsRNA plays an important role in JNK-2-and PKR-mediated cell death (Figure 7.2A). It has been reported that DNA viruses, such as adenovirus, HSV and vaccinia virus, can produce dsRNA during their replication cycles within few hours of infection (Weber et al., 2006). It is not exactly known if dsRNA is generated during

MDV replication, but an up-regulation of TLR3, which binds viral dsRNA (Guillot et al., 2005), was reported in lungs following MDV infection (Abdul-Careem et al., 2009b).

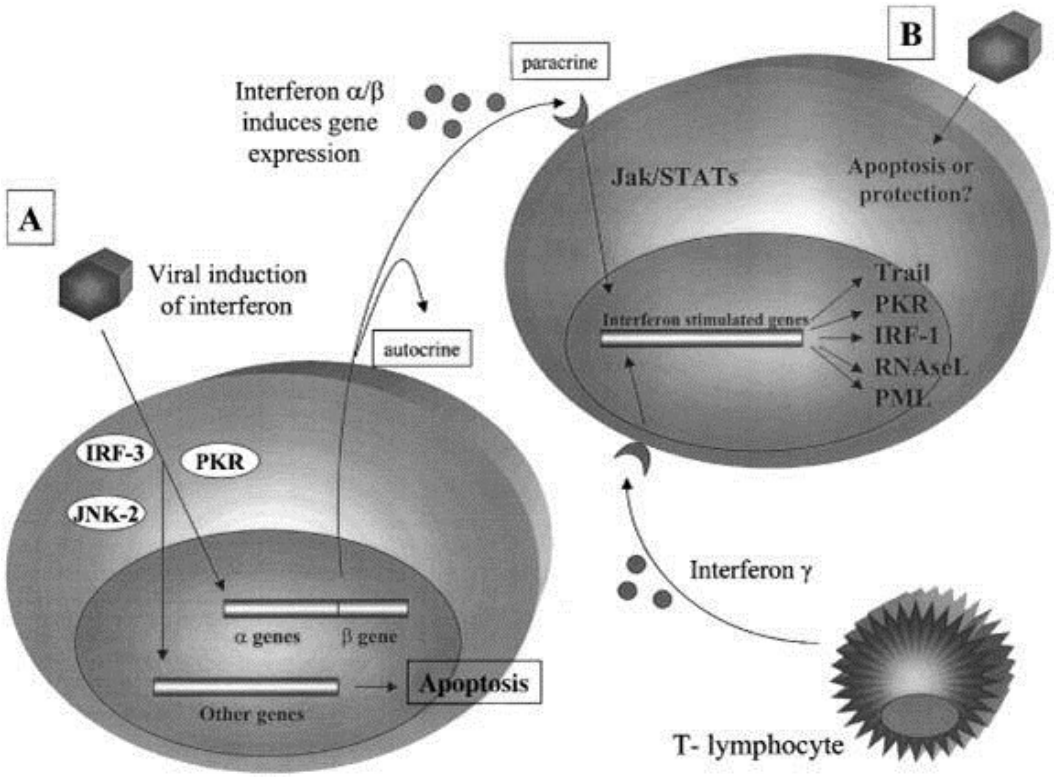

Figure 7.2. *(A) Virus invades the cell and triggers the activation of proteins involved in the induction of interferon (IFN). In response to virus infection, IRF-3 becomes phosphorylated and translocates to the nucleus to cooperate with transcription factors to induce IFN-beta. Viral dsRNA also activates JNK-2 and PKR, the latter assisting with IFN production perhaps through activation of the NF-kB pathway. Aside from inducing IFN, IRF-3, PKR and JNK-2 may also contribute towards regulating cell death or survival by inducing the activation of other genes. (B) Type I or II IFN binds to species specific cell surface receptors and through the JAK-STAT pathway induce the transcription of genes harbouring IFN-stimulated response elements (ISRE) or gamma-activation sequence (GAS) in their promoters regions, respectively. Genes known to be induced by IFN and to play a role in apoptosis include TRAIL, PKR, IRF-1 and PML. Adapted from Barber (2001) with permission from the Nature Publishing Group.*

The expression of TLR3 was also elevated in MDV-infected CEFs (Haunshi and Cheng, 2014), suggesting potential synthesis of dsRNA during MDV replication. DCs were infected at lower numbers than macrophages in both the lines but no differences were observed between the lines. Functional analyses revealed that similar biological pathways were activated in both the macrophages and DCs of the resistant line (6_1), while similar pathways were not involved with genes highly expressed in APCs of the susceptible line (7_2), suggesting that, like macrophages, DCs in line 6_1 are also involved in conferring resistance to MD.

7.5 Future plans

For establishing a new *in vitro* MDV-APC infection model, a recombinant virus construct of the MDV vaccine strain CVI988 was used in this study. Strains of vv or vv+ MDV produce higher levels of infection and infections are prevalent worldwide, but suitable recombinant strains of these viruses were not easily available for the studies. Therefore, these *in vitro* experiments need to be repeated using vv or vv+ strains of MDV in order to maximise infection *in vitro* and to reflect the pathogenicity of the viruses.

Further experiments are required to confirm MDV replication in APCs and the productiveness of MDV-macrophage infection regarding infection of B and T cells. In order to fully validate the transcriptomic differences between APCs of two lines, RT-PCR also need to perform in future.

The role of MZF1 (ZNF42) during MDV infection, especially its interactions with Meq, remains to be elucidated. It has been described as both a tumour-suppressing (Gaboli et al., 2001) and a tumour-promoting (Hseish et al., 2006) transcription factor. MZF1 TF binding sites were overrepresented in genes highly expressed in

line 6_1 (resistant) compared to genes highly expressed in line 7_2 (susceptible) infected APCs. Though MDV transforms lymphocytes in its life cycle, the expression of genes with enriched MZF1 TF binding sites in APCs might have an influence on tumourigenesis when the infection transmits from APCs to lymphocytes. However, the Meq oncoprotein of the MDV CVI988 strain is unable to induce lymphoma, as it has a 178 bp insertion which significantly diminishes its transactivation properties (Ajithdoss et al., 2009). Therefore, an oncogenic MDV strain should be used to clarify this.

7.6 Conclusions

An *in vitro* model of MDV-APC infection has been developed, for the first time, in this project. Carrying out MDV-infection studies *in vivo* is not always convenient for many labs around the world due to the lack of facilities as well as the risk of spreading MDV. This *in vitro* model will perhaps be helpful to perform intensive studies regarding MDV-APC interactions. This study also provides evidence that macrophages from resistant line 6_1 are involved in resistance to MD, most likely, at least in part, through the JAK-STAT signalling pathway-mediated anti-viral response.

References

Abdul-Careem MF, Haq K, Shanmuganathan S, Read LR, Schat KA, Heidari M and Sharif S (2009b). Induction of innate host responses in the lungs of chickens following infection with a very virulent strain of Marek's disease virus. *Virology*. 393:250-257.

Abdul-Careem MF, Hunter BD, Parvizi P, Haghighi HR, Thanthrige-Don N and Sharif S (2007). Cytokine gene expression patterns associated with immunization against Marek's disease in chickens. *Vaccine*. 25:424-432.

Abdul-Careem MF, Hunter BD, Sarson AJ, Mayameei A, Zhou H and Sharif S (2006). Marek's disease virus-induced transient paralysis is associated with cytokine gene expression in the nervous system. *Viral Immunol*. 19:167-176.

Abdul-Careem MF, Hunter BD, Sarson AJ, Parvizi P, Haghighi HR, Read L, Heidari M and Sharif S (2008). Host responses are induced in feathers of chickens infected with Marek's disease virus. *Virology*. 370:323-332.

Abdul-Careem MF, Read LR, Parvizi P, Thanthrige-Don N and Sharif S (2009a). Marek's disease virus-induced expression of cytokine genes in feathers of genetically defined chickens. *Dev Comp Immunol*. 33:618-623.

Aderem A and Underhill DM (1999). Mechanisms of phagocytosis in macrophages. *Annu Rev Immunol*. 17:593-623.

Afonso CL, Tulman ER, Lu Z, Zsak L, Rock DL and Kutish GF (2001). The genome of turkey herpesvirus. *J Virol*. 75:971-978.

Ajithdoss DK, Reddy SM, Suchodolski PF, Lee LF, Kung HJ and Lupiani B (2009). *In vitro* characterisation of the Meq proteins of Marek's disease virus vaccine strain CVI988. *Virus Res*. 142:57-67.

Alexis NE, Lay JC, Almond M, Bromberg PA, Patel DD and Peden DB (2005). Acute LPS inhalation in healthy volunteers induces dendritic cell maturation *in vivo*. *J Allergy Clin Immunol*. 115:345-350.

Ambagala AP and Cohen JI (2007). Varicella-Zoster virus IE63, a major viral latency protein, is required to inhibit the alpha interferon-induced antiviral response. *J Virol*. 81:7844-7851.

Anders S, Pyl PT and Huber W (2015). HTSeq-a Python framework to work with high-throughput sequencing data. *Bioinformatics*. 31:166-169.

Anderson AS, Parcells MS and Morgan RW (1998). The glycoprotein D (US6) homolog is not essential for oncogenicity or horizontal transmission of Marek's disease virus. *J Virol*. 72:2548-2553.

Baaten BJ, Butter C and Davison TF (2004). Study of host-pathogen interactions to identify sustainable vaccine strategies to Marek's disease. *Vet Immunol Immunopathol*. 100:165-177.

Baaten BJ, Staines KA, Smith LP, Skinner H, Davison TF and Butter C (2009). Early replication in pulmonary B cells after infection with Marek's disease herpesvirus by the respiratory route. *Viral Immunol*. 22:431-444.

Baigent SJ and Davison F (2004). Marek's disease virus: biology and life cycle. In: Davison F, Nair V (Eds), Marek's Disease: An Evolving Problem. Elsevier Academic Press, London, pp.62-77.

Baigent SJ, Ross LJN and Davison TF (1998). Differential susceptibility to Marek's disease is associated with differences in number, but not phenotype or location, of $pp38^+$ lymphocytes. *J Gen Virol*. 79:2795-2802.

Baigent SJ, Smith LP, Nair VK and Currie RJW (2006). Vaccinal control of Marek's disease: current challenges, and future strategies to maximize protection. *Vet Immunol Immunopathol*. 112:78-86.

Banchereau J and Steinman RM (1998). Dendritic cells and the control of immunity. *Nature*. 392:245-252.

Barber GN (2001). Host defence, viruses and apoptosis. *Cell Death Differ*. 8:113-126.

Barrow AD, Burgess SC, Baigent SJ, Howes K and Nair VK (2003). Infection of macrophages by a lymphotropic herpesvirus: a new tropism for Marek's disease virus. *J Gen Virol*. 84:2635-2645.

Bavisotto L, Kaushansky K, Lin N and Hromas R (1991). Antisense oligonucleotides from the stage-specific myeloid zinc finger gene MZF-1 inhibit granulopoiesis *in vitro*. *J Exp Med*. 174:1097-1101.

Bhattacharjee A, Shukla M, Yakubenko VP, Mulya A, Kundu S and Cathcart MK (2013). IL-4 and IL-13 employ discrete signalling pathways for target gene expression in alternatively activated monocytes/macrophages. *Free Radic Biol Med*. 54:1-16.

Bhoumik A, Lopez-Bergami P and Ronai Z (2007). ATF2 on the double - activating transcription factor and DNA damage response protein. *Pigment Cell Res*. 20:498-506.

Biggs PM (1961). A discussion on the classification of the avian leucosis complex and fowl paralysis. *Br Vet J*. 117:326-334.

Biggs PM and Payne LN (1967). Studies on Marek's disease. I. Experimental transmission. *J Natl Cancer Inst*. 39:267-280.

Blobel G and Dobberstein B (1975). Transfer of proteins across membranes. I. Presence of proteolytically processed and unprocessed nascent immunoglobulin light chains on membrane-bound ribosomes of murine myeloma. *J Cell Biol*. 67:835-851.

Blum JS, Wearsch PA and Cresswell P (2013). Pathways of antigen processing. *Annu Rev Immunol*. 31:443-473.

Boudny V and Kovarik J (2002). JAK-STAT signalling pathways and cancer. Janus kinases-signal transducers and activators of transcription. *Neoplasma*. 49:349-355.

Brass AL, Huang IC, Benita Y, John SP, Krishnan MN, Feeley EM, Ryan BJ, Weyer JL, van der Weyden L, Fikrig E, Adams DJ, Xavier RJ, Farzan M and Elledge SJ (2009). The IFITM proteins mediate cellular resistance to influenza A H1N1 virus, West Nile virus, and dengue virus. *Cell*. 139:1243-1254.

Breitfeld D, Ohl L, Kremmer E, Ellwart J, Sallusto F, Lipp M and Förster R (2000). Follicular B helper T cells express CXC chemokine receptor 5, localize to B cell follicles, and support immunoglobulin production. *J Exp Med*. 192:1545-1552.

Briles WE, Briles RW, Taffs RE and Stone HA (1983). Resistance to a malignant lymphoma in chickens is mapped to sub-region of major histocompatibility (B) complex. *Science*. 219:977-979.

Brown AC, Baigent SJ, Smith LP, Chattoo JP, Petherbridge LJ, Hawes P, Allday MJ and Nair V (2006). Interaction of Meq protein and C-terminal-binding protein is critical for induction of lymphomas by Marek's disease virus. *Proc Natl Acad Sci USA*. 103:1687-1692.

Brown AC, Nair V and Allday MJ (2012). Epigenetic regulation of the latency-associated region of Marek's disease virus in tumour-derived T-cell lines and primary lymphoma. *J Virol*. 86:1683-1695.

Brown MG, Dokun AO, Heusel JW, Smith HR, Beckman DL, Blattenberger EA, Dubbelde CE, Stone LR, Scalzo AA and Yokoyama WM (2001). Vital involvement of a natural killer cell activation receptor in resistance to viral infection. *Science*. 292:934-937.

Brownlie R, Zhu J, Allan B, Mutwiri GK, Babiuk LA, Potter A and Griebel P (2009). Chicken TLR21 acts as a functional homologue to mammalian TLR9 in the recognition of CpG oligodeoxynucleotides. *Mol Immunol.* 46:3163-3170.

Brun A, Albina E, Barret T, Chapman DA, Czub M, Dixon LK, Keil GM, Klonjkowski B, Le Potier MF, Libeau G, Ortego J, Richardson J and Takamatsu HH (2008). Antigen delivery systems for veterinary vaccine development: Viral-vector based delivery systems. *Vaccine*. 26:6508-6528.

Bublot M and Sharma J (2004). Vaccination against Marek's disease. In: Davison F, Nair V (Eds), Marek's Disease: An Evolving Problem. Elsevier Academic Press, London, pp.168-185.

Buckmaster AE, Scott SD, Sanderson MJ, Boursnell ME, Ross NL and Binns MM (1988). Gene sequence and mapping data from Marek's disease virus and herpesvirus of turkeys: implications for herpesvirus classification. *J Gen Virol*. 69:2033-2042.

Buelens C, Verhasselt V, De Groote D, Thielemans K, Goldman M and Willems F (1997). Human dendritic cell responses to lipopolysaccharide and CD40 ligation are differentially regulated by interleukin-10. *Eur J Immunol*. 27:1848-1852.

Bulow VV and Biggs PM (1975). Differentiation between strains of Marek's disease virus and turkey herpesvirus by immunofluorescence assays. *Avian Pathol*. 4:133-146.

Bumstead N (1998). Genomic mapping of resistance to Marek's disease. *Avian Pathol*. 27: S78-S81.

Bumstead N and Kaufman J (2004). Genetic resistance to Marek's disease. In: Davison F, Nair V (Eds), Marek's Disease: An Evolving Problem. Elsevier Academic Press, London, pp.112-125.

Bumstead N, Sillibourne J, Rennie M, Ross N and Davison F (1997). Quantification of Marek's disease virus in chicken lymphocytes using the polymerase chain reaction with fluorescence detection. *J Virol Methods*. 65:75-81.

Burgess SC and Davison TF (2002). Identification of the neoplastically transformed cells in Marek's disease herpesvirus-induced lymphomas: recognition by the monoclonal antibody AV37. *J Virol*. 76:7276-7292.

Burgess SC, Basaran BH and Davison TF (2001). Resistance to Marek's disease herpesvirus-induced lymphoma is multiphasic and dependent on host genotype. *Vet Pathol*. 38:129-142.

Burgoyne GH and Witter RL (1973). Effect of passively transferred immunoglobulins on Marek's disease. *Avian Dis*. 17:824-837.

Burnside J, Bernberg E, Anderson A, Lu C, Meyers BC, Green PJ, Jain N, Isaacs G and Morgan RW (2006). Marek's disease virus encodes MicroRNAs that map to Meq and the latency-associated transcript. *J Virol*. 80:8778-8786.

Buscaglia C and Calnek BW (1988). Maintenance of Marek's disease herpesvirus latency *in vitro* by a factor found in conditioned medium. *J Gen Virol*. 69:2809-2818.

Bustamante J, Bersier G, Romero M, Badin RA and Boveris A (2000). Nitric oxide production and mitochondrial dysfunction during rat thymocyte apoptosis. *Arch Biochem Biophys*. 376:239-247.

Buza JJ and Burgess SC (2007). Modelling the proteome of a Marek's disease transformed cell line: a natural animal model for CD30 overexpressing lymphomas. *Proteomics*. 7:1316-1326.

Calandra T and Roger T (2003). Macrophage migration inhibitory factor: a regulator of innate immunity. *Nat Rev Immunol*. 3:791-800.

Calnek BW (1972). Effects of passive antibody on early pathogenesis of Marek's disease. *Infect Immun*. 6:193-198.

Calnek BW (2001). Pathogenesis of Marek's disease virus infection. *Curr Top Microbiol Immunol*. 255:25-55.

Calnek BW, Hitchner SB and Adldinger HK (1970). Lyophilisation of cell-free Marek's disease herpesvirus and a herpesvirus from turkeys. *Appl Microbiol*. 20:723-726.

Calnek BW, Schat KA, Peckham MC and Fabricant J (1983). Field trials with a bivalent vaccine (HVT and SB-1) against Marek's disease. *Avian Dis*. 27:844-849.

Calnek BW, Schat KA, Ross LJ and Chen CL (1984a). Further characterisation of Marek's disease virus-infected lymphocytes. II. *In vitro* infection. *Int J Cancer*. 33:399-406.

Calnek BW, Schat KA, Ross LJ, Shek WR and Chen CL (1984b). Further characterisation of Marek's disease virus-infected lymphocytes. I. *In vivo* infection. *Int J Cancer*. 33:389-398.

Campadelli-Fiume G, Amasio M, Avitabile E, Cerretani A, Forghieri C, Gianni T and Menotti L (2007). The multipartite system that mediates entry of herpes simplex virus into the cell. *Rev Med Virol*. 17:313-326.

Campisano S, Mac Keon S, Gazzaniga S, Ruiz MS, Traian MD, Mordoh J and Wainstok R (2013). Anti-melanoma vaccinal capacity of CD11c-positive and -negative cell populations present in GM-CSF cultures derived from murine bone marrow precursors. *Vaccine*. 31:354-361.

Cantello JL, Anderson AS and Morgan RW (1994). Identification of latency-associated transcripts that map antisense to the ICP4 homolog gene of Marek's disease virus. *J Virol*. 68:6280-6290.

Cantello JL, Parcells MS, Anderson AS and Morgan RW (1997). Marek's disease virus latency-associated transcripts belong to a family of spliced RNAs that are antisense to the ICP4 homolog gene. *J Virol*. 71:1353-1361.

Carrozza JH, Fredrickson TN, Prince RP and Luginbuhl RE (1973). Role of desquamated epithelial cells in transmission of Marek's disease. *Avian Dis*. 17:767-781.

Chan C, Billard M, Ramirez SA, Schmidl H, Monson E and Kepler TB (2013). A model for migratory B cell oscillations from receptor down-regulation induced by external chemokine fields. *Bull Math Biol*. 75:185-205.

Chatzigeorgiou A, Lyberi M, Chatzilymperis G, Nezos A and Kamper E (2009). CD40/CD40L signaling and its implication in health and disease. *Biofactors*. 35:474-483.

Chen CL, Ager LL, Gartland GL and Cooper MD (1986). Identification of a T3/T cell receptor complex in chickens. *J Exp Med*. 164:375-380.

Chen Y, Zhang Z, Yang K, Du J, Xu Y and Liu S (2014). Myeloid zinc-finger 1 (MZF-1) suppresses prostate tumour growth through enforcing ferroportin-conducted iron egress. *Oncogene*. 2014:1-9.

Cheng HH, Perumbakka S, Black Pyrkosz AA, Subramaniam S, Preeyanon L, Dunn J, Van Sambeek F, Ansah G and Muir WM (2013). The Genetic Architecture of Genetic Resistance to Marek's Disease. In "*8th European Symposium on Poultry Genetics Proceedings*". p.12-13.

Cho KO, Mubarak M, Kimura T, Ochiai K and Itakura C (1996). Sequential skin lesions in chickens experimentally infected with Marek's disease virus. *Avian Pathol*. 25:325-343.

Churchill AE and Biggs PM (1967). Agent of Marek's disease in tissue culture. *Nature*. 215:528-530.

Churchill AE, Payne LN and Chubb RC (1969). Immunization against Marek's disease using a live attenuated virus. *Nature*. 221:744-747.

Ciraci C and Lamont SJ (2011). Avian-specific TLRs and downstream effector responses to CpG-induction in chicken macrophages. *Dev Comp Immunol*. 35:392-398.

Clement C, Tiwari V, Scanlan PM, Valyi-Nagy T, Yue BY and Shukla D (2006). A novel role for phagocytosis-like uptake in herpes simplex virus entry. *J Cell Biol*. 174:1009-1021.

Cole RK (1968). Studies on genetic resistance to Marek's disease. *Avian Dis*. 12:9-28.

Cook MK and Sears JF (1970). Preparation of infectious cell-free herpes-type virus associated with Marek's disease. *J Virol*. 5:258-261.

Cuadros MA, Martin C, Coltey P, Almendros A and Navascues J (1993). First appearance, distribution, and origin of macrophages in the early development of the avian central nervous system. *J Comp Neurol*. 330:113-129.

Cui X, Lee LF, Hunt HD, Reed WM, Lupiani B and Reddy SM (2005). A Marek's disease virus vIL-8 deletion mutant has attenuated virulence and confers protection against challenge with a very virulent plus strain. *Avian Dis*. 49:199-206.

Cui X, Lee LF, Reed WM, Kung HJ and Reddy SM (2004). Marek's disease virus-encoded vIL-8 gene is involved in early cytolytic infection but dispensable for establishment of latency. *J Virol*. 78:4753-4760.

Cui ZZ, Yan D and Lee LF (1990). Marek's disease virus gene clones encoding virus-specific phosphorylated polypeptides and serological characterization of fusion proteins. *Virus Genes*. 3:309-322.

Daniels CA, Kleinerman ES and Snyderman R (1978). Abortive and productive infections of human mononuclear phagocytes by type I herpes simplex virus. *Am J Pathol*. 91:119-136.

Davison AJ (2002). Evolution of the herpesviruses. *Vet Microbiol*. 86:69-88.

Davison AJ (2010). Herpesvirus systematics. *Vet Microbiol*. 143:52-69.

Davison F and Kaiser P (2004). Immunity to Marek's disease. In: Davison F, Nair V (Eds), Marek's Disease: An Evolving Problem. Elsevier Academic Press, London, pp.126-141.

de Geus ED, Jansen CA and Vervelde L (2012). Uptake of particulate antigens in a nonmammalian lung: phenotypic and functional characterisation of avian respiratory phagocytes using bacterial or viral antigens. *J Immunol*. 188:4516-4526.

Denesvre C (2013). Marek's disease virus morphogenesis. *Avian Dis*. 57:340-350.

Dhanasekaran DN and Johnson GL (2007). MAPKs: function, regulation, role in cancer and therapeutic targeting. *Oncogene*. 26:3097-3099.

Dinarello CA (2000). Proinflammatory cytokines. *Chest*. 118:503-508.

Djeraba A, Musset E, Bernardet N, Le Vern Y and Quere P (2002a). Similar pattern of iNOS expression, NO production and cytokine response in genetic

and vaccination-acquired resistance to Marek's disease. *Vet Immunol Immunopathol*. 85:63-75.

Djeraba A, Musset E, van Rooijen N and Quere P (2002b). Resistance and susceptibility to Marek's disease: nitric oxide synthase/arginase activity balance. *Vet Microbiol*. 86:29-44.

Doherty GJ and McMahon HT (2009). Mechanisms of endocytosis. *Annu Rev Biochem*. 78:857-902.

Dorange F, El Mehdaoui S, Pichon C, Coursaget P and Vautherot JF (2000). Marek's disease virus (MDV) homologues of herpes simplex virus type 1 UL49 (VP22) and UL48 (VP16) genes: high-level expression and characterization of MDV-1 VP22 and VP16. *J Gen Virol*. 81:2219-2230.

Dorange F, Tischer BK, Vautherot JF and Osterrieder N (2002). Characterisation of Marek's disease virus serotype 1 (MDV-1) deletion mutants that lack UL46 to UL49 genes: MDV-1 UL49, encoding VP22, is indispensable for virus growth. *J Virol*. 76:1959-1970.

Draghici S, Khatri P, Tarca AL, Amin K, Done A, Voichita C, Georgescu C and Romero R (2007). A systems biology approach for pathway level analysis. *Genome Res*. 17:1537-1545.

Durban EM and Boettiger D (1981). Replicating, differentiated macrophages can serve as *in vitro* targets for transformation by avian myeloblastosis virus. *J Virol*. 37:488-492.

Ellermann V (1921). A new strain of transmissible leukaemia in fowls (strain H). *J Exp Med*. 33:539-552.

Engel AT, Selvaraj RK, Kamil JP, Osterrieder N and Kaufer BB (2012). Marek's disease viral interleukin-8 promotes lymphoma formation through targeted recruitment of B cells and $CD4^+$ $CD25^+$ T cells. *J Virol*. 86:8536-8545.

Fabricant CG, Fabricant J, Litrenta MM and Minick CR (1978). Virus-induced atherosclerosis. *J Exp Med*. 148:335-340.

Fackler OT, Alcover A and Schwartz O (2007). Modulation of the immunological synapse: a key to HIV-1 pathogenesis? *Nat Rev Immunol*. 7:310-317.

Favoreel HW, Van Minnebruggen G, Adriaensen D and Nauwynck HJ (2005). Cytoskeletal rearrangements and cell extensions induced by the US3 kinase of an alphaherpesvirus are associated with enhanced spread. *Proc Natl Acad Sci USA*. 102:8990-8995.

Feng ZQ, Lian T, Huang Y, Zhu Q and Liu YP (2013). Expression pattern of genes of RLR-mediated antiviral pathway in different-breed chicken response to Mareks disease virus infection. *Biomed Res Int*. 2013:419256.

Ficken MD, Nasisse MP, Boggan GD, Guy JS, Wages DP, Witter RL, Rosenberger JK and Nordgren RM (1991). Marek's disease virus isolates with unusual tropism and virulence for ocular tissues: clinical findings, challenge studies and pathological features. *Avian Pathol*. 20:461-474.

Fragnet L, Blasco MA, Klapper W and Rasschaert D (2003). The RNA subunit of telomerase is encoded by Marek's disease virus. *J Virol*. 77:5985-5996.

Fukuchi K, Sudo M, Lee YS, Tanaka A and Nonoyama M (1984). Structure of Marek's disease virus DNA: detailed restriction enzyme map. *J Virol*. 51:102-109.

Gaboli M, Kotsi PA, Gurrieri C, Cattoretti G, Ronchetti S, Cordon-Cardo C, Broxmeyer HE, Hromas R and Pandolfi PP (2001). Mzf1 controls cell proliferation and tumourigenesis. *Genes Dev*. 15:1625-1630.

Garceau V, Smith J, Paton IR, Davey M, Fares MA, Sester DP, Burt DW and Hume DA (2010). Pivotal Advance: Avian colony-stimulating factor 1 (CSF-1), interleukin-34 (IL-34), and CSF-1 receptor genes and gene products. *J Leukoc Biol*. 87:753-764.

Garcia-Camacho L, Schat KA, Brooks Jr. R, and Bounous DI (2003). Early cell-mediated immune responses to Marek's disease virus in two chicken lines with defined major histocompatibility complex antigens. *Vet Immunol Immunopathol*. 95:145-153.

García-Cardeña G, Oh P, Liu J, Schnitzer JE and Sessa WC (1996). Targeting of nitric oxide synthase to endothelial cell caveolae via palmitoylation: implications for nitric oxide signalling. *Proc Natl Acad Sci USA*. 93:6448-6453.

Gavora JS and Spencer JL (1979). Studies on genetic resistance of chickens to Marek's disease-a review. *Comp Immunol Microbiol Infect Dis*. 2:359-371.

Gimeno I and Silva RF (2008). Deletion of the Marek's disease virus UL41 gene (vhs) has no measurable effect on latency or pathogenesis. *Virus Genes*. 36:499-507.

Gimeno IM (2008). Marek's disease vaccines: a solution for today but a worry for tomorrow? *Vaccine*. 3:C31-C41.

Gimeno IM, Witter RL and Reed WM (1999). Four distinct neurologic syndromes in Marek's disease: effect of viral strain and pathotype. *Avian Dis*. 43:721-737.

Gimeno IM, Witter RL, Hunt HD, Lee LF, Reddy SM and Neumann U (2001). Marek's disease virus infection in the brain: virus replication, cellular infiltration, and major histocompatibility complex antigen expression. *Vet Pathol*. 38:491-503.

Goody RJ, Beckham JD, Rubtsova K and Tyler KL (2007). JAK-STAT signalling pathways are activated in the brain following reovirus infection. *J Neurovirol*. 13:373-383.

Greider CW and Blackburn EH (1985). Identification of a specific telomere terminal transferase activity in Tetrahymena extracts. *Cell*. 43:405-413.

Greider CW and Blackburn EH (1989). A telomeric sequence in the RNA of Tetrahymena telomerase required for telomere repeat synthesis. *Nature*. 337:331-337.

Guillot L, Le Goffic R, Bloch S, Escriou N, Akira S, Chignard M and Si-Tahar M (2005). Involvement of toll-like receptor 3 in the immune response of lung epithelial cells to double-stranded RNA and influenza A virus. *J Biol Chem*. 280:5571-5580.

Haffer K, Sevoian M and Wilder M (1979). The role of the macrophages in Marek's disease: *in vitro* and *in vivo* studies. *Int J Cancer*. 23:648-656.

Hajjar DP, Fabricant CG, Minick CR and Fabricant J (1986). Virus-induced atherosclerosis: Herpesvirus infection alters aortic cholesterol metabolism and accumulation. *Am J Pathol*. 122:62-70.

Hanagata N and Li X (2011). Osteoblast-enriched membrane protein IFITM5 regulates the association of CD9 with an FKBP11-CD81-FPRP complex and stimulates expression of interferon-induced genes. *Biochem Biophys Res Commun*. 409:378-384.

Haunshi S and Cheng HH (2014). Differential expression of Toll-like receptor pathway genes in chicken embryo fibroblasts from chickens resistant and susceptible to Marek's disease. *Poult Sci*. 93:550-555.

Hayashi M, Kawamura T, Akaike H, Arai S and Okui T (1999). Antisense oligonucleotide complementary to the BamHI-H gene family of Marek's disease virus induced growth arrest of MDCC-MSB1 cells in the S-phase. *J Vet Med Sci*. 61:389-394.

Heidari M, Fitzgerald SD and Zhang H (2014). Marek's disease virus-induced transient cecal tonsil atrophy. *Avian Dis*. 58:262-270.

Heidari M, Huebner M, Kireev D and Silva RF (2008b). Transcriptional profiling of Marek's disease virus genes during cytolytic and latent infection. *Virus Genes*. 36:383-392.

Heidari M, Sarson AJ, Huebner M, Sharif S, Kireev D and Zhou H (2010). Marek's disease virus-induced immunosuppression: array analysis of chicken immune response gene expression profiling. *Viral Immunol*. 23:309-319.

Heidari M, Zhang HM and Sharif S (2008a). Marek's disease virus induces Th2 activity during cytolytic infection. *Viral Immunol*. 21:203-214.

Heinrich PC, Behrmann I, Haan S, Hermanns HM, Müller-Newen G and Schaper F (2003). Principles of interleukin (IL)-6-type cytokine signalling and its regulation. *Biochem J*. 374:1-20.

Heller ED and Schat KA (1987). Enhancement of natural killer cell activity by Marek's disease vaccines. *Avian Pathol*. 16:51-60.

Hicks JA and Liu HC (2013). Current state of Marek's disease virus microRNA research. *Avian Dis*. 57:332-329.

Higuchi M, Matsuo A, Shingai M, Shida K, Ishii A, Funami K, Suzuki Y, Oshiumi H, Matsumoto M and Seya T (2008). Combinational recognition of bacterial lipoproteins and peptidoglycan by chicken Toll-like receptor 2 subfamily. *Dev Comp Immunol*. 32:147-155.

Hong Y and Coussens PM (1994). Identification of an immediate-early gene in the Marek's disease virus long internal repeat region which encodes a unique 14 kilodalton polypeptide. *J Virol*. 68:3593-3603.

Hong Y, Frame M and Coussens PM (1995). A 14 kDa immediate-early phosphoprotein is specifically expressed in cells infected with oncogenic Marek's disease virus strains and their attenuated derivatives. *Virology*. 206:695-700.

Horner SM (2014). Activation and evasion of antiviral innate immunity by hepatitis C virus. *J Mol Biol*. 426:1198-1209.

Hotamisligil GS (2010). Endoplasmic reticulum stress and the inflammatory basis of metabolic disease. *Cell*. 140:900-917.

Hromas R, Boswell S, Shen RN, Burgess G, Davidson A, Cornetta K, Sutton J and Robertson K (1996). Forced over-expression of the myeloid zinc finger gene MZF-1 inhibits apoptosis and promotes oncogenesis in interleukin-3-dependent FDCP.1 cells. *Leukemia*. 10:1049-1050.

Hsieh YH, Wu TT, Huang CY, Hsieh YS and Liu JY (2007). Suppression of tumourigenicity of human hepatocellular carcinoma cells by antisense oligonucleotide MZF-1. *Chin J Physiol*. 50:9-15.

Hsieh YH, Wu TT, Tsai JH, Huang CY, Hsieh YS and Liu JY (2006). PKC alpha expression regulated by Elk-1 and MZF-1 in human HCC cells. *Biochem Biophys Res Commun*. 339:217-225.

Hu M, Pan Z, Yang Y, Meng C, Geng S, You M and Jiao X (2012). Different antigen presentation tendencies of granulocyte-macrophage colony-stimulating factor-induced bone marrow-derived macrophages and peritoneal macrophages. *In Vitro Cell Dev Biol Anim*. 48:434-440.

Huang da W, Sherman BT and Lempicki RA (2009). Systematic and integrative analysis of large gene lists using DAVID bioinformatics resources. *Nat Protoc*. 4:44-57.

Huang IC, Bailey CC, Weyer JL, Radoshitzky SR, Becker MM, Chiang JJ, Brass AL, Ahmed AA, Chi X, Dong L, Longobardi LE, Boltz D, Kuhn JH, Elledge SJ, Bavari S, Denison MR, Choe H and Farzan M (2011).

Distinct patterns of IFITM-mediated restriction of filoviruses, SARS coronavirus, and influenza A virus. *PLoS Pathog*. 7:e1001258.

Hugues S, Fetler L, Bonifaz L, Helft J, Amblard F and Amigorena S (2004). Distinct T cell dynamics in lymph nodes during the induction of tolerance and immunity. *Nat Immunol*. 5:1235-1242.

Hume DA (2008). Macrophages as APC and the dendritic cell myth. *J Immunol*. 181:5829-5835.

Igyártó BZ, Lackó E, Oláh I and Magyar A (2006). Characterisation of chicken epidermal dendritic cells. *Immunology*. 119:278-288.

Iizuka K, Naidenko OV, Plougastel BF, Fremont DH and Yokoyama WM (2003). Genetically linked C-type lectin-related ligands for the NKRP1 family of natural killer cell receptors. *Nat Immunol*. 4:801-807.

Improta T and Pine R (1997). Susceptibility to virus infection is determined by a Stat-mediated response to the autocrine effect of virus-induced type I interferon. *Cytokine*. 9:383-393.

Jakobisiak M, Golab J and Lasek W (2011). Interleukin 15 as a promising candidate for tumour immunotherapy. *Cytokine Growth Factor Rev*. 22:99-108.

Janeway CA and Medzhitov R (2002). Innate immune recognition. *Annu Rev Immunol*. 20:197-216.

Jarosinski KW and Du G (2014). Fluorescently-tagged RLORF4 for tracking reactivation of MDV in transformed cells. In "*10th International Symposium on Marek's Disease and Avian Herpesviruses Proceedings*". p.36.

Jarosinski KW, Arndt S, Kaufer BB and Osterrieder N (2012). Fluorescently tagged pUL47 of Marek's disease virus reveals differential tissue expression of the tegument protein in vivo. *J Virol*. 86:2428-2436.

Jarosinski KW, Njaa BL, O'connell P H and Schat KA (2005). Pro-inflammatory responses in chicken spleen and brain tissues after infection with very virulent plus Marek's disease virus. *Viral Immunol*. 18:148-161.

Jarosinski KW, Yunis R, O'Connell PH, Markowski-Grimsrud CJ and Schat KA (2002). Influence of genetic resistance of the chicken and virulence of

Marek's disease virus (MDV) on nitric oxide responses after MDV infection. *Avian Dis*. 46:636-649.

Jeurissen SH, Janse EM, Kok GL and De Boer GF (1989). Distribution and function of non-lymphoid cells positive for monoclonal antibody CVI-ChNL-68.2 in healthy chickens and those infected with Marek's disease virus. *Vet Immunol Immunopathol*. 22:123-133.

Jie H, Lian L, Qu LJ, Zheng JX, Hou ZC, Xu GY, Song JZ and Yang N (2013). Differential expression of Toll-like receptor genes in lymphoid tissues between Marek's disease virus-infected and noninfected chickens. *Poult Sci*. 92:645-654.

Jin S and Levine AJ (2001). The p53 functional circuit. *J Cell Sci*. 114:4139-4140.

Jones D, Lee L, Liu JL, Kung HJ and Tillotson JK (1992). Marek's disease virus encodes a basic-leucine zipper gene resembling the fos/jun oncogenes that is highly expressed in lymphoblastoid tumours. *Proc Natl Acad Sci USA*. 89:4042-4046.

Kaiser P (2010). Advances in avian immunology-prospects for disease control: a review. *Avian Pathol*. 39:309-324.

Kaiser P (2012). The long view: a bright past, a brighter future? Forty years of chicken immunology pre- and post-genome. *Avian Pathol*. 41:511-518.

Kaiser P, Underwood G and Davison F (2003). Differential cytokine responses following Marek's disease virus infection of chickens differing in resistance to Marek's disease. *J Virol*. 77:762-768.

Kamil JP, Tischer BK, Trapp S, Nair VK, Osterrieder N and Kung HJ (2005). vLIP, a viral lipase homologue, is a virulence factor of Marek's disease virus. *J Virol*. 79:6984-6996.

Kanehisa M and Goto S (2000). KEGG: Kyoto encyclopaedia of genes and genomes. *Nucleic Acids Res*. 28:27-30.

Kansas GS, Muirhead MJ and Dailey MO (1990). Expression of the CD11/CD18, leukocyte adhesion molecule 1, and CD44 adhesion molecules during normal myeloid and erythroid differentiation in humans. *Blood*. 76:2483-2492.

Karaca G, Anobile J, Downs D, Burnside J and Schmidt CJ (2004). Herpesvirus of turkeys: microarray analysis of host gene responses to infection. *Virology*. 318:102-111.

Kaspers B (2014). *In vitro* infection system for B and T cells: New avenues for Marek's disease virus (MDV) research. In "*10th International Symposium on Marek's Disease and Avian Herpesviruses Proceedings*". p.8.

Kato H, Takeuchi O, Mikamo-Satoh E, Hirai R, Kawai T, Matsushita K, Hiiragi A, Dermody TS, Fujita T and Akira S (2008). Length-dependent recognition of double-stranded ribonucleic acids by retinoic acid-inducible gene-I and melanoma differentiation-associated gene-5. *J Exp Med*. 205:1601-1610.

Kaufer BB, Arndt S, Trapp S, Osterrieder N and Jarosinski KW (2011). Herpesvirus telomerase RNA (vTR) with a mutated template sequence abrogates herpesvirus-induced lymphomagenesis. *PLoS Pathog*. 7:e1002333.

Kaufer BB, Trapp S, Jarosinski KW and Osterrieder N (2010). Herpesvirus telomerase RNA(vTR)-dependent lymphoma formation does not require interaction of vTR with telomerase reverse transcriptase (TERT). *PLoS Pathog*. 6:e1001073.

Kaufman J and Venugopal N (1998). The importance of MHC for Rous sarcoma virus and Marek's disease virus-some Payne-ful considerations. *Avian Pathol*. 27:S82-S87.

Kaufman J, Ferrone S, Flajnik M, Kilb M, Volk H and Parisot R (1990). MHC-like molecules in some nonmammalian vertebrates can be detected by some cross-reactive monoclonal antibodies. *J Immunol*. 144:2273-2280.

Kaufman J, Milne S, Göbel TW, Walker BA, Jacob JP, Auffray C, Zoorob R and Beck S (1999). The chicken B locus is a minimal essential major histocompatibility complex. *Nature*. 401:923-925.

Kaufman J, Völk H and Wallny HJ (1995). A "minimal essential Mhc" and an "unrecognized Mhc": two extremes in selection for polymorphism. *Immunol Rev*. 143:63-88.

Kawai T and Akira S (2006). Innate immune recognition of viral infection. *Nat Immunol*. 7:131-137.

Kedzierska K, Maerz A, Warby T, Jaworowski A, Chan H, Mak J, Sonza S, Lopez A and Crowe S (2000). Granulocyte-macrophage colony-stimulating factor inhibits HIV-1 replication in monocyte-derived macrophages. *AIDS*. 14:1739-1748.

Keestra AM, de Zoete MR, Bouwman LI and van Putten JP (2010). Chicken TLR21 is an innate CpG DNA receptor distinct from mammalian TLR9. *J Immunol*. 185:460-467.

Kim UJ, Shizuya H, De Jong PJ, Birren B and Simon MI (1992). Stable propagation of cosmid sized human DNA inserts in an F factor based vector. *Nucleic Acids Res*. 20:1083-1085.

Kingham BF, Zelnik V, Kopacek J, Majerciak V, Ney E and Schmidt CJ (2001). The genome of herpesvirus of turkeys: comparative analysis with Marek's disease viruses. *J Gen Virol*. 82:1123-1135.

Kodama H, Sugimoto C, Inage F and Mikami T (1979). Anti-viral immunity against Marek's disease virus infected chicken kidney cells. *Avian Pathol*. 8:33-44.

Kothlow S, Morgenroth I, Tregaskes CA, Kaspers B and Young JR (2008). CD40 ligand supports the long-term maintenance and differentiation of chicken B cells in culture. *Dev Comp Immunol*. 32:1015-1026.

Kuchipudi SV, Tellabati M, Sebastian S, Londt BZ, Jansen C, Vervelde L, Brookes SM, Brown IH, Dunham SP and Chang KC (2014). Highly pathogenic avian influenza virus infection in chickens but not ducks is associated with elevated host immune and pro-inflammatory responses. *Vet Res*. 45:118.

Kuhnlein U, Ni L, Weigend S, Gavora JS, Fairfull W and Zadworny D (1997). DNA polymorphisms in the chicken growth hormone gene: response to selection for disease resistance and association with egg production. *Anim Genet*. 28:116-123.

Kumar S, Buza JJ and Burgess SC (2009). Genotype-dependent tumour regression in Marek's disease mediated at the level of tumour immunity. *Cancer Microenviron*. 2:23-31.

Kumar S, Kunec D, Buza JJ, Chiang HI, Zhou H, Subramaniam S, Pendarvis K, Cheng HH and Burgess SC (2012). Nuclear Factor kappa B is central to Marek's Disease herpesvirus induced neoplastic transformation of CD30 expressing lymphocytes in vivo. *BMC Systems Biol*. 6:123.

La Boissiere S, Izeta A, Malcomber S and O'hare P (2004). Compartmentalisation of VP16 in cells infected with recombinant herpes simplex virus expressing VP16-green fluorescent protein fusion proteins. *J Virol*. 78:8002-8014.

Landman WJ and Verschuren SB (2003). Titration of Marek's disease cell-associated vaccine virus (CVI988) of reconstituted vaccine and vaccine ampoules from Dutch hatcheries. *Avian Dis*. 47:1458-1465.

Lanier LL and Phillips JH (1996). Inhibitory MHC class I receptors on NK cells and T cells. *Immunol Today*. 17:86-91.

Lauber K, Blumenthal SG, Waibel M and Wesselborg S (2004). Clearance of apoptotic cells: getting rid of the corpses. *Mol Cell*. 14:277-287.

Lee LF and Witter RL (1991). Humoral immune responses to inactivated oil-emulsified Marek's disease vaccine. *Avian Dis*. 35:452-459.

Lee LF, Cui X, Cui Z, Gimeno I, Lupiani B and Reddy SM (2005). Characterisation of a very virulent Marek's disease virus mutant expressing the pp38 protein from the serotype 1 vaccine strain CVI988/Rispens. *Virus Genes*. 31:73-80.

Lee LF, Kreager K, Heidari M, Zhang H, Lupiani B, Reddy SM and Fadly A (2013). Properties of a Meq-deleted rmd5 Marek's disease vaccine: protection against virulent MDV challenge and induction of lymphoid organ atrophy are simultaneously attenuated by serial passage *in vitro*. *Avian Dis*. 57:491-497.

Lee LF, Lupiani B, Silva RF, Kung HJ and Reddy SM (2008). Recombinant Marek's disease virus (MDV) lacking the Meq oncogene confers protection against challenge with a very virulent plus strain of MDV. *Vaccine*. 26:1887-1892.

Lee LF, Powell PC, Rennie M, Ross LJ and Payne LN (1981). Nature of genetic resistance to Marek's disease in chickens. *J Natl Cancer Inst*. 66:789-796.

Lee LF, Wu P, Sui D, Ren D, Kamil J, Kung HJ and Witter RL (2000a). The complete unique long sequence and the overall genomic organisation of the GA strain of Marek's disease virus. *Proc Natl Acad Sci USA*. 97:6091-6096.

Lee SH, Girard S, Macina D, Busa M, Zafer A, Belouchi A, Gros P and Vidal SM (2001a). Susceptibility to mouse cytomegalovirus is associated with deletion of an activating natural killer cell receptor of the C-type lectin superfamily. *Nat Genet*. 28:42-45.

Lee SH, Gitas J, Zafer A, Lepage P, Hudson TJ, Belouchi A and Vidal SM (2001b). Haplotypemapping indicates two independent origins for the Cmv1s susceptibility allele to cytomegalovirus infection and refines its localization within the Ly49 cluster. *Immunogenetics*. 53:501-505.

Lee SI, Takagi M, Ohashi K, Sugimoto C and Onuma M (2000b). Difference in the Meq gene between oncogenic and attenuated strains of Marek's disease virus serotype 1. *J Vet Med Sci*. 62:287-292.

Legler DF, Loetscher M, Roos RS, Clark-Lewis I, Baggiolini M and Moser B (1998). B cell-attracting chemokine 1, a human CXC chemokine expressed in lymphoid tissues, selectively attracts B lymphocytes via BLR1/CXCR5. *J Exp Med*. 187:655-660.

Lemon SM (2010). Induction and evasion of innate antiviral responses by hepatitis C virus. *J Biol Chem*. 285:22741-22747.

Levy AM, Gilad O, Xia L, Izumiya Y, Choi J, Tsalenko A, Yakhini Z, Witter R, Lee L, Cardona CJ and Kung HJ (2005). Marek's disease virus Meq transforms chicken cells via the v-Jun transcriptional cascade: a converging transforming pathway for avian oncoviruses. *Proc Natl Acad Sci USA*. 102:14831-14836.

Li H, Handsaker B, Wysoker A, Fennell T, Ruan J, Homer N, Marth G, Abecasis G, Durbin R and 1000 Genome Project Data Processing Subgroup (2009). The Sequence Alignment/Map format and SAMtools. *Bioinformatics*. 25:2078-2079.

Li Q and Verma IM (2002). NF-κB regulation in the immune system. *Nat Rev Immunol*. 2:725-734.

Lindholm PF, Tamami M, Makowski J and Brady JN (1996). Human T-cell lymphotropic virus type 1 Tax1 activation of NF-kappa B: involvement of the protein kinase C pathway. *J Virol*. 70:2525-2532.

Lingner J, Hughes TR, Shevchenko A, Mann M, Lundblad V and Cech TR (1997). Reverse transcriptase motifs in the catalytic subunit of telomerase. *Science*. 276:561-567.

Liu HC, Kung H-J, Fulton JE, Morgan RW and Cheng HH (2001). Growth hormone interacts with the Marek's disease virus SORF2 protein and is associated with disease resistance in chicken. *Proc Natl Acad Sci USA*. 98:9203-9208.

Liu HC, Niikura M, Fulton JE and Cheng HH (2003). Identification of chicken lymphocyte antigen 6 complex, locus E (LY6E, alias SCA2) as a putative Marek's disease resistance gene via a virus-host protein interaction screen. *Cytogenet Genome Res*. 102:304-308.

Liu J, García-Cardeña G and Sessa WC (1996). Palmitoylation of endothelial nitric oxide synthase is necessary for optimal stimulated release of nitric oxide: implications for caveolae localization. *Biochemistry*. 35:13277-13281.

Liu JL, Lin SF, Xia L, Brunovskis P, Li D, Davidson I, Lee LF and Kung HJ (1999). Meq and v-IL8: cellular genes in disguise? *Acta Virol*. 43:94-101.

Loudovaris T, Calnek BW, Yoo BH and Fahey KJ (1991b). Genetic susceptibility of chicken macrophages to in vitro infection with infectious laryngotracheitis virus. *Avian Pathol*. 20:291-302.

Loudovaris T, Yoo BH and Fahey KJ (1991a). Genetic resistance to infectious laryngotracheitis in inbred lines of White Leghorn chickens. *Avian Pathol*. 20:357-361.

Luo J, Teng M, Chi J-Q, Yu Z-H, Sun A-J, Cui Z-Z and Zhang G-P (2014). Critical roles of the Meq-clustered microRNAs of Marek's disease virus in oncogenesis. In "*10th International Symposium on Marek's Disease and Avian Herpesviruses Proceedings*". p.48.

Lupiani B, Lee LF, Cui X, Gimeno I, Anderson A, Morgan RW, Silva RF, Witter RL, Kung HJ and Reddy SM (2004). Marek's disease virus-

encoded Meq gene is involved in transformation of lymphocytes but is dispensable for replication. *Proc Natl Acad Sci USA*. 101:11815-11820.

Luzio JP, Poupon V, Lindsay MR, Mullock BM, Piper RC and Pryor PR (2003). Membrane dynamics and the biogenesis of lysosomes. *Mol Membr Biol*. 20:141-154.

MacEachern S, Muir WM, Crosby SD and Cheng HH (2011). Genome-wide identification and quantification of cis- and trans-regulated genes responding to Marek's disease virus infection via analysis of allelespecific expression. *Front Genet*. 2:113.

Maina JN (2002). Some recent advances on the study and understanding of the functional design of the avian lung: morphological and morphometric perspectives. *Biol Rev Camb Philos Soc*. 77:97-152.

Majorovits E, Nejmeddine M, Tanaka Y, Taylor GP, Fuller SD and Bangham CR (2008). Human T-lymphotropic virus-1 visualised at the virological synapse by electron tomography. *PLoS One*. 3:e2251.

Marek J (1907). Multiple Nervenentziindung (Polyneuritis) bei Hiihnern. *Dtsch Tieraerztl Wochenschr*. 15:417-421.

Markowski-Grimsrud CJ and Schat KA (2002). Cytotoxic T lymphocyte responses to Marek's disease herpesvirus-encoded glycoproteins. *Vet Immunol Immunopathol*. 90:133-144.

Mast J, Goddeeris BM, Peeters K, Vandesande F and Berghman LR (1998). Characterisation of chicken monocytes, macrophages and interdigitating cells by the monoclonal antibody KUL01. *Vet Immunol Immunopathol*. 61:343-357.

McElroy JP, Dekkers JC, Fulton JE, O'Sullivan NP, Soller M, Lipkin E, Zhang W, Koehler KJ, Lamont SJ and Cheng HH (2005). Microsatellite markers associated with resistance to Marek's disease in commercial layer chickens. *Poult Sci*. 84:1678-1688.

Meng F and Lowell CA (1997). Lipopolysaccharide (LPS)-induced macrophage activation and signal transduction in the absence of Src-family kinases Hck, Fgr, and Lyn. *Exp Med*. 185:1661-1670.

Messerle M, Crnkovic I, Hammerschmidt W, Ziegler H and Koszinowski UH (1997). Cloning and mutagenesis of a herpesvirus genome as an infectious bacterial artificial chromosome. *Proc Natl Acad Sci USA*. 94:14759-14763.

Meurs E, Chong K, Galabru J, Thomas NS, Kerr IM, Williams BR and Hovanessian AG (1990). Molecular cloning and characterization of the human double-stranded RNA-activated protein kinase induced by interferon. *Cell*. 62:379-390.

Meydan H, Yildiz MA, Dodgson JB and Cheng HH (2011). Allele-specific expression analysis reveals CD79B has a cis-acting regulatory element that responds to Marek's disease virus infection in chickens. *Poult Sci*. 90:1206-1211.

Milne DM, Campbell DG, Caudwell FB and Meek DW (1994). Phosphorylation of the tumour suppressor protein p53 by mitogen-activated protein kinases. *J Biol Chem*. 269:9253-9260.

Minick CR, Fabricant CG, Fabricant J and Litrenta MM (1979). Atheroarteriosclerosis induced by infection with a herpesvirus. *Am J Pathol*. 96:673-706.

Miyazawa K, Shinozaki M, Hara T, Furuya T and Miyazono K (2002). Two major Smad pathways in TGF-beta superfamily signalling. *Genes Cells*. 7:1191-1204.

Mizushima N, Levine B, Cuervo AM and Klionsky DJ (2008). Autophagy fights disease through cellular self-digestion. *Nature*. 451:1069-1075.

Moffatt P, Gaumond MH, Salois P, Sellin K, Bessette MC, Godin E, de Oliveira PT, Atkins GJ, Nanci A and Thomas G (2008). Bril: a novel bone-specific modulator of mineralization. *J Bone Miner Res*. 23:1497-1508.

Morgan R, Anderson A, Bernberg E, Kamboj S, Huang E, Lagasse G, Isaacs G, Parcells M, Meyers BC, Green PJ and Burnside J (2008). Sequence conservation and differential expression of Marek's disease virus microRNAs. *J Virol*. 82:12213-12220.

Morgan RW, Cantello JL and Mcdermott CH (1990). Transfection of chicken embryo fibroblasts with Marek's disease virus DNA. *Avian Dis*. 34:345-351.

Morgan RW, Sofer L, Anderson AS, Bernberg EL, Cui J and Burnside J (2001). Induction of host gene expression following infection of chicken embryo fibroblasts with oncogenic Marek's disease virus. *J Virol*. 75:533-539.

Moriguchi R, Fujimoto Y and Izawa H (1982). Chronological observations of feather pulp lesions in chickens inoculated with Marek's disease virus. *Avian Dis*. 26:375-388.

Moriguchi R, Yoshida H, Fujimoto Y, Mikami T and Izawa H (1987). Feather-pulp lesions in chickens with naturally occurring Marek's disease lymphomas. *Avian Dis*. 31:156-168.

Morimura T, Ohashi K, Sugimoto C and Onuma M (1998). Pathogenesis of Marek's disease (MD) and possible mechanisms of immunity induced by MD vaccine. *J Vet Med Sci*. 60:1-8.

Morissette G and Flamand L (2010). Herpesviruses and chromosomal integration. *J Virol*. 84:12100-12109.

Morris JF, Rauscher FJ, Davis B, Klemsz M, Xu D, Tenen D and Hromas R (1995). The myeloid zinc finger gene, MZF-1, regulates the CD34 promoter *in vitro*. *Blood*. 86:3640-3647.

Morrow C and Fehler F (2004). Marek's disease: a world-wide problem. In: Davison TF, Nair V (Eds), Marek's Disease: An Evolving Problem. Elsevier Academic Press, London, pp.49-61.

Mott KR, Underhill D, Wechsler SL, Town T and Ghiasi H (2009). A role for the JAK-STAT1 pathway in blocking replication of HSV-1 in dendritic cells and macrophages. *Virol J*. 6:56.

Mudduluru G, Vajkoczy P and Allgayer H (2010). Myeloid zinc finger 1 induces migration, invasion, and *in vivo* metastasis through Axl gene expression in solid cancer. *Mol Cancer Res*. 8:159-169.

Muylkens B, Coupeau D, Dambrine G, Trapp S, Rasschaert D (2010). Marek's disease virus microRNA designated Mdv1-pre-miR-M4 targets both cellular and viral genes. *Arch Virol*. 155:1823-1837.

Nair V (2005). Evolution of Marek's disease - a paradigm for incessant race between the pathogen and the host. *Vet J*. 170:175-183.

Nair V (2013). Latency and tumourigenesis in Marek's disease. *Avian Dis*. 57:360-365.

Nair V and Kung H-J (2004). Marek's disease virus oncogenicity: molecular mechanisms. In: Davison TF, Nair V (Eds), Marek's Disease: An Evolving Problem. Elsevier Academic Press, London, pp.32-48.

Nazerian K and Purchase HG (1970). Combined fluorescent-antibody and electron microscopy study of Marek's disease virus-infected cell culture. *J Virol*. 5:79-90.

Niikura M, Dodgson JB and Cheng H (2006b). Direct evidence of host genome acquisition by the alphaherpesvirus Marek's disease virus. *Arch Virol*. 151:537-549.

Niikura M, Dodgson JB and Cheng HH (2006a). Stability of Marek's disease virus 132-bp repeats during serial *in vitro* passages. *Arch Virol*. 151:1431-1438.

Niikura M, Kim T, Hunt HD, Burnside J, Morgan RW, Dodgson JB and Cheng HH (2007). Marek's disease virus up-regulates major histocompatibility complex class II cell surface expression in infected cells. *Virology*. 359:212-219.

Niikura M, Witter RL, Jang HK, Ono M, Mikami T and Silva RF (1999). MDV glycoprotein D is expressed in the feather follicle epithelium of infected chickens. *Acta Virol.* 43:159-163.

Nishikomori R, Usui T, Wu CY, Morinobu A, O'Shea JJ and Strober W (2002). Activated STAT4 has an essential role in Th1 differentiation and proliferation that is independent of its role in the maintenance of IL-12R beta 2 chain expression and signalling. *J Immunol*. 169:4388-4398.

O'Shea JJ, Gadina M and Schreiber RD (2002). Cytokine signalling in 2002: new surprises in the JAK-Stat pathway. *Cell*. 109:121-131.

Oeckinghaus A and Ghosh S (2009). The NF-kappaB family of transcription factors and its regulation. *Cold Spring Harb Perspect Biol*. 1:a000034.

Okamura H, Tsutsi H, Komatsu T, Yutsudo M, Hakura A, Tanimoto T, Torigoe K, Okura T, Nukada Y, Hattori K, Akita M, Namba M, Tanabe F, Konishi K, Fukada S and Kurimoto M (1995). Cloning of a new cytokine that induces IFN-gamma production by T cells. *Nature*. 378:88-91.

Okazaki W, Purchase HG and Burmester BR (1970). Protection against Marek's disease by vaccination with a herpesvirus of turkeys. *Avian Dis*. 14:413-429.

Omar AR and Schat KA (1996). Syngeneic Marek's disease virus (MDV)-specific cell-mediated immune responses against immediate early, late, and unique MDV proteins. *Virology*. 222:87-99.

Omar AR, Schat KA, Lee LF and Hunt HD (1998). Cytotoxic T lymphocyte response in chickens immunized with a recombinant fowlpox virus expressing Marek's disease herpesvirus glycoprotein B. *Vet Immunol Immunopathol*. 62:73-82.

Ooi EL, Chan ST, Cho NE, Wilkins C, Woodward J, Li M, Kikkawa U, Tellinghuisen T, Gale M Jr and Saito T (2009). Novel antiviral host factor, TNK1, regulates IFN signalling through serine phosphorylation of STAT1. *Proc Natl Acad Sci USA*. 111:1909-1914.

Orvedahl A, Alexander D, Tallóczy Z, Sun Q, Wei Y, Zhang W, Burns D, Leib DA and Levine B (2007). HSV-1 ICP34.5 confers neurovirulence by targeting the Beclin 1 autophagy protein. *Cell Host Microbe*. 1:23-35.

Osterrieder K and Vautherot J-F (2004). The genome content of Marek's disease-like viruses. In: Davison F, Nair V (Eds), Marek's Disease: An Evolving Problem. Elsevier Academic Press, London, pp.17-31.

Osterrieder N, Kamil JP, Schumacher D, Tischer BK and Trapp S (2006). Marek's disease virus: from miasma to model. *Nat Rev Microbiol*. 4:283-294.

O'Sullivan LA, Liongue C, Lewis RS, Stephenson SE and Ward AC (2007). Cytokine receptor signaling through the Jak-Stat-Socs pathway in disease. *Mol Immunol*. 44:2497-2506.

Paludan SR, Bowie AG, Horan KA and Fitzgerald KA (2011). Recognition of herpesviruses by the innate immune system. *Nat Rev Immunol*. 11:143-154.

Pappenheimer AM, Dunn LC and Cone V (1929a). Studies on fowl paralysis (neurolumphomatosis gallinarum): I. Clinical features and Pathology. *J Exp Med*. 49:63-86.

Pappenheimer AM, Dunn LC and Seidlin SM (1929b). Studies on fowl paralysis (neurolumphomatosis gallinarum): II. Transmission experiments. *J Exp Med*. 49:87-102.

Parcells MS, Arumugaswami V, Prigge JT, Pandya K and Dienglewicz RL (2003). Marek's disease virus reactivation from latency: changes in gene expression at the origin of replication. *Poult Sci*. 82:893-898.

Parcells MS, Lin SF, Dienglewicz RL, Majerciak V, Robinson DR, Chen HC, Wu Z, Dubyak GR, Brunovskis P, Hunt HD, Lee LF and Kung HJ (2001). Marek's disease virus (MDV) encodes an interleukin-8 homolog (vIL-8): characterisation of the vIL-8 protein and a vIL-8 deletion mutant MDV. *J Virol*. 75:5159-5173.

Parvizi P, Read LR and Sharif S (2014). Cytokine gene expression in lung mononuclear cells of chickens vaccinated with Herpesvirus of Turkeys and infected with Marek's disease virus. In "*10th International Symposium on Marek's Disease and Avian Herpesviruses Proceedings*". p.42.

Payne LN (2004). Pathological responses to infection. In: Davison F, Nair V (Eds), Marek's Disease: An Evolving Problem. Elsevier Academic Press, London, pp.78-97.

Payne LN and Rennie M (1976). The proportions of B and T lymphocytes in lymphomas, peripheral nerves and lymphoid organs in Marek's disease. *Avian Pathol*. 5:147-154.

Peng F, Specter S, Tanaka A and Nonoyama M (1994). A 7 kDa protein encoded by the bamhi-h gene family of Marek's disease virus is produced in lytically and latently infected-cells. *Int J Oncol.* 4:799-802.

Perera PY, Lichy JH, Waldmann TA and Perera LP (2012). The role of interleukin-15 in inflammation and immune responses to infection: implications for its therapeutic use. *Microbes Infect*. 14:247-261.

Perry ST, Prestwood TR, Lada SM, Benedict CA and Shresta S (2009). Cardif-mediated signalling controls the initial innate response to dengue virus *in vivo*. *J Virol*. 83:8276-8281.

Perumbakkam S, Muir WM, Black-Pyrkosz A, Okimoto R and Cheng HH (2013). Comparison and contrast of genes and biological pathways responding to Marek's disease virus infection using allele-specific expression and differential expression in broiler and layer chickens. *BMC Genomics*. 14:64.

Peterson FC, Hayes PL, Waltner JK, Heisner AK, Jensen DR, Sander TL and Volkman BF (2006). Structure of the SCAN domain from the tumour suppressor protein MZF1. *J Mol Biol*. 363:137-147.

Petherbridge L, Howes K, Baigent SJ, Sacco MA, Evans S, Osterrieder N and Nair V (2003). Replication-competent bacterial artificial chromosomes of Marek's disease virus: novel tools for generation of molecularly defined herpesvirus vaccines. *J Virol*. 77:8712-8718.

Petricevich VL, Reynaud E, Cruz AH and Possani LD (2008). Macrophage activation, phagocytosis and intracellular calcium oscillations induced by scorpion toxins from Tityus serrulatus. *Clin Exp Immunol*. 154:415-423.

Philbin VJ, Iqbal M, Boyd Y, Goodchild MJ, Beal RK, Bumstead N, Young J and Smith AL (2005). Identification and characterisation of a functional, alternatively spliced Toll-like receptor 7 (TLR7) and genomic disruption of TLR8 in chickens. *Immunology*. 114:507-521.

Powell PC, Hartley KJ, Mustill BM and Rennie M (1983). Studies on the role of macrophages in Marek's disease of the chicken. *J Reticuloendothel Soc*. 34:289-297.

Praslickova D, Sharif S, Sarson A, Abdul-Careem MF, Zadworny D, Kulenkamp A, Ansah G and Kuhnlein U (2008). Association of a marker in the vitamin D receptor gene with Marek's disease resistance in poultry. *Poult Sci*. 87:1112-1119.

Qian Z, Brunovskis P, Rauscher F, Lee L and Kung HJ (1995). Transactivation activity of Meq, a Marek's disease herpesvirus bZIP protein persistently expressed in latently infected transformed T cells. *J Virol*. 69:4037-4044.

Quere P and Dambrine G (1988). Development of anti-tumoural cell-mediated cytotoxicity during the course of Marek's disease in chickens. *Ann Rech Vet*.19:193-201.

Quere P, Rivas C, Ester K, Novak R and Ragland WL (2005). Abundance of IFN-alpha and IFN-gamma mRNA in blood of resistant and susceptible chickens infected with Marek's disease virus (MDV) or vaccinated with turkey herpesvirus; and MDV inhibition of subsequent induction of IFN gene transcription. *Arch Virol*. 150:507-519.

Qureshi MA and Miller L (1991). Signal requirements for the acquisition of tumoricidal competence by chicken peritoneal macrophages. *Poult Sci*. 70:530-538.

Reddy SM, Lupiani B, Gimeno IM, Silva RF, Lee LF and Witter RL (2002). Rescue of a pathogenic Marek's disease virus with overlapping cosmid DNAs: use of a pp38 mutant to validate the technology for the study of gene function. *Proc Natl Acad Sci USA*. 99:7054-7059.

Reese S, Dalamani G and Kaspers B (2006). The avian lung-associated immune system: a review. *Vet Res*. 37:311-324.

Reinke AW, Grigoryan G and Keating AE (2010). Identification of bZIP interaction partners of viral proteins HBZ, Meq, BZLF1, and K-bZIP using coiled-coil arrays. *Biochemistry*. 49:1985-1997.

Reis E Sousa C, Stahl PD and Austyn JM (1993). Phagocytosis of antigens by Langerhans cells *in vitro*. *J Exp Med*. 178:509-519.

Remouchamps C, Boutaffala L, Ganeff C and Dejardin E (2011). Biology and signal transduction pathways of the Lymphotoxin-αβ/LTβR system. *Cytokine Growth Factor Rev*. 22:301-310.

Reske A, Pollara G, Krummenacher C, Chain BM and Katz DR (2007). Understanding HSV-1 entry glycoproteins. *Rev Med Virol*. 17:205-215.

Rispens BH, Van Vloten H, Mastenbroek N, Maas HJ and Schat KA (1972a). Control of Marek's disease in the Netherlands. I. Isolation of an avirulent Marek's disease virus (strain CVI988) and its use in laboratory vaccination trials. *Avian Dis*. 16:108-125.

Rispens BH, Van Vloten H, Mastenbroek N, Maas JL and Schat KA (1972b). Control of Marek's disease in the Netherlands. II. Field trials on vaccination with an avirulent strain (CVI988) of Marek's disease virus. *Avian Dis*. 16:126-138.

Roberts KL and Baines JD (2011). Actin in herpesvirus infection. *Viruses*. 3:336-346.

Robertson KA, Hill DP, Kelley MR, Tritt R, Crum B, Van Epps S, Srour E, Rice S and Hromas R (1998). The myeloid zinc finger gene (MZF-1) delays

retinoic acid-induced apoptosis and differentiation in myeloid leukemia cells. *Leukemia*. 12:690-698.

Robinson MD and Smyth GK (2007). Moderated statistical tests for assessing differences in tag abundance. *Bioinformatics*. 23:2881-2887.

Robinson MD and Smyth GK (2008). Small-sample estimation of negative binomial dispersion, with applications to SAGE data. *Biostatistics*. 9:321-332.

Rogers SL and Kaufman J (2008). High allelic polymorphism, moderate sequence diversity and diversifying selection for B-NK but not B-lec, the pair of lectin-like receptor genes in the chicken MHC. *Immunogenetics*. 60:461-475.

Rothwell CJ, Vervelde L and Davison TF (1996). Identification of chicken Bu-1 alloantigens using the monoclonal antibody AV20. *Vet Immunol Immunopathol*. 55:225-234.

Saito T and Gale M Jr (2008). Regulation of innate immunity against hepatitis C virus infection. *Hepatol Res*. 38:115-122.

Sakata N, Patel HR, Terada N, Aruffo A, Johnson GL and Gelfand EW (1995). Selective activation of c-Jun kinase mitogen-activated protein kinase by CD40 on human B cells. *J Biol Chem*. 270:30823-30828.

Samuel MA and Diamond MS (2005). Alpha/beta interferon protects against lethal West Nile virus infection by restricting cellular tropism and enhancing neuronal survival. *J Virol*. 79:13350-13361.

Sareila O, Korhonen R, Kärpänniemi O, Nieminen R, Kankaanranta H and Moilanen E (2006). JAK inhibitors AG-490 and WHI-P154 decrease IFN-gamma-induced iNOS expression and NO production in macrophages. *Mediators Inflamm*. 2006:16161.

Sarmiento M (1988). Intrinsic resistance to viral infection: Mouse macrophage restriction of herpes simplex virus replication. *J Immunol*. 141:2740-2748.

Sarson AJ, Abdul-Careem MF, Read LR, Brisbin JT and Sharif S (2008a). Expression of cytotoxicity-associated genes in Marek's disease virus-infected chickens. *Viral Immunol*. 21:267-272.

Sarson AJ, Abdul-Careem MF, Zhou H and Sharif S (2006). Transcriptional analysis of host responses to Marek's disease viral infection. *Viral Immunol*. 19:747-758.

Sarson AJ, Parvizi P, Lepp D, Quinton M and Sharif S (2008b). Transcriptional analysis of host responses to Marek's disease virus infection in genetically resistant and susceptible chickens. *Anim Genet*. 39:232-240.

Sattentau Q (2008). Avoiding the void: cell-to-cell spread of human viruses. *Nat Rev Microbiol*. 6:815-826.

Scalzo AA, Lyons PA, Fitzgerald NA, Forbes CA, Yokoyama WM and Shellam GR (1995). Genetic mapping of *Cmv-1* in the region of mouse chromosome 6 encoding the NK gene complex-associated loci Ly49 and musNKr-P1. *Genomics*. 27:435-441.

Schat KA (1981). Role of the spleen in the pathogenesis of Marek's disease. *Avian Pathol*. 2:171-182.

Schat KA (2004). Marek's disease immunosuppression. In: Davison F, Nair V (Eds), Marek's Disease: An Evolving Problem. Elsevier Academic Press, London, pp.142-155.

Schat KA and Calnek BW (1978). Characterisation of an apparently non-oncogenic Marek's disease virus. *J Natl Cancer Inst*. 60:1075-1082.

Schat KA, Calnek BW and Fabricant J (1981). Influence of the bursa of Fabricius on the pathogenesis of Marek's disease. *Infect Immun*. 31:199-207.

Schlabach AJ, Martinez D, Field AK and Tytell AA (1979). Resistance of C58 mice to primary systemic herpes simplex virus infection: macrophage dependence and T-cell independence. *Infect Immun*. 26:615-620.

Schumacher D, Tischer BK, Fuchs W and Osterrieder N (2000). Reconstitution of Marek's disease virus serotype 1 (MDV-1) from DNA cloned as a bacterial artificial chromosome and characterisation of a glycoprotein B-negative MDV-1 mutant. *J Virol*. 74:11088-11098.

Schumacher D, Tischer BK, Trapp S and Osterrieder N (2005). The protein encoded by the US3 orthologue of Marek's disease virus is required for efficient de-envelopment of perinuclear virions and involved in actin stress fibre breakdown. *J Virol*.79:3987-3997.

Schwarz H, Schneider K, Ohnemus A, Lavric M, Kothlow S, Bauer S, Kaspers B and Staeheli P (2007). Chicken toll-like receptor 3 recognizes its cognate ligand when ectopically expressed in human cells. *J Interferon Cytokine Res*. 27:97-101.

Selgrade MK and Osborn JE (1974). Role of macrophages in resistance to murine cytomegalovirus. *Infect Immun*. 10:1383-1390.

Sharma JM (1983). Presence of adherent cytotoxic cells and non-adherent natural killer cells in progressive and regressive Marek's disease tumors. *Vet Immunol Immunopathol*. 5:125-140.

Sharma JM and Graham CK (1982). Influence of maternal antibody on efficacy of embryo vaccination with cell-associated and cell-free Marek's disease vaccine. *Avian Dis*. 26:860-870.

Sharma JM and Okazaki W (1981). Natural killer cell activity in chickens: target cell analysis and effect of antithymocyte serum on effector cells. *Infect Immun*. 31:1078-1085.

Shaw I, Powell TJ, Marston DA, Baker K, van Hateren A, Riegert P, Wiles MV, Milne S, Beck S and Kaufman J (2007). Different evolutionary histories of the two classical class I genes BF1 and BF2 illustrate drift and selection within the stable MHC haplotypes of chickens. *J Immunol*. 178:5744-5752.

Shek WR, Calnek BW, Schat KA and Chen CH (1983). Characterisation of Marek's disease virus-infected lymphocytes: discrimination between cytolytically and latently infected cells. *J Natl Cancer Inst*. 70:485-491.

Shepard JL and Zon LI (2000). Developmental derivation of embryonic and adult macrophages. *Curr Opin Hematol*. 7:3-8.

Sherer NM, Lehmann MJ, Jimenez-Soto LF, Horensavitz C, Pypaert M and Mothes W (2007). Retroviruses can establish filopodial bridges for efficient cell-to-cell transmission. *Nat Cell Biol*. 9:310-315.

Shizuya H, Birren B, Kim UJ, Mancino V, Slepak T, Tachiiri Y and Simon M (1992). Cloning and stable maintenance of 300-kilobase-pair fragments of human DNA in *Escherichia coli* using an F-factor-based vector. *Proc Natl Acad Sci USA*. 89:8794-8797.

Shkreli M, Dambrine G, Soubieux D, Kut E and Rasschaert D (2007). Involvement of the oncoprotein c-Myc in viral telomerase RNA gene regulation during Marek's disease virus-induced lymphomagenesis. *J Virol*. 81:4848-4857.

Shresta S, Sharar KL, Prigozhin DM, Snider HM, Beatty PR and Harris E (2005). Critical roles for both STAT1-dependent and STAT1-independent pathways in the control of primary dengue virus infection in mice. *J Immunol*. 175:3946-3954.

Silva RF and Gimeno I (2007). Oncogenic Marek's disease viruses lacking the 132 base pair repeats can still be attenuated by serial in vitro cell culture passages. *Virus Genes*. 34:87-90.

Silva RF, Dunn JR, Cheng HH and Niikura M (2010). A Meq-deleted Marek's disease virus cloned as a bacterial artificial chromosome is a highly efficacious vaccine. *Avian Dis*. 54:862-869.

Smith CM, Gill MB, May JS and Stevenson PG (2007). Murine gammaherpesvirus-68 inhibits antigen presentation by dendritic cells. *PLoS One*. 2:e1048.

Smith J, Sadeyen JR, Butter C, Kaiser P and Burt DW (2015). Analysis of the early immune response to infection by infectious bursal disease virus in chickens differing in their resistance to the disease. *J Virol*. 89:2469-2482.

Smith J, Sadeyen JR, Paton IR, Hocking PM, Salmon N, Fife M, Nair V, Burt DW and Kaiser P (2011). Systems analysis of immune responses in Marek's disease virus-infected chickens identifies a gene involved in susceptibility and highlights a possible novel pathogenicity mechanism. *J Virol*. 85:11146-11158.

Spatz SJ, Petherbridge L, Zhao Y and Nair V (2007). Comparative full-length sequence analysis of oncogenic and vaccine (Rispens) strains of Marek's disease virus. *J Gen Virol*. 88:1080-1096.

Staines K, Hunt LG, Young JR and Butter C (2014). Evolution of an expanded mannose receptor gene family. *PLoS One*. 9:e110330.

Stark GR, Kerr IM, Williams BR, Silverman RH and Schreiber RD (1998). How cells respond to interferons. *Annu Rev Biochem*. 67:227-264.

Strassheim S, Stik G, Rasschaert D and Laurent S (2012). MDV1-miR-M7–5p, located in the newly identified first intron of the latency-associated transcript of Marek's disease virus, targets the immediate-early genes ICP4 and ICP27. *J Gen Virol*. 93:1731-1742.

Subramaniam S, Johnston J, Preeyanon L, Brown CT, Kung HJ and Cheng HH (2013). Integrated analyses of genome-wide DNA occupancy and expression profiling identify key genes and pathways involved in cellular transformation by a Marek's disease virus oncoprotein, Meq. *J Virol*. 87:9016-9029.

Sugaya K, Bradley G, Nonoyama M and Tanaka A (1990). Latent transcripts of Marek's disease virus are clustered in the short and long repeat regions. *J Virol*. 64:5773-5782.

Tahiri-Alaoui A, Smith LP, Baigent S, Kgosana L, Petherbridge LJ, Lambeth LS, James W and Nair V (2009). Identification of an intercistronic internal ribosome entry site in a Marek's disease virus immediate-early gene. *J Virol*. 83:5846-5853.

Takahashi K, Matsumoto C and Ra C (2005). FHL3 negatively regulates human high-affinity IgE receptor beta-chain gene expression by acting as a transcriptional co-repressor of MZF-1. *Biochem J*. 386:191-200.

Tamiya T, Kashiwagi I, Takahashi R, Yasukawa H and Yoshimura A (2011). Suppressors of cytokine signalling (SOCS) proteins and JAK-STAT pathways: regulation of T-cell inflammation by SOCS1 and SOCS3. *Arterioscler Thromb Vasc Biol*. 31:980-985.

Tanaka N, Sato M, Lamphier MS, Nozawa H, Oda E, Noguchi S, Schreiber RD, Tsujimoto Y and Taniguchi T (1998). Type I interferons are essential mediators of apoptotic death in virally infected cells. *Genes Cells*. 3:29-37.

Tenney DJ and Morahan PS (1987). Effects of differentiation of human macrophage-like U937 cells on intrinsic resistance to herpes simplex virus type 1. *J Immunol*. 139:3076-3083.

Terunuma H, Deng X, Dewan Z, Fujimoto S and Yamamoto N (2008). Potential role of NK cells in the induction of immune responses: implications for NK cell-based immunotherapy for cancers and viral infections. *Int Rev Immunol*. 27:93-110.

Tian F, Luo J, Zhang H, Chang S and Song J (2012). Marek's disease virus challenge induced immune-related gene expression and chicken repeat 1 (CR1) methylation alterations in chickens. *Am J Mol Biol*. 2:232-241.

Tian F, Zhan F, VanderKraats ND, Hiken JF, Edwards JR, Zhang H, Zhao K and Song J (2013). DNMT gene expression and methylome in Marek's disease resistant and susceptible chickens prior to and following infection by MDV. *Epigenetics*. 8:431-444.

Tischer BK, Schumacher D, Messerle M, Wagner M and Osterrieder N (2002). The products of the UL10 (gM) and the UL49.5 genes of Marek's disease virus serotype 1 are essential for virus growth in cultured cells. *J Gen Virol*. 8:997-1003.

Tiwari V and Shukla D (2012). Nonprofessional phagocytosis can facilitate herpesvirus entry into ocular cells. *Clin Dev Immunol*. 2012:1-8.

Trapp S, Parcells MS, Kamil JP, Schumacher D, Tischer BK, Kumar PM, Nair VK and Osterrieder N (2006). A virus-encoded telomerase RNA promotes malignant T cell lymphomagenesis. *J Exp Med*. 203:1307-1317.

Treiber T, Treiber N and Meister G (2012). Regulation of microRNA biogenesis and function. *Thromb Haemost*. 107:605-610.

Tsai TT, Chuang YJ, Lin YS, Wan SW, Chen CL and Lin CF (2013). An emerging role for the anti-inflammatory cytokine interleukin-10 in dengue virus infection. *J Biomed Sci*. 20:40.

Tulman ER, Afonso CL, Lu Z, Zsak L, Rock DL and Kutish GF (2000). The genome of a very virulent Marek's disease virus. *J Virol*. 74:7980-7988.

Turner J, Nicholas H, Bishop D, Matthews JM and Crossley M (2003). The LIM protein FHL3 binds basic Krüppel-like factor/Krüppel-like factor 3 and its co-repressor C-terminal-binding protein 2. *J Biol Chem*. 278:12786-12795.

Vallejo RL, Bacon LD, Liu HC, Witter RL, Groenen MA, Hillel J and Cheng HH (1998). Genetic mapping of quantitative trait loci affecting susceptibility to Marek's disease virus induced tumours in F2 intercross chickens. *Genetics*. 148:349-360.

Vatter HA and Brinton MA (2014). Differential responses of disease-resistant and disease-susceptible primate macrophages and myeloid dendritic cells to simian haemorrhagic fever virus infection. *J Virol*. 88:2095-2106.

Vignais ML, Sadowski HB, Watling D, Rogers NC and Gilman M (1996). Platelet-derived growth factor induces phosphorylation of multiple JAK family kinases and STAT proteins. *Mol Cell Biol*. 16:1759-1769.

Vogelstein B, Lane D and Levine AJ (2000). Surfing the p53 network. *Nature*. 408:307-310.

von Bulow V and Klasen A (1983). Effects of avian viruses on cultured chicken bone marrow-derived macrophages. *Avian Pathol*. 12:179-198.

von Krosigk CM, McClary CF, Vielitz E and Zander DV (1972). Selection for resistance to Marek's disease and its expected effects on other important traits in White Leghorn Strain crosses. *Avian Dis*.16:11-19.

Warden C, Tang Q and Zhu H (2011). Herpesvirus BACs: past, present, and future. *J Biomed Biotechnol*. 2011:124595.

Wasson P (2011). Development of novel virus vectors for influenza vaccination. *PhD Thesis*. University of Edinburgh, UK.

Watkins SC and Salter RD (2005). Functional connectivity between immune cells mediated by tunnelling nanotubules. *Immunity*. 23:309-318.

Weber F, Wagner V, Rasmussen SB, Hartmann R and Paludan SR (2006). Double-stranded RNA is produced by positive-strand RNA viruses and DNA viruses but not in detectable amounts by negative-strand RNA viruses. *J Virol*. 80:5059-5064.

Wildy P (1973). Herpes: History and classification. In: Kaplan AS (Ed), The Herpesviruses. Academic Press, New York, pp.1-25.

Witter RL (1983). Characteristics of Marek's disease viruses isolated from vaccinated commercial chicken flocks: association of viral pathotype with lymphoma frequency. *Avian Dis*. 27:113-132.

Witter RL (1997). Increased virulence of Marek's disease virus field isolates. *Avian Dis*. 41:149-163.

Witter RL and Lee LF (1984). Polyvalent Marek's disease vaccines: safety, efficacy and protective synergism in chickens with maternal antibodies. *Avian Pathol*. 13:75-92.

Witter RL and Schat KA (2003). Marek's Disease. In: Saif YM (Ed), Diseases of Poultry. Blackwell Publishing, Iowa, Iowa State University Press, pp.407-465.

Witter RL, Sharma JM and Fadly AM (1980). Pathogenicity of variant Marek's disease virus isolants in vaccinated and unvaccinated chickens. *Avian Dis*. 24:210-232.

Wu L, Fossum E, Joo CH, Inn KS, Shin YC, Johannsen E, Hutt-Fletcher LM, Hass J and Jung JU (2009). Epstein-Barr virus LF2: an antagonist to type I interferon. *J Virol*. 8:1140-1146.

Wu L, Morahan PS and Leary K (1993). Regulation of herpes simplex virus type 1 gene expression in nonpermissive murine resident peritoneal macrophages. *J Leukoc Biol*. 53:61-65.

Wu P, Reed WM and Lee LF (2001). Glycoproteins H and L of Marek's disease virus form a hetero-oligomer essential for translocation and cell surface expression. *Arch Virol*. 146:983-992.

Wu Z, Hu T and Kaiser P (2011). Chicken CCR6 and CCR7 are markers for immature and mature dendritic cells respectively. *Dev Comp Immunol*. 35:563-567.

Wu Z, Rothwell L, Young JR, Kaufman J, Butter C and Kaiser P (2010). Generation and characterisation of chicken bone marrow-derived dendritic cells. *Immunology*. 129:133-145.

Xie Q, Anderson AS and Morgan RW (1996). Marek's disease virus (MDV) ICP4, pp38, and Meq genes are involved in the maintenance of transformation of MDCC-MSB1 MDV-transformed lymphoblastoid cells. *J Virol*. 70:1125-1131.

Xing Z and Schat KA (2000). Inhibitory effects of nitric oxide and gamma interferon on *in vitro* and *in vivo* replication of Marek's Disease Virus. *J Virol*. 74:3605-3612.

Xu H, Yao Y, Zhao Y, Smith LP, Baigent SJ and Nair V (2008). Analysis of the expression profiles of Marek's disease virus-encoded microRNAs by real-time quantitative PCR. *J Virol Methods*. 149:201-208.

Xu S, Xue C, Li J, Bi Y and Cao Y (2011). Marek's disease virus type 1 microRNA miR-M3 suppresses cisplatin-induced apoptosis by targeting Smad2 of the transforming growth factor beta signal pathway. *J Virol*. 85:276-285.

Yabe T, McSherry C, Bach FH, Fisch P, Schall RP, Sondel PM and Houchins JP (1993). A multigene family on human chromosome 12 encodes natural killer-cell lectins. *Immunogenetics*. 37:455-460.

Yamamoto K, Yamaguchi M, Miyasaka N and Miura O (2003). SOCS-3 inhibits IL-12-induced STAT4 activation by binding through its SH2 domain to the STAT4 docking site in the IL-12 receptor beta2 subunit. *Biochem Biophys Res Commun*. 310:1188-1193.

Yan QW, Reed E, Zhong XS, Thornton K, Guo Y and Yu JJ (2006). MZF1 possesses a repressively regulatory function in ERCC1 expression. *Biochem Pharmacol*. 71:761-771.

Yang XO, Panopoulos AD, Nurieva R, Chang SH, Wang D, Watowich SS and Dong C (2007). STAT3 regulates cytokine-mediated generation of inflammatory helper T cells. *J Biol Chem*. 282:9358-9363.

Yang Y, Contag CH, Felsher D, Shachaf CM, Cao Y, Herzenberg LA, Herzenberg LA and Tung JW (2004). The E47 transcription factor negatively regulates CD5 expression during thymocyte development. *Proc Natl Acad Sci USA*. 101:3898-3902.

Yonash N, Bacon LD, Witter RL and Cheng HH (1999). High resolution mapping and identification of new quantitative trait loci (QTL) affecting susceptibility to Marek's disease. *Anim Genet*. 30:126-135.

Yu GL, Bradley JD, Attardi LD and Blackburn EH (1990). *In vivo* alteration of telomere sequences and senescence caused by mutated Tetrahymena telomerase RNAs. *Nature*. 344:126-132.

Yu Y, Luo J, Mitra A, Chang S, Tian F, Zhang H, Yuan P, Zhou H and Song J (2011). Temporal transcriptome changes induced by MDV in Marek's disease-resistant and -susceptible inbred chickens. *BMC Genomics*. 12:501.

Zerboni L, Sen N, Oliver SL and Arvin AM (2014). Molecular mechanisms of varicella zoster virus pathogenesis. *Nat Rev Microbiol*. 12:197-210.

Zhang H, Xie Q, Chang S, He Y, Ernst CW, Heidari M, Black- Pykosz A and Song J (2014). Differential expression profiling of miRNAs between Marek's disease resistant and susceptible chickens. In "*10th International Symposium on Marek's Disease and Avian Herpesviruses Proceedings*". p.45.

Zhang L, Hong K, Zhang J and Pagano JS (2004). Multiple signal transducers and activators of transcription are induced by EBV LMP-1. *Virology*. 323:141-152.

Zhang W, Zhang L, Zan Y, Du N, Yang Y and Tien P (2015). Human respiratory syncytial virus infection is inhibited by IFN-induced transmembrane proteins. *J Gen Virol*. 96:170-182.

Zhao Y, Xu H, Yao Y, Smith LP, Kgosana L, Green J, Petherbridge L, Baigent SJ and Nair V (2011). Critical role of the virus-encoded microRNA-155 ortholog in the induction of Marek's disease lymphomas. *PLoS Pathog*. 7:e1001305.

Zimmerman TL, Thevananther S, Ghose R, Burns AR and Karpen SJ (2006). Nuclear export of retinoid X receptor alpha in response to interleukin-1beta-mediated cell signalling: roles for JNK and SER260. *J Biol Chem*. 281:15434-15440.

Appendix 1

Common buffers and solutions

1. General chemicals

General chemicals were of analytical or molecular biology grade, supplied by Sigma-Aldrich (Poole, UK) or Invitrogen (Paisley, UK).

2. Solutions

All solutions were made up in Milli-Q (reverse osmosis; ion-exchanged; activated charcoal filtration) water unless otherwise stated. All solutions for RNA-related work were made in RNase free H_2O or 0.1% diethyl pyrocarbonate (DEPC)-treated H_2O.

2.1 Composition of solutions

PBS	10 mM sodium phosphate, 140 mM sodium chloride (pH 7.4)
PBST	PBS with 0.05% Tween-20
SPGA-EDTA buffer	0.218 M $C_{12}H_{22}O_{11}$, 0.0038 M KH_2PO_4, 0.0072 M K_2HPO_4, 0.0049 M $C_5H_8NO_4Na$, 1% bovine serum albumin (BSA), 0.2% EDTA

3. Nucleic Acid Electrophoresis

Tris-Acetate EDTA (TAE)	40 mM Tris, 20 mM acetic acid, 1 mM EDTA (pH 8.0)
DNA loading dye	10 mM Tris-HCl (pH 7.6), 0.03% bromophenol blue, 0.03% xylene cyanol FF, 60% glycerol, 60 mM EDTA

4. Bacterial Media

LB broth	10 g bacto tryptone, 5 g bacto yeast extract, 10 g NaCl, adjust to pH 7.0 with 5 M NaOH. Made up to 1 litre with Milli-Q water

LB agar	As above with 1.5% bacto-agar

5. Buffer compositions of commercial kits

5.1 AEC substrate Kit (BD Pharmingen)

Acetate buffer	Aqueous mix of 2.5 M sodium acetate, pH 5.0
AEC chromogen	3-amino-9-ethylcarbazole (AEC) in N, N-dimethylformamide
Hydrogen peroxide	3% H_2O_2 in deionized water

5.2 EndoFree Plasmid Maxi Kit (Qiagen)

P1	50 mM Tris-HCl (pH 8.0), 10 mM EDTA, 100 µg/ml RNase A
P2	200 mM NaOH, 1% SDS (w/v)
P3	3 M potassium acetate (pH 5.5)
QBT	750 mM NaCl, 50 mM MOPS (pH 7.0), 15% isopropanol (v/v) and 0.15% Triton® X-100 (v/v)
ER	Details not provided by manufacturer
QC	1 M NaCl, 50 mM MOPS (pH 7.0) and 15% isopropanol (v/v)
QN	1.6 M NaCl, 50 mM MOPS (pH 7.0) and 15% isopropanol (v/v)
TE	10 mM Tris-HCl (pH 8.0) and 1 mM EDTA

5.3 NucleoBond® BAC100 Kit (Macherey-Nagel)

S1	50 mM Tris-HCl (pH 8.0), 10 mM EDTA, 100 µg/ml RNase A
S2	200 mM NaOH, 1% SDS

S3	2.8 M KAc (pH 5.1)
N2	100 mM Tris, 15% ethanol, 900 mM KCl, 0.15% Triton® X-100, adjusted to pH 6.3 with H_3PO_4
N3	100 mM Tris, 15% ethanol, 1.15 M KCl, adjusted to pH 6.3 with H_3PO_4
N5	100 mM Tris, 15% ethanol, 1 M KCl, adjusted to pH 8.5 with H_3PO_4

5.4 RNeasy® mini Kit (Qiagen)

RLT	Aqueous mix containing guanidine thiocyanate
RW1	Aqueous mix containing guanidine thiocyanate
RPE	Details not provided by manufacturer

5.5 Ambion® TURBO DNA-free™ Kit (Life Technologies)

10× DNase buffer	100 mM Tris-HCl pH 7.5, 25 mM $MgCl_2$, 5 mM $CaCl_2$

5.6 Qubit™ RNA Assay Kit (Invitrogen)

Qubit RNA reagent (Component A)	200× concentrate in DMSO
Qubit RNA Buffer (Component B)	Details not provided by manufacturer
Qubit RNA Standard #1 (Component C)	0 ng/µl in TE buffer
Qubit RNA Standard #2 (Component D)	10 ng/µl in TE buffer

Appendix 2

DE gene lists

Table S2.1: DE genes in line 6_1 control macrophages.

Line 6_1 control macrophages		
Gene	**Ensembl Gene ID**	**Fold Change**
AAED1	ENSGALG00000012624	3.871802
ABCA2	ENSGALG00000001226	2.446491
ADAM15	ENSGALG00000017301	2.51268
ADAMTS10	ENSGALG00000001544	2.24844
AGTPBP1	ENSGALG00000012595	2.729011
ALDH7A1	ENSGALG00000008229	2.293892
ALPK1	ENSGALG00000012074	2.16129
ANGPTL4	ENSGALG00000000619	4.322561
ANKRD6	ENSGALG00000015768	2.419207
AP1AR	ENSGALG00000028807	2.397185
ARHGEF10L	ENSGALG00000000449	2.036453
ARL4A	ENSGALG00000027757	3.808
ARSB	ENSGALG00000004438	3.099
ASAP3	ENSGALG00000001710	2.794424
ATP8B2	ENSGALG00000002326	2.390224
AUH	ENSGALG00000021843	2.054664
BAAT	ENSGALG00000005175	2.309857
BAIAP2	ENSGALG00000006915	2.068186
BAMBI	ENSGALG00000025919	8.996994
BARX2B	ENSGALG00000001197	2.992784
BCL2	ENSGALG00000012885	4.023935
BCL2A1	ENSGALG00000006511	2.040889
BDH1	ENSGALG00000006976	2.141704
BIN1	ENSGALG00000011541	2.510232
BLNK	ENSGALG00000006973	2.048154
BMP8B	ENSGALG00000024064	5.44633
BTF3	ENSGALG00000013512	2.184222
C8G	ENSGALG00000024004	2.491761
C9orf91	ENSGALG00000007186	2.193739
CATHL1	ENSGALG00000027973	3.34145
CD247	ENSGALG00000015441	3.3085
CDC14B	ENSGALG00000012627	2.192045
CDYL2	ENSGALG00000012978	3.248664
CHIR-B3	ENSGALG00000027486	7.524471
CHRNB2	ENSGALG00000002707	2.710536
CHTL1A	ENSGALG00000007174	5.467292
CLIC5	ENSGALG00000016707	3.963166
CNNM1	ENSGALG00000007489	2.500562
COL4A3BP	ENSGALG00000014952	2.310825
COMMD2	ENSGALG00000028001	2.183676

Line 6₁ control macrophages		
Gene	**Ensembl Gene ID**	**Fold Change**
CTSA	ENSGALG00000006876	2.339828
CUZD1	ENSGALG00000023424	13.7112
CYP46A1	ENSGALG00000011162	2.299543
DNAH5	ENSGALG00000013268	4.442247
DNAJA1	ENSGALG00000023066	2.066544
EFHD2	ENSGALG00000013698	2.650462
EPB41L4A	ENSGALG00000000234	2.786597
EXPH5	ENSGALG00000027243	5.54601
FAM46D	ENSGALG00000007157	4.165632
FAM47E-STBD1	ENSGALG00000027872	2.97738
FCGBP	ENSGALG00000014150	2.886056
FGF12	ENSGALG00000007219	3.973465
FXYD6	ENSGALG00000025937	2.020587
GAL1	ENSGALG00000022815	4.65347
GAL6	ENSGALG00000016668	30.14668
GBE1	ENSGALG00000015506	3.116434
gga-mir-142	ENSGALG00000018344	3.640504
gga-mir-1618	ENSGALG00000025287	3.078309
gga-mir-1661	ENSGALG00000025240	4.667173
gga-mir-3064	ENSGALG00000027517	2.413162
gga-mir-3533	ENSGALG00000027736	3.212579
GLRX	ENSGALG00000027483	2.005971
GP1BB	ENSGALG00000021529	3.401331
GPD1	ENSGALG00000012061	3.036604
GPR142	ENSGALG00000022536	3.177413
GPT2	ENSGALG00000004158	2.314629
GRHPR	ENSGALG00000005423	2.719062
HAVCR1	ENSGALG00000017362	2.236034
HERPUD1	ENSGALG00000001220	2.489729
HES4	ENSGALG00000028015	2.403829
HIC1	ENSGALG00000026718	4.088484
HIP1	ENSGALG00000000930	2.77431
HMGCS1	ENSGALG00000014862	2.200708
HSD17B1	ENSGALG00000027429	3.769768
IL17RC	ENSGALG00000028970	2.306222
IL1BETA	ENSGALG00000000534	2.77692
ILDR1	ENSGALG00000015136	3.226472
INSIG1	ENSGALG00000017394	2.079145
IRAK1BP1	ENSGALG00000015892	2.703687
ITGA1	ENSGALG00000014891	2.689838
ITM2B	ENSGALG00000016996	2.134191
JPH1	ENSGALG00000015653	5.363943

Line 6$_1$ control macrophages		
Gene	**Ensembl Gene ID**	**Fold Change**
KCTD12	ENSGALG00000009628	3.336448
KIAA0513	ENSGALG00000025938	3.447755
KIAA1147	ENSGALG00000012874	2.554401
KLF15	ENSGALG00000021702	26.23269
KLF2	ENSGALG00000003939	2.002845
KLHL13	ENSGALG00000009120	2.278936
LEFTY2	ENSGALG00000009256	5.239073
LGALS1	ENSGALG00000029043	2.02853
LGR4	ENSGALG00000012191	2.072203
LOC768803	ENSGALG00000003048	2.56365
LRMP	ENSGALG00000014011	2.227473
LYSMD3	ENSGALG00000014651	2.129185
MB21D2	ENSGALG00000007218	2.536567
ME1	ENSGALG00000015849	2.107392
MLPH	ENSGALG00000003904	5.473601
MPP3	ENSGALG00000002392	2.713062
MYLK3	ENSGALG00000004334	2.672483
N4BP2L1	ENSGALG00000017072	2.823663
NADK2	ENSGALG00000003558	2.06234
NAPEPLD	ENSGALG00000008285	2.453588
NCX1	ENSGALG00000008544	5.496456
NEDD4L	ENSGALG00000002917	3.065446
NPL	ENSGALG00000004614	2.353249
NSA2	ENSGALG00000014942	2.150103
ODF2L	ENSGALG00000006804	3.565713
OPRL1	ENSGALG00000027965	5.315932
OSBPL1A	ENSGALG00000015086	2.063202
PIM3	ENSGALG00000023576	2.570633
PINLYP	ENSGALG00000026884	2.620325
PLXDC1	ENSGALG00000023881	4.507664
POUV	ENSGALG00000026574	3.425265
PPAP2A	ENSGALG00000014711	2.401558
PPP4R4	ENSGALG00000010950	9.976112
PRRT3	ENSGALG00000006768	3.348119
PSAT1	ENSGALG00000015180	2.259765
RALGPS1	ENSGALG00000000906	4.149762
RASGRP3	ENSGALG00000010435	2.545871
RNF180	ENSGALG00000014743	4.469005
RPL17	ENSGALG00000002696	2.413544
RPS23	ENSGALG00000015617	2.449474
RPS6	ENSGALG00000015082	2.425489
SAT1	ENSGALG00000016348	2.277316

Line 6₁ control macrophages		
Gene	**Ensembl Gene ID**	**Fold Change**
SCARB1	ENSGALG00000003018	2.625295
SCN4A	ENSGALG00000000252	5.826144
SEC14L5	ENSGALG00000002111	4.381807
SELO	ENSGALG00000008694	2.082425
SFXN1	ENSGALG00000003263	2.307113
SLC1A4	ENSGALG00000008811	2.569569
SLC24A4	ENSGALG00000010793	2.263344
SLC7A5	ENSGALG00000027863	2.303132
SLC7A5	ENSGALG00000005845	2.232606
SMAD7A	ENSGALG00000018639	2.54909
SNCB	ENSGALG00000021542	5.139743
SNORD38	ENSGALG00000024758	2.570605
SOCS2	ENSGALG00000011295	3.297936
SSH2	ENSGALG00000021572	2.31678
STARD4	ENSGALG00000000241	2.404333
TBC1D8	ENSGALG00000016776	3.43013
TCN2	ENSGALG00000009536	2.876404
TGM3	ENSGALG00000004804	3.151073
THRSPB	ENSGALG00000028911	3.861224
TIMD4	ENSGALG00000003876	2.570163
TMC5	ENSGALG00000006911	2.737059
TMEM130	ENSGALG00000003569	2.397255
TMEM14A	ENSGALG00000019894	2.087553
TMEM186	ENSGALG00000027191	2.003926
TRIB1	ENSGALG00000016311	2.340359
TSNARE1	ENSGALG00000016161	4.445748
TSPAN18	ENSGALG00000014072	2.484887
TUSC1	ENSGALG00000017510	3.172573
TXN	ENSGALG00000015704	2.693107
UACA	ENSGALG00000008143	2.346389
UBA5	ENSGALG00000011707	3.069636
VPS37D	ENSGALG00000026044	2.51481
WBSCR17	ENSGALG00000001130	5.889157
WDR63	ENSGALG00000008696	4.206663
WSCD2	ENSGALG00000004849	2.437572
ZNF608	ENSGALG00000005016	3.716776
ZOV3	ENSGALG00000014877	2.082793
ZSWIM3	ENSGALG00000006848	2.242438
Uncharacterised	ENSGALG00000028154	3.460428
Uncharacterised	ENSGALG00000028418	4.557042
Uncharacterised	ENSGALG00000025824	3.741026
Uncharacterised	ENSGALG00000014551	2.50525

Line 6$_1$ control macrophages		
Gene	**Ensembl Gene ID**	**Fold Change**
Uncharacterised	ENSGALG00000016998	3.48027
Uncharacterised	ENSGALG00000027621	2.27809
Uncharacterised	ENSGALG00000028162	3.934173
Uncharacterised	ENSGALG00000005873	2.829919
Uncharacterised	ENSGALG00000007197	2.02185
Uncharacterised	ENSGALG00000027596	2.782688
Uncharacterised	ENSGALG00000027352	2.035917

Table S2.2: DE genes in line 7_2 control macrophages.

Line 7_2 control macrophages		
Gene	**Ensembl Gene ID**	**Fold Change**
ACAP3	ENSGALG00000001770	5.58647449
ACSL5	ENSGALG00000008840	2.086845944
ADAM8	ENSGALG00000003437	2.381783938
ADIPOQ	ENSGALG00000005554	4.208414513
ALDH6	ENSGALG00000007129	6.530275887
ANKRD13B	ENSGALG00000026000	4.013797676
ANKRD29	ENSGALG00000015034	3.618879408
ANO10	ENSGALG00000026562	2.147324076
APBB2	ENSGALG00000014262	3.432744823
ARHGAP32	ENSGALG00000025860	2.991742016
ATL2	ENSGALG00000000720	2.53961977
ATP1B3	ENSGALG00000002764	2.182597707
BAG3	ENSGALG00000009433	2.401920972
BLIMP-1	ENSGALG00000015388	3.378797263
BMPR1A	ENSGALG00000002003	3.683473105
C1R	ENSGALG00000014659	3.696859913
C1S	ENSGALG00000014603	10.91546432
C3H20ORF94	ENSGALG00000009016	2.71852822
CAMK1G	ENSGALG00000001319	3.534096756
CCDC186	ENSGALG00000008956	2.047452625
CCDC77	ENSGALG00000012987	3.604536489
CCNF	ENSGALG00000009201	2.407584033
CDCP1	ENSGALG00000011882	3.076342015
CDKN2C	ENSGALG00000010537	2.882035474
CENPN	ENSGALG00000013494	2.963625569
CENPO	ENSGALG00000016609	2.345592219
CEP19	ENSGALG00000006405	2.792350864
CHIR-A2	ENSGALG00000027817	3.65601729
CHIR-AB-502	ENSGALG00000028099	7.783366729
CHIR-B4	ENSGALG00000027971	66.84382305
CHIR-B4	ENSGALG00000023008	831.6999298
CHIR-B4	ENSGALG00000028718	722.605047
CHST2	ENSGALG00000026437	2.379693794
CIITA	ENSGALG00000007171	3.179096968
CIP1	ENSGALG00000028318	3.177156626
CLGN	ENSGALG00000009826	5.971209945
CLIC4	ENSGALG00000001262	3.559839642
CLIP2	ENSGALG00000001291	3.397773023
CMPK2	ENSGALG00000028982	7.647186156
CMTR1	ENSGALG00000010149	2.221045674

Line 7_2 control macrophages		
Gene	**Ensembl Gene ID**	**Fold Change**
CNKSR3	ENSGALG00000027159	2.297189867
CNTNAP1	ENSGALG00000003123	2.742176351
COL6A1	ENSGALG00000005974	4.662991137
COL6A2	ENSGALG00000006126	4.942517341
COL6A3	ENSGALG00000003923	3.520608147
CROT	ENSGALG00000008813	2.340632961
CSF1	ENSGALG00000028217	2.338229305
CSRP1	ENSGALG00000000318	2.010523748
CTNND1	ENSGALG00000007330	2.119984147
CTTNBP2NL	ENSGALG00000026182	2.022261019
CYP1A4	ENSGALG00000001325	16.94917599
CYP4V2	ENSGALG00000020688	3.036950689
DCHS1	ENSGALG00000004653	15.73701775
DENND5B	ENSGALG00000012944	9.683273816
DMB2	ENSGALG00000000166	3.09005219
DNAAF1	ENSGALG00000003258	3.668973778
DOCK7	ENSGALG00000010967	2.246662507
DUSP10	ENSGALG00000009450	2.511532947
DUSP8	ENSGALG00000006647	2.594852686
EAF2	ENSGALG00000011657	4.219791528
EDA2R	ENSGALG00000004599	2.853381726
EDARADD	ENSGALG00000014369	2.457884548
EIF2AK2	ENSGALG00000010560	2.368768188
ELOVL7	ENSGALG00000014730	7.53999656
ENG	ENSGALG00000005060	6.908284108
ENPP3	ENSGALG00000002869	2.770176176
EPHA2	ENSGALG00000023768	3.178721175
EPHB6	ENSGALG00000014749	2.359809851
EPN3	ENSGALG00000023279	3.21404597
FAM107B	ENSGALG00000028708	2.054521119
FAM114A1	ENSGALG00000013583	2.114063863
FLT1	ENSGALG00000017091	84.79895979
FLVCR1	ENSGALG00000009807	3.30300422
FMNL2	ENSGALG00000012525	2.828002165
FMO6P	ENSGALG00000003022	2.133413638
FN1	ENSGALG00000003578	2.003467501
FOXM1	ENSGALG00000013420	2.362225982
FRMD4A	ENSGALG00000006656	5.294633106
GABRD	ENSGALG00000001282	61.70928908
GADD45	ENSGALG00000025977	3.359823293
GALNT9	ENSGALG00000002242	3.876327129
GFOD1	ENSGALG00000012730	3.625408398

Line 7_2 control macrophages		
Gene	**Ensembl Gene ID**	**Fold Change**
GIMAP1	ENSGALG00000005650	3.015446908
GINS2	ENSGALG00000028131	2.356422989
GJC1	ENSGALG00000000997	3.694628293
GLIPR2	ENSGALG00000028821	2.447182064
GLUL	ENSGALG00000003678	5.291541415
GPAM	ENSGALG00000008795	2.220146899
GVINP1	ENSGALG00000016556	6.499811751
H2AFX	ENSGALG00000024338	2.703844102
H2A-VII	ENSGALG00000027425	3.310172694
H2B-I	ENSGALG00000027571	3.83479444
HAIRY1	ENSGALG00000002055	2.90479543
HAS2	ENSGALG00000016394	3.773983083
HELZ2	ENSGALG00000006138	6.000176774
HEPHL1	ENSGALG00000017214	6.82210564
HRASLS	ENSGALG00000007193	3.469678
HSD17B11	ENSGALG00000010979	2.634108106
HSP70	ENSGALG00000011715	3.785519814
HTR1B	ENSGALG00000015895	3.340330281
HTR2A	ENSGALG00000016992	7.027544443
ID1	ENSGALG00000006210	2.965040419
IFI27L2	ENSGALG00000021627	13.58998911
IFIH1	ENSGALG00000011089	4.173334126
IFITM5	ENSGALG00000026970	6.183513101
IGFBP2	ENSGALG00000011469	4.001163605
IL1RAPL2	ENSGALG00000008888	48.21464914
IQCK	ENSGALG00000028197	3.697301944
IRF1	ENSGALG00000006785	2.250762731
IRG1	ENSGALG00000016919	3.824919249
ISG12(2)	ENSGALG00000013575	9.711707091
ITGAV	ENSGALG00000002655	3.094613787
JAG1	ENSGALG00000009020	3.431176189
JAK3	ENSGALG00000028085	3.863499524
JSC	ENSGALG00000006346	4.022067529
KCNB2	ENSGALG00000022800	3.096651404
KIFC1	ENSGALG00000019837	2.147994548
KLF5	ENSGALG00000016927	2.286725851
KLHDC3	ENSGALG00000027645	4.57331162
KLHL25	ENSGALG00000006826	2.497132459
KNOP1	ENSGALG00000002042	2.098449943
LACC1	ENSGALG00000016969	7.069673254
LAMA5	ENSGALG00000005321	5.16725756
LAMB3	ENSGALG00000001343	4.401239837

Line 7_2 control macrophages		
Gene	**Ensembl Gene ID**	**Fold Change**
LARGE	ENSGALG00000012559	2.849930187
LGALS2	ENSGALG00000003213	14.79030328
LIG1	ENSGALG00000013384	2.093158254
LIMA1	ENSGALG00000006169	3.554803228
LIPI	ENSGALG00000015662	11.52030514
LRP8	ENSGALG00000010692	2.916801781
LRRC4	ENSGALG00000029160	3.426365904
MAD2L1	ENSGALG00000011967	2.070416488
MADPRT	ENSGALG00000000871	6.593057662
MANSC1	ENSGALG00000014147	2.784853202
MAPK8IP1	ENSGALG00000008430	7.354179877
MASTL	ENSGALG00000007507	3.163956226
MGAT3	ENSGALG00000012146	2.451175613
MGST3	ENSGALG00000003445	2.047386299
MICAL1	ENSGALG00000019751	2.165193348
MITD1	ENSGALG00000016759	2.328916277
MOV10	ENSGALG00000001558	2.426397915
MPP6	ENSGALG00000010988	3.104073795
MRC2	ENSGALG00000000461	3.57827136
MTFR2	ENSGALG00000019967	2.445735922
MTUS1	ENSGALG00000013615	2.890570873
MXRA8	ENSGALG00000001561	3.372132646
MYO1C	ENSGALG00000002709	3.183981751
MYO1E	ENSGALG00000004150	2.382677315
NACAD	ENSGALG00000005603	5.961886788
NAV2	ENSGALG00000003999	2.031552161
NDRG1	ENSGALG00000016216	2.496850372
NEFL	ENSGALG00000000314	8.701689709
NEU4	ENSGALG00000006361	15.11419911
NIN	ENSGALG00000012361	3.355535975
NOG	ENSGALG00000003114	28.42149679
NT5C1A	ENSGALG00000006608	2.732874671
NTN4	ENSGALG00000006325	12.81925292
OCSTAMP	ENSGALG00000004340	15.72061908
ODC1	ENSGALG00000016444	3.256505522
ORC2	ENSGALG00000008234	2.018960361
OSMR	ENSGALG00000003747	3.142476653
P2RX7	ENSGALG00000003863	2.880821337
PALM	ENSGALG00000001846	686.7271364
PAPSS2	ENSGALG00000003689	2.044728899
PARP14	ENSGALG00000012072	2.137566778
PARVB	ENSGALG00000014201	2.329433804

Line 7_2 control macrophages		
Gene	**Ensembl Gene ID**	**Fold Change**
PATL2	ENSGALG00000002167	2.970342484
PDE4DIP	ENSGALG00000011777	2.410267485
PDE7B	ENSGALG00000013941	2.400745783
PDIK1L	ENSGALG00000026301	2.587494394
PDLIM7	ENSGALG00000026159	2.133074247
PFKL	ENSGALG00000006543	2.223647424
PIK3AP1	ENSGALG00000005547	2.165293124
PISD	ENSGALG00000006872	2.458319088
PKD1	ENSGALG00000005714	2.144801021
PKN3	ENSGALG00000004689	2.360729272
PLACL2	ENSGALG00000011190	12.24393082
PLCG1	ENSGALG00000016141	2.221594027
PM20D2	ENSGALG00000015779	2.200681976
PNPLA2	ENSGALG00000014569	2.07816151
POGZ	ENSGALG00000002505	3.547167451
PPAR	ENSGALG00000022985	13.20642383
PRC1	ENSGALG00000012836	2.553010474
PRSS12	ENSGALG00000005156	3.353308624
PTCHD1	ENSGALG00000016358	4.388575404
PTGS1	ENSGALG00000001314	6.625913477
PTPRE	ENSGALG00000009823	2.246271693
PTTG1	ENSGALG00000001506	2.2818479
RAB34	ENSGALG00000026315	2.688320643
RACGAP1	ENSGALG00000006271	2.517730402
RASAL3	ENSGALG00000029030	2.771665224
RGSL1	ENSGALG00000003671	8.000150137
RHOC	ENSGALG00000001569	3.457512756
RHPN2	ENSGALG00000004814	3.316621667
RNF150	ENSGALG00000009865	3.576261702
RNF208	ENSGALG00000008911	2.700589914
RTTN	ENSGALG00000013745	2.409371228
RUFY4	ENSGALG00000025739	3.065413917
SAMD9L	ENSGALG00000009479	4.335827054
SCN1A	ENSGALG00000010943	4.674271764
SCN4B	ENSGALG00000007409	6.002679977
SDC4	ENSGALG00000003932	2.318118136
SEPT4	ENSGALG00000028193	2.504994692
SERPINE2	ENSGALG00000005135	4.624228596
SESN3	ENSGALG00000017204	2.767660386
SH3RF3	ENSGALG00000016810	3.462534018
SKA3	ENSGALG00000017128	2.040723394
SLC19A2	ENSGALG00000021092	9.024327669

Line 7_2 control macrophages		
Gene	**Ensembl Gene ID**	**Fold Change**
SLC19A3	ENSGALG00000003025	5.761852294
SLC2A6	ENSGALG00000002982	2.756368717
SLC41A3	ENSGALG00000006235	3.498249719
SLC7A3	ENSGALG00000005727	3.676171701
SLCO2B1	ENSGALG00000017302	4.844445243
SLCO4A1	ENSGALG00000005460	3.386073541
SLMO1	ENSGALG00000013830	2.78299333
SMC4	ENSGALG00000009553	2.028000423
SMTN	ENSGALG00000011865	2.590917506
SORCS3	ENSGALG00000008434	96.7393813
SPERT	ENSGALG00000016981	2425.992891
SPRY3	ENSGALG00000007448	33.30982895
SPTBN1	ENSGALG00000023241	2.795195301
SRGAP1	ENSGALG00000009825	3.656494705
ST8SIA1	ENSGALG00000013211	6.409817536
STOM	ENSGALG00000001434	2.171156283
SUSD4	ENSGALG00000009388	7.844970204
SYNDIG1L	ENSGALG00000010233	4.858235774
SYNE2	ENSGALG00000011811	3.93085666
TAAR1	ENSGALG00000013994	3.165421774
TACC2	ENSGALG00000009516	5.594353216
TAPBPL	ENSGALG00000014428	2.044491878
TBXA2R	ENSGALG00000027241	2.820602652
TFPI2	ENSGALG00000009512	9.673482581
THBS2	ENSGALG00000011200	5.71317378
TJP2	ENSGALG00000015109	9.667183245
TK1	ENSGALG00000007191	3.121176943
TLN2	ENSGALG00000003628	2.87988471
TMCC2	ENSGALG00000000673	3.422988581
TMEM201	ENSGALG00000002527	2.124849732
TMTC2	ENSGALG00000010975	3.435268209
TNFIP6	ENSGALG00000012481	3.771840757
TNNI2	ENSGALG00000006591	2.984885486
TOR1A	ENSGALG00000023709	6.270273117
TPCN2	ENSGALG00000007550	2.187598404
TRAF2	ENSGALG00000009014	2.035230306
TTC26	ENSGALG00000011847	2.891012355
TUBE1	ENSGALG00000015017	2.948307758
TWSG1	ENSGALG00000008400	2.66042892
TXNRD1	ENSGALG00000012714	2.093036522
UBXN2B	ENSGALG00000015431	2.132393869
UCK2	ENSGALG00000003510	3.781878673

Line 7_2 control macrophages		
Gene	**Ensembl Gene ID**	**Fold Change**
UNC13D	ENSGALG00000002234	3.285827849
USP12	ENSGALG00000017101	2.795555258
USP18	ENSGALG00000013057	6.962800793
VCAN	ENSGALG00000015624	2.333172351
VIPR1	ENSGALG00000005259	933.6545574
WNT11B	ENSGALG00000004401	7.761552371
ZDHHC8	ENSGALG00000002124	2.381638152
ZRANB3	ENSGALG00000012223	2.064620507
Uncharacterised	ENSGALG00000015276	4.902426345
Uncharacterised	ENSGALG00000020700	6.444272704
Uncharacterised	ENSGALG00000007846	63.80646277
Uncharacterised	ENSGALG00000027822	5.927773145
Uncharacterised	ENSGALG00000023068	13.18793007

Table S2.3: DE genes in line 6_1 infected macrophages.

Line 6_1 infected macrophages		
Gene	**Ensembl Gene ID**	**Fold Change**
ABI3	ENSGALG00000001287	2.885126032
ABTB2	ENSGALG00000011609	2.686976225
ADA	ENSGALG00000004170	2.606289839
ADAM9	ENSGALG00000013838	3.036049759
AGBL2	ENSGALG00000024097	3.558190174
ALDH3A2	ENSGALG00000003490	2.49653446
AMIGO3	ENSGALG00000028339	2.128645538
AMPD3	ENSGALG00000005662	2.149913351
ANGPT1	ENSGALG00000027520	3.662895618
ARSI	ENSGALG00000005616	20.80847226
ASB12	ENSGALG00000007594	3.077433713
ATP7B	ENSGALG00000017021	17.70034231
B3GNT9	ENSGALG00000021345	2.080622354
BATF	ENSGALG00000010323	3.138413833
BATF3	ENSGALG00000009816	5.596860906
BCAR1	ENSGALG00000028291	2.032273139
BDKRB1	ENSGALG00000020386	4.350207971
BDKRB2	ENSGALG00000011080	2.411805771
BEST4	ENSGALG00000010126	10.80578251
BPIFC	ENSGALG00000021025	4.623526845
BRICD5	ENSGALG00000005883	3.659003303
BUD13	ENSGALG00000025882	2.793408917
C14orf159	ENSGALG00000010703	3.279067056
C16orf93	ENSGALG00000021212	2.403234335
C4	ENSGALG00000017040	5.183964756
CA13	ENSGALG00000015820	2.339286065
CAB39L	ENSGALG00000017005	3.403533847
CACNA1S	ENSGALG00000000730	2.094571107
CCBL1	ENSGALG00000009407	2.707198698
CCDC65	ENSGALG00000028482	2.82125525
CCDC88C	ENSGALG00000027614	2.021492752
CCKBR	ENSGALG00000027913	2.429261322
CCL1	ENSGALG00000002329	22.61966865
CCL20	ENSGALG00000003003	5.057896837
CCR7	ENSGALG00000027572	4.952319266
CD1A1	ENSGALG00000012494	3.534067246
CD3E	ENSGALG00000007416	7.880156855
CDKN1A	ENSGALG00000026896	2.760567012
CELA2A	ENSGALG00000004568	2.953645327
CHRD	ENSGALG00000026983	3.955574349

Line 6$_1$ infected macrophages		
Gene	**Ensembl Gene ID**	**Fold Change**
CHRDL2	ENSGALG00000017308	3.054368286
CHRNA3	ENSGALG00000003014	3.823818256
CNGA2	ENSGALG00000007282	2.168905448
COCH	ENSGALG00000009920	6.28307773
COL13A1	ENSGALG00000004286	3.311831643
COL7A1	ENSGALG00000005811	3.885690745
CORO2A	ENSGALG00000001933	7.969053854
CPE	ENSGALG00000027788	6.741504545
CPNE2	ENSGALG00000001316	2.754450601
CPNE7	ENSGALG00000000507	8.39176448
CRMP1B	ENSGALG00000015042	6.402110707
CROCC	ENSGALG00000027085	2.096910323
CSF3	ENSGALG00000026420	2.498443545
CSGALNACT1	ENSGALG00000010125	4.503659877
CUBN	ENSGALG00000008704	2.068661611
CUTA	ENSGALG00000001620	4.332086462
CUX2	ENSGALG00000004598	2.381038252
CX3CL1	ENSGALG00000026663	5.033155941
CXCL13L2	ENSGALG00000010338	3.263677612
CYP3A37	ENSGALG00000004449	4.396369146
DGKH	ENSGALG00000003841	4.318612829
DIXDC1	ENSGALG00000007929	2.444657598
DNAH9	ENSGALG00000001111	3.276394398
DST	ENSGALG00000016289	2.655743993
DUSP16	ENSGALG00000028155	2.168386763
DZANK1	ENSGALG00000008731	2.165755677
EDA	ENSGALG00000004481	3.079990348
EPHA7	ENSGALG00000015593	13.04522977
ERICH3	ENSGALG00000011356	3.155575101
EVPL	ENSGALG00000002108	2.937918007
EX-FABP	ENSGALG00000024011	2.222775163
F2RL3	ENSGALG00000002570	2.203480451
F5	ENSGALG00000015207	2.202326928
FAM110D	ENSGALG00000001453	2.532812836
FAM134B	ENSGALG00000026200	2.025929844
FAM154A	ENSGALG00000027314	3.104733195
FAM181B	ENSGALG00000022713	5.869737427
FASN	ENSGALG00000025905	2.050296977
FBXO41	ENSGALG00000016087	3.816932967
FHAD1	ENSGALG00000017714	6.576526394
FLT4	ENSGALG00000005802	4.383895228
FSTL3	ENSGALG00000024328	23.11874632

Line 6$_1$ infected macrophages		
Gene	**Ensembl Gene ID**	**Fold Change**
FZD4	ENSGALG00000017242	2.820242672
G0S2	ENSGALG00000023933	2.838379078
GALR3	ENSGALG00000004127	2.005023215
GAREML	ENSGALG00000022838	2.807403996
GEM	ENSGALG00000015954	3.423282098
GNGT2	ENSGALG00000026333	2.491001379
GPAT2	ENSGALG00000014436	2.725948419
GPR174	ENSGALG00000004111	4.078799485
GPR39	ENSGALG00000012171	2.957593059
GRIP2	ENSGALG00000006449	23.51643915
GTSF1	ENSGALG00000001109	2.755232031
HEMGN	ENSGALG00000023061	2.974739553
HEY1	ENSGALG00000027364	4.717339011
HHLA2	ENSGALG00000022871	4.607573517
HLF	ENSGALG00000003059	2.281827868
HPCA	ENSGALG00000003573	3.458873918
HPD	ENSGALG00000004343	3.172186093
HSPA12A	ENSGALG00000028016	5.922633484
HSPA12A	ENSGALG00000009248	2.155061362
IGDCC3	ENSGALG00000007371	2.222165724
IGSF11	ENSGALG00000015084	2.915678966
IGSF3	ENSGALG00000015469	2.070897728
IL13RA2	ENSGALG00000020316	4.49295436
IL20RA	ENSGALG00000013869	6.865326748
IL23R	ENSGALG00000011212	7.11153038
IL2RA	ENSGALG00000006335	5.241353238
INHBB	ENSGALG00000028770	2.719880592
IRF4	ENSGALG00000012830	8.546411329
IRS2	ENSGALG00000016839	2.311884021
ITGB1BP2	ENSGALG00000005493	10.45135463
K123	ENSGALG00000006337	9.415051876
K60	ENSGALG00000011668	2.73039348
KBTBD3	ENSGALG00000028658	3.060382457
KCNAB1	ENSGALG00000010269	23.40541545
KCNH2	ENSGALG00000027043	8.140595457
KCNJ5	ENSGALG00000001181	2.238738963
KIAA1755	ENSGALG00000023590	2.610129237
KIFC3	ENSGALG00000001020	2.51972451
LAT2	ENSGALG00000029173	152.1779288
LEPR	ENSGALG00000011058	3.109279137
LHCGR	ENSGALG00000009095	3.036256301
LIMCH1	ENSGALG00000014258	10.48563592

Line 6$_1$ infected macrophages		
Gene	**Ensembl Gene ID**	**Fold Change**
LIPG	ENSGALG00000002712	2.68276657
LOXL3	ENSGALG00000013254	3.078675016
LRRC6	ENSGALG00000016244	2.901443706
LSAMP	ENSGALG00000015087	2.01906278
LYZ	ENSGALG00000009963	4.867377366
LZTS1	ENSGALG00000016001	3.790344364
MADCAM1	ENSGALG00000028341	10.93635636
MAMDC4	ENSGALG00000008995	4.62253841
MARCKSL1	ENSGALG00000021616	3.133070551
MIEN1	ENSGALG00000026328	2.047020503
MUC6	ENSGALG00000006740	3.675418211
MVK	ENSGALG00000013848	2.678900193
MYL4	ENSGALG00000000585	2.649272788
MYO10L	ENSGALG00000011172	2.340519692
NDNF	ENSGALG00000011962	2.622867607
NEB	ENSGALG00000012495	2.23561941
NINJ1	ENSGALG00000026891	2.3003172
NME1	ENSGALG00000007305	2.264954051
NR4A3	ENSGALG00000013568	2.356815885
NRN1	ENSGALG00000029089	3.128368385
ODZ3	ENSGALG00000010706	2.490415656
OLFML2A	ENSGALG00000001048	2.07162475
P4HA3	ENSGALG00000017311	2.25047525
PADI3	ENSGALG00000000479	2.474794321
PAQR7	ENSGALG00000009680	2.941980974
PCDH18	ENSGALG00000009732	2.517131234
PDLIM4	ENSGALG00000027627	2.312743005
PERM1	ENSGALG00000026875	3.797426826
PHYKPL	ENSGALG00000023920	2.009014426
PKD2L2	ENSGALG00000006120	3.902041719
PLCE1	ENSGALG00000028043	2.211014108
PLEKHN1	ENSGALG00000002121	5.294426519
PLOD2	ENSGALG00000006783	3.787488981
PROM1	ENSGALG00000007645	2.586154805
PRSS35	ENSGALG00000015847	2.425055502
PSD	ENSGALG00000005680	8.119824178
PSMD4	ENSGALG00000028505	4.041903398
PSMD4	ENSGALG00000026320	2.79399495
PTCHD1	ENSGALG00000023347	2.328939565
PTGES	ENSGALG00000027357	2.879877179
PTPN22	ENSGALG00000021656	2.053225759
PTPRB	ENSGALG00000000584	3.304958634

Line 6$_1$ infected macrophages		
Gene	**Ensembl Gene ID**	**Fold Change**
RAB11FIP3	ENSGALG00000002666	2.724481846
RAPGEF3	ENSGALG00000006348	4.877311512
RASSF7	ENSGALG00000006873	3.043780295
RELT	ENSGALG00000019033	6.34904231
RNaseP_nuc	ENSGALG00000025650	2.609890176
RNF157	ENSGALG00000002008	4.067590714
RRAD	ENSGALG00000005140	2.067169798
RUNX3	ENSGALG00000026821	3.523429118
RUSC2	ENSGALG00000002371	2.086567435
S100A11	ENSGALG00000009163	3.50947497
SAMD4A	ENSGALG00000012203	2.144478269
SCARNA7	ENSGALG00000025666	2.924232187
SDR42E1	ENSGALG00000005456	2.634376177
SEMA3B	ENSGALG00000013722	2.11385633
SEMA3C	ENSGALG00000008455	2.282269085
SEMA3F	ENSGALG00000013370	2.854706855
SEMA4D	ENSGALG00000003058	6.782338989
SERINC2	ENSGALG00000021685	3.421281291
SFRP5	ENSGALG00000006944	3.5324513
SH2D1B	ENSGALG00000028448	5.042172742
SH3BP5	ENSGALG00000011550	2.031664472
SHISA8	ENSGALG00000027568	5.573777113
SLC12A3	ENSGALG00000002957	2.400261548
SLC12A5	ENSGALG00000006930	3.367938384
SLC15A1	ENSGALG00000016884	2.606432403
SLC16A4	ENSGALG00000000417	4.992568735
SLC26A11	ENSGALG00000007018	2.218857794
SLC38A3	ENSGALG00000028871	3.467479421
SLC46A2	ENSGALG00000027345	2.265559988
SLC6A9	ENSGALG00000010098	2.956294151
SLCO3A1	ENSGALG00000006871	2.824683683
SLCO4C1	ENSGALG00000026768	2.060415124
SMTNL1	ENSGALG00000028884	2.280941234
SNORA27	ENSGALG00000017811	3.929658384
SNORA73	ENSGALG00000021931	2.745869301
SNORD35	ENSGALG00000021748	2.774445616
snoU2_19	ENSGALG00000025390	4.508887978
SPINT1	ENSGALG00000008469	2.106186417
SPIRE2	ENSGALG00000000521	11.08055555
ST3GAL1	ENSGALG00000016210	6.13833338
STARD10	ENSGALG00000028681	4.103890435
STAT2	ENSGALG00000028750	2.073040472

Line 6l infected macrophages		
Gene	**Ensembl Gene ID**	**Fold Change**
STAT4	ENSGALG00000025974	13.6460531
STRIP2	ENSGALG00000026181	2.648076101
SUGP2	ENSGALG00000003047	2.112050524
SYPL1	ENSGALG00000029006	2.280573422
SYT2	ENSGALG00000026033	9.877955567
SYTL4	ENSGALG00000006786	3.19578674
TBC1D24	ENSGALG00000001244	14.6929115
TDRP	ENSGALG00000016356	2.20411411
TMED6	ENSGALG00000000654	4.596052535
TMEM132E	ENSGALG00000002312	31.75883189
TMEM136	ENSGALG00000026316	2.325622149
TMEM51	ENSGALG00000013643	2.03951447
TNFRSF9	ENSGALG00000000543	2.177435955
TNIP3	ENSGALG00000011961	2.633283918
TNNC2	ENSGALG00000006835	2.731236752
TNXB	ENSGALG00000000182	2.322326451
TRPM2	ENSGALG00000005631	2.632437195
TSKU	ENSGALG00000000761	4.713068235
TTBK1	ENSGALG00000008627	2.055075262
TUBA3E	ENSGALG00000010439	2.915439388
TUBB3	ENSGALG00000000059	3.657756722
UCP	ENSGALG00000017316	2.605759001
UMODL1	ENSGALG00000016157	4.31446934
USP43	ENSGALG00000017417	9.767652134
VAV2	ENSGALG00000002699	2.858780351
VWA5B2	ENSGALG00000000193	2.355836041
WBSCR27	ENSGALG00000026762	2.15931029
WNT4	ENSGALG00000004790	3.732024814
WNT5B	ENSGALG00000012998	4.395598467
XG	ENSGALG00000029002	5.292523637
YF6	ENSGALG00000026292	10.44951891
ZPLD1	ENSGALG00000015347	3.766216383
ZSWIM5	ENSGALG00000010221	2.158446656
Uncharacterised	ENSGALG00000002614	16.34856499
Uncharacterised	ENSGALG00000022751	12.37891293
Uncharacterised	ENSGALG00000019325	5.475325603
Uncharacterised	ENSGALG00000027693	3.521908518
Uncharacterised	ENSGALG00000026622	3.098493533
Uncharacterised	ENSGALG00000023936	2.705520977
Uncharacterised	ENSGALG00000022080	2.53889931
Uncharacterised	ENSGALG00000020380	2.481085201
Uncharacterised	ENSGALG00000028330	2.274840479

Line 6_1 infected macrophages		
Gene	**Ensembl Gene ID**	**Fold Change**
Uncharacterised	ENSGALG00000028163	2.240868082
Uncharacterised	ENSGALG00000029010	2.224913092
Uncharacterised	ENSGALG00000026256	32.37965098
Uncharacterised	ENSGALG00000027955	5.287637564
Uncharacterised	ENSGALG00000028959	4.696291309
Uncharacterised	ENSGALG00000014600	4.213936831
Uncharacterised	ENSGALG00000024335	3.848697297
Uncharacterised	ENSGALG00000027839	3.47512769
Uncharacterised	ENSGALG00000027203	2.508321151
Uncharacterised	ENSGALG00000027780	2.482143989
Uncharacterised	ENSGALG00000018702	2.071794515

Table S2.4: DE genes in line 7_2 infected macrophages.

Line 7_2 infected macrophages		
Gene	**Ensembl Gene ID**	**Fold Change**
ABCA1	ENSGALG00000015433	2.284856259
ABCA1	ENSGALG00000015433	2.284856259
ABCB1LB	ENSGALG00000008912	4.388420445
ACOX2	ENSGALG00000007132	2.116000533
ACSS3	ENSGALG00000010940	132.3972858
ADAM12	ENSGALG00000012740	5.114999423
ADAMTS1	ENSGALG00000015792	2.613476819
AFAP1	ENSGALG00000015556	2.770025457
AKAP12	ENSGALG00000023073	2.636071774
AKAP6	ENSGALG00000009995	2.677849771
AKR1B1L	ENSGALG00000013067	2.345489388
ALPK2	ENSGALG00000002898	3.256460949
AMDHD1	ENSGALG00000011414	2.645963727
ANGPTL2	ENSGALG00000000927	2.123836445
ARHGAP31	ENSGALG00000015077	2.243209264
ARHGAP32	ENSGALG00000001192	2.667479125
ARMC2	ENSGALG00000015289	2.37348205
ARMC3	ENSGALG00000007864	3.76167533
ARNT2	ENSGALG00000006445	2.652962068
ART1	ENSGALG00000012603	2.155504116
ATCAY	ENSGALG00000001812	2.319862794
BCAR3	ENSGALG00000005816	2.00352537
BLK	ENSGALG00000016661	2.505825862
BTBD3	ENSGALG00000009028	2.137763807
C10orf54	ENSGALG00000004673	2.382841561
C11orf74	ENSGALG00000007941	2.984482827
C12ORF32	ENSGALG00000013422	2.061702106
C3AR1	ENSGALG00000013218	2.508183937
C3D	ENSGALG00000011509	2.317835814
C7orf50	ENSGALG00000004055	2.011600709
C8orf4	ENSGALG00000024083	2.399739867
CAMKK1	ENSGALG00000001617	2.507321104
CASS4	ENSGALG00000007744	4.463173808
CC2D2A	ENSGALG00000014514	2.070998064
CD244	ENSGALG00000027074	3.065817773
CD274	ENSGALG00000015032	2.239363806
CDC42BPA	ENSGALG00000009158	3.338876808
CELSR1	ENSGALG00000013399	3.026995125
CEP112	ENSGALG00000003975	2.009259245
CFAP70	ENSGALG00000002551	4.29889503

Line 7_2 infected macrophages		
Gene	**Ensembl Gene ID**	**Fold Change**
CFTII	ENSGALG00000009046	2.314490848
CHAC1	ENSGALG00000027874	2.641275999
CHANK3	ENSGALG00000003135	6.388131299
CHD1L	ENSGALG00000015038	2.0472633
CHIA	ENSGALG00000023760	2.693292214
CLCN4	ENSGALG00000016607	4.867920633
CNBP	ENSGALG00000027201	5.068905783
COL22A1	ENSGALG00000016195	4.302647895
COL5A2	ENSGALG00000002509	2.156004177
COL5A2	ENSGALG00000002509	2.156004177
COLEC12	ENSGALG00000014910	2.658889658
CPED1	ENSGALG00000009002	2.382349132
CR1L	ENSGALG00000023950	2.336040526
CREG2	ENSGALG00000026022	2.0099597
CRIP1	ENSGALG00000002771	4.792668267
CSF1R	ENSGALG00000005725	2.282746004
CSPG4	ENSGALG00000020561	2.146721293
CXXC5	ENSGALG00000000884	2.803204177
CYP3A4	ENSGALG00000004436	2.051461795
CYTIP	ENSGALG00000012545	2.838914077
D2HGDH	ENSGALG00000006347	2.103064713
DHFR	ENSGALG00000026757	2.544902446
DHRS13	ENSGALG00000004009	2.701364664
DHRS3	ENSGALG00000004256	2.466667635
DISP3	ENSGALG00000004662	2.619254779
DLC1	ENSGALG00000013715	3.340830997
DMC1	ENSGALG00000012236	12.32489135
DNASE1L3	ENSGALG00000005688	2.056467055
DOCK10	ENSGALG00000005030	2.026680734
DTNA	ENSGALG00000015211	3.409978656
DUSP4	ENSGALG00000011419	2.224808599
EFNA5	ENSGALG00000000280	2.326144379
ENTPD1	ENSGALG00000007078	2.200381235
EPB41L5	ENSGALG00000011605	3.772613538
EPHA3	ENSGALG00000015403	2.544264158
EPHX1	ENSGALG00000010303	2.994728829
ERMARD	ENSGALG00000011186	2.023083863
FABP3	ENSGALG00000000620	2.467862364
FAM171B	ENSGALG00000002646	2.463697055
FAT1	ENSGALG00000013579	3.208763007
FBXL8	ENSGALG00000003201	2.111170181
FGR	ENSGALG00000004785	2.732899098

Line 7_2 infected macrophages		
Gene	**Ensembl Gene ID**	**Fold Change**
FILIP1L	ENSGALG00000015271	2.295710038
FKBP10	ENSGALG00000025764	2.160043289
FTD	ENSGALG00000028696	2.867336572
FYN	ENSGALG00000026057	2.58279571
GALNTL4	ENSGALG00000005584	9.88860378
GCG	ENSGALG00000011104	3.566890111
gga-mir-22	ENSGALG00000024507	15.62169629
GINS1	ENSGALG00000008538	2.250126695
GLI3	ENSGALG00000012329	2.031254529
GMPR	ENSGALG00000012705	2.33264523
GPC1	ENSGALG00000002342	2.403584709
GPR126	ENSGALG00000013803	3.202171828
GPR149	ENSGALG00000010337	2.590854867
GPR161	ENSGALG00000015247	3.729185855
GPR35	ENSGALG00000005546	2.620583269
GPX7	ENSGALG00000010633	3.588262133
GTPBP8	ENSGALG00000015190	2.109192498
HHIPL1	ENSGALG00000011148	4.366191644
HIC2	ENSGALG00000001403	7.27980541
HLX	ENSGALG00000027554	2.704010002
HOMER2	ENSGALG00000006008	2.238729678
HSPB1	ENSGALG00000001926	2.563295346
IGF2	ENSGALG00000006555	2.582629281
IL15	ENSGALG00000009870	2.371391429
IL1RL2	ENSGALG00000016784	3.218722216
IQSEC1	ENSGALG00000005042	2.237588038
ITGB2	ENSGALG00000007511	2.12365685
JAM2	ENSGALG00000015746	2.556718106
JAM3	ENSGALG00000001472	5.665415182
KCTD14	ENSGALG00000017266	2.600795894
KIAA1161	ENSGALG00000005814	2.36111002
KIF3C	ENSGALG00000026973	2.923165642
KMO	ENSGALG00000007503	6.606353888
KYNU	ENSGALG00000012418	2.530235603
LAMA3	ENSGALG00000015056	3.078121415
LCAT	ENSGALG00000028928	5.157175475
LCT	ENSGALG00000012260	2.376153339
LGI2	ENSGALG00000028945	3.098630021
LYRM2	ENSGALG00000015762	2.136756125
MAP1A	ENSGALG00000008425	2.23846226
MAP1B	ENSGALG00000014999	4.17102957
MAP2K6	ENSGALG00000004370	2.865369609

Line 7_2 infected macrophages		
Gene	**Ensembl Gene ID**	**Fold Change**
MAP3K9	ENSGALG00000011008	2.290624759
MARVELD3	ENSGALG00000000882	4.106969992
MCM9	ENSGALG00000014883	2.163871722
MCMDC2	ENSGALG00000015526	5.534868238
MDM1	ENSGALG00000009905	2.209182435
MEF2C	ENSGALG00000014645	2.299681787
MND1	ENSGALG00000009212	3.993046652
MSC	ENSGALG00000019470	7.393650131
MTCL1	ENSGALG00000013357	2.378321146
MYCT1	ENSGALG00000013603	2.01206745
MYO10	ENSGALG00000012954	3.332734696
NCEH1	ENSGALG00000009170	2.127177057
NCKAP1	ENSGALG00000002750	2.325169544
NDRG4	ENSGALG00000000874	2.154684211
NEO1	ENSGALG00000001774	2.032750393
NHSL1	ENSGALG00000026388	2.38616603
NHSL2	ENSGALG00000028506	2.30848195
NT5M	ENSGALG00000004842	2.09394825
NTHL1	ENSGALG00000005617	2.512575778
NUDT15	ENSGALG00000016994	2.035045567
NUP210	ENSGALG00000005078	2.297325526
OSF-2	ENSGALG00000017046	3.536396883
P2RY13	ENSGALG00000010374	2.008564369
P2RY14	ENSGALG00000010380	2.612397981
PAG1	ENSGALG00000015758	3.037136371
PARD6B	ENSGALG00000007994	2.66316772
PARVG	ENSGALG00000014203	2.035043599
PATZ1	ENSGALG00000006934	3.365857826
PDGFC	ENSGALG00000009378	3.81349753
PHGDH	ENSGALG00000002988	8.230435015
PIWIL1	ENSGALG00000002645	2.252610305
PLCD4	ENSGALG00000003345	2.649349517
PLS1	ENSGALG00000002647	3.461525082
PON2	ENSGALG00000009689	3.071664185
PPAPDC3	ENSGALG00000018700	2.557407678
PPIC	ENSGALG00000005346	2.790484715
PRICKLE1	ENSGALG00000009556	2.292558682
PRMT8	ENSGALG00000013272	7.781317916
PSAP	ENSGALG00000004747	2.430919175
PTPN14	ENSGALG00000009784	2.939703975
PTPRG	ENSGALG00000007177	2.33074995
PTPRM	ENSGALG00000013902	8.402908144

Line 7_2 infected macrophages		
Gene	**Ensembl Gene ID**	**Fold Change**
PTX3	ENSGALG00000028284	3.135618705
PXDN	ENSGALG00000016377	2.863470942
PYGO1	ENSGALG00000004369	4.94905209
RAP1GAP2	ENSGALG00000005868	2.288083251
RARRES1	ENSGALG00000009594	2.15718124
RASSF8	ENSGALG00000014041	2.30040874
RIMS2	ENSGALG00000016074	2.842228852
SCML2	ENSGALG00000016537	2.518142196
SCN9A	ENSGALG00000027793	5.794355956
SDR9C7	ENSGALG00000026353	2.179627607
SERINC5	ENSGALG00000014798	2.38459441
SFT2D2	ENSGALG00000019228	2.273467666
SHC4	ENSGALG00000005011	2.065382859
SHISA9	ENSGALG00000002946	3.218896798
SHROOM3	ENSGALG00000011487	3.658144209
SLAMF1	ENSGALG00000006229	3.273106166
SLC11A1	ENSGALG00000011434	2.674946063
SLC12A2	ENSGALG00000014690	2.023693598
SLC13A3	ENSGALG00000004445	4.29513418
SLC16A9	ENSGALG00000003172	2.443230015
SLC1A6	ENSGALG00000000558	2.02395333
SLC23A1	ENSGALG00000011717	7.764930946
SLC2A11	ENSGALG00000006053	4.820204184
SLC35G1	ENSGALG00000027678	2.048617585
SLC39A10	ENSGALG00000007777	2.626997709
SLC47A1	ENSGALG00000021541	3.14460684
SORD	ENSGALG00000002317	3.133279802
SPECC1	ENSGALG00000004400	2.113303032
SPNS3	ENSGALG00000001410	5.221785782
SPON1	ENSGALG00000012027	2.983848873
SQRDL	ENSGALG00000005723	2.010400017
SRPK1	ENSGALG00000006544	3.328704878
STOX2	ENSGALG00000010646	2.899662063
STS	ENSGALG00000016622	56.78469533
STXBP4	ENSGALG00000003033	3.609754781
SYN2	ENSGALG00000004955	2.032059795
SYNM	ENSGALG00000007048	4.404670845
SYT8	ENSGALG00000006602	2.130803389
TBXAS1	ENSGALG00000012791	2.134254223
TCEANC	ENSGALG00000016581	6.440991004
TFPI	ENSGALG00000002594	10.86409282
THNSL2	ENSGALG00000015939	2.124080032

Line 7_2 infected macrophages		
Gene	**Ensembl Gene ID**	**Fold Change**
THSD1	ENSGALG00000017027	6.187235078
THSD4	ENSGALG00000004087	2.455470372
THY1	ENSGALG00000006751	3.211346775
TLR2B	ENSGALG00000009237	2.160125249
TMEM237	ENSGALG00000008381	2.256304766
TMEM242	ENSGALG00000013689	2.535126009
TMEM61	ENSGALG00000010801	4.588152654
TNFSF11	ENSGALG00000026163	2.924123432
TPTE2	ENSGALG00000017031	3.188251964
TRMT11	ENSGALG00000014831	2.191304036
TTBK2	ENSGALG00000009176	2.113799632
TUSC3	ENSGALG00000013674	4.658376226
URAHP	ENSGALG00000000549	2.058110576
USP13	ENSGALG00000008909	4.620459903
XYLT1	ENSGALG00000006757	2.45046257
YES1	ENSGALG00000014860	2.268606361
ZBTB40	ENSGALG00000004781	2.341049031
17.5	ENSGALG00000005183	3.066113076
Uncharacterised	ENSGALG00000020995	2.166029554
Uncharacterised	ENSGALG00000028509	2.239553003
Uncharacterised	ENSGALG00000028794	2.386081092
Uncharacterised	ENSGALG00000028298	2.960858814
Uncharacterised	ENSGALG00000016099	3.56102635
Uncharacterised	ENSGALG00000027045	8.751754006
Uncharacterised	ENSGALG00000027466	13.70587224
Uncharacterised	ENSGALG00000026489	382.9792573
Uncharacterised	ENSGALG00000028649	3.201264545
Uncharacterised	ENSGALG00000021451	5.898716014

Table S2.5: DE genes in line 6_1 control DCs.

Line 6_1 control DCs		
Gene	**Ensembl Gene ID**	**Fold Change**
ABAT	ENSGALG00000007334	4.362351
ABCB10	ENSGALG00000011096	2.241654
ABCB11	ENSGALG00000010891	3.526945
ACAD8	ENSGALG00000001557	2.460768
ACYP2	ENSGALG00000027632	3.969239
ADAMTS17	ENSGALG00000007069	3.535074
ALDH2	ENSGALG00000004725	2.367326
AMOTL2	ENSGALG00000006483	2.327923
ATP6V1E1	ENSGALG00000013036	2.66668
BCL2	ENSGALG00000012885	2.866962
BCL2A1	ENSGALG00000006511	2.14631
BIN1	ENSGALG00000011541	2.173061
C14orf159	ENSGALG00000010703	2.532588
C1orf123	ENSGALG00000026516	2.556338
C1orf216	ENSGALG00000002353	3.280162
C7orf50	ENSGALG00000004055	2.671745
C9orf91	ENSGALG00000007186	2.823948
CARTL	ENSGALG00000028845	3.092511
CCDC112	ENSGALG00000023042	2.766901
CCDC73	ENSGALG00000012103	3.521495
CCNJ	ENSGALG00000006955	4.153005
CD247	ENSGALG00000015441	3.252387
CD3D	ENSGALG00000007418	4.165199
CECR1	ENSGALG00000013031	2.114495
CLEC17A	ENSGALG00000026510	2.358043
CMTM7	ENSGALG00000011488	2.866281
CO6	ENSGALG00000002118	2.666077
COLEC12	ENSGALG00000014910	2.644773
COMTD1	ENSGALG00000005000	2.440063
CP	ENSGALG00000010434	2.836561
CXCR4	ENSGALG00000012357	5.728625
CYBRD1	ENSGALG00000026652	2.659156
CYP2U1	ENSGALG00000027908	2.795319
CYP2W1	ENSGALG00000004050	8.088998
CYP46A1	ENSGALG00000011162	2.725918
DBNDD1	ENSGALG00000000528	2.95906
DCXR	ENSGALG00000002849	2.683553
DERA	ENSGALG00000013095	2.787303
DIRC2	ENSGALG00000011679	2.347076
DNASE2	ENSGALG00000028790	2.44806

Line 6_1 control DCs		
Gene	**Ensembl Gene ID**	**Fold Change**
DOCK2	ENSGALG00000002080	2.124767
DZANK1	ENSGALG00000008731	3.019684
EFCAB1	ENSGALG00000009473	5.759721
EGLN1	ENSGALG00000011056	2.235434
EHBP1	ENSGALG00000008906	2.407525
EMP1	ENSGALG00000011803	2.192149
EP4	ENSGALG00000014824	4.027639
ESRRB	ENSGALG00000010365	4.16001
FAM134B	ENSGALG00000026200	3.873328
FAM169B	ENSGALG00000007016	2.7465
FAM180B	ENSGALG00000028710	4.304358
FANCA	ENSGALG00000000516	2.91829
FBP1	ENSGALG00000012613	2.959957
FUCA1	ENSGALG00000004112	2.462781
FUCA2	ENSGALG00000013773	2.240806
FZD10	ENSGALG00000002652	6.463517
GADD45B	ENSGALG00000028143	3.638979
GAL1	ENSGALG00000022815	24.16933
GAL2	ENSGALG00000016669	23.04836
GLDC	ENSGALG00000015053	3.322959
GLTP	ENSGALG00000019017	2.141519
GLUL	ENSGALG00000008518	2.303609
GOT1	ENSGALG00000007484	2.600721
GP1BB	ENSGALG00000021529	3.163247
GPD1	ENSGALG00000012061	5.046171
GPNMB	ENSGALG00000010949	3.288551
GPR157	ENSGALG00000002473	2.035751
GPR34	ENSGALG00000016227	2.577156
GPR35	ENSGALG00000005546	15.83732
GSTA3	ENSGALG00000016322	2.907114
GSTO1	ENSGALG00000008409	3.082421
GUK1	ENSGALG00000005336	2.055942
HAVCR1	ENSGALG00000017362	3.793223
HDAC11	ENSGALG00000005092	3.008842
HEXB	ENSGALG00000014933	2.700026
HEXDC	ENSGALG00000001612	2.383707
HOOK1	ENSGALG00000010889	2.709541
HPS3	ENSGALG00000010437	2.183508
HPSE	ENSGALG00000011203	2.276489
HYAL1	ENSGALG00000000785	2.306377
IDH1	ENSGALG00000008818	2.031954
IL12B	ENSGALG00000001409	6.354138

Line 6_1 control DCs		
Gene	**Ensembl Gene ID**	**Fold Change**
IL15	ENSGALG00000009870	2.645298
IL1R2	ENSGALG00000016782	4.361442
INPP5B	ENSGALG00000001606	2.598207
KCTD4	ENSGALG00000016975	2.643302
KCTD9	ENSGALG00000026855	3.665006
KNTC1	ENSGALG00000004515	4.610545
LAMTOR2	ENSGALG00000018760	2.150355
LECT2	ENSGALG00000006323	13.54734
LEFTY2	ENSGALG00000009256	11.89374
LGALS1	ENSGALG00000029043	3.393004
LINC00313	ENSGALG00000007526	4.315885
LIPA	ENSGALG00000023824	6.616439
LPAR5	ENSGALG00000014455	22.42557
LRRC32	ENSGALG00000004475	3.830536
MMEL1	ENSGALG00000001115	15.682
MMP13	ENSGALG00000017183	4.233303
MPHOSPH6	ENSGALG00000005477	2.476144
MPP2	ENSGALG00000002740	6.579817
MRRF	ENSGALG00000001333	2.272039
MYL12A	ENSGALG00000014852	2.23126
MYO16	ENSGALG00000016837	32.48761
NDUFS8	ENSGALG00000017675	2.346713
NHEJ1	ENSGALG00000011335	2.914904
NT5DC1	ENSGALG00000014964	3.870445
NTN3	ENSGALG00000029072	3.385016
OR8U1	ENSGALG00000003608	3.281856
ORC4	ENSGALG00000012448	2.00074
OSBPL1A	ENSGALG00000015086	2.592263
P4HA1	ENSGALG00000004325	2.075757
P4HTM	ENSGALG00000006937	2.016309
PADI3	ENSGALG00000000479	8.502655
PEX3	ENSGALG00000013777	2.203394
PGK1	ENSGALG00000007936	2.12676
PHYKPL	ENSGALG00000023920	4.106094
PIH1D3	ENSGALG00000004870	2.705887
PIM1	ENSGALG00000000742	2.059678
PLA2G7	ENSGALG00000016713	2.167974
PLTP	ENSGALG00000006894	4.357687
PNPLA8	ENSGALG00000009505	2.124734
PPAPDC1B	ENSGALG00000003268	2.558207
PPARGC1A	ENSGALG00000014398	19.36173
PRCP	ENSGALG00000017247	2.468665

Line 6_1 control DCs		
Gene	**Ensembl Gene ID**	**Fold Change**
PRODH	ENSGALG00000007728	3.184567
PTDSS2	ENSGALG00000004300	2.320722
PTPA	ENSGALG00000015995	2.221795
RAB33A	ENSGALG00000024049	4.068741
RABL2B	ENSGALG00000009770	2.494518
RAC2	ENSGALG00000012456	2.987144
RFFL	ENSGALG00000002225	2.234368
RHBDF1	ENSGALG00000007434	2.942536
RHBG	ENSGALG00000013232	2.471026
RHOU	ENSGALG00000025738	2.774213
RPAIN	ENSGALG00000001666	2.249619
RPLP1	ENSGALG00000016172	2.113429
RYBP	ENSGALG00000027845	2.380875
S100A13	ENSGALG00000013478	4.643169
S100A9	ENSGALG00000024272	37.15117
SCD	ENSGALG00000005739	3.951688
SFXN3	ENSGALG00000023621	2.355273
SLC15A1	ENSGALG00000016884	4.575215
SLC16A3	ENSGALG00000002728	2.10965
SLC24A4	ENSGALG00000010793	5.623099
SLC29A3	ENSGALG00000004585	2.06271
SLC48A1	ENSGALG00000018778	3.578205
SLC7A5	ENSGALG00000005845	2.446225
SNAPC5	ENSGALG00000007695	2.493589
SNAPIN	ENSGALG00000026796	2.010046
SOX5	ENSGALG00000021318	6.91782
SRGAP3	ENSGALG00000008378	6.547206
SULT2B1	ENSGALG00000027106	10.04862
SYTL2	ENSGALG00000014079	5.1697
TCN2	ENSGALG00000009536	2.08469
TESC	ENSGALG00000008206	19.50306
TEX264	ENSGALG00000003832	2.174396
TLCD1	ENSGALG00000003973	2.505061
TLR7	ENSGALG00000016590	3.167157
TM2D1	ENSGALG00000020614	2.252325
TMEM116	ENSGALG00000004760	5.885554
TMEM14A	ENSGALG00000019894	2.421552
TMEM186	ENSGALG00000027191	3.385683
TMEM233	ENSGALG00000020975	12.3687
TMEM55A	ENSGALG00000028264	2.287542
TNN	ENSGALG00000004538	7.080563
TPGS2	ENSGALG00000026547	2.222424

Line 6$_1$ control DCs		
Gene	**Ensembl Gene ID**	**Fold Change**
TPST2	ENSGALG00000005626	2.386787
TRABD	ENSGALG00000008705	2.471546
TRMT5	ENSGALG00000011904	2.13722
TTR	ENSGALG00000015143	2.936337
TTYH2	ENSGALG00000026940	2.005066
UACA	ENSGALG00000008143	2.444433
UQCRQ	ENSGALG00000007096	5.021424
VCAM1	ENSGALG00000005257	2.14985
ZNF395	ENSGALG00000016619	4.119581
ZNF518A	ENSGALG00000006966	2.107058
ZOV3	ENSGALG00000014877	4.488022
Uncharacterised	ENSGALG00000006003	2.766522
Uncharacterised	ENSGALG00000026436	5.692409
Uncharacterised	ENSGALG00000007320	8.938345
Uncharacterised	ENSGALG00000014551	2.049189
Uncharacterised	ENSGALG00000027621	2.039622
Uncharacterised	ENSGALG00000018386	2.024972

Table S2.6: DE genes in line 7_2 control DCs.

Line 7_2 control DCs		
Gene	**Ensembl Gene ID**	**Fold Change**
AAK1	ENSGALG00000025953	3.214161
AAK1	ENSGALG00000000019	2.82368
ABCC4	ENSGALG00000016896	3.220963
ACSL1	ENSGALG00000010628	2.28424
ACSS2	ENSGALG00000003362	2.194795
ADAM12	ENSGALG00000012740	5.166271
ADAMTS2	ENSGALG00000006000	3.333654
AKAP2	ENSGALG00000015656	2.441844
AKR	ENSGALG00000013072	4.11424
ALOX5	ENSGALG00000005857	2.516818
ANLN	ENSGALG00000012104	2.385838
ANTXR2	ENSGALG00000010892	3.055307
ANTXRL	ENSGALG00000005969	3.632429
AOX1	ENSGALG00000008185	3.027527
AP3B2	ENSGALG00000002136	4.835365
APBB2	ENSGALG00000014262	2.193241
APOBEC4	ENSGALG00000020926	8.661705
APOLD1	ENSGALG00000011784	3.931298
ARL16	ENSGALG00000019795	2.319814
ARNT2	ENSGALG00000006445	2.609273
ARVCF	ENSGALG00000002040	4.201827
ASB13	ENSGALG00000008401	2.915677
ASS1	ENSGALG00000023689	2.397823
ATF3	ENSGALG00000025887	3.401507
AVD	ENSGALG00000023622	6.607461
B3GNT5	ENSGALG00000008758	2.8124
BAFF	ENSGALG00000016852	2.328021
BARD1	ENSGALG00000003484	3.650705
BATF3	ENSGALG00000009816	3.30796
B-G	ENSGALG00000002102	2.530319
BRCA1	ENSGALG00000002781	2.532718
BUB1	ENSGALG00000008233	3.237123
C3H8ORF80	ENSGALG00000016572	2.079267
CA6	ENSGALG00000002390	5.212401
CALCRL	ENSGALG00000002632	3.064022
CAP2	ENSGALG00000012715	3.104264
CAV2	ENSGALG00000009396	4.792467
CCDC186	ENSGALG00000008956	2.091294
CCDC30	ENSGALG00000004878	4.168901
CCL4	ENSGALG00000000951	2.968543

Line 7_2 control DCs		
Gene	**Ensembl Gene ID**	**Fold Change**
CD2	ENSGALG00000015463	89.84604
CDC42BPA	ENSGALG00000009158	3.172591
CDR2	ENSGALG00000025743	4.465434
CDR2L	ENSGALG00000026295	5.141748
CEP135	ENSGALG00000013776	4.665311
CEP170	ENSGALG00000010733	2.026464
CEP170B	ENSGALG00000011639	3.89469
CFAP74	ENSGALG00000001288	3.579261
CHST3	ENSGALG00000024056	2.90404
CIDEC	ENSGALG00000026945	2.722033
CLSPN	ENSGALG00000002346	2.495311
CMPK2	ENSGALG00000028982	3.017821
CMYA5	ENSGALG00000026553	3.23926
COL27A1	ENSGALG00000006958	2.854133
COTL1	ENSGALG00000017644	2.0427
CRTAM	ENSGALG00000006527	3.450214
CSF1	ENSGALG00000028217	2.380597
CXorf21	ENSGALG00000016286	4.042675
DCN	ENSGALG00000011274	5.435235
DCSTAMP	ENSGALG00000016075	2.363014
DDX6	ENSGALG00000021251	2.070979
DGKD	ENSGALG00000001730	3.111149
DISP3	ENSGALG00000004662	3.519095
DLG3	ENSGALG00000005817	2.798845
DNER	ENSGALG00000002958	3.265334
DOC2B	ENSGALG00000004917	3.311658
DRAM1	ENSGALG00000012761	2.221845
E2F1	ENSGALG00000003045	2.030165
EHD4	ENSGALG00000008950	2.815592
EIF2AK2	ENSGALG00000010560	2.268471
EPAS1	ENSGALG00000010005	5.185308
EPB41L3	ENSGALG00000014770	3.46429
EPHA2	ENSGALG00000023768	3.654071
EPSTI1	ENSGALG00000016964	2.072505
EXOC3L1	ENSGALG00000011449	5.078498
FAM129A	ENSGALG00000004812	2.439999
FAM160A1	ENSGALG00000010090	5.182576
FAM92A1	ENSGALG00000015929	2.55281
FARP1	ENSGALG00000016886	2.361419
FGF14	ENSGALG00000016866	16.11005
FILIP1L	ENSGALG00000015271	3.512706
FKBP9	ENSGALG00000012193	2.007979

Line 7_2 control DCs		
Gene	**Ensembl Gene ID**	**Fold Change**
FLRT2	ENSGALG00000010589	2.944568
FLVCR1	ENSGALG00000009807	3.38302
FMNL2	ENSGALG00000012525	4.15545
FOXO6	ENSGALG00000026153	3.087849
FRMD4B	ENSGALG00000014627	2.132731
FST	ENSGALG00000014908	5.815029
GFPT2	ENSGALG00000013760	2.753026
GPR1	ENSGALG00000008589	3.312015
GPR64	ENSGALG00000016511	4.514469
GRIK1	ENSGALG00000015835	5.268596
HELZ2	ENSGALG00000006138	6.656276
HIVEP3	ENSGALG00000027365	2.707739
HSPA12A	ENSGALG00000009248	3.719682
ICA1	ENSGALG00000010708	3.233572
IFI27L2	ENSGALG00000021627	6.539193
IFIH1	ENSGALG00000011089	2.788292
IGSF1	ENSGALG00000026740	18.29941
IL13RA1	ENSGALG00000006032	3.03893
IL13RA2	ENSGALG00000020316	8.494457
IL20RA	ENSGALG00000013869	6.00459
INOS	ENSGALG00000005693	7.144601
INPPL1	ENSGALG00000004336	2.271568
IRF1	ENSGALG00000006785	2.676341
IRG1	ENSGALG00000016919	8.667193
ISG12(2)	ENSGALG00000013575	3.110708
ITGA2	ENSGALG00000014903	4.925297
ITGB3	ENSGALG00000000379	2.496299
ITPRIP	ENSGALG00000025780	4.033324
JAG1	ENSGALG00000009020	3.126474
KCNB2	ENSGALG00000022800	3.878832
KIF20B	ENSGALG00000006470	2.986937
KIF24	ENSGALG00000005806	3.043927
KIF4A	ENSGALG00000004195	2.223298
KLHL25	ENSGALG00000006826	2.838743
LACC1	ENSGALG00000016969	3.773694
LAMB1	ENSGALG00000007905	2.788371
LILRA6	ENSGALG00000027531	339.6525
LILRB3	ENSGALG00000029032	5.122908
LILRB4	ENSGALG00000027971	111.4473
LIMS1	ENSGALG00000016807	2.002092
LPIN2	ENSGALG00000014836	3.889093
LRCH2	ENSGALG00000005882	2.230532

Line 7_2 control DCs		
Gene	**Ensembl Gene ID**	**Fold Change**
LYZ	ENSGALG00000009963	10.99142
MAF	ENSGALG00000026258	3.330378
MAPK8IP1	ENSGALG00000008430	5.178984
MGLL	ENSGALG00000005990	6.85518
MLLT4	ENSGALG00000011329	5.717513
MOB3C	ENSGALG00000025946	2.326059
MSC	ENSGALG00000019470	2.906015
MTUS1	ENSGALG00000013615	2.944023
MX	ENSGALG00000016142	21.12414
MYCL	ENSGALG00000024047	2.947625
MYCT1	ENSGALG00000013603	2.080142
MYO10L	ENSGALG00000011172	4.623367
MYOM1	ENSGALG00000014847	3.275138
NCAPD3	ENSGALG00000001491	2.510597
NCF2	ENSGALG00000004700	2.317791
NECAB3	ENSGALG00000003065	2.637855
NRIP3	ENSGALG00000005903	6.850114
NRSN1	ENSGALG00000012670	5.269616
OAS*A	ENSGALG00000013723	3.14559
OSCAR	ENSGALG00000028805	2.444611
PALM	ENSGALG00000001846	3.559231
PARVA	ENSGALG00000005438	3.35183
PAX-6	ENSGALG00000012123	3.174655
PDE7B	ENSGALG00000013941	2.028292
PFKFB3	ENSGALG00000006324	2.681577
PGM2	ENSGALG00000000486	2.554383
PHLDB1	ENSGALG00000024033	2.130951
PHTF2	ENSGALG00000008335	2.649401
PID1	ENSGALG00000002963	2.492773
PIK3C2A	ENSGALG00000006121	2.035877
PIK3CG	ENSGALG00000008081	3.008285
PLA2G4A	ENSGALG00000005065	2.427602
PLACL2	ENSGALG00000011190	9.303286
PLAU	ENSGALG00000005086	3.724025
PLIN3	ENSGALG00000004157	3.023686
PPP1R3C	ENSGALG00000006670	7.221137
PPP1R9A	ENSGALG00000013233	2.500638
PSTPIP1	ENSGALG00000002786	2.273055
PSTPIP2	ENSGALG00000001745	4.165917
PTGS2	ENSGALG00000005069	8.067149
PTPN11	ENSGALG00000002005	2.219961
RAD54L	ENSGALG00000010356	3.12872

Line 7_2 control DCs		
Gene	**Ensembl Gene ID**	**Fold Change**
RANBP9	ENSGALG00000012696	2.287852
RBL1	ENSGALG00000001332	2.316836
RBM24	ENSGALG00000012712	3.277087
RGS2	ENSGALG00000002540	2.276782
RGSL1	ENSGALG00000003671	2.914143
RIF1	ENSGALG00000012484	2.238843
RSPO3	ENSGALG00000014829	7.163923
RTTN	ENSGALG00000013745	3.187675
SAMD9L	ENSGALG00000009479	4.165428
SCHIP1	ENSGALG00000009579	2.110766
SCN4B	ENSGALG00000007409	2.560368
SDC1	ENSGALG00000016480	2.173996
SEC24D	ENSGALG00000011998	2.082223
SEC61A1	ENSGALG00000005966	2.25264
SERPINE2	ENSGALG00000005135	2.307838
SH3KBP1	ENSGALG00000016420	2.170202
SH3PXD2A	ENSGALG00000008293	7.820266
SLBP	ENSGALG00000015712	4.656612
SLC17A9	ENSGALG00000028225	6.816613
SLC38A2	ENSGALG00000008497	2.410178
SLC39A6	ENSGALG00000013209	2.531121
SLC6A9	ENSGALG00000010098	2.401864
SNORD24	ENSGALG00000017870	3.5626
SNORD79	ENSGALG00000025527	7.089739
SNX10	ENSGALG00000011046	2.239761
SOGA1	ENSGALG00000003409	2.33502
ST6GALNAC2	ENSGALG00000006900	2.117608
STAG1	ENSGALG00000001277	2.215526
STK35	ENSGALG00000026301	2.927718
STXBP6	ENSGALG00000009847	2.396172
SYNJ2	ENSGALG00000013727	2.704691
TAAR1	ENSGALG00000013994	5.034264
TAPBPL	ENSGALG00000014428	2.00434
TARM1	ENSGALG00000028728	11.00142
TARM1	ENSGALG00000027348	5.221175
TBR1	ENSGALG00000011122	5.407805
TES	ENSGALG00000009398	2.029989
TGM2	ENSGALG00000006775	2.573378
TLN2	ENSGALG00000003628	2.035472
TMEM52	ENSGALG00000001304	2.446235
TNIP3	ENSGALG00000011961	18.00498
TOP2A	ENSGALG00000003922	2.547953

Line 7_2 control DCs		
Gene	**Ensembl Gene ID**	**Fold Change**
TOR1A	ENSGALG00000023709	4.283338
TRAF1	ENSGALG00000001583	2.976682
TRAF2	ENSGALG00000009014	2.858458
TRAF3	ENSGALG00000011389	2.377828
TRAIP	ENSGALG00000002908	2.743527
TRANK1	ENSGALG00000012057	2.359156
TRIB2	ENSGALG00000016457	2.607396
TSPAN5	ENSGALG00000012227	3.266713
TXNRD1	ENSGALG00000012714	2.277849
UBE2O	ENSGALG00000001971	2.242399
UBE3C	ENSGALG00000006461	2.424335
UCH-L1	ENSGALG00000014261	20.02871
UCK2	ENSGALG00000003510	2.596183
USP54	ENSGALG00000005232	2.419621
VNN1	ENSGALG00000013993	2.814097
WBSCR16	ENSGALG00000001174	3.032102
WFS1	ENSGALG00000015529	2.085233
ZDHHC20	ENSGALG00000017126	2.256786
ZFP92	ENSGALG00000015459	2.336782
ZNF488	ENSGALG00000026560	6.084261
Uncharacterised	ENSGALG00000005720	5.771738
Uncharacterised	ENSGALG00000028525	7.944605
Uncharacterised	ENSGALG00000028022	4.764888
Uncharacterised	ENSGALG00000027396	4.988047
Uncharacterised	ENSGALG00000028509	3.569299
Uncharacterised	ENSGALG00000027271	15.14941

Table S2.7: DE genes in line 6_1 infected DCs.

Line 6_1 infected DCs		
Gene	**Ensembl Gene ID**	**Fold Change**
AADACL2	ENSGALG00000010364	2.06318
AATK	ENSGALG00000006901	3.775925
ABCA1	ENSGALG00000015433	2.251189
ABCA2	ENSGALG00000001226	2.9117
ACTG2	ENSGALG00000006343	2.502703
ADAM15	ENSGALG00000017301	3.084329
ADAM28	ENSGALG00000000357	2.349058
ADAM33	ENSGALG00000016038	2.735453
ADAM8	ENSGALG00000003437	2.33543
ADAMTS20	ENSGALG00000009572	32.08151
ADAMTS4	ENSGALG00000026124	5.305531
ADAMTSL3	ENSGALG00000006104	2.341151
ADM	ENSGALG00000005666	2.205009
AEBP1	ENSGALG00000026047	2.527818
AEBP1	ENSGALG00000028533	2.295753
AHR	ENSGALG00000004322	3.81857
AMH	ENSGALG00000024368	2.047903
ANG	ENSGALG00000003196	2.54811
ANGPTL1	ENSGALG00000004290	4.622687
ANGPTL4	ENSGALG00000000619	2.945939
AQP1	ENSGALG00000005209	3.05925
ARHGEF10L	ENSGALG00000000449	2.941319
ARHGEF17	ENSGALG00000017326	3.017314
ARHGEF6	ENSGALG00000001894	6.102023
ARR3	ENSGALG00000004251	4.180882
ARRDC2	ENSGALG00000003527	2.970251
ARSI	ENSGALG00000005616	3.35109
ASAP3	ENSGALG00000029131	5.625763
ATHL1	ENSGALG00000004234	2.140033
AZIN2	ENSGALG00000003614	2.018402
BCAN	ENSGALG00000013237	2.919479
BDKRB1	ENSGALG00000020386	3.159899
BDKRB2	ENSGALG00000011080	2.608207
BEST1	ENSGALG00000007217	2.877149
BEST4	ENSGALG00000010126	4.422654
BMPER	ENSGALG00000012184	3.609248
BSN	ENSGALG00000001849	2.275616
BUD13	ENSGALG00000025882	3.126735
C1orf109	ENSGALG00000021645	4.59533
C1R	ENSGALG00000014659	2.207933

Line 6$_1$ infected DCs		
Gene	**Ensembl Gene ID**	**Fold Change**
CABYR	ENSGALG00000015076	2.824065
CACNA1E	ENSGALG00000003833	2.850454
CALD1	ENSGALG00000013071	3.419258
CAMK1G	ENSGALG00000001319	4.141536
CAPN6	ENSGALG00000008006	4.211775
CARD11	ENSGALG00000004398	2.185161
CBFA2T3	ENSGALG00000006234	2.52105
CCDC69	ENSGALG00000004354	2.22586
CCL1	ENSGALG00000002329	3.196265
CCLI10	ENSGALG00000014585	2.130617
CD164	ENSGALG00000015238	2.089832
CD180	ENSGALG00000023411	5.63282
CD200	ENSGALG00000027419	3.064961
CD40	ENSGALG00000007015	2.153177
CD72	ENSGALG00000002383	4.246101
CDC42EP1	ENSGALG00000026968	3.529627
CDKN2A	ENSGALG00000025805	3.749273
CDKN2B	ENSGALG00000026137	7.751854
CERCAM	ENSGALG00000004986	3.567019
CFTII	ENSGALG00000009046	2.64833
CHB1	ENSGALG00000005194	6.850073
CHRD	ENSGALG00000026983	2.455968
CISH	ENSGALG00000002260	3.86852
CKV1.1	ENSGALG00000000447	2.960743
CLMP	ENSGALG00000006507	3.007638
CNTF	ENSGALG00000026207	4.241655
COL12A1	ENSGALG00000015908	2.921718
COL16A1	ENSGALG00000026836	3.390311
COL18A1	ENSGALG00000004338	2.759308
COL1A1	ENSGALG00000023973	2.492793
COL1A2	ENSGALG00000009641	2.831143
COL25A1	ENSGALG00000010521	4.146638
COL3A1	ENSGALG00000002552	3.567479
COL5A1	ENSGALG00000002546	2.14859
COL6A1	ENSGALG00000005974	4.940321
COL6A2	ENSGALG00000006126	3.959898
COL6A3	ENSGALG00000003923	4.147334
COL7A1	ENSGALG00000005811	8.312927
COL9A2	ENSGALG00000027526	2.081889
CORO2A	ENSGALG00000001933	3.243526
CPNE4	ENSGALG00000011613	3.563191
CPNE7	ENSGALG00000000507	4.42526

Line 6$_1$ infected DCs		
Gene	**Ensembl Gene ID**	**Fold Change**
CR1L	ENSGALG00000023950	2.428168
CREB3L1	ENSGALG00000008393	2.231926
CROCC	ENSGALG00000027085	2.291571
CSF1R	ENSGALG00000005725	2.044342
CSF2RB	ENSGALG00000012518	2.166307
CSPG4	ENSGALG00000002678	4.947558
CTGF	ENSGALG00000002909	2.564298
CTSB	ENSGALG00000016666	2.282516
CUBN	ENSGALG00000008704	2.304798
CUTA	ENSGALG00000001620	2.450585
CX3CL1	ENSGALG00000026663	2.607379
CXCL12	ENSGALG00000028136	2.280116
DAB2	ENSGALG00000003803	2.134187
DAK	ENSGALG00000028767	2.004198
DAPK2	ENSGALG00000026070	2.391981
DBN1	ENSGALG00000026644	3.89009
DCHS1	ENSGALG00000017334	2.221799
DDX25	ENSGALG00000000463	2.58488
DDX60	ENSGALG00000009639	5.457969
DNAH17	ENSGALG00000007106	2.583594
DOCK2	ENSGALG00000025829	2.13143
DSG4	ENSGALG00000017398	5.923493
DYSF	ENSGALG00000016105	2.009864
ELFN1	ENSGALG00000004209	2.47501
EMILIN2	ENSGALG00000014815	2.74481
ENPP1	ENSGALG00000002896	3.87435
ENPP3	ENSGALG00000002869	3.123562
EPHA1	ENSGALG00000014687	2.817383
ERBB2	ENSGALG00000018828	2.264386
EX-FABP	ENSGALG00000024011	10.82013
F2RL2	ENSGALG00000023379	2.33234
FAM178B	ENSGALG00000028532	2.488818
FAM181B	ENSGALG00000022713	4.006557
FAM188B	ENSGALG00000023497	2.809656
FAM19A3	ENSGALG00000026585	4.565765
FAM78A	ENSGALG00000003789	2.010868
FBN1	ENSGALG00000004960	2.913064
FBN3	ENSGALG00000000327	5.080241
FCRL2	ENSGALG00000010507	3.45544
FES	ENSGALG00000008340	2.126706
FGFRL1	ENSGALG00000015725	2.518049
FKBP10	ENSGALG00000025764	2.926101

Line 6$_1$ infected DCs		
Gene	**Ensembl Gene ID**	**Fold Change**
FN1	ENSGALG00000003578	2.525055
FOLH1	ENSGALG00000017234	4.521771
FZD1	ENSGALG00000009064	2.014369
FZD2	ENSGALG00000008433	2.264741
G0S2	ENSGALG00000023933	4.514382
GAP43	ENSGALG00000015089	5.683525
GDPGP1	ENSGALG00000023246	2.108858
GEM	ENSGALG00000015954	3.865244
GFI1	ENSGALG00000005940	3.02677
gga-mir-3064	ENSGALG00000027517	2.589515
GGT5	ENSGALG00000006501	2.316257
GJA1	ENSGALG00000014873	2.54229
GPR27	ENSGALG00000027091	3.27862
GPR39	ENSGALG00000012171	3.385635
GVINP1	ENSGALG00000016556	2.877879
GZMA	ENSGALG00000013548	30.53686
HAS2	ENSGALG00000016394	3.18276
HDC	ENSGALG00000023436	2.250255
HLX	ENSGALG00000027554	2.638167
HPGD	ENSGALG00000010769	2.293296
HSD11B1	ENSGALG00000028858	6.197842
HSPB7	ENSGALG00000023772	2.386985
HTRA3	ENSGALG00000015575	3.491413
ID1	ENSGALG00000006210	2.128278
IFITM5	ENSGALG00000004239	2.207587
IGFBP4	ENSGALG00000028931	3.70241
IGFBP5	ENSGALG00000011468	4.483867
IL17RC	ENSGALG00000028970	2.208836
IL17RE	ENSGALG00000029177	2.108406
IL1B	ENSGALG00000000534	3.459698
IL1RL1	ENSGALG00000016785	3.974019
IL22RA1	ENSGALG00000004221	3.230995
IL6	ENSGALG00000010915	5.051559
INSRR	ENSGALG00000013253	4.867462
IRF-3	ENSGALG00000014297	2.075582
ISLR	ENSGALG00000021525	5.915629
ISLR2	ENSGALG00000029151	2.435596
ITGA11	ENSGALG00000008007	2.287078
ITGB5	ENSGALG00000011778	2.355724
JAK3	ENSGALG00000028085	2.140763
JSC	ENSGALG00000006346	3.554703
KANK3	ENSGALG00000000621	2.984422

Line 6$_1$ infected DCs		
Gene	**Ensembl Gene ID**	**Fold Change**
KANK4	ENSGALG00000010953	2.649729
KCNA4	ENSGALG00000012142	2.08187
KCTD3	ENSGALG00000009678	2.056386
KDELR3	ENSGALG00000012251	2.075624
KIF26A	ENSGALG00000011581	4.968181
KIR3DL3	ENSGALG00000018535	2.184211
KLF2	ENSGALG00000003939	2.839389
KLHDC8A	ENSGALG00000000684	3.046614
KLRG2	ENSGALG00000029035	4.397498
KREMEN1	ENSGALG00000005808	2.495434
LAMB3	ENSGALG00000001343	3.594461
LAMC2	ENSGALG00000004627	2.210837
LAMP3	ENSGALG00000008759	3.381034
LAMP5	ENSGALG00000008918	2.613694
LDLRAD1	ENSGALG00000020647	2.827957
LEPREL2	ENSGALG00000014490	4.568767
LEPREL4	ENSGALG00000027462	3.685885
LIF	ENSGALG00000008028	2.096912
LINGO1	ENSGALG00000002708	2.65109
LIPA	ENSGALG00000006378	2.063888
LIPI	ENSGALG00000015662	3.30116
LMCD1	ENSGALG00000008349	2.79749
LMO7	ENSGALG00000016920	2.540879
LMOD1	ENSGALG00000028721	3.369962
LOX	ENSGALG00000028063	3.323812
LOXL1	ENSGALG00000028247	2.036057
LOXL3	ENSGALG00000013254	2.34276
LPAR4	ENSGALG00000001701	2.38158
LRRC32	ENSGALG00000000818	2.43629
LRRC4	ENSGALG00000029160	3.144886
LSAMP	ENSGALG00000015087	2.241065
LTBP1	ENSGALG00000010448	2.202396
MADCAM1	ENSGALG00000028341	2.012223
MADPRT	ENSGALG00000000871	7.998343
MALL	ENSGALG00000023882	2.756876
MALT1	ENSGALG00000027961	2.274118
MAP3K12	ENSGALG00000026931	2.557896
MAPKAPK3	ENSGALG00000002283	2.416673
MCAM	ENSGALG00000006764	3.410349
MCF2L	ENSGALG00000016834	2.376608
MECOM	ENSGALG00000009437	2.037626
MED12L	ENSGALG00000010370	2.643939

Line 6₁ infected DCs		
Gene	**Ensembl Gene ID**	**Fold Change**
MEI1	ENSGALG00000011919	2.181186
MFAP2	ENSGALG00000027326	3.077756
MORN5	ENSGALG00000001352	6.814699
MPEG1	ENSGALG00000028536	2.255142
MPL	ENSGALG00000009965	3.034763
MPZL2	ENSGALG00000007412	2.643982
MR1	ENSGALG00000027693	3.300106
MRC1	ENSGALG00000028304	3.373405
MRC2	ENSGALG00000000461	3.279484
MRGPRX4	ENSGALG00000022324	2.232936
MRVI1	ENSGALG00000005632	2.545218
MT4	ENSGALG00000028451	2.27103
MT-ATP6	ENSGALG00000018368	2.146851
MTCL1	ENSGALG00000013357	2.043254
MTMR11	ENSGALG00000013350	3.456883
MT-ND4	ENSGALG00000018364	2.123227
MTSS1L	ENSGALG00000002467	2.866614
MXD1	ENSGALG00000013882	2.597616
MYL9	ENSGALG00000028567	2.01545
MYO1F	ENSGALG00000001571	2.288433
NANOS1	ENSGALG00000027980	2.418836
NARF	ENSGALG00000001603	2.066905
NCX1	ENSGALG00000008544	3.456327
NDNF	ENSGALG00000011962	3.081744
NDRG4	ENSGALG00000000874	2.023554
NEURL	ENSGALG00000008281	2.03377
NEURL1B	ENSGALG00000002846	2.163666
NFKBIZ	ENSGALG00000015346	2.105613
NOX4	ENSGALG00000017235	3.734981
NR4A3	ENSGALG00000013568	2.788466
NRP2	ENSGALG00000008621	2.923782
NT5E	ENSGALG00000015833	7.013233
NTM	ENSGALG00000001437	5.317819
NUMA1	ENSGALG00000001258	2.022952
NXPH2	ENSGALG00000029083	4.168325
ODZ2	ENSGALG00000001768	4.588546
OLFML2B	ENSGALG00000002667	2.325267
OMG	ENSGALG00000005594	2.295309
OSBPL10	ENSGALG00000011474	2.001044
P2RY12	ENSGALG00000010373	2.764976
P2RY13	ENSGALG00000010374	3.30708
P2RY2	ENSGALG00000017328	3.326679

Line 6$_1$ infected DCs		
Gene	**Ensembl Gene ID**	**Fold Change**
P4HA3	ENSGALG00000017311	2.60875
PAPPA2	ENSGALG00000004487	10.89811
PASD1	ENSGALG00000009063	2.622027
PCBP4	ENSGALG00000026397	3.21335
PCBP4	ENSGALG00000027695	2.669511
PCSK6	ENSGALG00000007238	2.822889
PCTP	ENSGALG00000003099	2.287935
PDGFRA	ENSGALG00000013929	2.433223
PDGFRB	ENSGALG00000021313	3.494216
PDLIM4	ENSGALG00000027627	2.734812
PERP	ENSGALG00000027207	2.18308
PHF7	ENSGALG00000001908	4.209984
PITPNM1	ENSGALG00000013185	2.518751
PLCD3	ENSGALG00000025771	2.094803
PLCD4	ENSGALG00000003345	2.332239
PLVAP	ENSGALG00000026147	3.188199
PLXDC1	ENSGALG00000023881	3.949544
PLXDC2	ENSGALG00000007956	2.349154
PLXNA2	ENSGALG00000001264	3.800204
PML	ENSGALG00000001478	2.809481
PPAP2C	ENSGALG00000026834	2.120839
PRELP	ENSGALG00000003551	2.539896
PROK2	ENSGALG00000007785	4.247384
PRRX1	ENSGALG00000003324	2.272129
PRRX2	ENSGALG00000028236	3.946995
PRSS35	ENSGALG00000015847	2.598932
PSMD4	ENSGALG00000028505	5.027432
PTGS1	ENSGALG00000001314	2.514512
PTX3	ENSGALG00000028284	6.444192
PVALB1	ENSGALG00000012522	2.760439
QPCT	ENSGALG00000010617	2.227785
RASGRP3	ENSGALG00000010435	2.079309
RGPD1	ENSGALG00000013985	65.84136
RGS13	ENSGALG00000026810	2.49157
RNF144A	ENSGALG00000028709	2.97246
RNF213	ENSGALG00000006988	2.329437
RPS6KA2	ENSGALG00000011473	2.430233
RSFR	ENSGALG00000027165	2.030674
RTN4RL2	ENSGALG00000023441	2.121126
RUFY4	ENSGALG00000025739	2.205498
RUNX2	ENSGALG00000026484	2.070984
S100A11	ENSGALG00000009163	2.086163

Line 6l infected DCs		
Gene	**Ensembl Gene ID**	**Fold Change**
SATB1	ENSGALG00000011254	3.65688
SCARA3	ENSGALG00000026651	2.733364
SCARNA7	ENSGALG00000025666	2.531302
SDK2	ENSGALG00000004464	3.533188
SEMA3B	ENSGALG00000013722	3.294215
SEPT4	ENSGALG00000028193	2.270539
SERPINF2	ENSGALG00000002987	2.605163
SERPING1	ENSGALG00000007381	2.508244
SERPINH1	ENSGALG00000011214	2.981399
SFRP4	ENSGALG00000012073	2.498264
SH3RF2	ENSGALG00000007415	8.383473
SHANK2	ENSGALG00000026110	2.184718
SHROOM4	ENSGALG00000027208	2.411571
SIGLEC1	ENSGALG00000028510	27.87116
SIGLEC15	ENSGALG00000021416	6.190811
SIRPA	ENSGALG00000006152	2.288473
SLAMF1	ENSGALG00000024118	2.616391
SLC10A4	ENSGALG00000014108	2.388347
SLC18A2	ENSGALG00000009289	2.408956
SLC38A4	ENSGALG00000009730	2.481271
SLC39A10	ENSGALG00000007777	2.224507
SLC43A2	ENSGALG00000002783	2.361197
SLC4A11	ENSGALG00000016017	8.398968
SLC9A5	ENSGALG00000007867	2.252328
SNAI2	ENSGALG00000015241	3.224584
SOCS1	ENSGALG00000007158	2.376085
SOCS3	ENSGALG00000027786	2.330686
SPON2	ENSGALG00000027109	3.090293
SRPX2	ENSGALG00000006796	2.710535
ST3GAL1	ENSGALG00000016210	2.010203
ST8SIA6	ENSGALG00000008671	2.451565
STAB1	ENSGALG00000001535	2.500814
STON2	ENSGALG00000010579	2.288269
SYDE1	ENSGALG00000026662	2.096622
SYNE2	ENSGALG00000011811	2.2916
SYNGR3	ENSGALG00000005589	2.088913
SYNPO	ENSGALG00000027330	2.77896
SYT8	ENSGALG00000006602	2.75983
SYTL4	ENSGALG00000006786	2.871941
TAGLN	ENSGALG00000011902	2.155361
TAP1	ENSGALG00000026269	2.01572
TBX3	ENSGALG00000008250	3.217643

Line 6$_1$ infected DCs		
Gene	**Ensembl Gene ID**	**Fold Change**
TESK1	ENSGALG00000027658	3.132473
TEX33	ENSGALG00000012490	8.467017
TGFB2	ENSGALG00000009612	2.734592
TGFBI	ENSGALG00000006319	2.775837
TIMP3	ENSGALG00000012568	3.387488
TLE1	ENSGALG00000026521	4.602383
TLE3	ENSGALG00000008120	3.047333
TLL1	ENSGALG00000009567	2.94316
TLL2	ENSGALG00000005519	3.483
TLR21	ENSGALG00000000774	2.33597
TLR2B	ENSGALG00000009239	2.094941
TMEM119	ENSGALG00000004893	2.58738
TMEM132A	ENSGALG00000003332	2.481927
TMEM132D	ENSGALG00000002671	2.147958
TMEM173	ENSGALG00000000852	2.634185
TMEM178A	ENSGALG00000028327	3.429086
TMEM178B	ENSGALG00000028444	2.647493
TMEM196	ENSGALG00000010865	2.130155
TMEM26	ENSGALG00000025862	3.049727
TMEM71	ENSGALG00000019426	2.024014
TNC	ENSGALG00000007113	2.134109
TNFAIP2	ENSGALG00000011446	2.720546
TNFIP6	ENSGALG00000012481	4.81799
TNFRSF11B	ENSGALG00000016114	4.642501
TNFRSF6B	ENSGALG00000006106	9.001829
TNNC1	ENSGALG00000001459	2.728508
TRAF3IP3	ENSGALG00000001373	2.363328
TRIM62	ENSGALG00000028437	2.055228
TRIM71	ENSGALG00000019622	2.408718
TSPAN15	ENSGALG00000004257	2.657924
TWIST1	ENSGALG00000026059	2.322944
VANGL2	ENSGALG00000024120	2.198111
VASN	ENSGALG00000007807	2.454177
VPS9D1	ENSGALG00000023468	2.220398
VSIG4	ENSGALG00000020326	2.20509
VTCN1	ENSGALG00000016211	2.208065
VTN	ENSGALG00000003589	2.963966
VWA5B2	ENSGALG00000028294	2.862563
WFDC1	ENSGALG00000005503	2.489335
WSCD2	ENSGALG00000004849	3.267168
XYLT1	ENSGALG00000006757	2.036287
YIPF6	ENSGALG00000004252	2.817773

Line 6$_1$ infected DCs		
Gene	**Ensembl Gene ID**	**Fold Change**
ZNF330	ENSGALG00000009868	2.123302
ZNF414	ENSGALG00000024378	2.570855
ZNF521	ENSGALG00000015112	2.167128
ZSCAN2	ENSGALG00000027097	4.008998
Uncharacterised	ENSGALG00000005873	3.083482
Uncharacterised	ENSGALG00000026220	488.8789
Uncharacterised	ENSGALG00000026256	13.5234
Uncharacterised	ENSGALG00000016484	9.557921
Uncharacterised	ENSGALG00000001629	4.01839
Uncharacterised	ENSGALG00000028016	3.903504
Uncharacterised	ENSGALG00000028922	3.718273
Uncharacterised	ENSGALG00000019325	3.46194
Uncharacterised	ENSGALG00000025973	2.91668
Uncharacterised	ENSGALG00000015276	2.786033
Uncharacterised	ENSGALG00000000819	2.606666
Uncharacterised	ENSGALG00000018781	2.571815
Uncharacterised	ENSGALG00000019932	2.559414
Uncharacterised	ENSGALG00000008629	2.4159
Uncharacterised	ENSGALG00000013973	2.387016
Uncharacterised	ENSGALG00000025728	2.245786
Uncharacterised	ENSGALG00000004854	2.220158
Uncharacterised	ENSGALG00000027352	2.217018
Uncharacterised	ENSGALG00000003670	2.184214
Uncharacterised	ENSGALG00000028182	2.136117
Uncharacterised	ENSGALG00000013542	2.018937

Table S2.8: DE genes in line 7_2 infected DCs.

Line 7_2 infected DCs		
Gene	**Ensembl Gene ID**	**Fold Change**
ADH1C	ENSGALG00000012250	2.331773
AKAP6	ENSGALG00000009995	2.302729
ALKBH8	ENSGALG00000017170	2.049126
APOA1	ENSGALG00000007114	13.44605
AREG	ENSGALG00000010866	2.423714
ARL5B	ENSGALG00000008557	2.752462
ATP5J	ENSGALG00000015751	2.260805
C6orf58	ENSGALG00000014823	2.020697
CCNE2	ENSGALG00000015985	2.60047
CCSAP	ENSGALG00000011084	2.034743
CCSER1	ENSGALG00000010392	2.777602
CD320	ENSGALG00000021688	2.87104
CDKN3	ENSGALG00000012220	2.051264
CELF3	ENSGALG00000028478	2.644073
CENPK	ENSGALG00000014753	2.142904
CENPL	ENSGALG00000026825	2.156348
CGNL1	ENSGALG00000004294	5.82571
CHIA	ENSGALG00000023760	3.767571
CHTL1A	ENSGALG00000007174	4.49272
CLCN4	ENSGALG00000016607	3.046699
COL14A1	ENSGALG00000016411	4.321688
CST7	ENSGALG00000008660	2.1898
CYB5A	ENSGALG00000013708	2.326181
DACH1	ENSGALG00000016933	2.355691
DAK	ENSGALG00000005961	2.159722
DMC1	ENSGALG00000012236	6.410244
DNAI2	ENSGALG00000004495	3.930177
ECHDC1	ENSGALG00000014828	2.77296
EFCAB3	ENSGALG00000000382	3.033619
ELOVL6	ENSGALG00000012131	2.00699
ELOVL7	ENSGALG00000014730	2.338781
EPHA5	ENSGALG00000011680	3.299416
FAM13C	ENSGALG00000001825	3.666876
FAM161A	ENSGALG00000008810	2.176809
FAM175A	ENSGALG00000011210	2.555401
FBXL2	ENSGALG00000011975	2.344007
FILIP1	ENSGALG00000015903	2.182781
GALNTL4	ENSGALG00000005584	3.512756
GIMAP2	ENSGALG00000029112	2.382143
GLT1D1	ENSGALG00000002679	2.449182

Line 7_2 infected DCs		
Gene	**Ensembl Gene ID**	**Fold Change**
GMNN	ENSGALG00000013626	3.130713
GPR132	ENSGALG00000027407	2.480896
GPR37	ENSGALG00000027861	6.240084
HCN4	ENSGALG00000001764	5.468598
IQCK	ENSGALG00000028197	2.170153
JAG2	ENSGALG00000011696	2.939021
KIF21A	ENSGALG00000007098	2.275882
KLF15	ENSGALG00000006245	2.747173
LEF1	ENSGALG00000010529	3.092974
LGI2	ENSGALG00000028945	5.783854
LILRA3	ENSGALG00000028229	2.729724
LRP8	ENSGALG00000010692	2.304365
LY6E	ENSGALG00000025879	3.197661
MAMDC2	ENSGALG00000015115	2.715423
MAPK12	ENSGALG00000019384	2.116528
MCM9	ENSGALG00000014883	2.111067
MCMDC2	ENSGALG00000015526	5.953758
MED30	ENSGALG00000026340	2.345239
MR1	ENSGALG00000027045	41.44911
MRPS33	ENSGALG00000028879	2.078087
MVK	ENSGALG00000027759	2.547073
MYH13	ENSGALG00000000779	7.006279
MYH1G	ENSGALG00000028612	2.588246
NEGR1	ENSGALG00000011350	4.732262
NMRK2	ENSGALG00000025751	4.073974
NOG	ENSGALG00000003114	2.101714
NRN1	ENSGALG00000028813	3.133779
NSG1	ENSGALG00000015010	2.959432
NUBPL	ENSGALG00000009983	2.015691
PDE6C	ENSGALG00000006626	2.712235
PHGDH	ENSGALG00000002988	2.470862
PLCL1	ENSGALG00000008113	2.076025
PLS1	ENSGALG00000002647	4.211592
PODXL	ENSGALG00000006409	3.285219
PROSER2	ENSGALG00000006700	2.342766
PRSS23	ENSGALG00000017244	2.260082
PYGO1	ENSGALG00000004369	15.06014
RDH10	ENSGALG00000026505	2.103382
RHPN1	ENSGALG00000016143	2.568768
RPL14	ENSGALG00000011523	2.266084
RPP30	ENSGALG00000006486	2.111477
RPS21	ENSGALG00000005338	2.041015

Line 7_2 infected DCs		
Gene	**Ensembl Gene ID**	**Fold Change**
S100A10	ENSGALG00000028774	2.318623
SALL3	ENSGALG00000012657	2.366587
SBSPON	ENSGALG00000015634	9.63557
SEC61G	ENSGALG00000013107	2.245488
SESN3	ENSGALG00000017204	2.210621
SETD4	ENSGALG00000016024	3.503497
SETD6	ENSGALG00000028890	2.850795
SH3BGRL2	ENSGALG00000015877	8.648823
SHISA9	ENSGALG00000002946	2.139714
SIPA1L2	ENSGALG00000011025	2.328392
SKIDA1	ENSGALG00000017395	2.307617
SLC13A3	ENSGALG00000004445	2.212562
SLC25A15	ENSGALG00000017032	2.576981
SLC2A5	ENSGALG00000002466	2.073321
SLC44A5	ENSGALG00000011379	3.950476
SNORA68	ENSGALG00000025464	3.11009
SPAG6	ENSGALG00000007892	2.176209
SRD5A1	ENSGALG00000013063	2.902929
SSX2IP	ENSGALG00000008763	2.442534
STS	ENSGALG00000016622	18.18441
STXBP4	ENSGALG00000003033	3.642529
SULT4A1	ENSGALG00000014189	2.271469
TCEANC	ENSGALG00000016581	2.530349
TMCC3	ENSGALG00000011320	2.37792
TMEM169	ENSGALG00000011493	2.869265
TNFSF11	ENSGALG00000026163	11.69926
TPTE2	ENSGALG00000017031	2.152685
TREM-A1	ENSGALG00000023781	4.559349
TSPAN12	ENSGALG00000009029	2.123325
TSPAN13	ENSGALG00000027240	2.375663
TUBA3E	ENSGALG00000010439	2.558806
U3	ENSGALG00000025958	3.14576
UBXN2B	ENSGALG00000015431	2.036169
UCHL5	ENSGALG00000002524	2.197277
UTP23	ENSGALG00000016120	2.366037
WNT9A	ENSGALG00000005401	3.409731
ZNF800	ENSGALG00000028694	2.927765
Uncharacterised	ENSGALG00000002923	2.240975
Uncharacterised	ENSGALG00000026584	5.005097
Uncharacterised	ENSGALG00000025939	7.802344

Appendix 3

MDV QTL candidate gene lists

Table S3.1: Line 6_1 control macrophages.

Line 6_1 control macrophages				
Gene	**QTL**	**Chr.**	**Fold Change**	**Ensembl Gene ID**
AAED1	MD25-30	Z	4	ENSGALG00000012624
AGTPBP1	MD25-30	Z	3	ENSGALG00000012595
ARSB	MD25-30	Z	3	ENSGALG00000004438
AUH	MD25-30	Z	2	ENSGALG00000021843
BCL2	MD16-17	2	4	ENSGALG00000012885
BLNK	MD22	6	2	ENSGALG00000006973
CD247	MD1	1	3	ENSGALG00000015441
CDC14B	MD25-30	Z	2	ENSGALG00000012627
CNNM1	MD22	6	2	ENSGALG00000007489
COL4A3BP	MD25-30	Z	2	ENSGALG00000014952
CYP46A1	MD19-21	5	2	ENSGALG00000011162
EPB41L4A	MD25-30	Z	3	ENSGALG00000000234
FAM47E-STBD1	MD7	4	3	ENSGALG00000027872
gga-mir-1618	MD23	8	3	ENSGALG00000025287
GLRX	MD25-30	Z	2	ENSGALG00000027483
HMGCS1	MD25-30	Z	2	ENSGALG00000014862
ITGA1	MD25-30	Z	3	ENSGALG00000014891
LGALS1	MD7	4	2	ENSGALG00000029043
LGR4	MD19-21	5	2	ENSGALG00000012191
LYSMD3	MD25-30	Z	2	ENSGALG00000014651
MLPH	MD10	7	5	ENSGALG00000003904
NADK2	MD25-30	Z	2	ENSGALG00000003558
NPL	MD23	8	2	ENSGALG00000004614
NSA2	MD25-30	Z	2	ENSGALG00000014942
ODF2L	MD23	8	4	ENSGALG00000006804
PINLYP	MD25-30	Z	3	ENSGALG00000026884
PPAP2A	MD25-30	Z	2	ENSGALG00000014711
PPP4R4	MD19-21	5	10	ENSGALG00000010950
PSAT1	MD25-30	Z	2	ENSGALG00000015180
RNF180	MD25-30	Z	4	ENSGALG00000014743
RPS23	MD25-30	Z	2	ENSGALG00000015617
RPS6	MD25-30	Z	2	ENSGALG00000015082
SAT1	MD2	1	2	ENSGALG00000016348
SCARB1	MD24	15	3	ENSGALG00000003018
SLC24A4	MD19-21	5	2	ENSGALG00000010793
SNORD38	MD23	8	3	ENSGALG00000024758
STARD4	MD25-30	Z	3	ENSGALG00000000241
TBC1D8	MD2	1	3	ENSGALG00000016776
TCN2	MD24	15	3	ENSGALG00000009536
TSPAN18	MD19-21	5	2	ENSGALG00000014072

Line 6_1 control macrophages				
Gene	**QTL**	**Chr.**	**Fold Change**	**Ensembl Gene ID**
TXN	MD25-30	Z	3	ENSGALG00000015704
WDR63	MD23	8	4	ENSGALG00000008696
WSCD2	MD24	15	2	ENSGALG00000004849
ZOV3	MD25-30	Z	2	ENSGALG00000014877
Uncharacterised	MD16-17	2	4	ENSGALG00000013268
Uncharacterised	MD19-21	5	2	ENSGALG00000027352
Uncharacterised	MD9	7	3	ENSGALG00000012061
Uncharacterised	MD13	12	3	ENSGALG00000006768
Uncharacterised	MD24	15	3	ENSGALG00000005873
Uncharacterised	MD24	15	4	ENSGALG00000028162
Uncharacterised	MD25-30	Z	2	ENSGALG00000002326
Uncharacterised	MD25-30	Z	2	ENSGALG00000013512

Table S3.2: Line 7_2 control macrophages.

Line 7_2 control macrophages				
Gene	**QTL**	**Chr.**	**Fold Change**	**Ensembl Gene ID**
ADAM8	MD22	6	2	ENSGALG00000003437
CDKN2C	MD23	8	3	ENSGALG00000010537
CLGN	MD8	4	6	ENSGALG00000009826
COL6A3	MD10	7	4	ENSGALG00000003923
CTNND1	MD19-21	5	2	ENSGALG00000007330
DOCK7	MD23	8	2	ENSGALG00000010967
DUSP8	MD19-21	5	3	ENSGALG00000006647
ELOVL7	MD25-30	Z	8	ENSGALG00000014730
ENG	MD14	17	7	ENSGALG00000005060
FN1	MD10	7	2	ENSGALG00000003578
GADD45	MD23	8	3	ENSGALG00000025977
GALNT9	MD24	15	4	ENSGALG00000002242
GFOD1	MD16-17	2	4	ENSGALG00000012730
GLIPR2	MD16-17	2	2	ENSGALG00000028821
GLUL	MD23	8	5	ENSGALG00000003678
IRG1	MD2	1	4	ENSGALG00000016919
ISG12(2)	MD16-17	2	10	ENSGALG00000013575
ITGAV	MD10	7	3	ENSGALG00000002655
KLF5	MD2	1	2	ENSGALG00000016927
LRP8	MD23	8	3	ENSGALG00000010692
MAPK8IP1	MD19-21	5	7	ENSGALG00000008430
MGST3	MD23	8	2	ENSGALG00000003445
MITD1	MD2	1	2	ENSGALG00000016759
NAV2	MD19-21	5	2	ENSGALG00000003999
OSMR	MD25-30	Z	3	ENSGALG00000003747
P2RX7	MD24	15	3	ENSGALG00000003863
PAPSS2	MD22	6	2	ENSGALG00000003689
PIK3AP1	MD22	6	2	ENSGALG00000005547
PISD	MD24	15	2	ENSGALG00000006872
PKN3	MD14	17	2	ENSGALG00000004689
PNPLA2	MD19-21	5	2	ENSGALG00000014569
PTCHD1	MD2	1	4	ENSGALG00000016358
RGSL1	MD23	8	8	ENSGALG00000003671
RNF150	MD8	4	4	ENSGALG00000009865
SH3RF3	MD2	1	3	ENSGALG00000016810
SLC41A3	MD13	12	3	ENSGALG00000006235
SMTN	MD24	15	3	ENSGALG00000011865
SORCS3	MD22	6	97	ENSGALG00000008434
SYNDIG1L	MD19-21	5	5	ENSGALG00000010233
TJP2	MD25-30	Z	10	ENSGALG00000015109

Line 7_2 control macrophages				
Gene	**QTL**	**Chr.**	**Fold Change**	**Ensembl Gene ID**
TNNI2	MD19-21	5	3	ENSGALG00000006591
TPCN2	MD19-21	5	2	ENSGALG00000007550
UCK2	MD23	8	4	ENSGALG00000003510
VCAN	MD25-30	Z	2	ENSGALG00000015624
Uncharacterised	MD19-21	5	6	ENSGALG00000026970
Uncharacterised	MD19-21	5	3	ENSGALG00000006608
Uncharacterised	MD22	6	16	ENSGALG00000004653
Uncharacterised	MD22	6	3	ENSGALG00000005156
Uncharacterised	MD9	7	2	ENSGALG00000012072
Uncharacterised	MD23	8	6	ENSGALG00000020700
Uncharacterised	MD11	8	3	ENSGALG00000020688
Uncharacterised	MD13	12	13	ENSGALG00000006325

Table S3.3: Line 6_1 infected macrophages.

Line 6_1 infected macrophages				
Gene	**QTL**	**Chr.**	**Fold change**	**Ensembl Gene ID**
ABTB2	MD19-21	5	3	ENSGALG00000011609
AMIGO3	MD13	12	2	ENSGALG00000028339
AMPD3	MD19-21	5	2	ENSGALG00000005662
BATF	MD19-21	5	3	ENSGALG00000010323
BDKRB1	MD19-21	5	4	ENSGALG00000020386
BDKRB2	MD19-21	5	2	ENSGALG00000011080
BEST4	MD23	8	11	ENSGALG00000010126
C14orf159	MD19-21	5	3	ENSGALG00000010703
COCH	MD19-21	5	6	ENSGALG00000009920
COL13A1	MD22	6	3	ENSGALG00000004286
COL7A1	MD13	12	4	ENSGALG00000005811
CPE	MD8	4	7	ENSGALG00000027788
CRMP1B	MD5	4	6	ENSGALG00000015042
CSGALNACT1	MD8	4	4	ENSGALG00000010125
CUX2	MD24	15	2	ENSGALG00000004598
CXCL13L2	MD8	4	3	ENSGALG00000010338
ERICH3	MD23	8	3	ENSGALG00000011356
FAM134B	MD16-17	2	2	ENSGALG00000026200
FAM154A	MD25-30	Z	3	ENSGALG00000027314
GRIP2	MD13	12	24	ENSGALG00000006449
HHLA2	MD1	1	5	ENSGALG00000022871
HPD	MD24	15	3	ENSGALG00000004343
IGSF3	MD1	1	2	ENSGALG00000015469
IL23R	MD23	8	7	ENSGALG00000011212
IRF-4	MD16-17	2	9	ENSGALG00000012830
IRS2	MD2	1	2	ENSGALG00000016839
K60	MD7	4	3	ENSGALG00000011668
LEPR	MD23	8	3	ENSGALG00000011058
NINJ1	MD13	12	2	ENSGALG00000026891
NR4A3	MD16-17	2	2	ENSGALG00000013568
PCDH18	MD8	4	3	ENSGALG00000009732
PLCE1	MD22	6	2	ENSGALG00000028043
PSD	MD22	6	8	ENSGALG00000005680
RASSF7	MD19-21	5	3	ENSGALG00000006873
RNaseP_nuc	MD23	8	3	ENSGALG00000025650
RUSC2	MD25-30	Z	2	ENSGALG00000002371
SEMA3B	MD13	12	2	ENSGALG00000013722
SEMA3F	MD13	12	3	ENSGALG00000013370
SH2D1B	MD1	1	5	ENSGALG00000028448
SLC15A1	MD2	1	3	ENSGALG00000016884

Line 6_1 infected macrophages				
Gene	**QTL**	**Chr.**	**Fold change**	**Ensembl Gene ID**
SLC38A3	MD13	12	3	ENSGALG00000028871
SLC46A2	MD25-30	Z	2	ENSGALG00000027345
SLC6A9	MD23	8	3	ENSGALG00000010098
SMTNL1	MD19-21	5	2	ENSGALG00000028884
SPINT1	MD19-21	5	2	ENSGALG00000008469
UMODL1	MD2	1	4	ENSGALG00000016157
ZPLD1	MD1	1	4	ENSGALG00000015347
ZSWIM5	MD23	8	2	ENSGALG00000010221
Uncharacterised	MD2	1	5	ENSGALG00000029002
Uncharacterised	MD2	1	12	ENSGALG00000022751
Uncharacterised	MD19-21	5	4	ENSGALG00000006740
Uncharacterised	MD19-21	5	4	ENSGALG00000027520
Uncharacterised	MD19-21	5	2	ENSGALG00000020380
Uncharacterised	MD19-21	5	3	ENSGALG00000013838
Uncharacterised	MD22	6	3	ENSGALG00000007645
Uncharacterised	MD13	12	4	ENSGALG00000006944
Uncharacterised	MD24	15	3	ENSGALG00000013848
Uncharacterised	MD25-30	Z	2	ENSGALG00000026768

Table S3.4: Line 7_2 infected macrophages.

Line 7_2 infected macrophages				
Gene	**QTL**	**Chr.**	**Fold change**	**Ensembl Gene ID**
ABCA1	MD25-30	Z	2	ENSGALG00000015433
ACOX2	MD13	12	2	ENSGALG00000007132
ADAMTS1	MD2	1	3	ENSGALG00000015792
AFAP1	MD5	4	3	ENSGALG00000015556
AKAP6	MD19-21	5	3	ENSGALG00000009995
BCAR3	MD23	8	2	ENSGALG00000005816
C10orf54	MD22	6	2	ENSGALG00000004673
C11orf74	MD19-21	5	3	ENSGALG00000007941
CC2D2A	MD5	4	2	ENSGALG00000014514
CD274	MD25-30	Z	2	ENSGALG00000015032
CHAC1	MD19-21	5	3	ENSGALG00000027874
CHANK3	MD22	6	6	ENSGALG00000003135
CLCN4	MD2	1	5	ENSGALG00000016607
COL5A2	MD10	7	2	ENSGALG00000002509
CREG2	MD2	1	2	ENSGALG00000026022
DHFR	MD25-30	Z	3	ENSGALG00000026757
DNASE1L3	MD13	12	2	ENSGALG00000005688
DUSP4	MD7	4	2	ENSGALG00000011419
EFNA5	MD25-30	Z	2	ENSGALG00000000280
ENTPD1	MD22	6	2	ENSGALG00000007078
EPHA3	MD1	1	3	ENSGALG00000015403
FAM171B	MD10	7	2	ENSGALG00000002646
FAT1	MD6	4	3	ENSGALG00000013579
FTD	MD19-21	5	3	ENSGALG00000028696
GALNTL4	MD19-21	5	10	ENSGALG00000005584
GLI3	MD16-17	2	2	ENSGALG00000012329
GMPR	MD16-17	2	2	ENSGALG00000012705
GPX7	MD23	8	4	ENSGALG00000010633
HHIPL1	MD19-21	5	4	ENSGALG00000011148
IGF2	MD19-21	5	3	ENSGALG00000006555
IL15	MD8	4	2	ENSGALG00000009870
IQSEC1	MD13	12	2	ENSGALG00000005042
JAM2	MD2	1	3	ENSGALG00000015746
LGI2	MD5	4	3	ENSGALG00000028945
MAP1B	MD25-30	Z	4	ENSGALG00000014999
MEF2C	MD25-30	Z	2	ENSGALG00000014645
MND1	MD8	4	4	ENSGALG00000009212
MYO10	MD16-17	2	3	ENSGALG00000012954
NCKAP1	MD10	7	2	ENSGALG00000002750
NUP210	MD13	12	2	ENSGALG00000005078

Line 7_2 infected macrophages				
Gene	**QTL**	**Chr.**	**Fold change**	**Ensembl Gene ID**
PATZ1	MD24	15	3	ENSGALG00000006934
PDGFC	MD8	4	4	ENSGALG00000009378
PIWIL1	MD24	15	2	ENSGALG00000002645
PTPRG	MD13	12	2	ENSGALG00000007177
SCML2	MD2	1	3	ENSGALG00000016537
SERINC5	MD25-30	Z	2	ENSGALG00000014798
SHROOM3	MD7	4	4	ENSGALG00000011487
SLC12A2	MD25-30	Z	2	ENSGALG00000014690
SLC16A9	MD22	6	2	ENSGALG00000003172
SLC35G1	MD22	6	2	ENSGALG00000027678
SPON1	MD19-21	5	3	ENSGALG00000012027
STS	MD2	1	57	ENSGALG00000016622
SYN2	MD13	12	2	ENSGALG00000004955
SYT8	MD19-21	5	2	ENSGALG00000006602
TCEANC	MD2	1	6	ENSGALG00000016581
TFPI	MD10	7	11	ENSGALG00000002594
THNSL2	MD5	4	2	ENSGALG00000015939
TMEM61	MD23	8	5	ENSGALG00000010801
TTBK2	MD19-21	5	2	ENSGALG00000009176
Uncharacterised	MD2	1	3	ENSGALG00000016784
Uncharacterised	MD8	4	2	ENSGALG00000009237
Uncharacterised	MD5	4	5	ENSGALG00000027201
Uncharacterised	MD22	6	2	ENSGALG00000004747
Uncharacterised	MD23	8	4	ENSGALG00000016099
Uncharacterised	MD13	12	3	ENSGALG00000006544
Uncharacterised	MD24	15	5	ENSGALG00000006053
Uncharacterised	MD25-30	Z	2	ENSGALG00000005814
Uncharacterised	MD25-30	Z	2	ENSGALG00000020561
Uncharacterised	MD25-30	Z	3	ENSGALG00000028298

Table S3.5: Line 6_1 control DCs.

Line 6_1 control DCs				
Gene	**QTL**	**Chr.**	**Fold change**	**Ensembl Gene ID**
BCL2	MD16-17	2	3	ENSGALG00000012885
C14orf159	MD19-21	5	3	ENSGALG00000010703
C1orf123	MD23	8	3	ENSGALG00000026516
CCDC73	MD19-21	5	4	ENSGALG00000012103
CCNJ	MD22	6	4	ENSGALG00000006955
CD247	MD1	1	3	ENSGALG00000015441
COMTD1	MD22	6	2	ENSGALG00000005000
CYP46A1	MD19-21	5	3	ENSGALG00000011162
DNASE2	MD23	8	2	ENSGALG00000028790
EP4	MD25-30	Z	4	ENSGALG00000014824
ESRRB	MD19-21	5	4	ENSGALG00000010365
FAM134B	MD16-17	2	4	ENSGALG00000026200
FAM180B	MD19-21	5	4	ENSGALG00000028710
FBP1	MD25-30	Z	3	ENSGALG00000012613
FZD10	MD24	15	6	ENSGALG00000002652
GLDC	MD25-30	Z	3	ENSGALG00000015053
GOT1	MD22	6	3	ENSGALG00000007484
GPR34	MD2	1	3	ENSGALG00000016227
GSTO1	MD22	6	3	ENSGALG00000008409
HDAC11	MD13	12	3	ENSGALG00000005092
HEXB	MD25-30	Z	3	ENSGALG00000014933
HOOK1	MD23	8	3	ENSGALG00000010889
IL15	MD8	4	3	ENSGALG00000009870
IL1R2	MD2	1	4	ENSGALG00000016782
KNTC1	MD24	15	4	ENSGALG00000004515
LGALS1	MD7	4	3	ENSGALG00000029043
MYO16	MD2	1	32	ENSGALG00000016837
P4HA1	MD22	6	2	ENSGALG00000004325
P4HTM	MD13	12	2	ENSGALG00000006937
PPARGC1A	MD5	4	19	ENSGALG00000014398
PTDSS2	MD19-21	5	2	ENSGALG00000004300
RYBP	MD13	12	2	ENSGALG00000027845
SCD	MD22	6	4	ENSGALG00000005739
SFXN3	MD22	6	2	ENSGALG00000023621
SLC15A1	MD2	1	5	ENSGALG00000016884
SLC24A4	MD19-21	5	6	ENSGALG00000010793
SLC29A3	MD22	6	2	ENSGALG00000004585
SRGAP3	MD13	12	7	ENSGALG00000008378
TCN2	MD24	15	2	ENSGALG00000009536
TESC	MD24	15	19	ENSGALG00000008206

Line 6$_1$ control DCs				
Gene	**QTL**	**Chr.**	**Fold change**	**Ensembl Gene ID**
TEX264	MD13	12	2	ENSGALG00000003832
TLR7	MD2	1	3	ENSGALG00000016590
TM2D1	MD23	8	2	ENSGALG00000020614
TMEM116	MD24	15	6	ENSGALG00000004760
TNN	MD23	8	7	ENSGALG00000004538
TPGS2	MD25-30	Z	2	ENSGALG00000026547
TPST2	MD24	15	2	ENSGALG00000005626
VCAM1	MD23	8	2	ENSGALG00000005257
ZNF518A	MD22	6	2	ENSGALG00000006966
ZOV3	MD25-30	Z	4	ENSGALG00000014877
Uncharacterised	MD22	6	7	ENSGALG00000023824
Uncharacterised	MD9	7	5	ENSGALG00000012061
Uncharacterised	MD24	15	2	ENSGALG00000004725
Uncharacterised	MD24	15	12	ENSGALG00000020975
Uncharacterised	MD24	15	3	ENSGALG00000007728

Table S3.6: Line 7_2 control DCs.

Line 7_2 control DCs				
Gene	**QTL**	**Chr.**	**Fold change**	**Ensembl Gene ID**
ABCC4	MD2	1	3	ENSGALG00000016896
AKAP2	MD25-30	Z	2	ENSGALG00000015656
ALOX5	MD22	6	3	ENSGALG00000005857
APOBEC4	MD23	8	9	ENSGALG00000020926
AVD	MD25-30	Z	7	ENSGALG00000023622
BAFF	MD2	1	2	ENSGALG00000016852
BARD1	MD10	7	4	ENSGALG00000003484
CALCRL	MD10	7	3	ENSGALG00000002632
CAP2	MD16-17	2	3	ENSGALG00000012715
CD2	MD1	1	90	ENSGALG00000015463
CHST3	MD22	6	3	ENSGALG00000024056
CMYA5	MD25-30	Z	3	ENSGALG00000026553
CXorf21	MD2	1	4	ENSGALG00000016286
EHD4	MD19-21	5	3	ENSGALG00000008950
FAM129A	MD12	8	2	ENSGALG00000004812
FAM160A1	MD8	4	5	ENSGALG00000010090
FARP1	MD2	1	2	ENSGALG00000016886
FGF14	MD2	1	16	ENSGALG00000016866
FLRT2	MD19-21	5	3	ENSGALG00000010589
FRMD4B	MD13	12	2	ENSGALG00000014627
FST	MD25-30	Z	6	ENSGALG00000014908
GPR64	MD2	1	5	ENSGALG00000016511
GRIK1	MD2	1	5	ENSGALG00000015835
IRG1	MD2	1	9	ENSGALG00000016919
ISG12(2)	MD16-17	2	3	ENSGALG00000013575
ITGA2	MD25-30	Z	5	ENSGALG00000014903
ITPRIP	MD22	6	4	ENSGALG00000025780
KIF20B	MD22	6	3	ENSGALG00000006470
KIF24	MD25-30	Z	3	ENSGALG00000005806
LIMS1	MD2	1	2	ENSGALG00000016807
MAPK8IP1	MD19-21	5	5	ENSGALG00000008430
MGLL	MD13	12	7	ENSGALG00000005990
MOB3C	MD23	8	2	ENSGALG00000025946
MX	MD2	1	21	ENSGALG00000016142
NCF2	MD23	8	2	ENSGALG00000004700
NRIP3	MD19-21	5	7	ENSGALG00000005903
NRSN1	MD16-17	2	5	ENSGALG00000012670
OAS*A	MD13	12	3	ENSGALG00000013723
PARVA	MD19-21	5	3	ENSGALG00000005438
PAX-6	MD19-21	5	3	ENSGALG00000012123

Line 7_2 control DCs				
Gene	**QTL**	**Chr.**	**Fold change**	**Ensembl Gene ID**
PIK3C2A	MD19-21	5	2	ENSGALG00000006121
PLA2G4A	MD23	8	2	ENSGALG00000005065
PLAU	MD22	6	4	ENSGALG00000005086
PPP1R3C	MD22	6	7	ENSGALG00000006670
PTGS2	MD12	8	8	ENSGALG00000005069
RAD54L	MD11	8	3	ENSGALG00000010356
RANBP9	MD16-17	2	2	ENSGALG00000012696
RBM24	MD16-17	2	3	ENSGALG00000012712
RGSL1	MD23	8	3	ENSGALG00000003671
SEC61A1	MD13	12	2	ENSGALG00000005966
SH3KBP1	MD2	1	2	ENSGALG00000016420
SH3PXD2A	MD22	6	8	ENSGALG00000008293
SLBP	MD5	4	5	ENSGALG00000015712
SLC39A6	MD16-17	2	3	ENSGALG00000013209
SLC6A9	MD23	8	2	ENSGALG00000010098
SNORD24	MD23	8	4	ENSGALG00000017870
SNORD79	MD23	8	7	ENSGALG00000025527
STXBP6	MD19-21	5	2	ENSGALG00000009847
TRAF3	MD19-21	5	2	ENSGALG00000011389
TRAIP	MD13	12	3	ENSGALG00000002908
TSPAN5	MD6	4	3	ENSGALG00000012227
UCK2	MD23	8	3	ENSGALG00000003510
USP54	MD22	6	2	ENSGALG00000005232
WFS1	MD5	4	2	ENSGALG00000015529
ZFP92	MD1	1	2	ENSGALG00000015459
Uncharacterised	MD22	6	4	ENSGALG00000005969

Table S3.7: Line 6_1 infected DCs.

Line 6_1 infected DCs				
Gene	**QTL**	**Chr.**	**Fold change**	**Ensembl Gene ID**
ABCA1	MD25-30	Z	2	ENSGALG00000015433
ACTG2	MD22	6	2	ENSGALG00000006343
ADAM8	MD22	6	2	ENSGALG00000003437
ADM	MD19-21	5	2	ENSGALG00000005666
ANG	MD22	6	3	ENSGALG00000003196
ANGPTL1	MD23	8	5	ENSGALG00000004290
ATHL1	MD19-21	5	2	ENSGALG00000004234
BDKRB1	MD19-21	5	3	ENSGALG00000020386
BDKRB2	MD19-21	5	3	ENSGALG00000011080
BEST1	MD19-21	5	3	ENSGALG00000007217
BEST4	MD23	8	4	ENSGALG00000010126
BSN	MD13	12	2	ENSGALG00000001849
CACNA1E	MD23	8	3	ENSGALG00000003833
CD180	MD25-30	Z	6	ENSGALG00000023411
CD72	MD25-30	Z	4	ENSGALG00000002383
CERCAM	MD14	17	4	ENSGALG00000004986
CHB1	MD25-30	Z	7	ENSGALG00000005194
CNTF	MD19-21	5	4	ENSGALG00000026207
COL25A1	MD8	4	4	ENSGALG00000010521
COL3A1	MD10	7	4	ENSGALG00000002552
COL6A3	MD10	7	4	ENSGALG00000003923
COL7A1	MD13	12	8	ENSGALG00000005811
CREB3L1	MD19-21	5	2	ENSGALG00000008393
CXCL12	MD22	6	2	ENSGALG00000028136
DAB2	MD25-30	Z	2	ENSGALG00000003803
F2RL2	MD25-30	Z	2	ENSGALG00000023379
FGFRL1	MD5	4	3	ENSGALG00000015725
FN1	MD10	7	3	ENSGALG00000003578
GFI1	MD23	8	3	ENSGALG00000005940
GGT5	MD24	15	2	ENSGALG00000006501
GPR27	MD13	12	3	ENSGALG00000027091
GZMA	MD25-30	Z	31	ENSGALG00000013548
HTRA3	MD5	4	3	ENSGALG00000015575
IFITM5	MD19-21	5	2	ENSGALG00000004239
IL1RL1	MD2	1	4	ENSGALG00000016785
IRF-3	MD19-21	5	2	ENSGALG00000014297
ITGB5	MD9	7	2	ENSGALG00000011778
KANK4	MD23	8	3	ENSGALG00000010953
KCNA4	MD19-21	5	2	ENSGALG00000012142
KLRG2	MD25-30	Z	4	ENSGALG00000029035

Line 6_1 infected DCs				
Gene	**QTL**	**Chr.**	**Fold change**	**Ensembl Gene ID**
KREMEN1	MD24	15	2	ENSGALG00000005808
LAMC2	MD23	8	2	ENSGALG00000004627
LDLRAD1	MD23	8	3	ENSGALG00000020647
LIF	MD24	15	2	ENSGALG00000008028
LIPA	MD22	6	2	ENSGALG00000006378
LMCD1	MD13	12	3	ENSGALG00000008349
LMO7	MD2	1	3	ENSGALG00000016920
MCF2L	MD2	1	2	ENSGALG00000016834
MPEG1	MD19-21	5	2	ENSGALG00000028536
MPL	MD23	8	3	ENSGALG00000009965
MRVI1	MD19-21	5	3	ENSGALG00000005632
NEURL	MD22	6	2	ENSGALG00000008281
NFKBIZ	MD1	1	2	ENSGALG00000015346
NR4A3	MD16-17	2	3	ENSGALG00000013568
PAPPA2	MD23	8	11	ENSGALG00000004487
PROK2	MD13	12	4	ENSGALG00000007785
PRRX1	MD23	8	2	ENSGALG00000003324
PRRX2	MD14	17	4	ENSGALG00000028236
RSFR	MD22	6	2	ENSGALG00000027165
RTN4RL2	MD19-21	5	2	ENSGALG00000023441
SATB1	MD4	2	4	ENSGALG00000011254
SEMA3B	MD13	12	3	ENSGALG00000013722
SERPING1	MD19-21	5	2	ENSGALG00000007381
SPON2	MD5	4	3	ENSGALG00000027109
STON2	MD19-21	5	2	ENSGALG00000010579
SYT8	MD19-21	5	3	ENSGALG00000006602
TBX3	MD24	15	3	ENSGALG00000008250
TESK1	MD25-30	Z	3	ENSGALG00000027658
TLL1	MD8	4	3	ENSGALG00000009567
TLL2	MD22	6	3	ENSGALG00000005519
TLR2-2	MD8	4	2	ENSGALG00000009239
TMEM119	MD24	15	3	ENSGALG00000004893
TMEM132D	MD24	15	2	ENSGALG00000002671
TMEM178A	MD19-21	5	3	ENSGALG00000028327
TMEM26	MD22	6	3	ENSGALG00000025862
TSPAN15	MD22	6	3	ENSGALG00000004257
WSCD2	MD24	15	3	ENSGALG00000004849
ZNF330	MD8	4	2	ENSGALG00000009868
Uncharacterised	MD1	1	3	ENSGALG00000027419
Uncharacterised	MD2	1	2	ENSGALG00000016211
Uncharacterised	MD2	1	66	ENSGALG00000013985
Uncharacterised	MD8	4	5	ENSGALG00000009639

Line 6_1 infected DCs				
Gene	**QTL**	**Chr.**	**Fold change**	**Ensembl Gene ID**
Uncharacterised	MD7	4	2	ENSGALG00000025728
Uncharacterised	MD19-21	5	2	ENSGALG00000027352
Uncharacterised	MD13	12	3	ENSGALG00000027695
Uncharacterised	MD24	15	2	ENSGALG00000004854
Uncharacterised	MD24	15	3	ENSGALG00000005873

Table S3.8: Line 7_2 infected DCs.

Line 7_2 infected DCs				
Gene	**QTL**	**Chr.**	**Fold change**	**Ensembl Gene ID**
AKAP6	MD19-21	5	2	ENSGALG00000009995
ATP5J	MD2	1	2	ENSGALG00000015751
CCSER1	MD8	4	3	ENSGALG00000010392
CENPK	MD25-30	Z	2	ENSGALG00000014753
CENPL	MD23	8	2	ENSGALG00000026825
CLCN4	MD2	1	3	ENSGALG00000016607
DACH1	MD2	1	2	ENSGALG00000016933
ELOVL6	MD6	4	2	ENSGALG00000012131
ELOVL7	MD25-30	Z	2	ENSGALG00000014730
EPHA5	MD7	4	3	ENSGALG00000011680
GALNTL4	MD19-21	5	4	ENSGALG00000005584
GLT1D1	MD24	15	2	ENSGALG00000002679
KLF15	MD13	12	3	ENSGALG00000006245
LGI2	MD5	4	6	ENSGALG00000028945
LRP8	MD23	8	2	ENSGALG00000010692
MAMDC2	MD25-30	Z	3	ENSGALG00000015115
NEGR1	MD23	8	5	ENSGALG00000011350
NRN1	MD16-17	2	3	ENSGALG00000028813
NSG1	MD5	4	3	ENSGALG00000015010
NUBPL	MD19-21	5	2	ENSGALG00000009983
PDE6C	MD22	6	3	ENSGALG00000006626
RPP30	MD22	6	2	ENSGALG00000006486
SALL3	MD16-17	2	2	ENSGALG00000012657
SEC61G	MD16-17	2	2	ENSGALG00000013107
SETD4	MD2	1	3	ENSGALG00000016024
SLC44A5	MD23	8	4	ENSGALG00000011379
SRD5A1	MD16-17	2	3	ENSGALG00000013063
SSX2IP	MD23	8	2	ENSGALG00000008763
STS	MD2	1	18	ENSGALG00000016622
TCEANC	MD2	1	3	ENSGALG00000016581
Uncharacterised	MD6	4	2	ENSGALG00000012250
Uncharacterised	MD19-21	5	8	ENSGALG00000025939
Uncharacterised	MD19-21	5	5	ENSGALG00000026584

Appendix 4

Genes with enriched TF binding sites

Table S4.1: Line 6$_1$ infected macrophages - enriched ZNF42 TF binding sites.

Line 6$_1$ infected macrophages	
Gene	**Ensembl Gene ID**
ARSI	ENSGALG00000005616
BATF	ENSGALG00000010323
C14orf159	ENSGALG00000010703
CCR7	ENSGALG00000027572
CHRDL2	ENSGALG00000017308
CORO2A	ENSGALG00000001933
CRMP1B	ENSGALG00000015042
CUTA	ENSGALG00000001620
CXCL13L2	ENSGALG00000010338
DIXDC1	ENSGALG00000007929
EVPL	ENSGALG00000002108
GPR174	ENSGALG00000004111
GPR39	ENSGALG00000012171
HLF	ENSGALG00000003059
HSPA12A	ENSGALG00000009248
IGDCC3	ENSGALG00000007371
IGSF3	ENSGALG00000015469
ITGB1BP2	ENSGALG00000005493
K123	ENSGALG00000006337
LIPG	ENSGALG00000002712
LZTS1	ENSGALG00000001727
P4HA3	ENSGALG00000017311
RELT	ENSGALG00000019033
RNF157	ENSGALG00000002008
SAMD4A	ENSGALG00000012203
SDR42E1	ENSGALG00000005456
SFRP5	ENSGALG00000007515
SH3BP5	ENSGALG00000011550
SLC15A1	ENSGALG00000016884
ST3GAL1	ENSGALG00000016210
STAT4	ENSGALG00000025974
STRIP2	ENSGALG00000026181
SYPL1	ENSGALG00000029006
TRPM2	ENSGALG00000005631
TUBA3E	ENSGALG00000010439
WNT4	ENSGALG00000004790
WNT5B	ENSGALG00000012998
Uncharacterised	ENSGALG00000010336

Table S4.2: Line 6_1 infected DCs - enriched ZNF42 TF binding sites.

Line 6_1 infected DCs	
Gene	**Ensembl Gene ID**
ACTG2	ENSGALG00000006343
ADAM33	ENSGALG00000016038
AHR	ENSGALG00000010836
AMH	ENSGALG00000024368
ANGPTL4	ENSGALG00000000619
AQP1	ENSGALG00000005209
ARHGEF6	ENSGALG00000006439
ARR3	ENSGALG00000004251
ARRDC2	ENSGALG00000003527
ARSI	ENSGALG00000005616
BDKRB2	ENSGALG00000011080
CAMK1G	ENSGALG00000001319
CARD11	ENSGALG00000004398
CCDC69	ENSGALG00000004354
CCL1	ENSGALG00000002329
CD164	ENSGALG00000015238
CD40	ENSGALG00000007015
CD72	ENSGALG00000002383
CERCAM	ENSGALG00000004986
CISH	ENSGALG00000002260
COL18A1	ENSGALG00000004338
COL1A2	ENSGALG00000009641
COL25A1	ENSGALG00000010521
COL3A1	ENSGALG00000002552
COL5A1	ENSGALG00000002546
COL6A3	ENSGALG00000003923
CORO2A	ENSGALG00000001933
CPNE4	ENSGALG00000011613
CTSB	ENSGALG00000016666
CUBN	ENSGALG00000008704
CUTA	ENSGALG00000001620
CX3CL1	ENSGALG00000026663
CXCL12	ENSGALG00000028136
DAK	ENSGALG00000005227
DAK	ENSGALG00000005961
DDX25	ENSGALG00000000463
DNAH17	ENSGALG00000007106
DOCK2	ENSGALG00000002080
ELFN1	ENSGALG00000004209
EMILIN2	ENSGALG00000014815
F2RL2	ENSGALG00000023379
FAM78A	ENSGALG00000003789
FBN2	ENSGALG00000014686
FZD1	ENSGALG00000009064
GAP43	ENSGALG00000015089
GEM	ENSGALG00000015954
GJA1	ENSGALG00000014873
GPR39	ENSGALG00000012171

Line 6$_1$ infected DCs	
Gene	**Ensembl Gene ID**
HPGD	ENSGALG00000010769
HTRA3	ENSGALG00000015575
ID1	ENSGALG00000006210
IFITM5	ENSGALG00000004239
IL1RL1	ENSGALG00000016785
IL6	ENSGALG00000010915
ITGA11	ENSGALG00000008007
KCNA4	ENSGALG00000012142
KDELR3	ENSGALG00000012251
KLHDC8A	ENSGALG00000000684
LAMB3	ENSGALG00000001343
LAMC2	ENSGALG00000004627
LAMP3	ENSGALG00000008759
LIF	ENSGALG00000008028
LINGO1	ENSGALG00000002708
LMCD1	ENSGALG00000008349
LRRC32	ENSGALG00000000818
MALL	ENSGALG00000023882
MAPKAPK3	ENSGALG00000002283
MCAM	ENSGALG00000006764
MPL	ENSGALG00000009965
MRC2	ENSGALG00000000461
MXD1	ENSGALG00000013882
MYL9	ENSGALG00000028567
NDRG4	ENSGALG00000000874
NEURL	ENSGALG00000008281
NFKBIZ	ENSGALG00000015346
NR4A3	ENSGALG00000013568
NT5E	ENSGALG00000015833
NTM	ENSGALG00000001437
NUMA1	ENSGALG00000001258
OSBPL10	ENSGALG00000011474
P4HA3	ENSGALG00000017311
PAPPA2	ENSGALG00000004487
PCSK6	ENSGALG00000007238
PCTP	ENSGALG00000003099
PDGFRB	ENSGALG00000021313
PERP	ENSGALG00000027536
PLXDC2	ENSGALG00000007956
PRELP	ENSGALG00000003551
PRRX2	ENSGALG00000028236
RSFR	ENSGALG00000027165
RTN4RL2	ENSGALG00000023441
RUNX2	ENSGALG00000026484
S100A11	ENSGALG00000009163
SDK2	ENSGALG00000004464
SERPINH1	ENSGALG00000011214
SFRP4	ENSGALG00000012073
SLC18A2	ENSGALG00000009289
SLC38A4	ENSGALG00000009730

Line 6$_1$ infected DCs	
Gene	**Ensembl Gene ID**
SLC43A2	ENSGALG00000002783
SLC4A11	ENSGALG00000016017
SNAI2	ENSGALG00000015241
SOCS1	ENSGALG00000007158
ST3GAL1	ENSGALG00000016210
STON2	ENSGALG00000010579
SYTL4	ENSGALG00000006786
TAGLN	ENSGALG00000011902
TAP1	ENSGALG00000026269
TBX3	ENSGALG00000008250
TIMP3	ENSGALG00000012568
TLE1	ENSGALG00000012575
TMEM119	ENSGALG00000004893
TMEM26	ENSGALG00000025862
TNFAIP2	ENSGALG00000011446
TNFRSF11B	ENSGALG00000016114
TNNC1	ENSGALG00000001459
TRIM71	ENSGALG00000019622
TSPAN15	ENSGALG00000004257
VANGL2	ENSGALG00000024120
VTN	ENSGALG00000003589
WFDC1	ENSGALG00000005503
WSCD2	ENSGALG00000004849
XYLT1	ENSGALG00000006757
YIPF6	ENSGALG00000004584
ZNF414	ENSGALG00000024378
ZNF521	ENSGALG00000015112